Proceedings

of the

1st

National Communications Engineering Conference, 2018

Held at
ASSEMBLY HALL,
AHMADU BELLO UNIVERSITY, ZARIA

DATE: 17TH – 19TH OCTOBER, 2018

Published by
Department of Communications Engineering
Ahmadu Bello University, Zaria.

Copyright©2018

LOCAL ORGANISING COMMITTEE (LOC)

LOC Chairman – Dr A. D. Usman

Secretary - Dr. M. J. Musa

Publication Committee
Dr. M. J. Musa (Head)
Dr. K. A. Abu-Bilal
Dr. Y. A. Shehu
S. G. Zubairu
A. M. Abba
M. A. Hudu
U. Abubakar (Student)

Finance Committee
Dr. A. D. Usman (Head)
Dr. A. M. S. Tekanyi
I. Ya'u
F. S. Dadah (Student)
R. F. Onundi (Student)

Venue and equipment's committee
Dr. U. F. Aguye (Head)
A. Y. Kassim
M. Suleiman
M. Tijjani
S. Aminu
Safiya Yusuf (Student)

Technical Sessions Committee
Dr. K. A. Abu-Bilal (Head)
Dr. H. A. Abdulkareem (Chair session 1)
Dr. E. A. Adedokun (Co-Chair session 1)
Dr. U. F. Abdu-Aguye (Chair session 1)
Dr. A. T. Salawudeen (Co-Chair session 1)
Dr. S. M. Sani (Chair session 1)
Dr. I. J. Umoh (Co-Chair session 1)
Dr. A. M. S. Tekanyi (Chair session 1)
Dr. Y. A. Sha'aban (Co-Chair session 1)

Protocol, Publicity and Mini excursion Committee
H. A. Abdulkareem (Head)
M. Z. Zaya'ulhaq
I. K. Musa
A. B. Kunya
M. Itse (Student)

Entertainment Committee
M. A. Zanna (Head)
E. Obi
E. E. Agbon
A. A. Olaniyan
A. Mazamaza (Student)
P. Guyah (Student)

Exhibition Committee
M. A.Ogbole (Head)
S. Bako
J. Olorunpomi
A. Buhari
M. Francis (Student)
I. Musa (Student)

TABLE OF CONTENT

Botnet Detection Technique Using Artificial Neural Network

Suleiman Muhammad Nasir, Olalere Morufu Olajide.
Ojeniyi Joseph. A.
Cyber Security Science Department
Federal University of Technology
Minna, Nigeria
suleiman.pg611993@st.futminna.edu.ng,
lerejide@futminna.edu, ojeniyija@futminna.edu.ng

Mebawondu Jacob Olorunshogo
Computer Science Department
Federal Polytechnic
Nasarawa, Nigeria

ABSTRACT - As the cyber space grows so also are it challenges. The most severe security challenges bothering cyber security researchers around the globe is botnet: a network of systems that is taken over by a hacker to launch attack or perform an unwholesome activity. Botnet as a means of cyber-attack delivery has more far reaching effect that any other means. It is a prime factor in the delivery of Distributed Denial of Service (DDoS), SPARM (mail or fake review), and click fraud among other cyber related crimes. It is equally implicated in most of the activities that are termed cyber warfare. The paper reviews the incidence and purulence of botnet and proposes an Artificial Neural Network based Botnet Detection and classification system. The model was implemented on an ISCXbotnet dataset and an accuracy of 98% was achieved in detection and classification.

KEYWORDS: Botnet, command & Control channel, botmaster/botherder, zombie,

INTRODUCTION

Botnet is coined from the words roBOT and NETwork. It describes a kind of attack where a set of connected computer systems (possibly over the internet) is taken over by a distance or remote system to launch a systematic and simultaneous attack on a target system. [1, 2,3]. The controlled systems are referred to as the bot while the controlling system is called the botmaster. The bots are mostly the end user host systems which are a priori infested or compromised while the botmaster can be a human user at a remote end or a system operating the various hosts[4, 5]. The malware system deployed to enable a remote control of a system is also be called a bot.

Botnet employs vulnerable machines using techniques that are employed by other types of malware (remote software vulnerability exploitation, social engineering etc). The defining chrematistics of a botnet is that is that it uses *Command and Control Channels*. This channel enhances the dissemination of botmaster's commands to the various bots or armies[6, 7].

Botnets happens to be the most severe security challenges bothering cyber security researchers around the globe [8]. The botnet can be used in implementing so many hazardous effects in an organization. It can be used to transfer secret information to a competitor or an adversary, to spread denial of Service attack (DoS) for phishing activities, key logging activities forward spam activities and click fraud etc. Unlike other classes of malware that are generally used to exhibit technical prowess botnets are mostly employed for illegal and illicit undertakings. These undertakings may take the form of extortion, identity theft and software piracy. Hence the reason for a concerted research in this area.

Recently many of the cyber-attacks have employed botnet in one way or the other [6, 9]. It signifies a vivid and cogent treat to the information systems across the globe.[10]. Botnet has the ability to obfuscate the identity of the attacker and easily multiply the source of attack. It has evolved from a simple spam factory to and elaborate big masquerade behind mammoth criminal activities. According to [11] the number of computers enrolled as bot increases by 8% per seek. Extracting from this every computer system is a potential victim. Another study has reported a botnet of up to 400,000 bots.

A botnet can be defined as a coordinated group of compromised machines controlled via Command & Control (C&C) communication channels that are connected to some C&C servers/peers managed by botmaster/botherder. In other words, it is an army of infested end-user systems under the influence of a remote instructor, which has the capability to unleash havoc or spread malicious software or conduct a malicious activity on a target system [12, 13, 1]. We can also define a botnet as an *assemblage* of *malware* instances that are *controlled* through a C&C communication channels

Through the botnet attack the identity of the botmaster is effectively concealed while the master can effectively conduct a multiple and simultaneous attack on the target. The bots can generally be used to conduct any attack as the botmaster deems fit. The essential characteristics of a botnet are that the bots communicate with some C&C servers/peers, enact some activities that can be said to be malicious, and these activities are in a similar or correlated the C&C

In the botnet world according to [14] there are three actors: the botmaster, the vulnerable systems and the defenders. The botmaster is actively involved in recruiting the bots and controlling them to perform his nefarious act. His motive is always economic gain. The vulnerable systems are the end users' systems whose vulnerability could be employed by the botmaster to get them recruited as zombies into the botnet. These system, if unpatched, remain tools in

the hands of a botmaster in conducting his criminal activities. The defender intends to prevent, detect, track host and trace the botmaster. He is always on the side of the law and protected by the law enforcement agency.

The botnet life circle divided into four phases: formation, C&C, attack and post attack phases [9]. At the formation phase a botmaster attempts to and compromise any available vulnerable machines. It uses all the available methods including social Engineering to recruit vulnerable hosts to become part of his network of zombies. At the C&C phase, the master communicates with the bot through the C&C mechanism. The botmaster always keep track of the bots by relaying regular instruction which may include when and how to attack. At this point a defender may intervene and disrupt the botmaster activity thereby binging the botnet system down.

The attack phase starts when the botmaster issues instruction to the bots to launch attack. The victim may be the host system itself or another system entirely depending on the mode of attack in the intention of the botmaster. During the post attack phase the bots may get exposed to the defender and it is brought down and the system patched. However, if the botnet remains active the botmaster increases the number of bots in his botnet by requiring more vulnerable systems for his future attack.

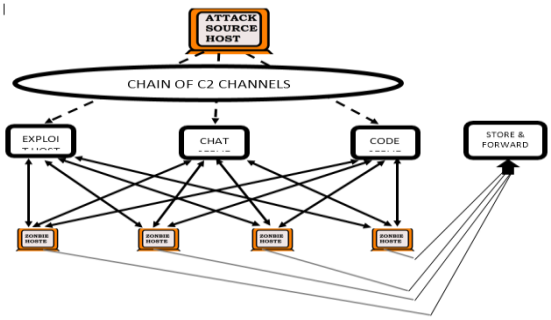

Figure 1 Chat based botnet architecture using a C2 char service

A. Architectures

There are two basic topologies available in thorough which a botnet can be deployed. These are Centralized Command and Control (C&C) architecture or distributed Command and Control (C&C) architecture [7]. Centralized C&C architecture is a simple and widely used architecture. In (C&C) architecture the botmaster simply communicates with the bots using the C&C server to send commands to the botnet. The architecture is one way and therefore suffers a single point failure. Once the C&C server is brought down the whole botnet is down. The famous approaches used in centralized botnet include Internet Relay Chat (IRC) and Hypothec Transfer Protocol (HTTP).[15]

Decentralized C&C is a relatively new architecture aimed at elevating the single point of entry setback suffers by a Centralized C&C architecture. In Decentralized C&C infrastructure all peers in the network works like a bot and a C&C Server at the same time. Here the botmaster's role is only to send command to any recruited peer. The life cycle of a distributed botnet (particularly the P2P architecture) consists of initial infection, peer propagation, secondary injection and attack[16; 15, 8 5]

B. History

The first observable botnet-like behavior was in 1988 when Robet Marris, released the internet first worm which was designed to "phone home" to a command & Control Server. In 1999 Sub7 – a Trojan and Pretty Perk – a worm were released. These malwares are known to connect infected systems to an IRC channel to listen to malicious commands. In 2000 was the emergence of the Global Threat bot GTbot which was known to to run custom scripts in response to IRC event. Agabot emerged in 2002 and in 2004 its variant phanbot was released. Phanbot Rbot was among the first known P2P based botnet.

2003 witnessed the rise of spybots with new features like key logging and data miming and Rbot (a family of bots which used compression and encryption algorithms to evade detection). Others in the series include Zeus (2006) Grum (2008) and Gameover Zeus (2011)

C. Artificial Neural Network

Artificial neural network is an information processing approach that is inspired by the way biological neurons process information. It is a computing system made up of simple highly connected elements (the neurons), which process information by their dynamic state response to external input working together to solve a particular problem [34, 35, 37]. As human being learn by examples, so is the Artificial Neural Network does. ANN can be configured for applications such as pattern recognition, data classification etc. through a learning process. ANN has a remarkable ability to derive meanings from complicated or impressive data. Hence it can be used to extract patterns and detect trends that are too complex to be noticed by either man or other computer techniques. A trained neural network can be thought of as an "expert" in the category of information it has been given to analyze. The expert can then be used to provide trajectory given a new situation of interest [35, 37]

As human being learns by examples, repeating the examples to create relationships so is the Artificial Neural Network does. The process of learning is referred to as training. The training problem is modeled as a minimization of loss function. This function is in general composed of and error term and regularization term. The error term evaluates how neural network fits the data set while the regulator tern

is sued to prevent out fitting by controlling the effective complexity of the network [37]

The loss function depends on the adaptive parameters (biases and synaptic) and can be conveniently grouped together into a single n-dimensional weigh factor w. The fundamental element of ANN is the neuron. Each neuron handles:

i. The multiplication of the network inputs, x1, x2, x3, . . .xn (from original data, or from the output of other neurons in a neural network) by the associated input weights,

ii. The summation of the weight and input product to the bias value associated with the neuron, and

iii. The passage of the summation result, u, through a linear or nonlinear transformation called the activation function, φ. The neuron's output, y, is the result of the action of the activation function.

$$\varphi = f(u) \quad (1)$$

$$y = \varphi(\sum_{i=1}^{n} \quad X_i W_i + b) \quad (2)$$

$$y = \varphi(W^T X + b) \quad (3)$$

where b is the bias value (or external threshold), W_i, is the weight of the respective inputs xi, u is the argument of the activation function and W^T is a transpose of the weight vector. The weight and bias are adjustable parameters of the neuron that causes the network to exhibit some desired or interesting behaviours. Fig 2 shows an illustration of an artificial neuron. [37]

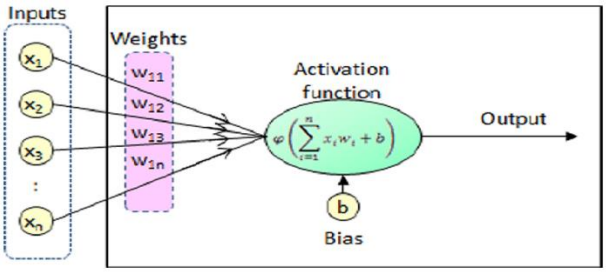

Figure 2 ANN Network [35, 37]

D. Training algorithms

There are five popular training algorithms. These are:

i. Gradient Decent (Steepest descent)
ii. Newton's Method
iii. Conjugate Gradient
iv. Quasi Newton
v. Levenberg Marquidt [35, 37]

II RELATED WORKS

The authors of [23] proposed a BotSniffer: an anomaly base botnet Command and Control detection system, although it is mainly sued for detecting centralized command and control activities. A BotMiner described and proposed by [22] uses a horizontal correlation approach that examines correlation between multiple host. BotMiner is independent of the botnet C&C protocol, structure and infection mode. The frame work of BotMiner targeted both centralized IRC and P2P botnets. The design of a BotMiner woks on the assumption that bots are coordinated malware that exhibit similar communication pattern and similar behavior both malicious and otherwise. Its major drawback is that it targets a group of compromised machines within a monitored network. However, it may fail if only one or two hosts are infected in a network but the hosts belong to a larger group of botnet with spans the monitored network. Again, it may fail to detect bots that exchange covert C&C messages without undertaking any malicious activity.

Another approach was introduced by the authors of [24]. This was based on the analysis of network behavior. The approach focused on the characteristics of IRC flows. Hence the approach is divided in to four stages. The first sage filtered off the not likely varying bot C&C data (given some prior knowledge of IRC bot commands) the second stag clustered the remaining flows into predefined network application clusters using machine learning. The third stage, the correlator stage, where clustered chat-like applications are clustered again in to a group of flows showing similar characteristic. Then the correlated flows are passed in to topology analysis to determine flows with common controllers. The last stage, an offline stage where a human factor analyzed the flows to determine whether they are botnet or not. This last stage spelled the setback of the proposed system.

The authors of [33] in their work identified some TCP related features for the detection of HTTP botnets. With these features a Multi-Layer Feed Forward Neural Network training model using Bold Driver Back-propagation learning algorithm was created. This algorithm had the advantage of dynamically changing the learning rate parameter during weight updating process. With this approach, Spyeye and Zeus botnets are efficiently identified.

In [25] the authors' work is focused on detecting botnet C&C commination on an end host. This is based on the fact that a recruited host need to keep in touch with the botmaster to remain relevant. This is always done by frequent communication between the bot and the botmaster such that such communication exhibits some temporal regularity over a period of irregular large time period. Evaluation of this approach using a real network traces yields low false positive rate.

The authors of [26] proposed a 2P2 botnet detaching technique using multi-phased flow model. In its proposal, 2P2 botnets are identified by observing similar flow occurring between a group of hosts in the network on a regular basis. Flow with similar behavior are groped and a transition model of the grouped flow is constructed using a probability matrix. Then a likelihood ratio is computed and used for bot detection. An accuracy of above 95 was achieved with experimental evaluation

In [27] the authors proposed a P2P botnet detection model using data mining technique. They explained the possibility of detaching host infected with a bot by analyzing bot traffic behavior. They introduced a set of metrics that could be used to differentiate between bot traffic, normal traffic, gaming traffic and general internet traffic. The evaluation of the proposed approach involved studying one 2P2 botnet virus known as Trojanpeacomm and achieved a detection rate of over 87%. However, the approach has not been applied on other categories of botnet to see how it performs. However according to [9] the approach had not been applied on other categories of botnet to see how it performs.

Since the botnet technology is evolving there is the need to consider distributed approach to bot dissemination. Hence the authors of [28] considered other types of network and streaming technologies and proposed artificial neural network for botnet detection.

The authors of [9] proposed a new approach to characterize and detect network traffic (Particularly the P2P bots) before it launches an attack. Using machine learning technique, they extracted and analyzed a set of C&C traffic behavior and its characteristics. It applied all the five machine learning techniques and compared them. The work in [29] observed that focusing on statistics network flow rather than packet content was unable to differentiate between IRC traffic and benign graphic. He pointed the setbacks on previous methods as Principle component analysis, (PCA), Correlation Feature Selection (CFS), minimum redundancy minimum relevance (mRmR) and improper evaluation of feature sets on test bed datasets. He built a dataset which incorporates different varieties of botnet of different protocols in realistic environment.

In their work [3], the authors modeled classifier using an assemble algorithm for botnet classification. It employed K-nearest Neighbor and decision tree and bagging and Ada Boost for soft voting.

III. METHODOLOGY

A. Proposed ANN Model for Based Botnet Detection

The proposed MLP network for botnet detection consists of 11 nodes at the input layer, one hidden layer and 4 nodes at the output layer. In the proposed model, 3 most frequently used activation functions have been considered. These are:

i. Logistic sigmoid activation function also known as logsig.

$$f(u) = \frac{1}{1+e^{-u}} \quad (4)$$

ii. Hyperbolic tangent sigmoid activation function also known as tansig.

$$f(u) = \frac{2}{1+e^{-2u}} - 1 \quad (5)$$

iii. Linear activation function also known as purelin.

$$f(u) = u \quad (6)$$

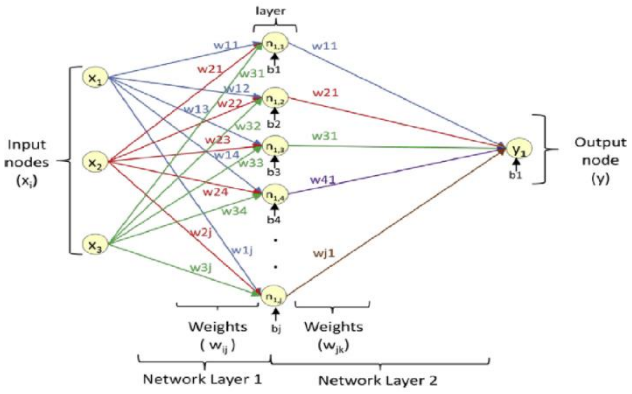

Figure 3

A schematic of the proposed ANN network with variable neurons in the hidden layer is shown inin fig 4 .where x_i ($1 \le i \le 11$) are the set of inputs; w_{ij} and w_{jk} are adjustable weight values: w_{ij} connects the ith input to the jth neuron in the hidden layer, w_{jk} connects the jth output in the hidden layer to the kth node in the output layer; yk ($1 \le k \le 5$) are the output.

Each neuron and output node has associated adjustable bias values: bj (where j = number of neurons) is associated with the jth neuron in network layer 1, bk ($1 \le k \le 5$) is associated with the node in the network layer 2. Within each network layer are: the weights, w, the multiplication and summing operations, the bias, b, and the activation function, u.

B. Data Acquisition and Pre-Processing

For the purpose of the work the use iscxbot2014 dataset. The dataset was originally created by [29]. It is made up of data set from three different sources. These sources are:

i. ISOT data set created by fusing different available data sets [30]. (French chapter of honeynet project, Eriksson Research in Hungary and Lawrence Berkeley National Library).
ii. ISCX 2012 IDS dataset generated in a physical testbed implementation using real devices that generated real traffic that mimic user behavior [31]
iii. Botnet traffic generated by the malwares capture facility project. A research project with the purpose of generating and capturing botnet traces in long term. [32.]

The dataset was extracted using Wireshark: a foremost and widely used network analyzer to generate an excel version of the set. The data set contain Forty-two (42] attributed out of which 11 were selected for our purpose.

C. Model Development

MATLAB was used to write the script files for the developed botnet detection and classification model and performance analysis to determine the weight and bias values, number of neurons and activation function type to be used in the optimal model equation. The script files were written to compare the relative effect of number of hidden layer neurons and activation function type on the performance of a designed network. A feedforward network topology and the default Matlab Neural Network Toolbox learning algorithm, Levenberg– Marquardt, were used.

The number of neurons in the hidden layer was varied from 5 to 33 in incremental steps of 2. Logsig, purelin and tansig type of activation functions were used to create 9 different pairs of activation functions. Thus, each of the 15 different numbers of neurons was used with 9 different pairs of activation functions. Each run of the script file generates 135 networks. For networks in which activation function pairs with logsig or tansig functions were used in the output layer, the input and target output data were pre-processed into 0–1 or _1 to +1 range using bellow respectively.

$$X_{norm\_0\_1} = \frac{X - X_{min}}{X_{max} - X_{min}} \quad (7)$$

$$X_{norm\_-1\_1} = 2 * \frac{X - X_{min}}{X_{max} - X_{min}} - 1 \quad (8)$$

The network outputs from the simulation process were then post processed to the original range. To compare the relative effect of number of runs on network performance, the script file was run 20 times and 20 runs generated 2700 trained networks for performance evaluation. The flow diagram of the ANN script file is shown in Fig. 3 flowchart.

Out of the over 1million iscxbot2014 dataset downloaded and extracted through Wireshark into excel file, 9040 samples were used while training the network and 4040 were used for testing. During the training process, the input and target output data were applied to the network and the network computed its output. The initial weight and bias values and their subsequent adjustments were done by the Matlab Neural Network Toolbox software. For each set of output in the output data, the error, e, (the difference between the target output, t, and the network's output, y,) was computed. The computed errors were used by the network performance function to optimize the network and the default network performance function for feedforward networks is mean squared error, MSE (the mean of the sum of the squared errors) which is given by:

$$MSE = \frac{1}{N}\left(\sum_{i=1}^{N} (e_i)^2\right) \quad (9)$$

$$MSE = \frac{1}{N}\left(\sum_{i=1}^{N} (t_i - y_i)^2\right) \quad (10)$$

where N is the number of sets in the output data. The weight and bias values are adjusted so as to minimize the mean squared error and thus increase the network performance. After the adjustments, the network undergoes a retraining process, the mean square error is recomputed and the weight and bias values are readjusted. The retraining continues until the training data achieves the desired mapping to obtain minimum mean square error value.

D) Developed Model

Mathematically, fig 4can be represented as:

$$y_i = \varphi_2\left(\sum_{j=1}^{m} w_{j1}\varphi_1\left[\sum_{i=1}^{11} w_{ij}x_i + b_j\right] + b_1\right) \quad (11)$$

where m is the total number of neurons in the hidden layer. The operations within an N layered network can be mathematically represented by;

$$y_i = \frac{\varphi_N\left(\sum_{j=1}^{p} w_{ki} \cdots \frac{\varphi_2\left(\sum_{j=1}^{m} w_{jk}\frac{\varphi_1\left(\sum_{i=1}^{n} w_{ij}x_i + b_j\right)}{Layer\ 1} + b_k\right)}{Layer\ 2} + \cdots + b_i\right)}{Layer\ N} \quad (12)$$

where i is the number for the ith neuron in layer N, p is the maximum number of neurons in layer N and N is the total number of network layers.

For linear activation function in both hidden and output layers and the use of m number of neurons in the hidden layer, eqn. (10)is transformed into:

$$y = LW[IW * X + b_I] + b_2 \quad (13)$$

$$y = [LW * IW] * X + [LW * b_1] + b_2 \quad (14)$$

Where

Layer weights, LW = [1,m] matrix

Input weights, IW = [m,11] matrix
Layer 1 bias, b1 = [m,1] matrix
Layer 2 bias, b2 = c
Input vector, X = [11,1] matrix

Thus

$$[LW * IW] = [\alpha\ \beta\ \gamma\ ] \quad (15)$$

$$[LW * IW] * X = [\alpha\ \beta\ \gamma\ ][TRD] \quad (16)$$

The proposed model equation is:

$$y = \alpha T + \beta R + \gamma D + c \quad (17)$$

IV RESULT AND DISCUSSION

In order to get best performance of the intelligent model, dynamic thresholding algorithm was developed to get the best threshold value using training dataset between 0.4 and 0.6 with an increment 0f 0.05. The best three threshold values ware recorded: 0.5, 0.505 and 0.58 as displayed in table 4.1

Table 4.1: Dynamic thresholding for training dataset

Thres-hold	Accuracy						Average Accuracy	Standard Deviation
0.485	99	96	99.14286	98.85714	95.85714	97.77143	97.77142857	1.686077443
0.49	99.85714286	99.2857143	99.71429	98.28571	98.42857	99.11429	99.11428571	0.724216677
0.495	98.85714286	99.2857143	99.57143	99.28571	98.71429	99.14286	99.14285714	0.349927106
0.5	99.71428571	99.7142857	99.42857	99.71429	99.42857	99.6	99.6	0.156492159
0.505	99.85714286	99.4285714	98.85714	99.71429	99.28571	99.42857	99.42857143	0.391230398
0.51	99	97.4285714	99.71429	99.57143	99.57143	99.05714	99.05714286	0.950832074
0.515	99.28571429	99.2857143	99.57143	98.57143	99.14286	99.17143	99.17142857	0.369776546
0.52	99.71428571	96.2857143	99.71429	99.71429	99.85714	99.05714	99.05714286	1.550510122

Table 4.2. Performance Evaluation of Activation Function Combinations and DTA

Acti-vation Functio n Pair	Accu-racy (%)	Correct Rate (%)	Error Rate (%)	Last Correct Rate (%)	Last Error Rate (%)	Inco n clusi ve Rate (%)	Classi fied Rate (%)	Sensi -tivity (%)	Speci -ficity (%)	False Positi ve Rate (%)	False Negati ve Rate (%)
PP	66.113	79.18	20.82	79.18	20.82	0	100	71.78	87.65	12.35	28.22
PT	66.113	79.51	20.49	79.51	20.49	0	100	71.37	88.84	11.16	28.63
PL	65.448 5	79.29	20.71	79.29	20.71	0	100	70.95	88.84	11.16	29.05
TP	99.6	99.89	0.11	99.89	0.11	0	100	99.79	99.52	0.48	0.21
TT	75.083 1	86.16	13.84	86.16	13.84	0	100	89.63	82.19	17.81	10.37
TL	66.113	79.51	20.49	79.51	20.49	0	100	71.37	88.84	11.16	28.63
LP	79.734 2	84.05	15.95	84.05	15.95	0	100	80.29	88.36	11.64	19.71
LT	82.059 8	84.83	15.17	84.83	15.17	0	100	82.16	87.89	12.11	17.84
LL	81.395 3	84.05	15.95	84.05	15.95	0	100	82.57	85.75	14.25	17.43

The performance evaluation of the activation function pairs and the Dynamic Thresholding Algorithm (DTA) ispresented in table 4.2 above. The metrics used in evaluating the performance are accuracy, correct rate, error rate, last correct rate, last error rate, inconclusive rate, classified rate, sensitivity, specificity, false positive rate and false negative rate. The performance evaluation report clearly indicates that all the traffic data were classified. There is no unclassified traffic. With reference to all the performance metrics, tansig-purelin (TP) activation function combination achieved the best values. The accuracy, sensitivity and specificity of TP pair are 99.6678%, 99.79% and 100%. With these values, the false positive rate of 0% and false negative rate of 0.21% were attained.

V CONCLUSION AND RECOMMENDATION

A. Conclusion

An Artificial neural network classifier for botnet detection and classification have been presented to for the. The model and its implantation on the chosen data set has shown to be of a comparative very efficiency given an average accuracy of 98%. The SCIX data set has also shown to be very relevant in the researches on botnet detection and classification.

B. Recommendation

We hereby recommend that more than one training algorithm could be combined to generate of more flexible and robust detection system.

REFERENCES

[1] M. Khosroshahy, M. K. M. Ali,& D. "SIC botnet lifecycle model: A step beyond traditional epidemiological models". *Computer Networks*, 2013, *57*(2), 404–421.

[2] E. Alparslan, A Karahoca, & D. Karahoca, "BotNet Detection : Enhancing Analysis by Using Data Mining Techniques", 2012.

[3] A. Bijalwan., N Chand, E. Shubhakar, & C. R. Krishna, "Botnet analysis using ensemble classifier". *Perspectives in Science*, 2016. PP *8*, 502–504.

[4] J. Zarfoss, "A Multifaceted Approach to Understanding the Botnet", 2006. PP 41–52.

[5] P.Torres, & C. Catania, "An Analysis of Recurrent Neural Networks for Botnet Detection Behavior". 2017.

[6] P. Wang, & C.C Zou, "An Advanced Hybrid Peer-to-Peer Botnet". 2010.

[7] M. Alauthaman, N. Aslam, L. Zhang, & R. Alasem, "A P2P Botnet detection scheme based on decision tree and adaptive multilayer neural networks" in. *Neural Computing and Applications*. 2016. https://doi.org/10.1007/s00521-016-2564-5

[8] P. Barthakur, B.T. Park, & C.V.Ramannagar, "A Framework for P2P Botnet Detection Using SVM", 2012. https://doi.org/10.1109/CyberC.2012.40

[9] S. Saad, I. Traore, A. Ghorbani, B. Sayed, D, Zhao,W. Lu, & P. Hakimia. "Detecting P2P Botnets through Network Behavior Analysis and Machine Learning". 2011.

[10] S.S.C Silva, R.M.P. Silva, R.C.G. Pinto, & R.M. Salles, "Botnets : A survey", *57*, 378–403. 2013. https://doi.org/10.1016/j.comnet.2012.07.021

[11] A. Hardikar, & F. Bégin, BYOB: "Build Your Own Botnet Botnets". *SANS Institute InfoSec Reading Room*. 2011.

[12] D. Dagon, C. Zou & W. Lee. "Modeling botnet propagation using timezones". In *13th Annual Network and Distributed System Security Symposium NDSS'06,* 2006.

[13] F.Haddadi, J. Morgan, E.G. Filho & A.N. Zincir-heywood, "Botnet Behaviour Analysis using IP Flows", 2014. PP 1–6. https://doi.org/10.1109/WAINA.2014. 19

[14] J. Leonard, S. Xu & R. Sandhu, "A framework for understanding botnets". *Proceedings - International Conference on Availability, Reliability and Security, ARES*, 2009. PP 917–922. https://doi.org/10.1109/ARES.2009.65

[15] M. Bailey, E. Cooke, F. Jahanian, Y. Xu, A. Arbor & A. Arbor, "A Survey of Botnet Technology and Defenses" 2006.

[16] S. Anwar, & A. Karim, "A Statistics Approach towards Mobile Botnet Detection", 563–567. (2016).

[17] F. Freiling, Holz, T., & G.Wicherski, "Botnet tracking: Exploring a root-cause methodology to prevent denial of service attacks" In *European symposium on research in compute security*,2005.

[18] M. Reiter, & T. F Yen, "Traffic Aggregation for Malware Detection" 2007.1–22. https://doi.org/10.1007/978-3-540-70542-0_11

[19] A. Karasaridis, B. Rexroad, & D. Hoeflin:Wide-scale Botnet Detection and Characterization". 2007.

[20] J. Goebel, & T. Holz, & Rishi: "identify bot contaminated hosts by IRC nickname evaluation" *HotBots'07 Proceedings of the First Conference on First Workshop on Hot Topics in Understanding Botnets*, 2007.PP 8. https://doi.org/10.1.1.177.8170

[21] G. Gu, P. Porras, V. Yegneswaran, M. Fong & W. Lee, "Bothunter:Detecting malware infection through IDS-driven dialog correlation". In *16th USENIX Security Symposium*, 2007.

[22] G. Gu, R. Perdisci, J. Zhang, & W. Lee, « BotMiner: Clustering Analysis of Network Traffic for Protocol- and Structure-Independent Botnet Detection" 2008.

[23] G. Gu, J. Zhang & W. Lee, "BotSniffer: Detecting Botnet Command and Control Channels in Network Traffic", 2008.

[24] T. Strayer, & R. Walsh, "Botnet Detection", *36*(October), 2008 PP 0–29..https://doi.org/10.1007/978-0-387-68768-1

[25] F. Giroire, J.N. Chandrashekar, E. Taft, Schooler, & D. Papagiannaki, "Exploiting temporal persistence to detect covert botnet channels". *Lecture Notes in Computer Science (Including Subseries Lecture Notes in Artificial Intelligence and Lecture Notes in Bioinformatics)*, 2009. *5758 LNCS*, 326–345, https://doi.org/10.1007/978-3-642-04342-0_17

[26] S.K Noh, J.H. Oh, J.S. Lee, B.N. Noh, & H.C Jeong, "Detecting P2P botnets using a multi-phased flow model". *Proceedings of the 3rd International Conference on Digital Society*, (2009).*ICDS 2009*, PP 247–253. https://doi.org/10.1109/ICDS.2009.37

[27] D. Liu, Y. Li, Y. Hu, & Z. Liang, "A P2P-botnet detection model and algorithms based on network streams

analysis", *International Conference on Future Information Technology and Management Engineering, FITME 2010*, PP *1*, 55–58. https://doi.org/10.1109/FITME.2010.5655788

[28] P. Salvador, C. Santiago, De & N. Siemens, "A Botnet Detection System based on Neural Networks", 2010. PP 57–62. https://doi.org/10.1109/ICDT.2010.19

[29] E.B. Beigi, H.H. Jazi, N. Stakhanova & A. A Ghorbani, "Towards Effective Feature Selection in Machine Learning-Based Botnet Detection Approaches", 2014. PP 247–255.

[30] D. Zhao, I. Traore, B. Sayed, W. Lu, S. Saad, A. Ghorbani, & D. Garant, "Botnet detection based on traffic behavior analysis and flow intervals". *Computers & Security*, 2013. PP *39*, 2–16. https://doi.org/10.1016/j.cose.2013.04.007

[31] A. Shiravi, H. Shiravi, M. Tavallaee & A.A Ghorbani, "Toward developing a systematic approach to generate benchmark datasets for intrusion detection". *Computers & Security*, 2011. *31*(3), 357–374. https://doi.org/10.1016/j.cose.2011.12.012

[32] S. Garcia. (n.d.). "Malware capture facility project, cvut university". Retrieved February 12, 2017, from https://mcfp.agents.fel.cvut.scz

[33] G. Kirubavathi Venkatesh & R. Anitha Nadarajan, "HTTP Botnet Detection Using Adaptive Learning Rate Multilayer Feed-Forward Neural Network". *Information Security Theory and Practice. Security, Privacy and Trust in Computing Systems and Ambient Intelligent Ecosystems*,2012. - *5*, *7322*, 38–48. https://doi.org/10.1007/978-3-642-30955-7_5

[34] J.O Eichie, O.D. Oyedum, M.O. Ajewole, & A.M. Aibinu, "Artificial Neural Network model for the determination of GSM Rxlevel from atmospheric parameters" in. *Engineering Science and Technology, an International Journal*, *20*(2), 795–804. 2017. https://doi.org/10.1016/j.jestch.2016.11.002

[35] I. Masood, N.Z. Abidin, N.R., Roshdi, N.A Rejab & M.F. Johari, "Design of an Artificial Neural Network Pattern Recognition Scheme Using Full Factorial Experiment". *Applied Mechanics and Materials*, 2014. *466*, 1149–1154. https://doi.org/doi: I0.4028/www.scient~c.net/AMM.465-466.1

[36] S. Stockt, & X. Van Der., "A Generic Neural Network Framework Using Design Patterns". *University of Pretoria, Pretoria*, 2017 (October).

Comparison between ANN and ANFIS-Based Algorithms for Detection and Classification of Fault on Transmission Lines

Abubakar Isa
Department of Electronics and Energy Storage Devices
Sheda Science and Technology Complex
Abuja, Nigeria abuabakarisa@yahoo.com

Shamsu Idris Abdullahi
Department of Electrical and Electronic Engineering
Kano State Polytechnic
Kano, Nigeria
shamsuabdullahi114@gmail.com

Rabiu Aliyu Abdulkadir
Department of Electrical Engineering
Kano University of Science and Technology, Wudil
Kano, Nigeria
rabiukk@gmail.com

Yakubu Muhammad Muhammad
System Operation Engineer
Transmission Company of Nigeria
Abuja, Nigeria
ymmuhammad33@gmail.com

ABSTRACT— This paper presents a comparison between relaying algorithm based on Artificial Neural Network (ANN) and adaptive neuro-fuzzy inference system (ANFIS) technique for the protection of transmission line. A feed forward ANN with six inputs and eleven outputs has been developed for the detection and classification of faults. Data was generated by simulating a 400 kV, 50Hz, 100 km transmission line in PSCAD/EMTDC at a sampling frequency of 2 kHz. Three ANN and ANFIS configurations with different combinations of inputs have been attempted. Initially all the three ANN and ANFIS configurations were trained and tested using truncated data for their comparative performance. ANFIS configuration has been found to be the best one and different set of data have been used for training and testing with different number of epochs and membership function. 'gbell' membership function found to be the best membership function in performance for both training and testing with least error, been 100% accuracy and lesser number of epochs and faster than ANN.

KEYWORDS— artificial neural network, fault detection, phase selection, power system faults, transmission line.

INTRODUCTION

A transmission line is one of the main components in electric power system which provides a path to transfer power from generation to load. The transmission line is exposed to different types of faults namely phase-to-earth, two-phase-to- earth, phase-to-phase, three phase faults. The fault on the transmission line needs to be detected and then isolated quickly to prevent the disturbance in the line. It is important to detect, classify and clear the faults with high speed, selectivity and accuracy in order to prevent instability which can cause damage to the system. Several techniques have been reported in the literature for detection and location of faults on transmission lines [1,2]. The objective is to protect the transmission line in such a way that the power system is stable and only the faulty part is to be isolated leaving the rest part of the system in operation. Hence, it is essential to detect the fault quickly and separate the faulty section of the transmission line for safety, economy and power quality. A fault detector that uses artificial neural networks (ANN) has been described in [3]. It performs the fault defection problem as a pattern classification process. However it does not classify the faults. Back-propagation ANN has been used as a pattern classifier for a distance of 100 km with two sources at both ends in [4]. However, only one type of fault, phase to ground fault, was simulated varying the fault distance, fault resistance, fault inception angles, sources impedance, source capacities and power transfer angle. ANN used six inputs, namely normalized Ia, Ib, Ic and Va, Vb, Vc and had six nodes in the input layer, six nodes in the first hidden layer, two nodes in the second hidden layer and one node in the output layer.ANN was successfully trained to detect fault in protection zone only with accuracy at 78.82% of the protection zone. Fault detection and classification has been achieved in [5]. Two hidden layers with (30-20-15-11) have been used. However, it requires large memory as the number of inputs is more. Faults have been detected and classified using ANN with the relay operating time of 1 cycle in [6]. Single-line-ground faults have been classified with the relay operating time of 1 cycle in [7]. The prime motive behind the present work was an accurate fault classification as well as fault detection in such a way that the maximum accuracy is achieved with minimum relay operating time. Paper reports improved algorithm which does classification as well as detection and has accuracy of 100% and requires less memory with relay operating time of less than ¾ cycle which is an improvement over work achieved by the earlier researchers.

ANN has been trained and tested using Back-propagation algorithm with a large amount of data. The inputs to ANN were the rms values of phase voltages, line voltages, line currents and ratios of sequence components of currents in different combinations and the same data used for training and testing for ANFIS.

The transmission line was simulated using an electromagnetic transient program, EMTDC/PSCAD on a sample three-phase power system. The data has been generated for all the types of faults at two different locations with two values of fault resistance and eight values of fault inception angles at a sampling rate of 2 kHz. Three ANN configurations (ANN-1, ANN-2, ANN-3) with six inputs and eleven outputs have been attempted. The three configurations differ in the inputs. The inputs were Va, Vb, Vc and Ia, Ib, Ic to ANN-1, Vab, Vbc, Vca and

In/Ip, Io/Ip, Ip/Iload to ANN-2 and. Va, Vb, Vc and In/Ip, Io/Ip, Ip/Iload to ANN-3. The same configuration used for ANFIS.

All the three ANN and ANFIS configurations were attempted and compared. ANFIS has been found as the best configuration in terms of accuracy and performance as 100% accuracy has been achieved in both training and testing with a minimum delay.

II. DATA GENERATION FOR TRAINING AND TESTING OF ANNS AND ANFIS

A. Simulation

Simulations were performed using an electromagnetic transient program, EMTDC/PSCAD, on a sample three-phase power system. Fig. 1 shows the three phase model of the system that has been studied. The system consists of a generator of 400 kV located on one side of the transmission line. The transmission line (line-1 and line-2 together) is 100 km long. The line has been modeled using distributed parameters. A three phase fault module is used to simulate different types of faults with different inception angles, different fault resistances, and different source and load impedances at various locations on the transmission line.

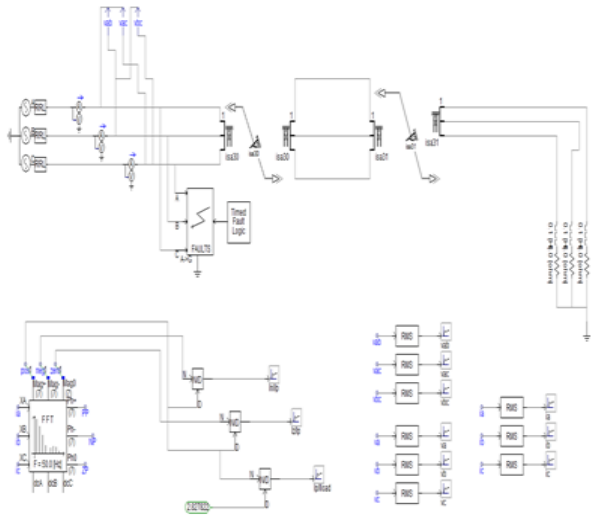

Fig. 1. Model simulated in PSCAD (fault location at 0km)

B. Dataset

As the input signals to the protective relay are currents and voltages. In the same way these inputs have to be fed to the ANN. However, some other parameters are needed to differentiate between the types of faults. Those parameters are zero sequence currents (Io), positive sequence currents (Ip) and negative sequence currents (In). Twelve quantities are needed to select the best set of input combinations for the neural network. The quantities include Ia, Ib,I c, Va, Vb, Vc, Vab, Vbc, Vca and In/Ip, Io/Ip, Ip/Iload. Balanced faults and unbalanced faults are differentiated by the ratio of negative sequence current to positive sequence currents (In/Ip), the ratio of zero sequence currents to positive sequence currents (Io/Ip) is used to differentiate between the ground faults to phase faults and the balanced fault and no fault condition is differentiated by the ratio of positive sequence currents to load currents (Ip/Iload). C. Generated Data The values of three-phase rms voltages and currents are measured. The rms voltages include the rms line to line voltages and rms phase voltages. The line components are first processed using FFT algorithm and then the sequence components at the fundamental frequency are derived.

Fig. 2 shows the graphs obtained during single line-to-ground fault of the system.

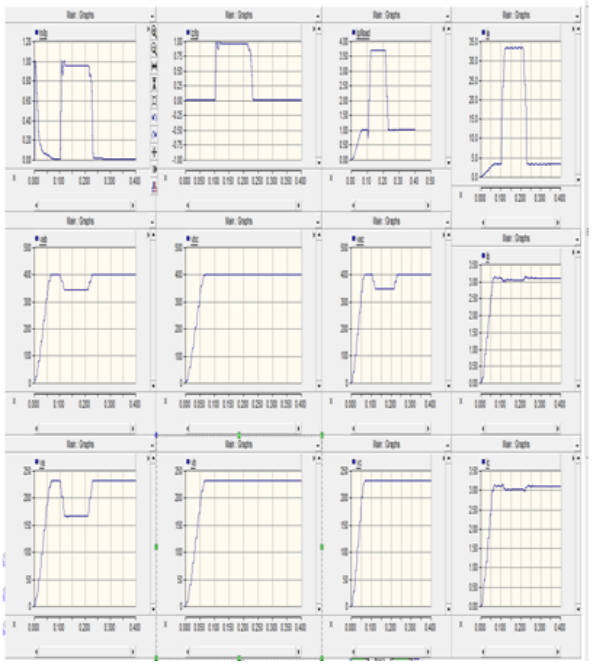

Fig. 2. Rms graphs of 12 parameters during single-line-to-` 1ground fault.

III. ANN INPUTS AND CONFIGURATION

Three ANN configurations have been attempted. The configurations differ in the input signals applied. The three combination of inputs include (Va, Vb, Vc and Ia, Ib, Ic) for ANN-1, (Vab, Vbc, Vca and In/Ip, Io/Ip, Ip/Iload) for ANN-2 and (Va, Vb, Vc and In/Ip, Io/Ip, Ip/Iload) for ANN-3. but the combination of ANN-2 have better accuracy compare ANN-1and ANN-3, due to this ANN-2 will be consider.

A. ANN-2

1) Inputs Line voltages and sequence current ratios were used as inputs to ANN-2. The six inputs used include Vab, Vbc, Vca and In/Ip, Io/Ip, Ip/Iload. The outputs were eleven which consists of AG, BG, CG, AB, BC, CA, ABG, BCG, CAG, ABCG and no-fault. One hidden layer was used with different number of neurons for optimization.

2) Results The numbers of iterations required for the training process were 48. The mean square error in fault detection achieved by the end of the training process was 4.57e-07 and the number of validation check fails was zero by the end of the training process. Fig. 3 shows the training performance plot of the neural network.

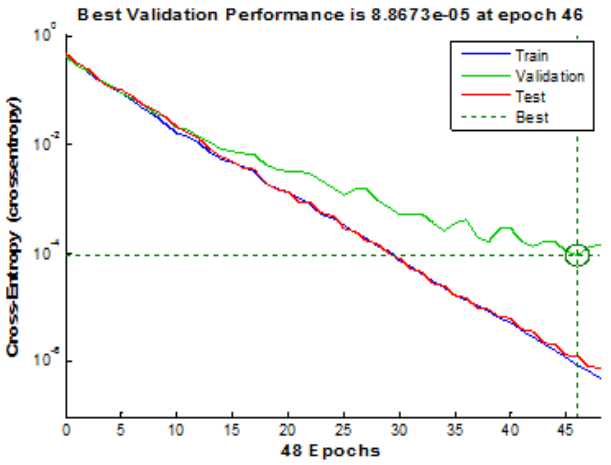

Fig. 3. Mean-square error performance of ANN-2 (6-20-11)

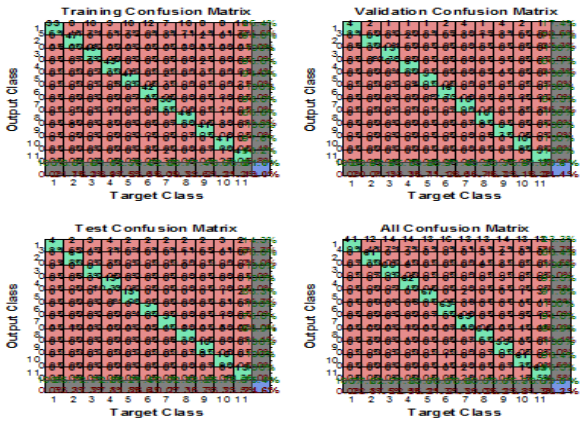

Fig. 4. Confusion matrices for Training, Testing and Validation Phases of ANN-2 (25 sample delay)

The accuracy of training for ANN-2 for fault classification with no delay was 79.8%. In order to increase the accuracy 5 samples were removed and the accuracy was still 83.2%. Then the accuracy reached a value of 94.1% at a delay of 10 samples, 99.4% at a delay of 15 samples, 99.2% at a delay of 20 samples. The accuracy of 100% was obtained at a delay of 25 samples as shown in Fig. 6. Further delay would make no sense. Confusion matrices for a delay of 25 samples (12.5 ms) are shown in Fig. 4. Similarly ANN-2 was tested and the accuracy of testing for ANN-2 for fault classification with no delay was 81.3%. In order to increase the accuracy 5 samples were removed and the accuracy was still 84.9%. Then the accuracy reached a value of 93.5% at a delay of 10 samples, 98.0% at a delay of 15 samples, 98.8% at a delay of 20 samples. An accuracy of 100% was obtained at a delay of 25 samples as shown in Fig. 5.

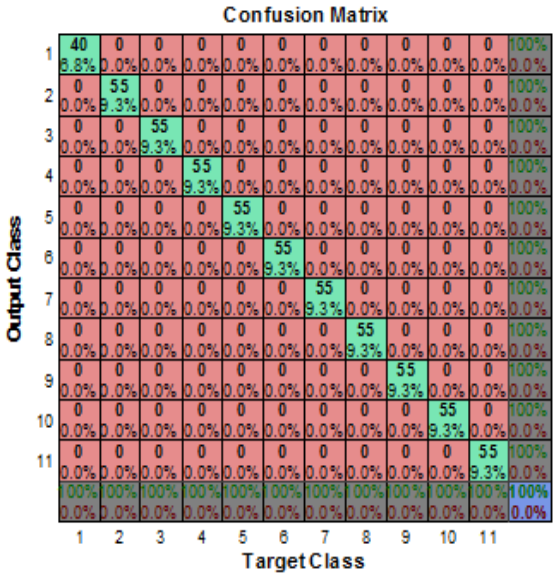

Fig. 5. ANN-2 Confusion matrix for testing of ANN-2 with 25 sample delay

IV. ANFIS INPUTS AND CONFIGURATION

Three ANFIS configurations have been attempted. The configurations differ in the input signals applied. The three combination of inputs include (Va, Vb, Vc and Ia, Ib, Ic) for ANFIS-1, (Vab, Vbc, Vca and In/Ip, Io/Ip, Ip/Iload) for ANFIS-2 and (Va, Vb, Vc and In/Ip, Io/Ip, Ip/Iload) for ANFIS-3. but the combination of ANFIS-2 have better accuracy compare ANFIS-1and ANFIS-3, due to this ANFIS-2 will be consider.

A. ANFIS-2

1) Inputs Line voltages and sequence current ratios were used as inputs to ANFIS-2. The six inputs used include Vab, Vbc, Vca and In/Ip, Io/Ip, Ip/Iload. The outputs were eleven which consists of AG, BG, CG, AB, BC, CA, ABG, BCG, CAG, ABCG and no-fault.

B. ANFIS DATA TRAINING AND TESTING

The data is classified as training data and testing data in ANFIS's learning process. Testing data should be in the range of training data for the purpose of testing procedures. The number of training epoch also gives a good result in predicting the target. Accurate targets consider a minimum prediction error from the result of ANFIS training. The error can be reduced by adjusting the variable membership function (MF) and epoch parameters. With increasing in number of MF and epoch, the error will reduce accordingly. Sometimes, no reducing in error can be noticed even though the epoch was increased up to 5000 and above. This is due to the way the data is assembled. Therefore effective input data assembly will result good prediction. For this work, effective configuration of the data has been reached by preparing a wide data range between their elements and arranging the data from small to large values.

During the training process, MF parameters are varied so as to yield the ANFIS's output as target values. The

minimum error percentage is a small difference between target and prediction values and it is used to measure the success level of a training process.

C. TESTING AND TRAINING OF ANFIS WITH GBELLMF WITH EXPANDED DATA SET

I. In this part the number of samples data increased for both training and testing,in the training similarly six inputs were used i.e. V_{ab}, V_{bc}, V_{ca} *and* $I_n/I_p, I_o/I_p, I_p/I_{load}$ together with the 0 and 90 degree faults inception angles and 50km fault location. While for testing the same set of inputs were used with 45 and 135 degree inception angles. The figures below show the training and testing results starting from 10 epochs to 20epochs of the gbellmf.

D. RULE

In this part, an ANFIS model has been developed with 12 fuzzy 'IF-THEN' rules for the task of determining the ten faults and no-fault condition. Since, the number of block functions represents the rules for every input data, it is difficult to describe the operational process of the model due to lack of space. However, a rule viewer is shown in Fig.5.1.8 for that purpose. There are five stages of ANFIS operational process that includes fuzzification, 'IF-THEN' rules, normalization, defuzzification and neuron addition. Figure 5.4.1:show the rule viewer of gbellmf with 12 rules

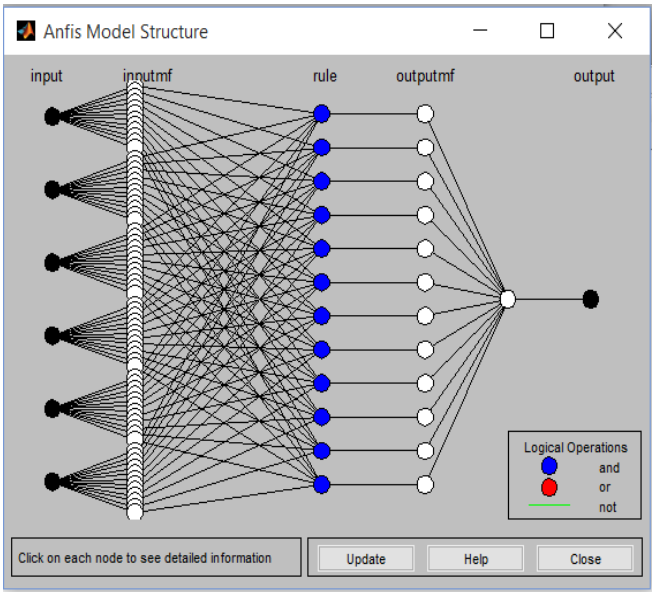

Fig. 6: An ANFIS model structure for the task of identifying ten fauts and no-faults condition

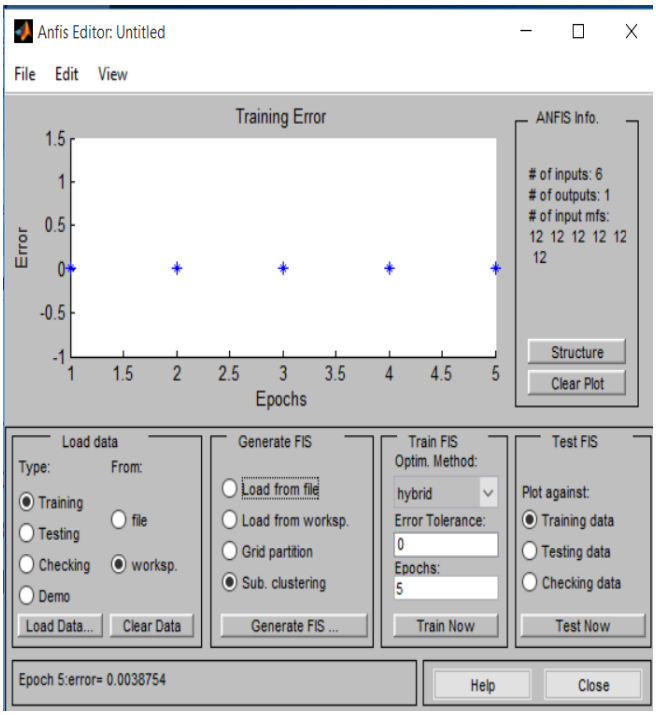

Figure 7:train result of gbellmf with 5 epochs

E. Testing results

About 1640 samples of data set were tested with six inputs i.e. V_{ab}, V_{bc}, V_{ca} *and* $I_n/I_p, I_o/I_p, I_p/I_{load}$ and ten faults and no-fault condition used as output with different fault inception angles and epochs. The results are show in the figures below;

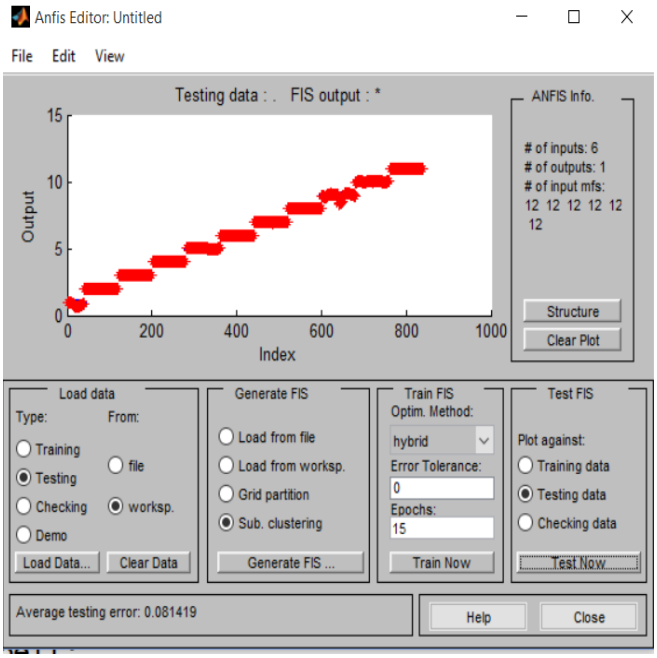

Figure 8:test result of gbellmf with 15 epochs

V. FINDINGS

A. ANFIS

- Gbellmf has the best performance for both training and testing data.
- The error are reduced with increased the number of epochs
- The optimum number epochs for both testing and training was found to be 5epochs
- Training error = 0.0038754
- Testing error =0.0814
- Faster than ANN

B. .ANN

- 20 neurons is the optimums number for training
- 22 neurons is the optimum number for testing
- The optimum delay is 25 samples i.e.12.5ms

VI. CONCLUSION

ANFIS technique involves more computation, but it provides better accuracy for detection and classification all types faults in transmission lines than ANN .Different set of data had been trained and tested with different number of epochs and membership function and gbellmf was found to be the best membership function in performance for both training and testing with least error, high accuracy and less number of epochs and faster than ANN with less delay.

REFERENCES

[1] G Das R, Novosel D, "Review of fault location techniques for transmission and sub – transmission lines". Proceedings of 54th Annual Georgia Tech Protective Relaying Conference, 2000. .

[2] IEEE guide for determining fault location on AC transmission and distribution lines. IEEE Power Engineering Society Publ., New York, IEEE Std C37.114, 2005

[3] E. Vazquez, O. L. Chacon, and H. J. Altuve, "Neural-network-based fault detector for transmission line protection," inProceedings of the Mexico- USA Collaboration in Intelligent Systems Technologies (ISAI/IFIS '96), pp. 180–185, November 1996K. Elissa, "Title of paper if known," unpublished.

[4] D.V. Coury and D.C. Jorge, "The Back propagation Algorithm Applied to Protective Relaying", IEEE International Conference on Neural Networks, Vol. 1, pp. 105–110, 1997

[5] M.Kezunovic , I Rikalo and D.J Sobajic"High-Speed fault detection and classification with neural nets," Electric Power Systems Research, vol. 34,no. 2, pp. 109–116, 1995.

[6] A. Jain, A. S. Thoke, and R. N. Patel, "Fault classification of double circuit transmission line using artificial neural network," International Journal of Electrical Systems Science and Engineering, vol. 1, no. 4, pp. 750–755, 2008

[7] A. Jain, A. S. Thoke, and R. N. Patel, "Fault classification of double circuit transmission line using artificial neural network," International Journal of Electrical Systems Science and Engineering, vol. 1, no. 4, pp. 750–755, 2008.

Design of Millimeter Wave Micro Strip Patch Antenna for 5G Mobile Application

Muhammad Surajo, Amos.O.Ataguba, Charles joe Garba
Department of Communication engineering,
Ahmadu Bello University Zaria, Nigeria
ephraimamos62@gmail.com, smdgw2002@gmail.com, charlesjoegarba@yahoo.com

Abstract*—This paper present the design and simulation of a single band micro strip patch antenna for 5G wireless application operating at 60GHz with a maximum reflection coefficient of -41.648731dB,a very wide bandwidth of 30GHz and a gain of 8.82dB.The transmission line of the antenna used is an inset feed. The substrate used is Rogers RT5880 which has a dielectric constant of 2.2, loss tangent 0.0009, and height 1.6mm.The antenna dimensions were calculated and simulated results have been displayed and analyzed using CST software.

Keywords—millimeter-wave, 5G, u slot and H slot, microstrip, 60GHz

I. INTRODUCTION

Today and in the recent future, to fulfill the presumptions and challenges of the near future, the wireless based networks of today will have to advance in various ways. The 5G technology uses a higher frequency range of 28-72 propose by FCC on October 22nd 2015 as the FCC 15138 rule, which is able to deliver a high data of multi-Gbp and will be able to support as much as 1000x by 2030.With the competence of 5G,a lot of industries will be enhanced such as Artificial intelligence, and the Internet of Things (IoT) that is fueling a need for massive connectivity of devices, and also a need for ultra-reliable, ultra-low-latency connectivity over Internet Protocol (IP).

In this paper, the propose single patch antenna is designed to resonate at 60GHz millimeter wave frequency.The patch is design using the substrate Roger RT5880 with a dielectric constant of 2.2,thickness of 0.254mm with 3.5mm × 2.9mm as the dimension of the patch. The design antenna uses the 50Ω microstrip line feeding and simulated by the CST software.

II. MATERIALS AND METHODS

The proposed micro strip patch antenna operating at 60GHz for 5G is shown in Figure 1

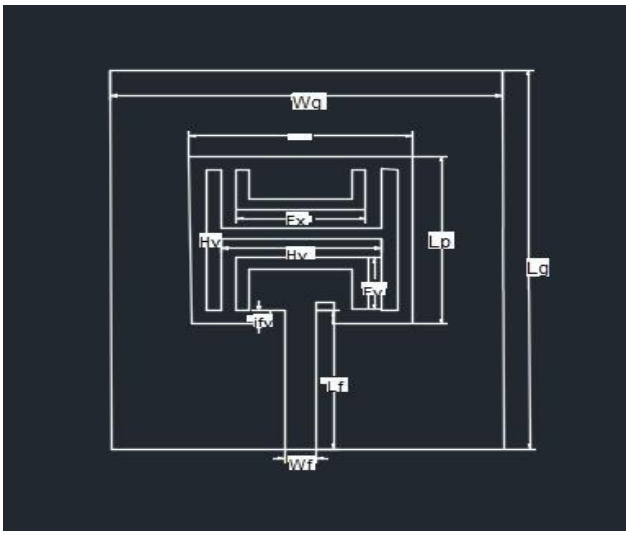

Figure 1: Proposed Micro strip Patch Antenna

TABLE I. Dimension of proposed antenna

Parameter	Dimension (mm)
wg	8
lg	7.5
Wp	3.5
Lp	2.9
Wf	0.41
Lf	2.15
Ifx	0.2
Ify	0.2
Hx	2.4
Hy	2.5
Ex	1.5
Ey	1.35
D	0.3

The copper plate with dimensions of 8mm x 7.5mm and thickness of 0.003 mm is used as the ground plane. The H and U slot cut on the patch help to enhance the impedance bandwidth, the length and width is 1.5 mm and 1.35 mm. The feed lines have a length and width of 0.41mm and 3.25 mm. The single band antenna has been designed at work 60 GHz millimeter wave frequency.

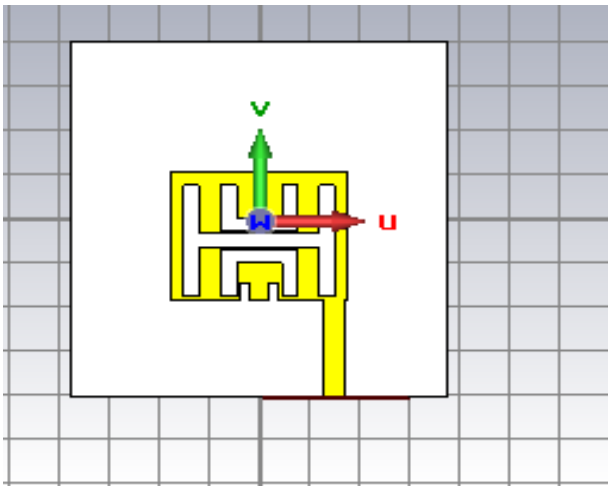

Figure2: The Simulated Micro Strip Patch Antenna

III. RESULTS AND DISCUSSIONS

The antenna was modeled and simulated using CST Microwave commercial software programs and each layer of the proposed design was assigned with its respective physical and electrical properties. The result of the return loss, VSWR (Voltage Standing Wave Ratio), gain and the radiation pattern of the single patch element obtained is shown in Figure 3 - 7. The S11 parameters were obtained to be -41.65 dB taken as the base value which is favorable for mobile communication. The single patch resonates at 60 GHz with a return loss of -41.65 dB as seen in Figure 3 below. The acceptable level of VSWR for wireless application should be less than 2 and as seen in Figure 4, the VSWR of the single patch antenna is 1.8 The antenna achieved a high gain of 8.82 dB which is considered excellent in terms of a compact micro strip patch antenna as shown in Figure 4. The radiation pattern at phi=0° and theta = 90 is presented in Figure 5 and 6. An omnidirectional pattern of the proposed antenna is seen with a small back lobe.

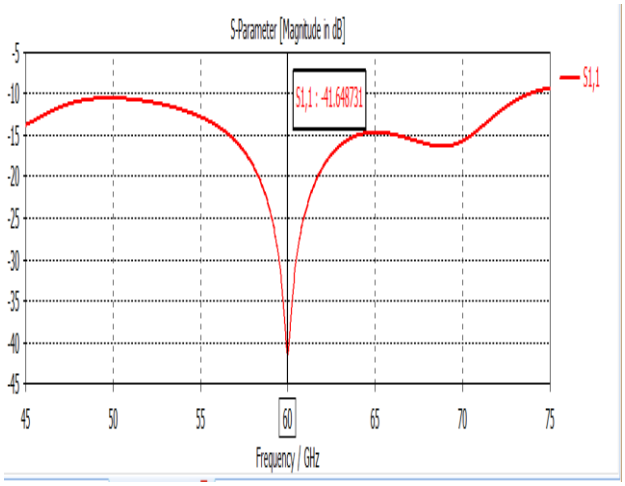

Figure 3: Return Loss

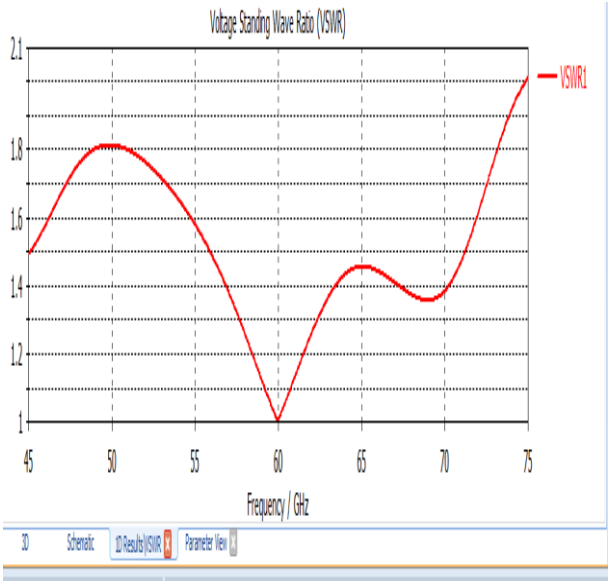

Figure. 4: VSWR curve of proposed antenna

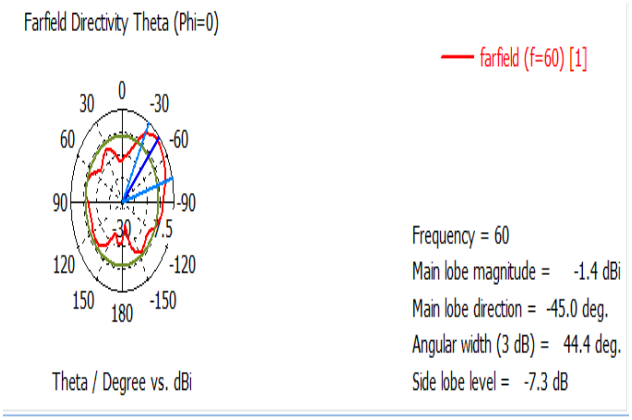

Figure 5: Radiation Pattern

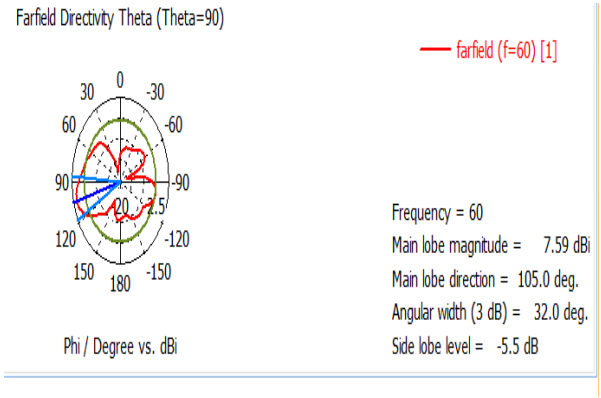

Figure 6: Radiation Pattern at 90

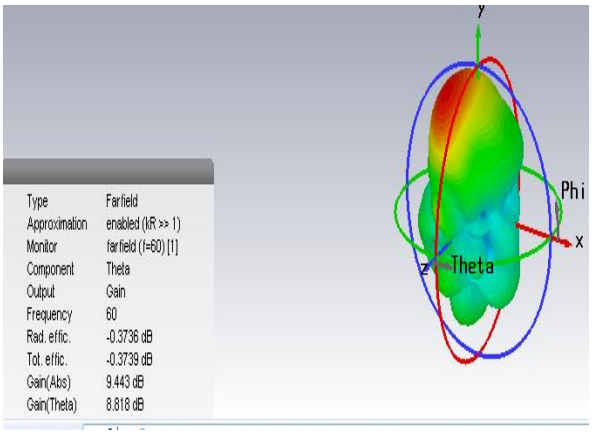

Figure 7: 3D Display of antenna gain

The summary of result is shown in Table 2 below. The obtained parameters shows that the proposed antenna is a suitable for 5G mobile communication.

Table 2: Summary of Results

Antenna parameter	S11 parameter	VSWR	Realized Gain	bandwidth
Specification Detail	60 GHz at -41.65 dB	1.8	8.82 dB	30 GHz

IV. CONCLUSION

In this paper, a rectangular micro strip patch antenna has been proposed for 5G wireless communication. The antenna resonates at 60 GHz with a return loss of -41.65 dB. The achieved gain of the antenna is 8.84 dB and the radiation pattern is omnidirectional. The integration of the antenna can be done in devices where space is a major concern and can be used in future 5G wireless devices.

REFERENCE

[1] S. L. S. Yang, A. A. Kishk, K. F. Lee, "*Frequency reconfigurable U-slot microstrip patch antenna", IEEE Antennas and Wireless Propagation Letters,* vol. 7, pp. 127–129,2008.[Online].Available: http://dx.doi.org/10.1109/LAWP.2008.921330

[2] D. Sanchez-Hernandez, I. Robertson, "*60 GHz-band active microstrip patch antenna for future mobile systems applications*", *Electronics Letters,*vol. 30, no. 9, pp. 677–678, 1994. [Online]. Available: http://dx.doi.org/10.1049/el:19940488

[3] A. Adane, F. Gallée, C. Person, "*Bandwidth improvements of 60GHz micromachining patch antenna using gap coupled U-microstrip feeder*", in *Proc. 4th European Conf. Antennas and Propagation (EuCAP)*, 2010, pp. 1–5.

[4] Y. Coulibaly, M. Nedil, L. Talbi, T. A. Denidni, "*Design of high gain and broadband antennas at 60 GHz for underground communications systems*", *Int. J. Antennas and Propagation*, pp. 1–7, 2012. [Online]. Available: http://dx.doi.org/10.1155/2012/386846

[5] R. Garg, P. Bhartia, I. Bahl, and A. Ittipiboon, *Microstrip Antenna Design Handbook*, Artech House, 2000

[6] Z. Nasimuddin, N. Chen, "*Multipatchs multilayered UWB microstrip antennas*", *IET Microwaves, Antennas & Propagation*, vol. 3, no. 3, pp. 379–386, 2009. [Online]. Available: http://dx.doi.org/ 10.1049/iet-map.2008.0181

[7] A.Z Adane, F. Gallée, C. Person, "*Bandwidth improvements of 60GHz micromachining patch antenna using gap coupled U-microstrip feeder*", in *Proc. 4th European Conf. Antennas and Propagation (EuCAP)*, 2010, pp. 1–5

[8] D. Liu, J. Akkermans, B. Floyd, "*A superstrate patch antenna for 60 GHz applications*", in *Proc. 3rd European Conf. Antennas and Propagation (EuCAP)*, 2009, pp. 2592–2594

[9] Jyoti Saini, S. K. Agarwal "*Design a Single Band Microstrip Patch Antenna at 60 GHz Millimeter Wave for 5G Application*",International Conference on Computer, Communications and Electronics (Comptelix),July 2017

[10] Iskandar Fitri, Al Amin Akbar T "*A New Gridded Parasitic Patch Stacked Microstrip Antenna for Enhanced Wide Bandwidth in 60GHz Band*", IEEE Transaction on Antennas and Propagation, 2017.

[11] Y. Coulibaly, M. Nedil, L. Talbi, T. A. Denidni, *"Design of high gain and broadband antennas at 60 GHz for underground communications systems*", *Int. J. Antennas and Propagation*, pp. 1–7, 2012. [Online]. Available: http://dx.doi.org/10.1155/2012/386846

Comparative Analysis of GSM Networks Communication Congestion in Zaria

Dr. A.D. Usman Dr. A.M.S. Tekanyi, Engr. A.A. Sadiq
Department of Communications Engineering,
Faculty of Engineering
Ahmadu Bello University Zaria, - Nigeria.
adusman@abu.edu.ng, amtekanyi@abu.edu.ng,aasadiq@abu.edu.ng

ABSTRACT-The study of congestion on GSM networks in Nigeria is necessary as congestion remains a major challenge to telecommunications services provision both to service providers and subscribers. The subscribers are compelled to quit the service provider who fails to meet up with the services required by them. This occurs at a time when the wide spread use of mobile communication has heightened consumers' demand for quality of service anytime, anywhere. Today, network operators face challenges of improving the quality of services. Operators are fast realizing that they are in a highly competitive environment, where subscribers can easily quit them. Dissatisfaction by subscribers gives rise to a high rate of subscriber churn (a situation of stopping doing business with the company or service) and low revenue for the operator. Congestion is a problem all GSM service providers are facing and trying to resolve. Drive test was conducted using Transmission Evaluation and Monitoring System (TEMS) software and congestion was analyzed to check the performance of Etisalat, and MTN Networks in Zaria and methods for its improvement were suggested.
Keywords- QoS, KPIs, ITU, Cellular Network and Congestion

I. INTRODUCTION

A cellular telephone is designed to give the user maximum freedom of movement. As a result of this freedom, the number of mobile users keep growing at an alarming rate. The role of cellular phones has risen with the improvement in services, reduction in service cost, and the ever increasing range of services available through cell phones and as a result, subscribers possess multiple lines on the same or various networks, all of which have contributed to the challenge of congestion (Kuboye etal, 2010).The cellular system began in the United States of America with the release of the Advanced Mobile Phone Service (AMPS) system in the year 1983, Asia, Latin America, and Oceanic countries adopted the AMPS standard
creating the largest potential market in the world for cellular service (Mehrotra, 2015).

GSM was introduced to solve the problem of capacity, high-level of interference, high power consumption, signaling issues, inefficient use of radio spectrum and so on, which were faced in the analogue mobile system. The technology was embraced by everybody considering the advantages a GSM has, such as increase in the number of simultaneous user and clarity of voice communication, in addition to those problems of AMPS it resolved. GSM revolution in Nigeria started in August 2001, and this brought a great change in the ICT. The Nigerian telecommunications industry is rapidly growing, and many operators and their operations put forth different services, but in the diverse services provided, most of the subscribers do not receive satisfaction due to the poor nature of services available on these networks. With the rapid growth of the wireless industry, GSM networks are rolling out and expanding at a high rate. The industry is also becoming intensely competitive. In this environment, high quality service is a competitive advantage for service providers. A lot of effort is made by a network operator to monitor the network and maintain current, comprehensive and accurate status of its quality. This status together with new traffic demand data is used by the operators to improve the Quality of Service (QoS) of their networks and adjust their Operations QoS of mobile cellular networks which was defined by ITU-T Rec E. 800 as "the collective effect of service performance that determine the degree of satisfaction of a user of the service" has many performance attributes or metrics which have continue to give telecommunications experts and operators lot of keen consideration for continual optimality. In GSM, parameters used include network accessibility, retain-ability, mobility, and service integrity. According to ITU standard, all these are affected by system configuration or/and dimensioning. Since the QoS is very important, then researching into factors affecting this QoS is equally very important. This research work focuses on carrying out investigation on the parameters that determine the QoS in GSM technologies for the mutual benefits of both subscribers and network operators.

II. RELATEDWORKS

Popoola *et al.*, (2012) evaluated the network performance and QoS of GSM cellular system in Nigeria using Key Performance Indicators (KPIs). The result of the study showed that the QoS of GSM system in the country was unreliable, poor, and unsatisfactory. The limitation in their work was the fact that the assessment and the performance evaluation were carried out by using structured questionnaire which could not be appropriate for standard QoS measurement analysis.

Shoewu *et al*., (2011) presented a report on the QoS of network optimization and evaluation of KPIs provided by GSM operators considering the ability to establish and maintain call connections, call retention, handover, inter and intra network call setup. The work consequently developed a model of service quality and a set of dimensions for comparative evaluation which were opined to direct regulators and service providers. The major problem of this work was that, the ability to establish and maintain call connections, call retention, handover, inter and intra network call setup could not be used for the comparison of the QoS Performance of various GSM Operators.

Louge, (2011) used subscribers' perception of the quality of service of GSM services in Nigeria to determine the network performance through a questionnaire titled "user perception of

the QoS of GSM Service providers in Ibadan, Nigeria to gather responses from users. The responses were presented using descriptive statistics and data collated using inferential statistics. Finding from the questionnaire showed that a significant number of respondents were not satisfied with the QoS provided by the operators. They experienced epileptic services, call drops, low voice call quality, poor interconnectivity, and poor reception on the network. The major problem of this work was that the work seemed like work that was carried out based on sample opinion. Just using questionnaire to take statistics by sample opinion could not establish or justify assessment or performance evaluation of QoS.

Agago *et al*., (2012) optimized GSM network performance with respect to efficiency by developing a pilot study. Simulations were carried out to assess various parameters and recommendations were made on how to improve the efficiency of the wireless communication network. The limitation of this work was the fact that the work was based on optimizing the efficiency of wireless communication network which could not be used to determine or compare the QoS of GSM Network.

Ndife *et al.*, (2013) carried out an evaluation and optimization of QoS of mobile cellular networks in Nigeria using drive test but without considering the KPIs. With this, a holistic network optimization model using an Adaptive Network-based Tuzzu Inference System (ANFIS) algorithm was developed. The limitation of this work was that drive test could not give a standard performance measurement of QoS Analysis in a GSM network.

Innocent(2015) uses ANFIS and ANN features to evaluate the performance of GSM network Call Set-up Success Rate(CSSR) of MTN Kano region. Innocent's paper focused only on corporate analysis of the measured (CSSR) to that of estimated using (ANFISS) and (ANN) model.

Marshal, (2015) carried out the assessment ofQoS over GSM network using KPIs, in his work Marshal,2015 selected Etisalat Nigeria in Kano and Katsina as a case study, only that the study covers virtually the areas mentioned and the results may not be specific.

Having observed the limitations of the above literatures reviewed, this research came up with a better method in accordance with the standard for Congestion Comparative Analysis and measurement of the QoS in GSM Cellular network. The work considered the major KPIs such as TCH and SDCCH that were used in Congestion Comparative Analysis in GSM Cellular Network. The data used in this research were obtained directly from network operators through drive testnot through opinion sampling. The data were directly from BSC and BTSs of Etisalat, and MTN in Zaria. The research also described the causes and impacts of TCH and SDCCH congestion rate and provided measures to reduce the congestion rate and optimize the KPIs. The research also provided the models for allocation of calls within GSM network based on the network capacity and traffic, distribution procedure and optimization method and algorithm for implementing the models to manage congestion of calls in GSM network. All these are what the operator needs to use to improve service level of a GSM Communication Network.

III. Methodology/Materials

The methodology adopted in carrying out this research included the following;

Collection of data(by means of drive test) from BSC and BTSs of Etisalat and MTN-Zaria from 1st January to 30th June,2017

Generating the data collected to a MapInfo-format for the purpose of plotting drive test information, view a cellular network with sites and cells and for analysing key performance indicators(KPIs) of the system.

Analysis and Extraction of relevant parameters from the data collected for comparing the performance of the two networks.

Transmission Evaluation and Monitoring System (TEMS) investigation software was used to analyse the data to achieve the improved voice quality, increased accessibility, more successful call attempts and better service performance.

Materials

The drive test equipments required in performing cluster test and data collection are;

- Laptop as a user interface that displays all information during RF drive testing. It is the user interface where drive test software such as Transmission, Evaluation and Monitoring System (TEMS), MapInfo and MS-excel are installed and hardware such as scanner, external GPS and mobile phone are connected
- Dongle as a small modem that enables a user to connect to the Internet using mobile phone.
- TEM software from ASCOM as the backbone of RF drive testing optimization tool. It is used to obtain all RF parameters for data collection and data analysis.
- Laptop as a user interface that displays all information during RF drive testing. It is the user interface where drive test software such as Transmission, Evaluation and Monitoring System (TEMS), MapInfo and MS-excel are installed and hardware such as scanner, external GPS and mobile phone are connected
- Dongle as a small modem that enables a user to connect to the Internet using mobile phone.
- TEM software from ASCOM as the backbone of RF drive testing optimization tool. It is used to obtain all RF parameters for data collection and data analysis.
- External GPS (Global Positioning System) as a device connected externally to Laptop collecting the data of latitude and longitude of each point/measurement data, time, speed, etc.
- MS-Sony Ericsson TEMS phone used for collecting data such as signal strength, best service, etc. It is also used for making short call and long call during RF drive testing for drop call rate optimization evaluation.
- Scanner that is used in collecting data through the network because mobile radio is limited and does not handle all the necessary data for complete RF analysis.

Figure 1. Laptop

Methods of Data Collection

The data were obtained from Etisalat and MTN Nigeria, Zaria Metro-police, comprising TCH, SDCCH, CSSR, CCR, CDR, CST, and TCHASR for the period of 6 months (from 1st January to 31st June 2017). Test routes were planned to include all the roads(around PZ) which are covered by different sectors of the sites under study. Also, the main streets around the BTSs, BSC were included. The test routes reached the overlapping areas of surrounding neighbour cells. This ensured the proper verification of the actual coverage area of the sites and the handover functions.

Drive Test

Drive test is the process of data collection from the GSM network so as to check the network performance by means of coverage evaluation, system availability, network capacity, network retain-ability and call quality. This is accomplished by checking the status of KPIs like receive level, receive quality, Speech quality and so on, in order to make appropriate recommendations where necessary for effective optimization. The drive test was carried out in a dedicated manner to identify the eventual black spots(radio coverage, holes) present within Zaria Metropolis. The logs recorded during the test were analysed and recommendations were made to improve the QoS in the City. The drive test investigated what the mobile users experienced on the radio network in the area. This was done by collecting data related to the radio network itself, services running on the network, radio frequency scanner information, and geographical positioning data to enable mobile station location logging.

Benchmarking drive test involves comparing the network performance in terms of network accessibility, retain-ability, mobility, data throughput and service integrity. This enables the network operator to know its rank among other competitors and where necessary improvement action needed. After drive test data collection using TEMS software, the data were analysed to check the event summary such as call attempts, call completion, drop calls, and blocked calls. Also, graphical representation of the data was drawn to be able to understand how the network plots of 2G and 3G signal levels, 2G and 3G signal quality, and other events summary that were represented graphically.

TEMS Investigation Interface

TEMS investigation is the industry-leading solution for troubleshooting, verification, optimization, and maintenance of wireless networks. TEMS investigation has powerful, versatile features that are essential throughout the network's lifecycle. Using TEMS investigation, operators can achieve improved voice quality, increased accessibility, more successful call attempts, and better service performance. Support for GSM, GPRS, EDGE, WCDMA, HSPA, and GAN (UMA), CDMA (IS-95 to EV-DO Rev A),and now the addition of WiMAX technology functionality, further demonstrates that TEMS investigation is the ideal choice for network operators. TEMS investigation also offers true multi-vendor support in addition to its multi-technology infrastructure support. It supports handsets from all major vendors across multiple technologies. Its measurement and reporting functions have general features that can be applied to any event or radio parameter that is measured. These features include a real-time map display and a report generator, allowing quick verification of the cell coverage. The map functionality in TEMS investigation provides basic statistics and the distribution of an arbitrary area selection plotted on the map. The route analysis module allows the user to work with multiple log files when post-processing the data by performing tasks such as statistical binning and benchmarking. TEMS investigation offers operators one tool with the ability to collect, analyse, and post-process the network data used on a daily basis for network monitoring, troubleshooting, and optimization. This complete solution eliminates the need for multiple tools, reducing costs and saving time, and effort for operations staff. In addition, TEMS investigation gives operators a way to utilize all the benefits of network data while at the same time protecting its integrity. TEMS Investigation collects data beyond the abilities of other tools on the market. In addition to all standard parameters, it employs specialized developed algorithms to collect unique information not available in other vendors' tools. For example, the Sony Ericsson Z750 (Triband HSDPA/WCDMA, Quadband GSM/EDGE) now offers powerful WCDMA scanning capabilities. This model is a cost-effective, conveniently slim tool for solution for the agile field engineer. TEMS investigation gives efficient work processes that allow operators to focus on network quality.

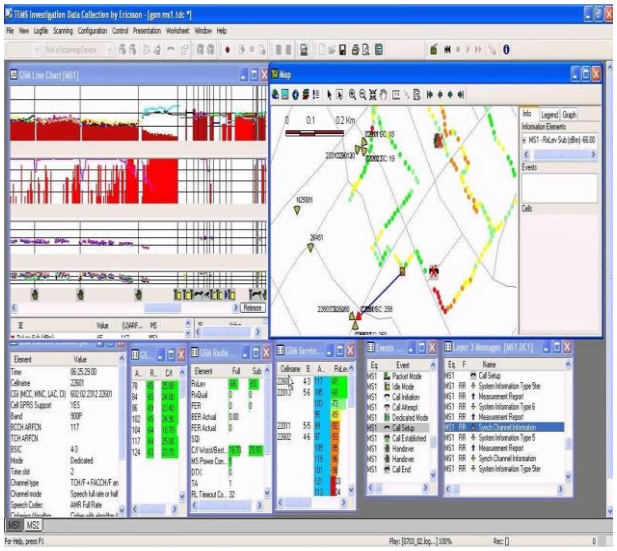

Figure 2 TEMS Investigation Interface

TEMS Discovery

TEMS discovery is the wireless industry's most holistic network analytical and optimization platform, providing mobile operators and their service providers with unparalleled insight into network performance as it is perceived by subscribers at the device, the application and the network level. This holistic approach is unique to TEMS Discovery, empowering operators to lock-in premium subscribers by validating that customers receive the service levels they demand, around-the-clock, from any location, and across voice, data and integrated media services. TEMS Discovery automatically analyses drive-test, User Equipment (UE), network OSS, crowdsourced, and application data, providing actionable intelligence via a Web-based management dashboard. TEMS Discovery enterprise offers a variety of analytical packages for customer experience, VoLTE, indoor, capacity (traffic hotspots and small cell); SON; handset analysis; subscriber KPIs, and benchmarking. TEMS Discovery is available in its flagship enterprise edition, as well as desktop editions that enables engineers to drill down into UE (collected from TEMS and third-party tool vendors) and OSS data (collected from Ericsson, Nokia Siemens Networks and Huawei).

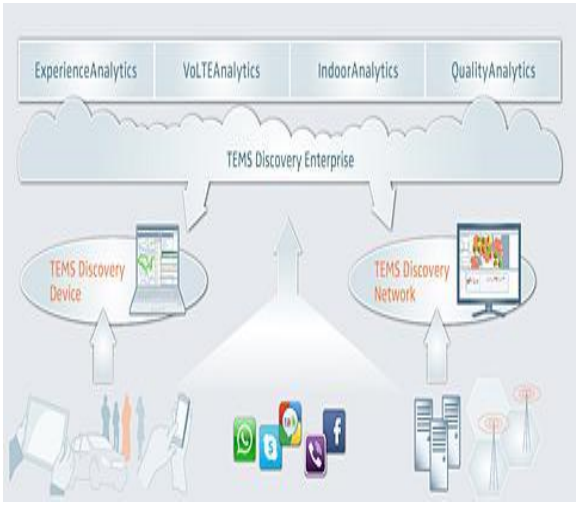

Figure 3 TEMS Discovery

Drive Test Route

Quality routes are pre-defined pathways and that must be performed periodically, usually 2 to 2 months. These routes should cover the relevant areas of the network, such as large customers and companies, bridges and major Avenues, etc. long ago. These routes were marked in printed maps and delivered to the staff responsible for performing the Drive Test. Currently, it is more common the creation and use of these routes in vector files, lines drawn on GIS programs such as Map-info and Google Earth.

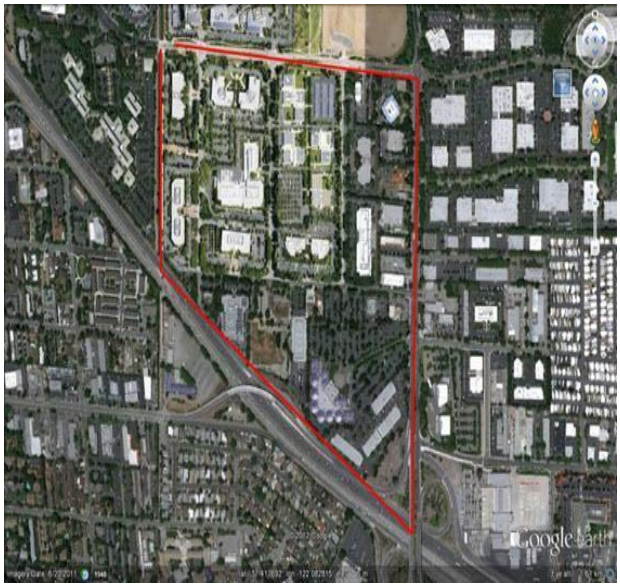

Figure 4 Drive Test Route

Figure 5 Zaria Test Route

IV. Results and Discussion

From the data obtained in the site, the Tables 1 and 2 show the call events statistics results which compare the performance of the two networks.

Table 1 Summary of 2G Call Events Statistics Overall Voice

Event details	Etisalat	MTN
Call attempt	153	334
Call attempt retry	02	31
Call initiation	152	335
Call end	152	321
Call established	150	321
Call setup	150	1
Blocked call	0	1
Dropped call	1	3
Handover	559	526
Handover failure	0	13
Location area update	42	49

Table 2 Summary of 3G Call Events Statistics Overall Voice

Event detail	Etisalat	MTN
Call attempt	170	356
Call attempt retry	2	34
Call initiation	170	361
Call end	169	323
Call established	168	332
Call setup	169	332
Blocked call	0	21
Drop call	0	9
Handover	83	396
Handover failure	0	10
Location area update	42	112

Speech Quality Index

Speech Quality Index (SQI) is a quality of speech of a network. It is designed to cover all factors that Received Signal Quality (RxQual) lack to measure. SQI computation considers the Bit Error Rate (BER), the Frame Erasure Rate (FER) and data on handover events. The Figures4.1 and 4.2 show the speech quality index for Etisalat and MTN network operators from data collected.

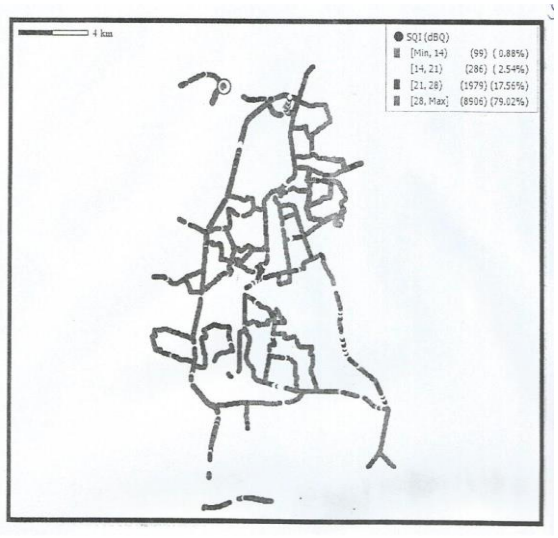

Figure 6 Etisalat 2G SQI Drive

Figure 6 shows the speech quality index of Etisalat 2G network the best SQI is 28 and above whose measurement counts of 8906 points and it also has the highest proportion of counts. Below 14 represent or bad SQI and it has the smallest measurement point of 99. This indicates that the SQI of this network is strong and better than MTN.

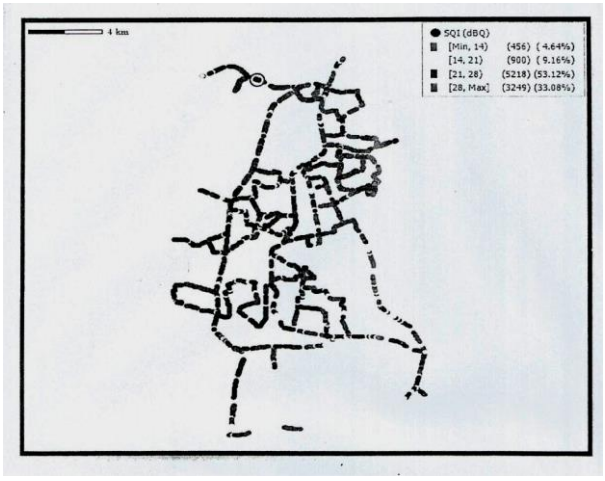

Figure 7 MNT 2G SQI Drive

Figure 7 shows the SQI of MTN 2G network. The best SQI is 28 and above whose measurement counts of 3249 point while the SQI with the highest proportion of counts falls within 21-28 with a point of 5218. Below 14 represent a bad SQI and it has the smallest measurement point of 456. This indicates that the SQI of this network is strong but not as strong as Etisalat.

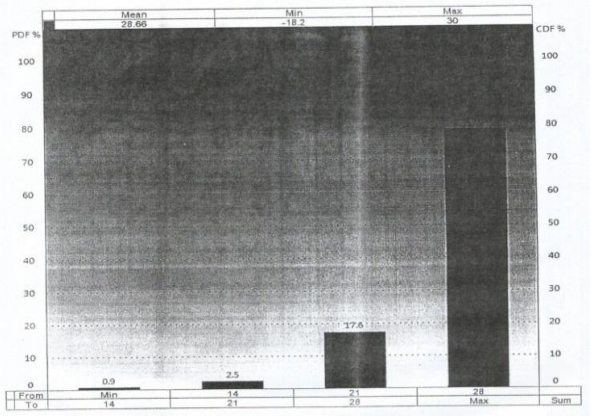

Figure 8 Etisalat 2G SQI Histogram Plot

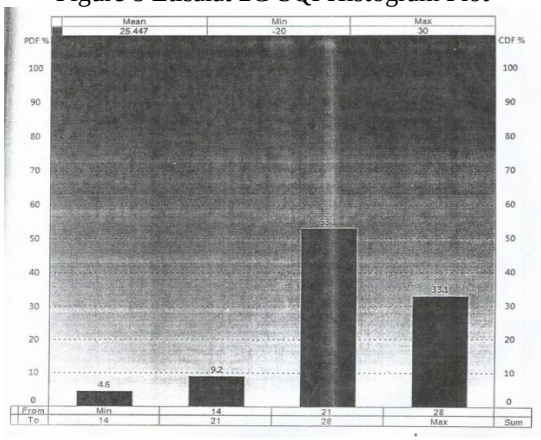

Figure 9: MTN 2G SQI Plot

Figures 8 and 9 show SQI histogram plots for Etisalat and MTN networks, respectively. From the histogram it is observed that the SQI for Etisalat network is the best because it has higher percentage of maximum SQI. The congestion rate of MTN network is higher than that of the Etisalat network.

Signal Quality

For 2G network, it is denoted as received signal quality (Rx Qual) and for 3G energy per chip per noise density (Ec/Lo). It is the measure of signal quality and the unit is dBm. The Figure 10 shows the signal quality for Etisalat and MTN network operators from the data collected.

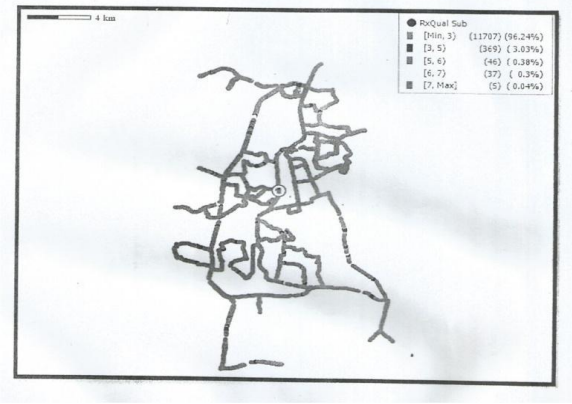

Figure 10 Etisalat 2G RxQual Drive Test

Figure 10 shows the received signal quality level Etisalat 2G network, measured base on BER. The value is between 0 and 7, the lower it is the better. The received signal quality of a larger proportion of the measurement point (11707) falls within the range of 0-3. Also the best received signal quality level of the lowest received signal quality falls into 7 and has the measurement points 5.

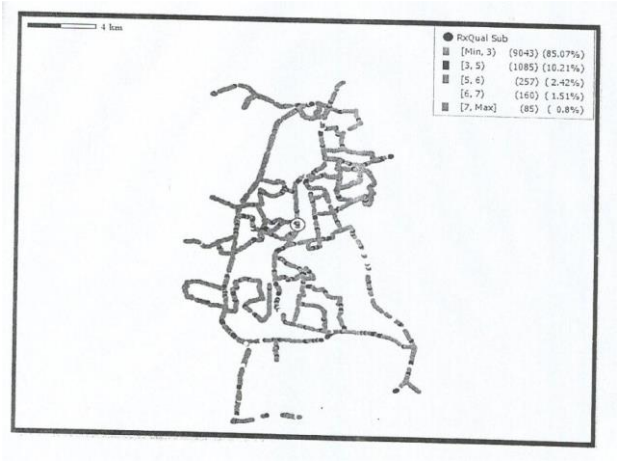

Figure 11 MNT 2G Rx Qual Drive

Figure 11 shows the received signal quality level for MTN 2G network, measured based on BER. The value is between 0 and 7. The RxQual of a larger proportion of the measurement point (9043) falls within the range of 0-3. Also the best received signal quality level and the lowest received signal quality falls into 7 and has the measurement point 85.

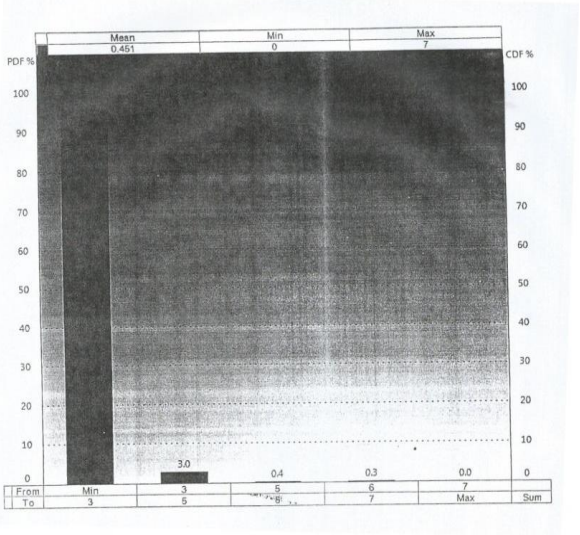

Figure 12 Etisalat2GRxQualPlot

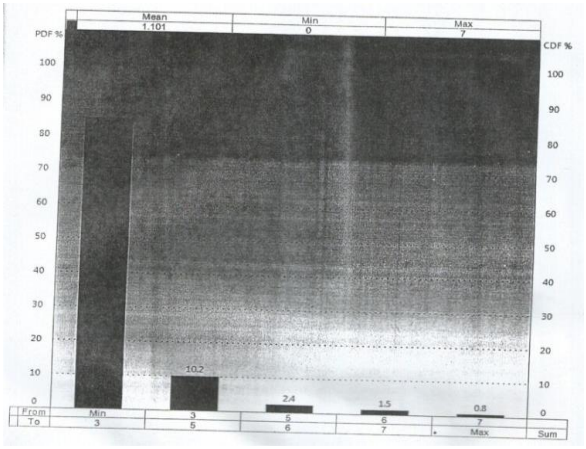

Figure 13 MTN "2G RxQual Plot

Figure 12 and 13 show RxQual histogram plots of Etisalat and MTN 2G networks, respectively. The plots show how the comparison of RxQual between Etsialat and MTN networks. It is observed that the RxQual of Etisalat is the better because it has highest percentage of minimum BER. Thus, it implies that Etisalat subscribers experience better received signal quality and low congestion compared to MTN subscribers in the area.

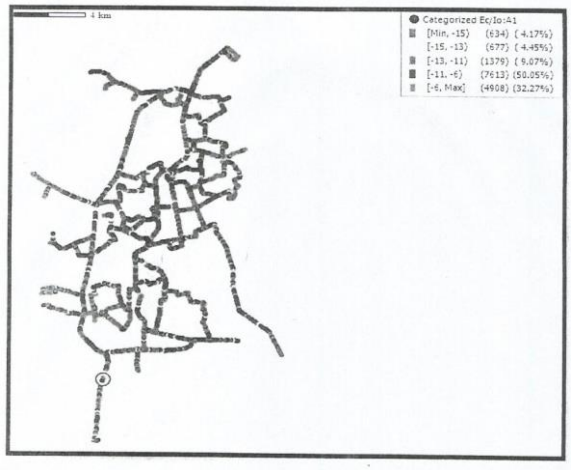

Figure 14 Etisalat 3G Ec/Lo Drive

Figure 14 show the received signal quality level Etisalat 3G network Ec/Lo, measured base on BER. The value is between -15 and - 6, the it is higher the better. The received signal quality of a larger proportion of the measurement point (7613) falls within the range of -11 to –6, and it is a good received signal quality level of the lowest received signal quality that falls into-15 and has the measurement point of 634.

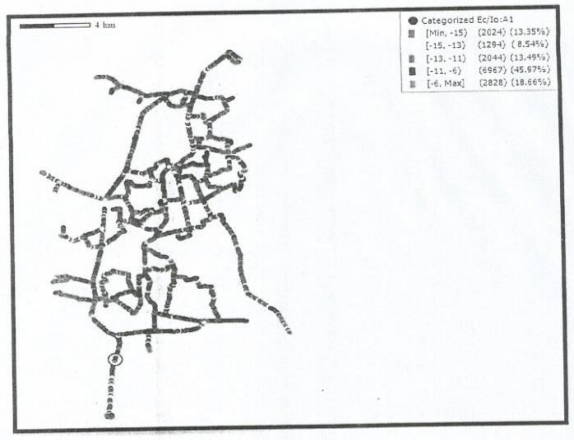

Figure 15 MNT 3G Ec/Lo Drive

Figure 15 shows the received signal quality level for MTN 3G network Ec/Lo, measured base on BER. The value is between -15 and -6. The received signal quality of a larger proportion of the measurement point of 6967 falls within the range of -11 to -6 and it is a good received signal quality level and the lowest received signal quality that falls within the range of -15 to -13 and has the measurement point of 1294.

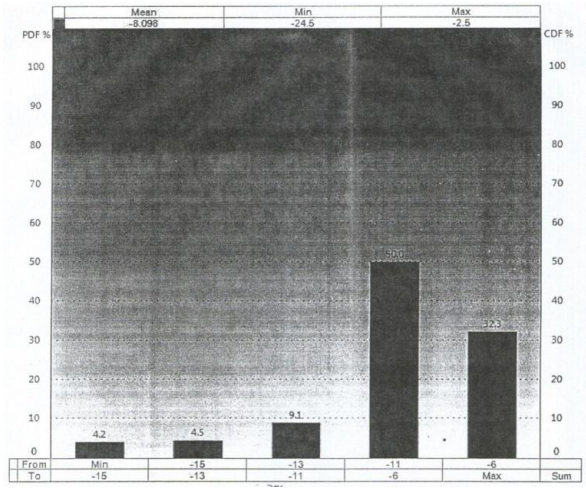

Figure 16 Etisalat 3G Ec/Lo Plot

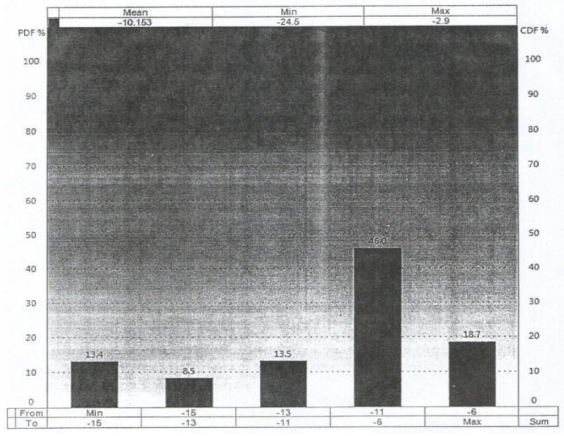

Figure 17 MTN 3G Ec/Lo Plot

Figure 16and 17 show energy per chip per noise density Ec/Lo histogram plots of Etisalat and MTN networks, respectively.

It can be observed that the Ec/Lo for Etisalat network is better than MTN network because it has higher percentage of best Ec/Lo level. Thus the network quality of Etisalat is better than MTN network.

Network Coverage

This determines the area that a network can cover. For 2G networks it is termed as Received Signal Level (Rx Level) and for 3G networks it is termed as Received Signal Code Power (RSCP). This is the signal power level (signal strength).The pilot channel of a cell is received and usually expressed in dBm. With this parameter different cell using the same career can be compared and handover or cell reselection decision can be taken. Figures 16 and 17show the network strength for Etisalat and MTN network operators from data collected.

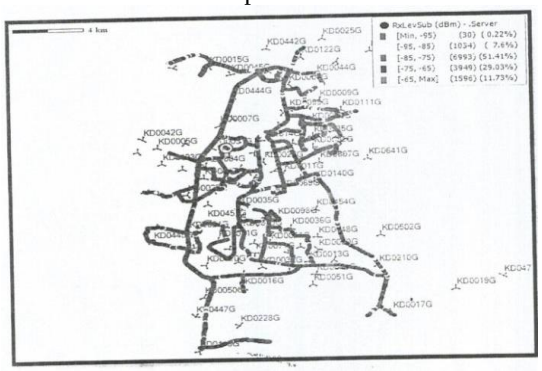

Figure 18 Etisalat 2G Rx Level Drive

Figure 18 shows the coverage plot of the received signal level obtainable on the networks at different mobile user locations for Etisalat 2G network. The analysis of this result revealed that approximately 13,600 measurement points were collected during the drive test. The received signal strength of a larger proportion of the measurement points (6993 points) fell within the range of -85 to -75 dBm. Higher signal values of -65 to 0 dBm were received at 1596 measurement points. The lowest received signal level range of below – 95dBm was experienced at 30 measurement points within the coverage area.

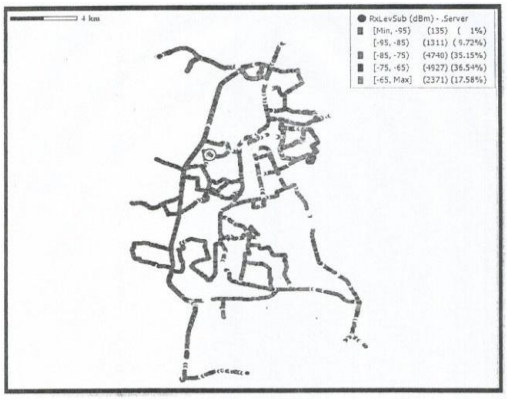

Figure 19 MTN 2G Rx Level Drive

Figure 19 shows the coverage plot of the received signal level obtainable on the networks at different mobile user locations for MTN 2G network. The analysis of this result revealed that approximately 13, 480 measurement points were collected during the drive test. The received signal strength of a larger proportion of the measurement points of 4927 points fall within the range of -75 to -65 dBm. Higher signal level values of -65 to 0 dBm were received at 2371 measurement points. The lowest received signal level range of below -95dBm was experienced at 135 measurement point within the coverage area.

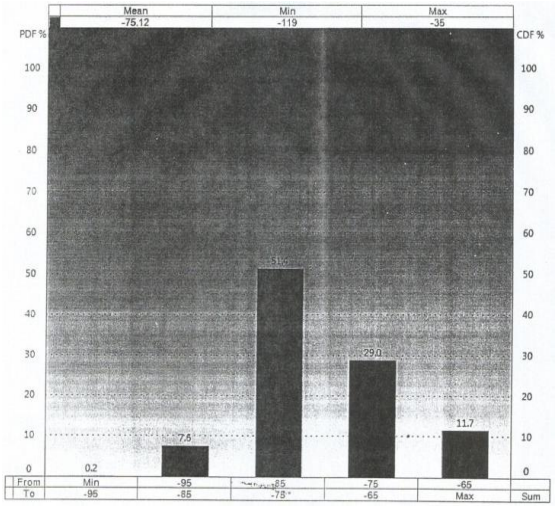

Figure 20 Etisalat 2G Rx Level Plot

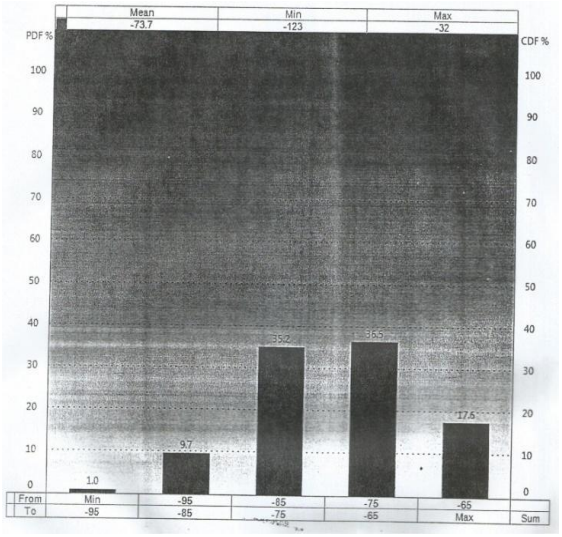

Figure 21 MTN 2G Rx Level Plot

Figure 20 and 21 show Rx Level histogram plots of Etisalat and MTN networks, respectively. From the plots it was deduced that the Rx Level of MTN network is better than Etisalat because it has higher percentage of best Rx Level.

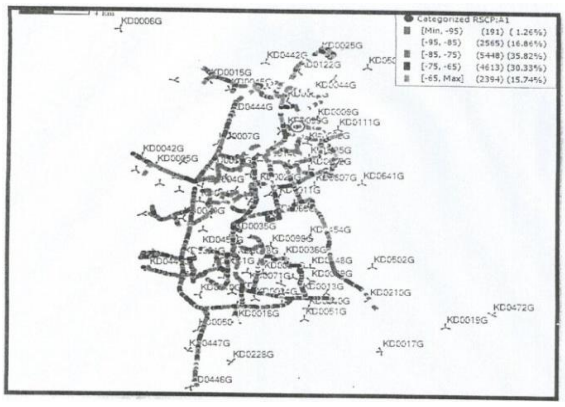

Figure 22 Etisalat 3G RSCP Drive

Figure 22 shows the coverage plot of the received signal level obtainable on the networks at different mobile user locations for Etisalat 3G network RSCP. The analysis of this result revealed that approximately 15,200 measurement points were collected during the drive test. The received signal strength of a larger proportion of the measurement points of 5448 fall within the range of -85 to -75 dBm. Higher signal level value of -65 to 0 dBm were received at 2394 measurement points. The lowest received signal level range of below -95dBm was experienced at 191 measurement points within the coverage area.

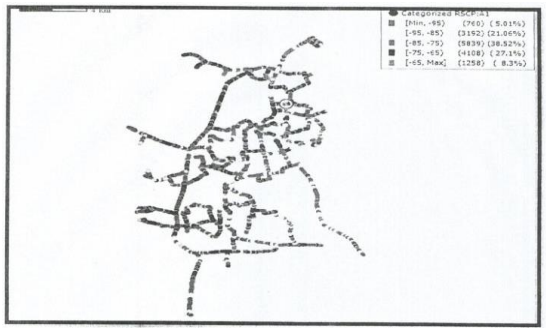

Figure 23 MTN 3G RSCP Drive

Figure 23 shows the coverage plot of the received signal level obtainable on the networks at different mobile user locations for MTN 3G network RSCP. The analysis of this result revealed that approximately 15,100 measurement points were collected during the drive test. The received signal strength of a larger proportion of the measurement points of 5839 fall within the range of -85 to -75 dBm. Higher signal level values of 65 to 0 dBm were received at 1258 measurement points. The lowest received signal level range of below -95 dBm was experienced at 760 measurement points within the coverage area.

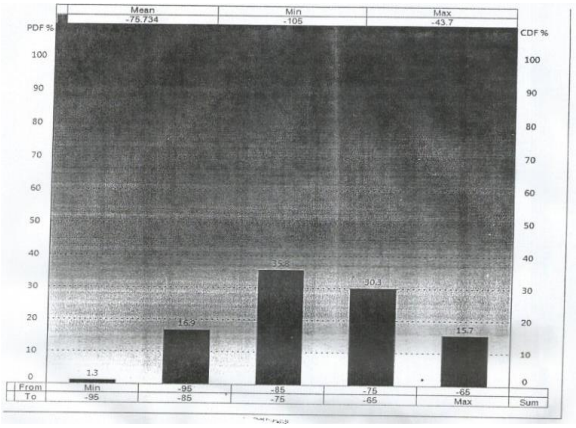

Figure 24:Etisalat3GRSCPPlot

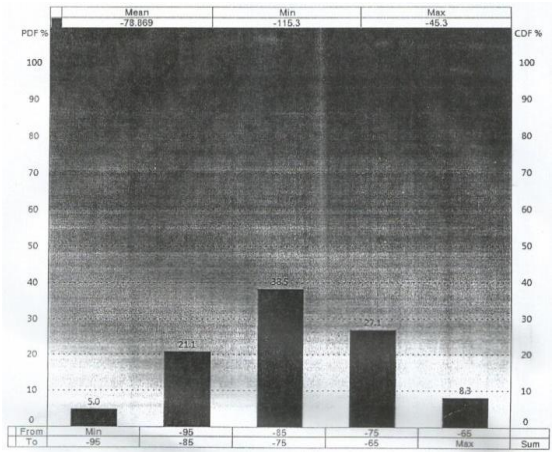

Figure 25 MTN 3G RSCP Plot

Figure 24 and 25 show received signal code power histogram plots of Etisalat and MTN networks respectively. It is observed, from the plots that RSCP for Etisalat network is better than MTN network because it has the high percentage of best RSCP and this has significant effect on the network performance in general.

Discussion

From the results analysed, the received signal code power and energy per chip per noise density for 3G Etisalat network is better than that 3G MTN network. Also, signal quality index received signal level and received signal quality for 2G ETISALAT network is better than that of 2G MTN network. In general, the ETISALAT network performance is the better in the area where the drive test was conducted which implied that subscribers on ETISALAT network experienced low congestion.

V. Conclusions

With technological advancement in this age, 2G and 3G planning has been a very interesting task due to availability of updated digital terrain data. 0Subscribers' growth has posed a great demand for network rollout and expansion, software and hardware upgrade basically towards coverage and capacity expansion. In order to achieve the best performance, service providers have to monitor and optimize their network continuously. Therefore, good optimization models will go a

long way in helping the GSM operators to deliver good and qualitative service to the subscribers.

KPI monitoring schedule should be done in such a timely manner of routine checks on networks, network audit, performance test, cluster acceptance test, and analysis to ensure compliance with NCC regulations.

References;

[1] Alexander N. Ndife et al (2013). "Evaluating and optimization of QoS of mobile cellular networks in Nigeria", *International Journal of Information and Communication Technology Research*, 2(9).

[2] Harte, L., Levine, R., and Livingston, G. (2009). "GSM super phones
McGraw-Hill 71:45-47

[3] Idigo, V.E. Azubogu, A.C.O., Ohaneme, C.O. and Akpado, K.A. (2012). "Real-Time Assessments of QoS of Mobile cellular network in Nigeria", *International Journal of Engineering Inventions*, 1(6), pp. 64-68.

[4] ITU-T E. 800, "Definition of terms related to QoS", ITU recommendations E. 800 09/2008.

[5] Jahangir Khan, (2010). "Handover Management in GSM cellular system", in international journal of computer applications, 8(12), pp 14-24.

[6] Kuboye, B.M., Alese, B.K., & Fajuyigbe, O. (2010). "Congestion analysis on the Nigerian global system for mobile communication (GSM) Network", *The Pacific Journal of Science and Technology*, 10(1).

[7] Longe, F.A. (2011). "Subscribers' perception of the quality of service (QoS) of the global system for mobile services in Ibadan, Nigeria". *Computing, Information System & Development Informatics Journal*2(2).

[8] Shoewu, O. and Edeko, F.O. (2011). "Outgoing call Quality Evaluation of GSM Network Services in Epe, Lagos State". American Journal of Scientific and Industrial Research, AJSIR, 2(3), pp. 409-417.

[9] Syski, R. (2016). "Introduction to congestion theory in telephone system" Elserier Science Publishers B.V.

[10] Ugwoke F.N., et al., (2014). "Using software engineering approach in mitigating QoS challenges in mobile communication networks in Nigeria". *Computing, Information Systems, Development Information and Allied Research Journal*, 5(1).

Improved Automatic Eggs' Turner Device for Effective Incubation

P. Samuel
Department of Agric Engineering Technology, Ramat Polytechnic Maiduguri
Peter3ng2001@yahoo.com

A. Dahiru
Department of Agricultural and Bio-Environmental Engineering Technology. College of Agriculture Jalingo, Taraba

S. G. Zubairu
Institute of Computing & ICT, Ahmadu Bello University, Zaria. Nigeria
sgzubairu@abu.edu.ng

Y. M. Abdullahi
Electrical Engineering Department, Umaru Ali Shinkafi Polytechnic, Sokoto

M. J. Musa
Communications Engineering Department, Ahmadu Bello University, Zaria. Nigeria
mjmusa@abu.edu.ng

ABSTRACT—*In natural means of incubation, the mother hen occasionally used her beak to turn her eggs twice to four times per day to avoid the embryo from sticking to the egg shell. In semi-artificial incubation, the eggs turning was done using hand to laterally keep the eggs horizontally four to six times per day. The natural way by the mother hen yield good result but is by far less than the number of chicks required worldwide. While the semi-artificial of eggs turning process using hands provided large number of chicks but transmitted diseases due to the direct contact to the eggs, is labor intensive and always leakage out the trapped head of incubation in the process of turning the eggs. This paper proposed an automatic eggs' turning device using a timing integrated circuit configured in an astable multi vibration mode of high time 1.8 ks, low time 1.5 ks and a duty circle of 50%. In every high time pin 3 of the timing circuit goes high and activated the relay which in turn switched a bi-directional DC motor that tilted the eggs at an angle of 45^0 in the clock wise direction and deactivated the relay which will resulted to the tilting of the egg trays in the anti-clock wise direction. Incubation efficiency was compared with the conventional incubator using hand turning and that with the proposed device, it resulted to hatchability of about 87% was achieved. The turning control was cost effective with the cost of only three thousand naira, in which the cost of production will drastically fall in mass production.*

KEYWORDS: bi-directional, egg, hatching, turning.

I. INTRODUCTION

Egg turning is usually done by the mother hen to enable the spray of even required temperature to the egg for development. The mother hen used its beak to turn the egg at some interval while laying on them [1]. The turning by the mother hen is efficient for embryo development and to avoid the sticking of the embryo to the egg's shell. The challenge of the conventional (mother hen) method is due to the production of small number of chicks, which are not enough to the demand. This challenge lead to the actualization of the artificial incubator, which produces large number of chicks at a time. Researchers proved that egg turning is crucial for a successful hatching apart from temperature and humidity control. The problem of egg turning in an artificial incubator is always a challenging control problem and hence this paper proposed a method for egg turning. The proposed techniques will turn all the eggs within an angle of 45^0 bi directional, this is to enable maintain the embryo at the center of the egg to prevent it from sticking [2].

Section II of this paper describes the design of the circuitry for the turning mechanism and the timing unit were mathematical analysis will be conducted. Section III provide the design and analysis of the eggs'–turner delay circuit, Testing results are shown in section II. Section V concludes on the presented results.

II. DESIGN AND ANALYSIS OF EGG TURNER MANIPULATOR

The egg turner manipulator shown in Figure I is a designaimed at frequent changing the polarity of the supply terminals of the bi-directional DC motor, which in turn tilts the eggs trays to an angle of 45^o [2]. The tilt angle will prevent the egg's embryo against sticking to the warm shell during incubation.

This was achieved by connecting the terminals namely 'A' and 'B' with the astable multivabrator relay's RL_A control terminals of Figure II. When RL_A is energized the terminals A and B will be connected and the energized RL_C and RL_D simultaneously. Now, the normal open of the relays (RL_C and RL_D) will both be closed, results in feeding the terminals 'a' and 'b' of the bidirectional DC motor with negative and positive supply from the standby battery respectively. This results in tilting the eggs' turner anticlockwise.

When RL_A is de-energized, terminals A and B will be open and will result to de-energize of RL_C and RL_D simultaneously. Now, the normal close of the relays (RL_C and RL_D) will both be closed, resulting in feeding the terminals 'a' and 'b' of the bidirectional DC motor with positive and negative supply

from the standby battery respectively. This results to the tilting the eggs' tray in bi-directionmanner [3].

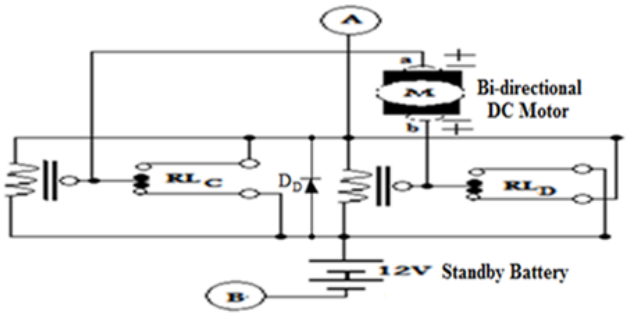

Figure I. Egg Turner Manipulator Circuit Diagram

A summary of the components required and used is shown in Table I.

Table I Egg Turner Manipulator Components

COMPONENT	CALCULATED VALUE	STANDARD VALUE
RL_C, RL_D	----------	12 V RELAY
D_D	----------	1N4001
BI-DIRECTION DC MOTOR	----------	12 V BI-DIRECTION MOTOR
BATTERY	----------	12 V

Relay 'RL_C and RL_D' are SPDT with 2 A at 220 V switch, coil voltage 12 V; coil resistance 200 Ω to 300 Ω was used.

III. Design and Analysis of Eggs' – Turner Delay Circuit

The eggs' turner delay circuit is designed and implemented using the circuit diagram of Figure II.

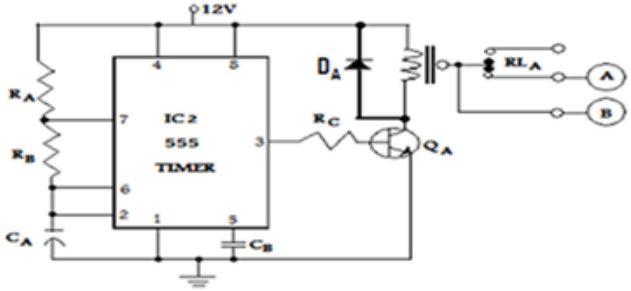

Figure II. Delay Circuit Diagram

Figure II was designed using an astable multivabrator by utilizing 555 IC. Efficient delays of 30 mins and 25 mins were chosen for the design oft_h (time high) and t_l (time low) respectively. The said period was selected to enable us to achieve a duty circle 'D' where D is approximately 55%, which leads toa pair of trays tilting per hour and 26 pairs of per day. The t_h and t_l can be computed by using equations (1) and (2) [4]:

$$t_h = 0.693(R_A + R_B)C_A (1)$$

$$t_l = 0.693(R_B C_A) (2)$$

Hence t_h is 30 mins $= 1800$ sand t_l is 25 mins $=$ 1500 s and the capacitor C_A is selected as $3300\ \mu F, 50$ V. Using equation (2), the value of the resistor R_B is obtained as:

$$R_B = 787.09\ k\Omega$$

But standard value resistors of 680 kΩand 100 kΩresistors in series with $\pm 10\%$ tolarance are used.Using equation (1), the value of the resistor R_A is calculated as:

$$R_A = 131.2\ k\Omega$$

But a standard value of 130 kΩ with $\pm 10\%$ tolarance is used.

The period of oscillation 'T' can also be determined from equations (1) and (2), which yield the relationship in equation (3) [5]:

$$T = t_h + t_l = 0.693(R_A + 2R_B)C_A (3)$$

Hence, $T = 55$ mins $= 3300$ s

The frequency of oscillation 'f' of the timer was calculated using the relation in equation (4) [5]:

$$f = 1/T = \frac{1}{0.693(R_A + 2R_B)C_A} \quad (4)$$

Therefore, the frequency $f = 260\ \mu Hz$

The duty cycle 'D' as in equation (6) was derived from equations (1) and (3).

$$D = \left({}^{t_h}/_{T}\right) x\ 100\% \quad (5)$$

$$\because D = (R_A + R_B/R_A + 2R_B)\ x\ 100\% \quad (6)$$

Using equation (6), gives the duty cycle of:
D ≅ 55%.

The output of the timer IC at pin-3 is connected to the base of transistor Q_A through resistor R_C for further amplification. The transistor used is a general purpose NPN transistor with the following specifications:

Turn-on voltage$V_{BE} = 0.7$ V, Collector current $I_C =$ 450 mA, Power dissipation $P_D = 500$ mW.
Current gain factor $\beta = 250$. The part number of the transistor is BC548.

The base current of the transistor Q_A is obtained as follows [6]:

$$I_B = I_C/\beta\ (7)$$

Using equation (7) where I_B is 1.8 mA:

$$R_C = \frac{V_{CC} - V_{BE}}{I_B} \quad (8)$$

Using equation (8), the value of the resistor R_C is calculatedas:
$R_C = 6.2\ 8\ k\Omega$
But a standard value of 6.8 kΩ with $\pm 10\%$ tolarance is used.

A summary of the components required and used is shown in Table II.

Table II Eggs' - Turning Delay Components

Relay 'RL_A' is SPDT with 2A at 220V switch, coil voltage 12V; coil resistance 200Ω to 300 Ω was used.

RESULTS

The egg turner was implemented using the presented analysis. Standard component values were used in the physical system. The egg turner was placed in an existing incubator (HEFINC840) of capacity 840 and it was found to provide egg tilting at an angle of 45^0 for each design delay. The same HEFINC840 and the same type and number of eggs were used but with manual (hand) egg turning. Hatchability was taking as the performance index of the two turning methods. Using the proposed turning method hatchability of 732 eggs were recorded and a failure of 108 eggs. While with the manual egg turning method hatchability of 4336 was recorded, and a failure of 404 eggs. Table III shows the comparison between the proposed automatic egg tilting system with the manual egg turning method.

COMPONENT	CALCULATED VALUE (kΩ)	STANDARD VALUE
R_A	131.20	130 kΩ
R_B	787.09	780 kΩ
R_C	6.28	6.80 kΩ
C_A	----------	3300 µF, 50 V
QA	----------	C945

Table III. Comparison of the Proposed and Manual Egg Turning Method

Proposed method Hatch success %	Proposed method Hatch failure %	Manual method Hatch success %	Manual method Hatch failure %
87	13	52	48

DESIGN OF THE EGG TURNING PARTS

The egg turning parts is made up of metal of different shapes (i.e. rectangular pipe, straight bar, flat sheet, angle bar and cylindrical rod) were used in building the turning frames. Figure III to Figure IV shows the major turning parts.

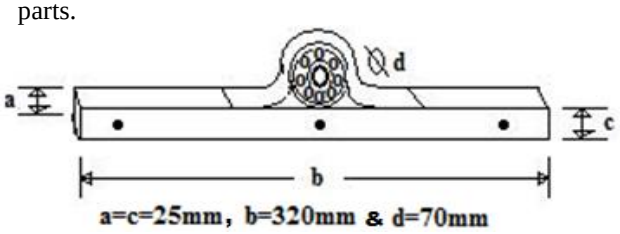

Figure III. Egg Turning Tray Pivot

Figure III is made up of rectangular pipe, straight bar and bearing all welded together to form pivoting part for the egg's turning tray. Three (3) holes were made on the rectangular pipe to ease fixing it on the wooding casing. Three (3) of its kind were made to support and permit free turning of the eggs' turning tray.

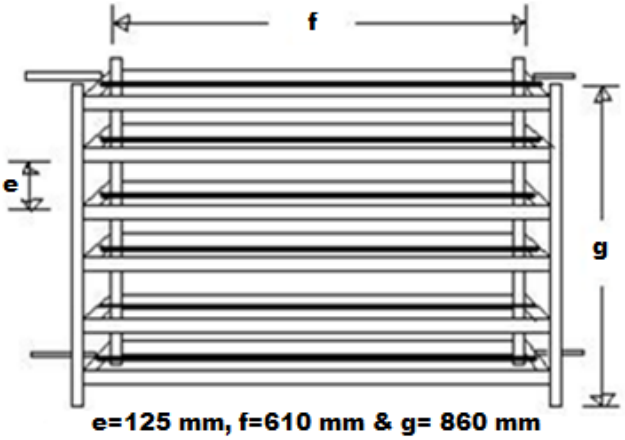

Figure IV. Egg Turning Shelve

Figure IV shows the egg turning device which was constructed using straight bar, rectangular bar, angle bar and cylindrical rod.

This mechanism was deliberately designed in such a way to freely tilt clockwise and counter clockwise. On completion of the design, the eggs' turning trays was found tilting smoothly at an angle of 45^0 in both directions without damaging any of the eggs. Such angular displacement was achieved using the equation (9) [3].

$$c = [\mathrm{Cos}\theta(a + b)] - a \qquad (9)$$

Wherea is the thickness of the bar used,b is the wideness between the two tray bars,c is the required gap between trays andθ is the angle of tilting required (45^0).

CONCLUSION

The proposed egg turning system was designed with an efficiency of 35% ahead of the manual egg turning method which is also porous to uneven turning and it can also transmit diseases to the eggs. Exactly egg tilting of 45^0 was achieved using the proposed method as against the manual turning which a random turning is administered. It can now be concluded that the proposed method of automatic egg turning at an angle of 45^0 in both directions is encourage to the used by the hatchers than the hand turning method.

REFERENCES

[1] A. B. Umar, K. Lawal, M. Mukhtar and M. S. Adamu "Construction of an Electrically-OperatedEgg Incubator" International Journal of Modern Engineering Sciences, vol. 5, issue 1, Florida, USA. p. 1-18, 2016

[2] A. Mohammad, M. J. Musa; K. Ahmad, S. Garba and M.D. Almustapha "Design and Performance of HEFINC840 Micro-controller Based Incubator" NIAE International Conference, Uyo 2013 University of Uyo, Nigeria. October 21-24, 2013, p. 685-692, 2013

[3] Z. N. Oriolowo; Z. Haruna; K.I. Ali; M. J. Musa; Tekanyi A. M. S. (2015) "Symbolic Modeling and Simulation of a Planar Seven-Body Mechanism using MapleSim" Zaria Journal of Electrical Engineering Technology, Department of Electrical and Computer Engineering, A. B. U. Zjeet Volume 1 & 2. No. 5/10-14

[4] U. F. Abdu-Aguye, S. Garba, M. J. Musa, K. Ahmad, and A.M.S. Tekanyi "Development of an Embedded Light Activated Remote for fan Regulator" Proceedings of Academia Industry Conference. Faculty of Engineering, Bayero University Kano 9th-11th December 2014.

[5] M. J. Musa; Y. M. Abdullah; M. J. Bello and J.A. Ignatius (2009) "Design and Construction of an Automatic Bird (Pest) Repeller" 3rd West Africa Society for Agricultural Engineering and 9th Nigerian Institute of Agricultural Engineering "Agricultural Technologies and the African Poverty Eradication Challenge" WASAE/ NIAEIFE 2009. 25th-29th January 2009. Pp.396-400

[6] K. Ahmed, Y. A. Sha'aba, M. J. Musa, A. S. Musa and A. M. S. Tekanyi "Design, Development and Reliability Assessment of four-in-one Electronics Security Assistant" 46TH Annual Conference of Science Association of Nigeria. ZAZZAU 2011.

Dragonfly Algorithm-based Detection Technique for Man-In-The-Middle Attack in Fog Computing Environment: A Conceptual Framework

Yakubu Jimoh[1], Shafi'i Muhammad Abdulhamid[2]
[1]*Department of Computer Science,*
[2]*Department of Cyber Security Science,*
Federal University of Technology Minna, Nigeria.
jimm.yack@futminna.edu.ng, shafii.abdulhamid@futminna.edu.ng

ABSTRACT—Fog computing is a recent model of computing, in a distributed way that extends the cloud computing operation to the network edges. Fog computing enables storage execution and tasks processing, which relies on the cooperation of users and resource sharing among various devices. The fog being the new shift to cloud computing addresses some critical challenges associated with cloud model by providing notable advantages which are location sensitivity, latency minimization, geographical accessibility, wireless connectivity, mobility support and improved data streaming. Nevertheless, fog computing concept is never an option for replacing cloud computing model. In spite of the attractive solutions found in fog computing, it also inherited some security problems from the cloud. Most of the proposed techniques to solve security issues in fog computing could not completely addressed the security challenges due to the limitation of the various techniques. A fog computing security approach that is based on man- in- the middle attack using Dragonfly algorithm (DA) detection algorithm is conceptualized here. This paper is a framework for detection of MITM attacks that exist between the fog nodes and the cloud and vice versa using swarm intelligence optimization techniques called the DA algorithm which is be implemented on the platform of ifogsim simulator.

KEYWORDS: **Fog computing, DA, MITM attack, Cloud computing, Fog security**

I. INTRODUCTION

Cloud computing model is viewed as the main integration of internet system because it possessed computational and storage ability, which does not exist in other devices. The increase in internet computation leads the web expansion, and is growing with complexity because of the addition of new technologies and solutions. The need for data processing and storage demands is astronomically on the increase. To address this phenomenon, Web architecture must be developed to meet user's data processing need [1]. Fog computing paradigm is a new concept developed to meet the latency requirement of the web architecture. The design greatly reduces latency and enhances network performance[2].

Fog computing emergence is still very new; this technology has already been embraced by the modern data center and the cloud. The technology is built upon the distributed computing paradigm especially the network's content delivery which ultimately paves way to additional complex services delivery through the use of cloud model technologies. Nonetheless, the distinction of fog computing from cloud is therefore, it nearness to the end user since they offers computation, data storage and provision of application services to the client. Fog computing model is never a replacing option of cloud computing rather, it is viewed as complementary to many applications and services in order to eliminate the inadequacies of the cloud [3].

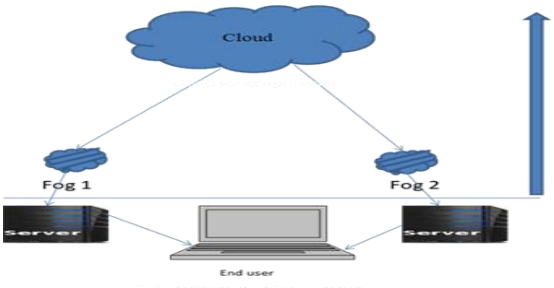

Figure 1: Fog and the cloud

The major contributions of our conceptual framework paper include:

i. We compare the fog and cloud computing environment and show case the structural design of fog architecture.
ii. We present and analyze the scenario of MITM attack in fog environment.
iii. We proposed swarm intelligence optimization techniques *(*Dragonfly algorithm*)* framework to detect MITMattack in fog computing environment.

The major purpose of our proposed paper is to develop a conceptual framework that will use swarm-intelligence optimization techniques called DA to detect Man-in-the-middle attack in fog computing environment using ifogsim simulator. The remaining section of this framework is structured as below: the Section II gives the overview of fog computing, section III summarized the reviewed similar research works, while section IV described the problem formulation and design model. Section V presents the Proposed DA Framework for MITM Attack, section VI introduced the dragonfly algorithm (DA) optimization and

the associated equations, section VII describe the expected outcome of the model, section VIII recommends the future research direction and finally, section IX contain the conclusion of the paper.

II. FOG COMPUTING OVERVIEW

Fog computing idea was put forward by CISCO team of researchers in year 2012. The term was used to imply extension of cloud computing[4]. The main purpose is to deviate from the usual computing from cloud datacenters to heterogeneous users and edge devices. Fog computing enhances the operation of computation, data storage, and linking of datacenters with networking services between user devices and the cloud. Cloud computing has solutions of protecting network but these solutions in most cases might be unfit to fog environment. Fog computing is generally nearer to the end users and operated in a distributed approach since the various devices are working together at the network edge [5].

However, implementing fog computing technology introduces more number of security challenges. Although there are presently several techniques for detecting and handling the data security and also privacy problems in cloud environment. But these challenges are inherited in fog computing and it remains a major problem[6]. Organizations and data processing center need to find a medium through which more centralize distributed architectural design transmit data and information to the end-users. Fog computing idea was generated to distribute data in order to move it closer to the end-user, and to remove latency issues and give support to mobile computing as well as streaming of data [7].

III.RELATED WORKS

Stand-alone authentication mechanism to authenticate user when connection is not available to the cloud server was introduced by [3]. This was achieved through hybrid-encryption and attribute-based encryption. The former is a procedure to share data with a particular party in encryption while the latter is information like smart grid. Extending hybrid-encryption into one -to-many setting can address the connection issue if the two fog devices are in different areas. This authentication method enables users to be authenticated and have permission to establish connection between the fragile cloud and the fog devices. The team pointed out that this approach create another problem of calculating increase in smart users card especially if a new equipped devices that is to act as stand-alone is added. This problem according to the authors can be subdued through cryptographically primitive – Attribute-based encryption method. The authors described the attribute-based encryption as a viable tool, for providing data without necessarily having the fore-knowledge of the receiver of the data. This provides flexible sharing of data in flexible way more than the usual end-to-end encryption. However, the proposed technique is not capable of authenticating and authorizing user in a setup that is being distributed.

In fog environment, There exist gateways that represent fog devices that can be compromise by the activities of man-in-the middle attack[8] .The authors explained that it is difficult to use encryption and decryption algorithm to secure communication between the fog devices and IoT devices because the formal and the later consumes large amount of battery on mobile devices. As a result, it becomes difficult to detect the rootkit and the various types of malicious code that is present in the fog nodes. The team combined a fog node and the cloud to visualized a fog computing paradigm that produce high quality of services to the users to make up for the lapses of cloud in internet of things environment. Conversely, the result of the experiment conducted could not address MITM attack.

Insecure authentication protocols are viewed as the major security threat to fog computing platform and the end – user application devices [9]. The authors stressed that spoofing attack and data tampering are exposed to IoT devices that exist in smart grids which ultimately can prevent using infrastructure, intrusion detection techniques and Hellman key exchange. The investigation of Video call between 3g and Wireless LAN users in a fog network was conducted for Man-in-the middle attack which result shows that the attack did not reveal obvious changes in the memory utilization and CPU consumption of fog node. Also, Authentication scheme through securing communication channels between the fog environments was suggested by the authors to be adopted as preventive measure. Similarly Advanced encryption standard (AES) was also recommended as a viable encryption techniques for fog platform. Conversely, the security solutions put forward by the team are individualistic and therefore, not dynamic enough to secure fog platform in terms of confidentiality, integrity and availability.

IV. PROBLEM FORMULATION

Man-in-the middle attack (MITM) is demonstrated in Figure 2where the attacker inserted himself in-between the flow of traffic, the fog node and the cloud. The attacker can then inject false information and intercept the data transferred between them. More so, from the survey and the research analyses, Man-in-the-middle attack investigation remains a top priority for researchers due the stealthy nature of the attack

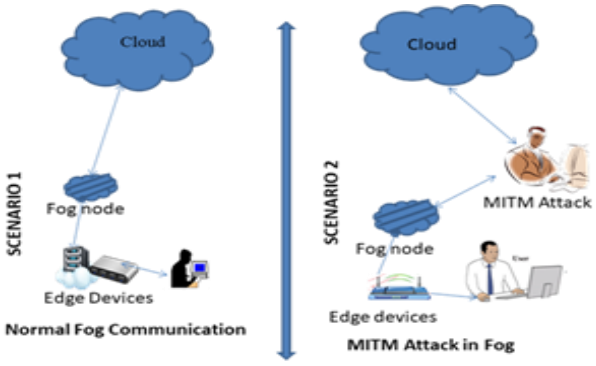

Figure 2. MITN attack scenario in fog environment

In the proposed model in Figure 3, the DA detects any malicious attacker, whose intention is to intercept all relevant information that is moving from fog node to the cloud or vices versa and inject false information in fog computing environment.

V. PROPOSED DA FRAMEWORK FOR MITM ATTACK

The proposed framework consists of 1st, 2nd and 3rd phases. The first phase contains problem formulation, planning and dataset description. The second Phase contains design and implementation which include Dragonfly Algorithm (DA) detection on ifogsim Simulator Platform, Model flowchart and Pseudocode. The third phase of the framework is the implementation, testing performance evaluation stage. This includes experimental setup, performance metric, and testing, and performance evaluation. Figure 3 shows the proposed DA detection framework for MITM attacks.

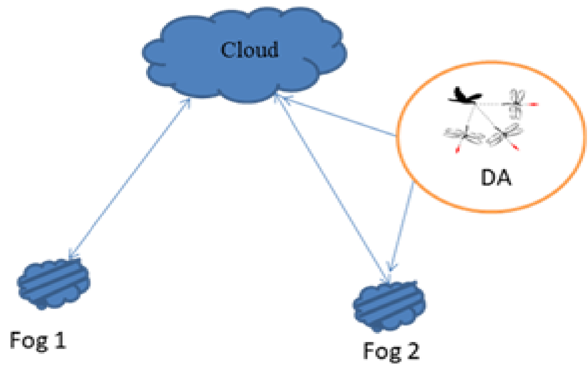

I.

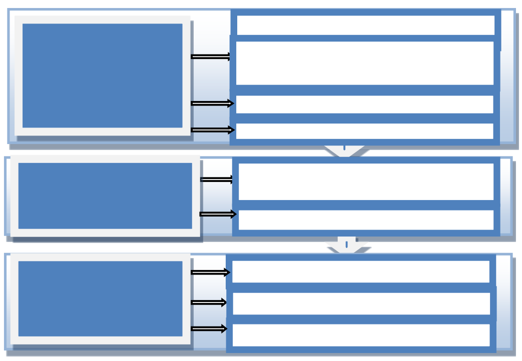

VI.D

VI. DRAGONFLY ALGORITHM (DA) OPTIMIZATION

*D*ragonflyin comparison to other insects has exceptional good vision. It possesses two huge compound eyes, which has about 360 ° visions. Each of the compound eyes contains almost 30,000 lenses. A dragonfly uses almost 80% of the brain to process all the information within it view. The vision assists the insect to detect how the other insects move in order to avoid collisions when flying. Dragonfly possesses an active gaze control, with fixed eyes which enable them rotate their heads. This compels it to focus its target within five degree from the central view.

Seyedali Mirjalili proposed (DA) in 2015. It was derived from static and dynamic swarming insert behaviors. These behaviors are synonymous to the two main phases of optimization that uses meta-heuristics. They are exploration and exploitation. Dragonflies create sub swarms and then usually fly over different areas in a static form, which is the major objective in the exploration phase. The algorithm, described and model dragonflies social behavior in interaction when navigating, foods exploration and dynamically avoid enemies when swarming. There are two versions of the DA which are: binary DA (BDA) and multi-objective DA (MODA).There are five existing principles of swarming in dragonfly which have been utilized for aiding the swarming behavior of insects: separation, alignment, cohesion, attraction to food source, and distraction from enemies [10-14].

Separation indicates the static collision avoidance of the individuals from other individuals in the neighborhood. **Alignment** shows the velocity matching of individuals to another individual in neighborhood. **Cohesion** is the ability of individuals moving along the center of the mass of the neighborhood. All swarm exhibit struggle for Survival which is the major purpose of swarm existence; all the individuals should therefore, be attracted towards food sources and distracted outward enemies.

The swarm's behaviors approach is evaluating for each individual as follows.

The separation is obtained as

$$Si = -\sum_{j=1}^{N} X - XjSi = -\sum_{j=1}^{N} X - Xj \quad \textbf{(1)}$$

X is the position of the present individual, Xj indicate the position j-th neighboring individual While N is the number of neighboring individuals.

Alignment is obtained as

$$Ai = \sum_{j=1}^{N} Xj/NAi = \sum_{j=1}^{N} Xj/N \quad \textbf{(2)}$$

Where Xj shows the velocity of j-th neighboring individual.

Cohesion is obtained as

$$Ci = \sum_{j=1}^{N} Xj/N - XCi = \sum_{j=1}^{N} Xj/N - X \quad \textbf{(3)}$$

X is the position of the present individual; N is the number of neighborhoods while Xj indicate the position j-th neighboring individual.

The Attraction of the insect moving along a food source is obtained as;

X is the position of the current individual, and X^+ shows the position of the food source.

Dist fraction outwards an enemy is calculated as;

X is the position of the present individual, while X^- shows the position of the enemy.

The step vector indicates the direction of the movement of the dragonflies and obtained as;

the separation weight, Si shows the separation of the i-th individual, shows the alignment weight, A is the alignment of i-th individual, c shows the cohesion weight, Ci indicate cohesion of the i-th individual,

f is known as the food factor, Fi is the food source of the i-th individual, e is the enemy factor, Ei is the position of enemy of the i-th individual, a is the alignment weight, A is the alignment of i-th individual, c indicates the cohesion weight, Ci is the cohesion of the i-th individual, Fi is the food source of the i-th individual, e is the enemy factor, Ei is the position of enemy of the i-th individual, w is the inertia weight, and t is the iterationcounter.

The position vector can be calculated as follows;

In order to enhance the randomness, stochastic behavior, and exploration of the artificial dragonflies, using a random walk (Le´vy flight) when there are no neighboring solutions the position of dragonflies is updated using the following equation:

PSEUDO-CODES OF THE DA DETECTION ALGORITHM

Initialize the dragonflies population Xi (i=2,2, ...,n)
Initialize step vectors ΔXi (i=1,2,----n)
While the end condition is not satisfied
Calculate the objective values of all dragonflies
Update the food source and the enemy
Update w, s, a, c, f, and e
Calculate S, A, C, F, and E using **(1)** *to* **(5)**
Update neighbouring radius
if a dragonfly has at least one neighbouring dragonfly
Update velocity vector using **(6)**
Update position vector using **(7)**
else
Update position vector using **(8)**
end if
Check and correct the vector new position base
boundaries of variable
end while

Figure 5. Pseudo-codes of DA detection algorithm

VII. INITIAL RESULTS AND EXPECTED OUTCOME

To demonstrate the workability of our proposed framework, we test the threshold consumption of CPU in MITM attack based on the percentage of CPU utilization in scenarios 1 and 2 illustrated in Figure 2. It shows that the CPU utilization of memory usage is less in a normal communication between the fog and the cloud environment [15-18]. This is as compared with the CPU usage when there is a MITM attack taking place. Figure 6 shows the results of an initial or preliminary experiment in the two scenarios depicted above. This implies that, the CPU usage can be used as a threshold value in detection of MITM attack in a Fog computing environment.

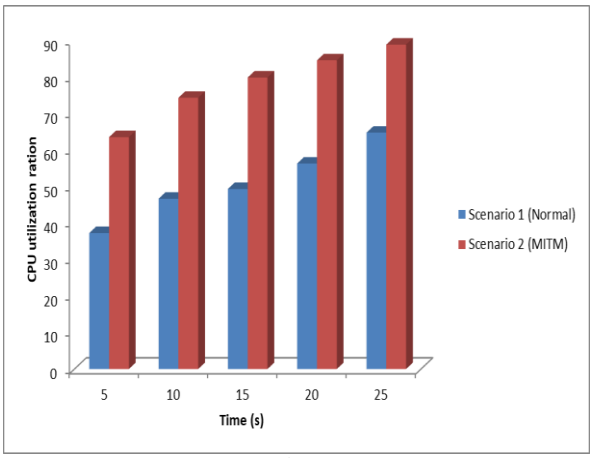

Figure 6. Initial results of CPU utilization with time

The DA detection model is expected to detect MITM attacks in fog computing environment. The introduction of DA algorithm in the proposed model would help significantly to detect MITM attack, as information moves from the cloud to fog environment and vice-versa without visible feature of the attack when collected from the fog. The experimental setup will be achieved through ifogsim simulator to determine the stealthy nature of Man-in-the middle attack.

VIII. FUTURE RESEARCH WORK

Future direction is to extend the DA algorithm to detect MITM attack at the edge of fog devices in fog computing environment. Traditional anomaly detection algorithms are not capable enough to expose MITM attack in fog to cloud scenario. Therefore, application of swarm intelligence optimization techniques using ifogsim simulator is expected to properly classify and detect the MITM attacks in fog devices.

IX. CONCLUSION

We have discussed the concept of fog computing paradigm and the security challenges. We observed that MITM attack remain security threat in fog computing environment as previous researcher's result shows insignificant effect. It is therefore difficult to detect MITM attack without visible feature of the attack when collected from the fog. This framework proposed the introduction of Dragonfly algorithm detection in MITM which it implementation through ifogsim simulator would help significantly to detect MITM, as information moves from the cloud to the fog environment and vice-versa. The DA is expected to detect any malicious attacker, whose intention is to intercept all relevant information that is moving from fog node to the cloud or cloud to the fog node and inject false information in fog computing environment. We recommend the extension of the DA to detect MITM attack at the edge of fog devices in fog computing environment.

REFERENCES

[1] J. Shropshire, "Extending the Cloud with Fog : Security Challenges & Opportunities," *Am. Conf. Inf. Syst.*, pp. 1–10, 2014.

[2] R. Rios, R. Roman, J. A. Onieva, and J. Lopez, "From SMOG to Fog: A security perspective," *2017 2nd Int. Conf. Fog Mob. Edge Comput. FMEC 2017*, pp. 56–61, 2017.

[3] I. Stojmenovic, S. Wen, X. Huang, and H. Luan, "An overview of Fog computing and its security issues," *Concurr. Comput. Pract. Exp.*, vol. February, no. April 2015, pp. 2991–3005, 2016.

[4] I. Stojmenovic and S. Wen, "The Fog Computing Paradigm: Scenarios and Security Issues," *Proc. 2014 Fed. Conf. Comput. Sci. Inf. Syst.*, vol. 2, pp. 1–8, 2014.

[5] Y. Sun, F. Lin, and N. Zhang, "Saudi Journal of Biological Sciences Original article A security mechanism based on evolutionary game in fog computing," *Saudi J. Biol. Sci.*, vol. 25, no. 2, pp. 237–241, 2018.

[6] Y. Guan, J. Shao, G. Wei, and M. Xie, "Data Security and Privacy in Fog Computing," *IEEE Netw.*, pp. 1–6, 2018.

[7] P. Kumar, N. Zaidi, and T. Choudhury, "Fog computing: Common security issues and proposed countermeasures," *Proc. 5th Int. Conf. Syst. Model. Adv. Res. Trends, SMART 2016*, pp. 311–315, 2017.

[8] J. Kang, R. Yu, X. Huang, Y. Zhang, and S. Member, "Privacy-Preserved Pseudonym Scheme for Fog Computing Supported Internet of Vehicles," *IEEE Trans. Intell. Transp. Syst.*, pp. 1–11, 2017.

[9] S. Khan, S. Parkinson, and Y. Qin, "Fog computing security : a review of current applications and security solutions," 2017.

[10] S. Mirjalili, "Dragonfly algorithm: a new meta-heuristic optimization technique for solving single-objective, discrete , and multi-objective problems," *Neural Comput. Appl.*, vol. 27, no. 4, pp. 1053–1073, 2016.

[11] SM Abdulhamid, Latiff MS, Chiroma H, Osho O, Abdul-Salaam G, Abubakar AI, Herawan T. A Review on Mobile SMS Spam Filtering Techniques. IEEE Access. 2017;5, pp. 15650-66.

[12] SH Madni, Latiff MS, Abdullahi M, Usman MJ. Performance comparison of heuristic algorithms for task scheduling in IaaS cloud computing environment. PloS one. 2017 May 3;12(5): e0176321.

[13] MS Latiff, Madni SH, Abdullahi M. Fault tolerance aware scheduling technique for cloud computing environment using dynamic clustering algorithm. Neural Computing and Applications. 2018 Jan 1;29(1), pp. 279-93.

[14] I. Idris, Abdulhamid SM. An improved AIS based e-mail classification technique for spam detection. arXiv preprint arXiv:1402.1242. 2014 Feb 6.

[15] SH Madni, Latiff MS, Coulibaly Y. Recent advancements in resource allocation techniques for cloud computing environment: a systematic review. Cluster Computing. 2017 Sep 1;20(3), pp. 2489-533.

[16] Abdullahi M, Ngadi MA. Symbiotic Organism Search optimization based task scheduling in cloud computing environment. Future Generation Computer Systems. 2016 Mar 1; 56:640-50.

[17] Latiff MS, Abdul-Salaam G, Madni SH. Secure scientific applications scheduling technique for cloud computing environment using global league championship algorithm. PloS one. 2016 Jul 6;11(7): e0158102.

[18] Latiff MS. A checkpointed league championship algorithm-based cloud scheduling scheme with secure fault tolerance responsiveness. Applied Soft Computing. 2017 Dec 1; 61:670-80.

An Enhanced Logic-gate Based Automatic Water Drinking System for Chicks

M. J. Saidu
Department of Agricultural and Bio-Environmental Engineering Technology. College of Agriculture Jalingo, Taraba
msjauro2020@gmail.com

Y. M. Abdullahi
Electrical Engineering Department, Umaru Ali Shinkafi Polytechnic, Sokoto

A. Mohammed
Department of Physics, Kaduna State University, Kaduna-Nigeria

M. J. Musa
Communications Engineering Department, Ahmadu Bello University, Zaria. Nigeria
mjmusa@abu.edu.ng

A. M. Kauji
Department of Agric Engineering Technology, Ramat Polytechnic Maiduguri

ABSTRACT—*Water is a resource that need to be conserved. Large volume of water is wasted due to the manual way of water supplied to chick from the batten houses to the chicken grown up cages. This traditional water drinking practice of placing a container of water for chicks to drink does not only waste the water, but it also leads to high mortality when a chick mistakenly falls into the water full container. Similarly, when the chicks pour away the water in the container or drink all the water at night, they will remain stave till the owner noticed and refilled again. This paper proposed an automatic water drinking system using the three not-or (NOR) gates of CD4001 as the heart of the design. Two probes were used as water sensors, which are fixed at different level in the water container to enable completed the logic circuit and triggered a 12 V relay. The relay acted as a switched that energizes and de-energizes a mini water pump, which on/off the water supplied respectively to the container through a complex logic strategy. The chicks water drinking system provided an efficiency of about 79% as compared to the traditional practice of manual refilling of the water container with the same number of chicks*.

KEYWORDS: chick, control, refilling, drinking water.

INTRODUCTION

Chicks usually drink water from any available source for survival, sometimes they do drink the water even when they do not need it to an extend that it become harm to the chicks [1-3]. Occasionally chick die as a result of falling into the water way pan. Research has been conducted ad is ongoing in this area of interest to enable provide an automatic way of water supply to the chicks. In this paper, an automatic chick drinking water was proposed, which used logic gates and solid-state components.

Section II of this paper describes the design of the circuitry and the mathematical analysis of the proposed design based on the components used. Testing results are shown in section III with respect to the traditional practice of drinking water. Section IV concludes on the presented results.

IV. DESIGN OF AN AUTOMATIC CHICK DRINKING SYSTEM

Water is essential in life, but the amount of drinking water needs to be regulated to in such a way that the water will only be available to a safe level when needed by the chicks. Hence the control of water flow to the chicks drinking pan is necessary. The proposed drinking system was controlled as shown in Figure I, which only allows water flow when needed and cased when not.

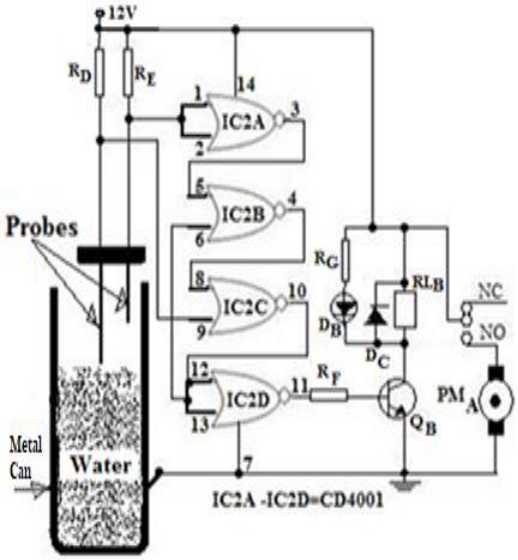

Figure I. Water Refilling Control Diagram

This water refilling circuit is designed and constructed using quad 2 - input NOR gate CMOS IC1 (CD 4001) as the active component that generates the oscillation. The arrangement of the logic gates is a deliberate design to pump water to the metal container whenever water in the container fall below to a set safety level and to cut off water supply when the water reaches the desired safety level.

A. Pumping Water to the drinking Container

When the steel rods (probes) are not immersed into water the input pins 1 and 2 of IC1A NOR gate will be high and its

output pin 3 will be low. The output of pin 3 will serve as one of the input of IC1B pin 6 due to the deliberate design any signal at the second input (pin 5 of IC1B) will not have effect on the output pin 4, hence pin 4 which remain high. The low signal of pin 4 will serve as one of the input terminal of IC1C pin 8, while the second input pin 9 of the same IC1C will be high since the longest probe is not in the water and so the output pin 10 of the gate will be low. Pin 10 will be connected to the input terminals (pin 12 and 13) of IC1D, this holds the output of IC1D pin 11 high and hence saturate the transistor, which in turn energies the relay to switch - ON the water pump and fill the container to the required safer level.

B. Stop Refilling Water to the drinking Container

When the two probes are both immersed in the water (container fills up to required level) the input terminals of IC1A will be tied low and the output terminal pin 3 will be high. Pin 3 is connected to pin 6 as one of the new input of IC1B will assume the feedback high signal from pin 10 of IC1C, hence the output of pin 4 will be low. Pin 4 is connected to one of the input of IC1C pin 8, since both probes are immersed in water pin 9 will be low and this results in making pin 10 high. Pin 10 is tied to both inputs of IC1D (pin 12 and 13) hence, the output pin 11 will be low. The low signal from pin 11 is fed to the base of transistor QB, which cut off the transistor and results in de-energizing of the relay RLB. Therefore, the water pump stops pumping water to the drinking container [3]

C. Design of the water Refilling Control Circuit

From data sheet, the specifications of the transistor Q_B are β is 220 , V_{BE} is 0.7 V and I_B is 1.36 mA.Using equation (1) [4] the value of resistor R_F is obtained as:

$$R_F = \frac{V_{CC} - V_{BE}}{I_B} \quad (1)$$

R_F is 8.3 kΩ

where V_{CC} is 12 V. A standard value of 10kΩ±20% tolerance is used.

R_G is a current limiting resistor to the LED D_B,which is designed using equation (2) as [5]:

$$R_G = \frac{V_{CC} - V_d}{I_d} \quad (2)$$

From data sheet, it was found that voltage drop across D_B is $V_d = 2.2$ V, it can also take current $'I_d'$ ranging from10 mA to 15 mA. In this design, a minimum I_d of 10 mA was selected for safety.

Using equation (2) R_G was calculated as:

R_G is 0.92 kΩ.

A standard value of 10kΩ±20% tolerance was used.

Quad 2 input NOR gate CMOS IC CD4001 can operate on the current I_{in} ranging from 0.5mA to 1mA. In this design a current of 0.8 mA was used since it falls within the accepted range.

The two input limiting resistors are selected to be of equal value(R_D is R_E) R_D and R_E are calculated using equation (3) as [6]:

$$R_D = \frac{V_{CC}}{I_{in}} \quad (3)$$

$R_D = R_E$ is 15 kΩ.

A germanium diodeD_C (IN4148) was used as the freewheeling diode to prevent a reverse emf, which may be generated in the relay's coil. Relay 'RL_B' is SPDT with 2A at 220V switch, coil voltage 12 V, coil resistance of 200Ω to 300 Ω was used for safety.

Two steel rods (probes) of same length are used as sensors to switch ON/OFF the water pump to provide water in the drinking container when empty/full respectively. A summary of the components required and used is as shown in Table I.

Table I. Water Refilling System Components

COMPONENT	CALCULATED VALUE (kΩ)	STANDARD VALUE (kΩ)
R_D	15	15
R_E	15	15
R_F	8.3	10
F_G	0.92	1

V. RESULTS

The automatic drinking water system was compared with the traditional method of pouring water in a container for 120 chicks. A reservoir of water was provided were the automatic chick drinking system gets its supply from. Same volume of reservoir was provided for the traditional practice of pouring the water for the chicks manually. The two methods were compared for a period of two weeks. Table II shows the comparison when a preset safer volume of 1000 cm^3 was set.

Table II. Results Comparison

Days	Proposed chick drinking system (cm^3)	Manual chick drinking system (cm^3)
1	984	1202
2	999	1350
3	1000	1104
4	978	1026
5	1000	1207
6	1000	1224
7	1000	1193
8	996	1211
9	997	1009
10	998	1312
11	998	1233

12	1000	1215
13	970	1032
14	960	1239
Average Total	991.428571	1182.64286

From Table II a significant variation was recorded from the desire level in day 1, 4, 13 and 14 with a shortest set value of 984 cm^3, 978 cm^3, 970 cm^3 and 960cm^3. These fall in the chicks drinking water level may lead to uneven growth of the chicks though it may prevent them from falling in the drinking water and die [1]. The traditional method shows that excess of water was supply to the chick throughout the weeks, which may result drinking excess water by the chicks. Taking excess water will make the chick plumb and eventually die [1]. Similarly, supplying excess water to the drinking pan in the traditional method as shown in Figure II do lead to the chicks fall in to the container and die. As a result of the excess water supply, three chicks were death in two weeks and this number of mortalities may rise when the traditional method is adopted.

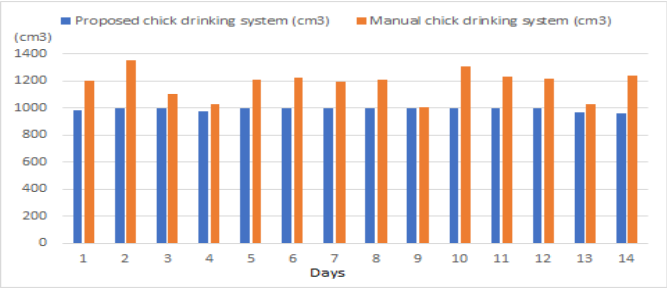

VI. CONCLUSION

From the above fact, the proposed design has an efficiency of about 79% because it only malfunction in four days out of the 14 weeks of testing. However, the traditional method is discouraged to be applicable to chick drinking water due to the excess supply of water throughout the fourteen days of testing. It can now be concluded that the proposed method of using logic gave in implementing the chick drinking water is encourage to the used by poultry farmers than the traditional method.

REFERENCES

1) A. Mohammad, M. J. Musa; K. Ahmad, S. Garba and M.D. Almustapha "Design and Performance of HEFINC840 Micro-controller Based Incubator" NIAE International Conference, Uyo 2013 University of Uyo, Nigeria. October 21-24, 2013, p. 685-692, 2013
2) K. Ahmad, M. J. Musa; Y. A. Shaaban, A.M.S Tekanyi, A. Muhhamad "Design and Development of Automatic Drip Irrigation System" NIAE International Conference, Uyo 2013 University of Uyo, Nigeria. October 21-24, 2013, p. 712-719, 2013.
3) K. Ahmad, M. J. Musa, M. J. Saidu, A. J. Abubakar and I. Rilwanu "Development of Micro-Controller Based Home-Garden Watering System with GSM Remote Control" (NIAE) International Conference, Minna 2016, Federal University of Technology, Minna, Niger State, Nigeria. October 4-7th, Vol. 27, 2016, Pp. 521-527, 2016.
4) U. F. Abdu-Aguye, S. Garba, M. J. Musa, K. Ahmad, and A.M.S. Tekanyi "Development of an Embedded Light Activated Remote for fan Regulator" Proceedings of Academia Industry Conference. Faculty of Engineering, Bayero University Kano 9th-11th December 2014.
5) M. J. Musa, K. Ahmad, I. Umar, M. A. Aminu; A. Ahmed (2013) "Control and Monitoring of Green House Environment Microcontroller-Based Approach" NIAE International Conference, Uyo 2013 University of Uyo, Nigeria. October 21-24, 2013, Pp. 757-773
6) K. Ahmed, Y. A. Sha'aba, M. J. Musa, A. S. Musa and A. M. S. Tekanyi "Design, Development and Reliability Assessment of four-in-one Electronics Security Assistant" 46TH Annual Conference of Science Association of Nigeria. ZAZZAU 2011

Artificial Neural Network Based Plant Species Identification

Rabiu Aliyu Abdulkadir
Department of Electrical Engineering,
Kano University of Science and Technology, Wudil.
Kano, Nigeria
rabiukk@gmail.com

Khalipha Abubakar Imam,
Shamsu Idris Abdullahi
Department of Electrical Engineering,
School of Technology, Kano State Polytechnic. Kano, Nigeria
khaliphaaimam@yahoo.com,
shamsuabdullahi114@gmail.com

Abubakar Isa
Physics Advanced Research Centre,
Sheda Sceince and Tecgnology Complex, Abuja, Nigeria
abuabakarisa@yahoo.com

ABSTRACT—*in this research, we proposed an algorithm for the identification of plant leaves based on image processing techniques and artificial neural networks. Image processing techniques help in improving the quality of the images, and hence increase the performance of the identification process and reduce the rate of error. The processed images are used to train an artificial neural network (ANN) for the different plant types. After the training process, the network will be ready to classify and identify the different types of leaves even if there were not presented before. In order to validate the algorithm an experiment is conducted on ten different plant species. The experimental result indicated that the proposed algorithm is able to classify the leaves at high speed with high accuracy.*

KEYWORDS—plant identification, image processing, ANN.

INTRODUCTION

Plant leaves identification is an important process with application in different fields, including medicinal plant collection and classification, and study of the environmental life. Manual identification of plant species using their leaves and stems is a very difficult task that requires a lot of experience in addition to huge books that shows the different types of plants and their leaves. However, the increasing capabilities of the new cameras and mobile phones gives opportunity for picturing plant leaves and using automatic ways to identify them. The majority of the existing algorithms are based on segmentation technique [1]. The main disadvantage of these approaches is that any error in the segmentation will lead to a wrong identification of the leaf.

In this work, we proposed a novel plant identification algorithm that utilizes image processing techniques to enhance the quality of the image, and employ the learning capability of artificial neural networks for identification. These improved the performance of the identification process and reduce the rate of error, in addition to flexibility and reliability. An experiment is conducted in order to validate our algorithm.

VII. DIGITAL IMAGE PROCESSING

Digital image processing is described as processing of digital images by means of a digital computer [2]. Many methods of image processing are available and have been successfully utilized in many applications such as; Intelligent eye tumor detection system [3], face recognition, finger print recognition, automatic traffic control systems and video surveillance [4, 5]. For simplicity some of the important DIP processes that are related to our work will be presented here. This includes image representation, image filtering, and image segmentation.

A. Digital Image Representation

When an image is captured on a digital camera, it captures the analogue information of the image and transforms it to tinny blocs of digital values known as pixels. Digital images can be stored in different formats as it is well known. RAW images, JPEG, PNG, JIF, and BMP images are all types of images represented using different compression methods [6]

B. Edge Detection in Digital Images

Edge detection is the process in which significant object properties in digital images are being detected and captured. These properties include discontinues lines in the characteristics of the object. The main aim of edge detection is to identify and separate these variations in the property of objects within the image. It is very useful in detecting and identifying the region of interest (ROI) in an image. Famous edge detection techniques include:

Sobel edge detection: Sobel operator applies a two dimensional space gradient calculation to highlight the high frequency regions in the spatial domain. It finds the gradient of each pixel in gray scale images. Sobel edge detection method employs two kernels of 3x3 matrixes. The two matrixes are shown as follow.

$$G_x = \begin{bmatrix} -1 & 0 & 1 \\ -2 & 0 & 2 \\ -1 & 0 & 1 \end{bmatrix} \quad (1)$$

$$G_y = \begin{bmatrix} 1 & 2 & 1 \\ 0 & 0 & 0 \\ -1 & -2 & -1 \end{bmatrix} \quad (2)$$

The magnitude of the gradient of the image can be found by

$$|G| = \sqrt{G_x^2 + G_y^2} \quad (3)$$

Sobel edge detection is less affected by the image noise [7].

- **Prewitt edge detection:** Prewitt edge detection is similar to the Sobel method as it also uses similar

kernel to find the gradient in an image. The kernel in Prewitt method is isotropic as shown in the next equations defining the horizontal and vertical kernels [8].

$$G_x = \begin{bmatrix} -1 & 0 & 1 \\ -1 & 0 & 1 \\ -1 & 0 & 1 \end{bmatrix} \quad (4)$$

$$G_y = \begin{bmatrix} 1 & 1 & 1 \\ 0 & 0 & 0 \\ -1 & -1 & -1 \end{bmatrix} \quad (5)$$

- **Canny edge detection:** Canny edge detection is one of the most common edge detection algorithm employed to increase the signal to noise ratio and identify the different features of the image. Generally, Canny edge detection algorithm is composed of several steps; At the beginning, the image is smoothed to remove noise and blur, followed by filtering using Gaussian filter. Finally, the gradient of the image is obtained. The more the change in the image pixels the higher the gradient is. This fact is used to identify the sharp changes in the mage pixels. Canny edge detection uses threshold to eliminate the unwanted regions of the image and highlight the regions of interest (ROIs) [9].
- **Robert's edge detection:** The Robert operator is used to approximate the gradient of image using discrete differentiation. Robert mask is a 2x2 kernel that convolve with the whole image using its horizontal and vertical versions [8].

C. *Wiener Filter*

Wiener filter is an adaptive filter type which uses the error minimization formulas to reject the noise from images. It is based on the mean squared error approximations. It is considered as a frequency filter that can be used with discrete Fourier transform of the image. The reconstruction of the image is carried out by applying the inverse version of discrete wavelet transform. Wiener filter performs greatly in many applications of image filtering and restoration [10].

ARTIFICIAL NEURAL NETWORK

An Artificial Neural Network (ANN) is an information processing tool that is motivated by the biological nervous system such as the brain. Artificial Neural Networks (ANN) are widely used to approximate complex systems that are difficult to model using conventional modelling techniques such as mathematical modelling. The most common applications are function approximation (feature extraction), and pattern recognition and classification. There is no exact available formula to decide what architecture of ANN and which training algorithm will solve a given problem [11]. The best solution is obtained by trial and error. One can get an idea by looking at a problem and decide to start with simple networks; going on to complex ones till the solution is within the acceptable limits of error. There are different neural network architectures. The basic architectures include multi-layered feed-forward networks (Figure 1) that are trained using back-propagation training algorithms.

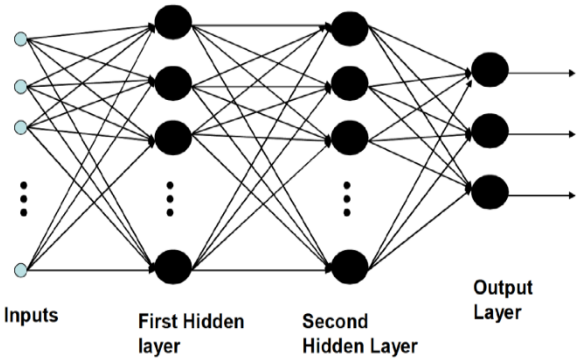

Figure 1: Multi-layered feed-forward neural network

SYSTEM DESIGN

D. *Dataset Description and Pre-processing*

The dataset is composed of approximately 200 leaves images of 10 different plants. These images were all taken as jpg format. The sample images are shown in Figure 2. All the images were obtained in RGB format and converted to gray scale format to make it more suitable for processing. The next step will be to scale down these images so that it will be less size to be fed to neural networks.

The data set file is saved in the matlab folder as plantleaves.mat. The file is loaded using the command loadplantleaves; in the code. This command uploads the file and includes all the variables setup in the current workspace. The data is divided into training, testing and validation. Once the network has been trained, it has to be tested on data that it has not seen before in order to determine the performance of the trained network.

Figure 2: Sample of the used plant leaves

E. Algorithm Flowchart

The flowchart of the overall algorithm is presented in Figure 2. The algorithm is made up of 3 fundamental components; data pre-processing, image processing (edge detection and filtering), building the neural network.

Figure 3: Flowchart of the proposed work

SIMULATION RESULT

The simulation was carried out using Intel ® core ™ i5-4200U CPU @ 2.29 GHz PC with 4GB RAM, windows 10, 64-bit OS, and MATLAB 2016b software.

Three different methods of edge detection were applied in this work to test the effect of each of them on the efficiency of our system. Figure 4 shows the results of the edge detection. Sobel method has given the best region of interest detection and hence used as the main edge detection method in this work.

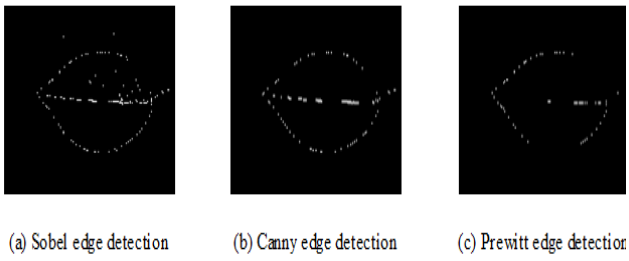

Figure 4: Edge detection results

Figure 5 presents the results obtained from the application of the different image processing techniques. The first image (a) is the original image in RGB format, (b) is the gray scale converted image, while (c) is the filtered image using Wiener filter and (d) is the segmented version of the leaf showing the edges of the leaf.

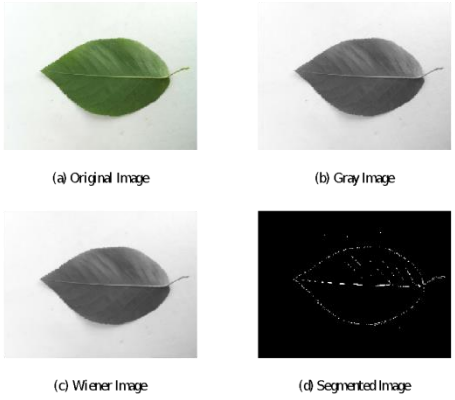

Figure 5: Image processing result

The structure of the used artificial neural network is presented in Figure 6. The network consists of 1 input layer, three hidden layers, and 1 output layer. Hidden layers are all sigmoid transfer functions while the output layer is a linear transfer function.

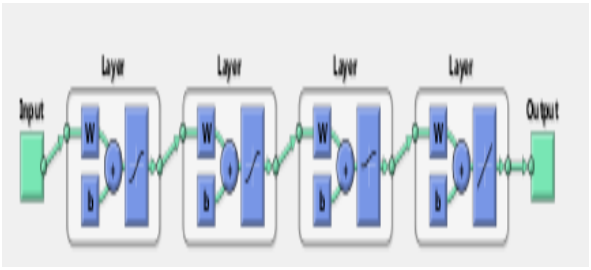

Figure 6: Structure of the ANN

TABLE I. TABLE I. ANN PARAMETERS

Parameter	***Value***
Input neuron size	2500
Output neuron size	10
Hidden neuron 1	250
Hidden neuron 2	280
Hidden neuron 3	200
Learning rate	0.01
Momentum factor	0.1
Epochs	2800
MSE	0.000002

The performance of the developed network was assessed by testing the network with a different 50 samples of the plant leaves data (5 from each plant). The parameters of the successfully trained neural network are presented in Table I. The successfully trained neural network classified the testing data correctly; hence, 100% recognition is achieved.

CONCLUSION

An algorithm has been developed for the identification of plant leaves based on image processing techniques and artificial neural networks. The simulation is by writing a matlab code that uses matlab commands. The performance of the developed network was evaluated by testing the algorithm with different samples of the plant leaves image dataset. The successfully trained neural network classified the testing data correctly; indicating 100% recognition.

REFERENCES

1. Amin, A. H. M., and Khan, A. I, "One-shot Classification of 2-D Leaf Shapes Using Distributed Hierarchical Graph Neuron (DHGN) Scheme with k-NN Classifier," in Procedia Computer Science, Vol. 2, pp.84–96, 2013.
2. R. C. Gonzalez and R. E. Woods, Digital Image Processing, New jersey: Parentice Hall, 2008.
3. K. Dimililer, Y. K. Ever and H. Ratemi, "Intelligent eye tumour detection system," in Procedia Computer Science 102 (2016) 325 – 332, Austria, 2016.

4. M. J. Kumar, D. G. R. Kumar and R. V. K. Reddy, "REVIEW ON IMAGE SEGMENTATION TECHNIQUES," International Journal of Scientific Research Engineering & Technology, vol. III, no. 6, p. 2278 – 0882, 2014.
5. Y. K. Dilpreet Kaur, "Various Image Segmentation Techniques: A Review," International Journal of Computer Science and Mobile Computing, vol. III, no. 5, p. 809 – 814, 2014.
6. Boran Sekeroglu. (2004). *Intelligent Banknote Identification System (IBIS)*. Near East University.
7. Robert, F., Simon, P., Ashley Walker; & Wolfart, E. (2003). Hypermedia Image Processing Reference. Retrieved from http://homepages.inf.ed.ac.uk/rbf/HIPR2/sobel.htm
8. Chaple, G. N., Daruwala, R. D., & Gofane, M. S. (2015). Comparisions of Robert, Prewitt, Sobel operator-based edge detection methods for real time uses on FPGA. In *2015 International Conference on Technologies for Sustainable Development (ICTSD)* (pp. 1–4).
9. Shen, D., & Tang, Z. (n.d.). Canny Edge Detection Algorithm for Image Processing Using FPGA. In *Second International Conference on Electric Information and Control Engineering* (pp.419–442).Washington. https://doi.org/10.1109/ICEICE.2012.110
10. Khajwaniya, K. K., & Tiwari, V. (2015). Satellite image denoising using Weiner filter with SPEA2 algorithm. In *9th International Conference on on Intelligent Systems and Control* (pp. 1–6). India. https://doi.org/10.1109/ISCO.2015.7282324
11. R.A.Abdulkadir1, K. A. Imam and M. Jibril, "Simulation of Back Propagation Neural Network for Iris Flower Classification," American Journal of Engineering Research (AJER), vol. 6, no. 1, pp. 200-205, 2017.

Non Orthogonal Multiple Access Based Interference Mitigation Schemes in the Emerging 5G Cellular Mobile Networks

Ndagi Muhammad Hassan, Habeeb Bello-Salau, Caroline Omoanatse Alenoghena, and Bala Alhaji Salihu
Department of Telecommunication Engineering,
Federal University of Technology Minna, Nigeria
ndagi@futminna.edu.ng, habeeb.salau@futminna.edu.ng, carol@futminna.edu.ng, salbala@futminna.edu.ng

ABSTRACT— ***The emerging 5G mobile cellular network is envisaged to accommodate the increasing data traffic growth from the unprecedented proliferation of smart devices. The developments in the internet of things (IoT) have also led to the emergence of radio access technologies that can only be handled by a network with ultra-reliable low latency. The non- orthogonal multiple access (NOMA) technology is being proposed by 3GPP for 5G network because of its high spectrum efficiency. But interference management remains a major challenge in deploying NOMA techniques. This paper studies the working principles of NOMA techniques, reviews existing NOMA based interference mitigation schemes and proposes multi antenna zero-forcing beamforming vector, two user NOMA clustering algorithm and formulates an optimization problem for power allocation to mitigate inter-cluster and inter user interference in a NOMA based 5G mobile network.***

KEYWORDS— ***Non orthogonal multiple access; 5G network; interference mitigation; Zero-forcing beamforming; power allocation; successive interference cancellation***

I. INTRODUCTION

The increasing demand for higher data rates and capacity of wireless communication systems led to evolution from the first generation (1G) to the present fourth generation (4G) and Long term Evolution (LTE) networks. Multiple access techniques have been the major technology distinguishing these different generations. The frequency division multiple access (FDMA) used in 1G, time division multiple access (TDMA) mostly for 2G, code division multiple access (CDMA) in 3G and orthogonal frequency division multiple access (OFDMA) for 4G are primarily orthogonal multiple access (OMA) schemes [7]. However, the fast growth of mobile internet propelled by unprecedented proliferation of smart devices has given rise to anticipated 1000-fold data traffic by 2020 for the fifth generation (5G) networks [6]. Moreover, due to developments in the internet of things (IoT), the 5G is envisioned to support massive connectivity of users and devices. According to the standard organizational partners; the 3rd generation partnership project (3GPP), 5G network should support three key families of applications; enhanced mobile broadband networks, massive machine type communication, and ultra-reliable low latency communications [1].

The OFDMA in 4G supports heterogeneous networks informs of femtocells and picocells but will be unable to meet new demands for massive machine type communication in 5G due to the limitation in its orthogonal resource blocks [5]. Non orthogonal multiple access (NOMA) is being introduced as an effective approach to increasing spectrum efficiency and providing the massive connectivity required in 5G. Power domain NOMA superposes multiple user signals at the transmitter over same channel (same time-frequency resources) and uses multiuser detection algorithms known as successive interference cancellation (SIC) at the receiver to detect desired signal [13].
Although NOMA offers higher spectrum efficiency and ensures massive connectivity of devices, it is prone to more signal interference because users share same spectrum at different power levels. Interference mitigation remains a major challenge in the implementation of multiple access technologies to realize 5G mobile networks. Recent research works on interference mitigation tends towards the actualization of NOMA for 5G networks. Power domain NOMA is believed to be a promising multiple access scheme for 5G. Specifically, a downlink version of NOMA known as multiuser superposition transmission (MUST) has been approved by 3GPP LTE Release 14 to identify techniques that will enable LTE support MUST. A downlink NOMA with two superposed user signals is shown in Figure 1.

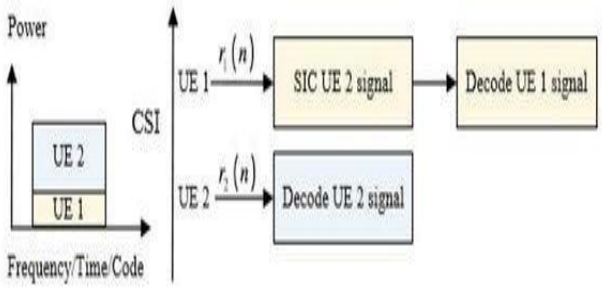

Figure 1: Downlink of a Non-orthogonal Multiple Access

The capacity gain of NOMA over conventional OMA can be illustrated by a simple SNR analysis. With OMA, two users A and B have achievable data rates as $\frac{1}{2}\log_2(1+\rho|h_A|^2)$ and $\frac{1}{2}\log_2(1+\rho|h_B|^2)$ respectively, where $\frac{1}{2}$ indicates a split of the bandwidth resources between users A and B. ρ is the SNR, h_A and h_B are channel gains for users A and B respectively. Assume $|h_A|^2 < |h_B|^2$, At high SNR $\rho \to \infty$, the sum rate can be approximated as $\frac{1}{2}\log_2(\rho|h_A|^2) + \frac{1}{2}\log_2(\rho|h_B|^2)$. While with NOMA, the achievable rates are $\log_2(1+\frac{\rho\alpha_A|h_A|^2}{1+\alpha_B\rho|h_B|^2})$ and $\log_2(1+\rho\alpha_B|h_B|^2)$, respectively where α_A and α_B are the power alloaction

coefficients. At SNR $\rho \to \infty$, the sum rate is approximated as $\log_2(\rho|h_B|^2)$, which is much more than the sum of OMA. The reason for the performance gain of NOMA over OMA can be attributed to the $\frac{1}{2}$ factor outside the logarithms of the sum rate for OMA which is due to the splitting of bandwidth resources between two users.

The basic operational principle of NOMA techniques entails multiple users been clustered and simultaneously served over the same time –frequency resources by either having their messages superposed in the power domain or code domain [7]. The inherent mutual intra-cluster and inter-cluster interference can only be managed with properly designed resource allocation techniques in conjunction with successive interference cancellation (SIC) schemes [7].
In this paper, the working principle of NOMA is described in section II, a review of NOMA based 5G interference mitigation techniques is in section III. The proposed interference aware NOMA multi antenna beamforming, two user clustering algorithm and optimized power allocation scheme is captured in section IV. Conclusions with recommendation for future works is in section V.

WORKING PRINCIPLE OF NOMA

A. Downlink NOMA Principle

The general principle of NOMA is to allow superposition of unique message signals at the BS of users in a NOMA cluster and decode desired message signal at the receiver by applying SIC. In downlink NOMA, BS transmits a superimposed signal

$$x = \sum_{i=1}^{U} \sqrt{p_i} x_i \qquad (1)$$

where x_i is the unit message signal intended for user i, $p_i$is power allocated to user i and U is total number of users in a NOMA cluster. The power allocated to a user depends on power of other users due to power constraint at BS,

$$p_t = \sum_{i=1}^{U} p_i \qquad (2)$$

where p_t is BS total power. The received i^{th} user signal is given by

$$y_i = h_i x + w_i \qquad (3)$$

where h_i is the channel gain between BS and user i, and w_i denotes Gaussian noise at the reciever for user i [16].

B. Uplink NOMA Principle

In the downlink, NOMA utilizes a power allocation and control mechanism to enable higher transmission power to be allocated to users with poor channel condition and low power to channels with higher gain [4]. Thus in a given cluster the strong interfering signals comes from the high power message signal of the relatively weak channel users. Subsequently, the user with the highest channel gain cancels all interferences while the lowest channel gain users receive all the interferences.
In the uplink NOMA, each user transmits x_i signal with p_i transmit power such that the received signal at BS can be defined by

$$y = \sum_{i=1}^{U} \sqrt{p_i} h_i x_i + w_i \qquad (4)$$

where w denotes reciever noise. The power transmitted per user is limited by their maximum battery power. Power control mechanism can be developed to enhance the performance of NOMA by allocating power coefficient to users mitigate intra-cluster interference.

C. Successive Interference Cancellation in NOMA

Successive interference cancellation (SIC) is one of the principles of NOMA implemented at the receiver terminal. The basic idea of SIC is that user signals are successively decoded. A user's signal is decoded and subtracted from the combined signals before the next user's signal is decoded. During SIC, one user's signal is decoded treating the other user's signal as an interferer, which can also be decoded with the help of the first having been already removed [11]. Prior to SIC implementation, the users are ordered according to their signal strength so that the receiver can decode stronger signals first, subtract it from the combined signals and isolate the weaker one from the residue. In brief the processes involved in decoding superposed messages can be mathematically expressed as follows: [18]. At user 1, single-user decoder g_1 decodes the message $S_1(n)$ by treating $S_2(n)$ as noise. User 2, performs the following steps to successfully recover its message from the receive signal $Y_2(n)$:

i. Decode user 1's message $S_1(n)$ by using single-user decoder g_1

ii. Subtract $\sqrt{p\beta_1} h_2 S_1(n)$ from the received signal $Y_2(n)$

$$Y'_2(n) = Y_2(n) - \sqrt{p\beta_1} h_2 S_1(n) \qquad (5)$$

a. Where h_2 is the complex channel gain at user 2

iii. Decode user's 2 messages $S_2(n)$ by applying another single user decoder on $Y'_2(n)$

SIC based receivers are prone to error propagation which may degrade the performance of some users. Therefore in designing SIC, some non-linear detection algorithms with higher detection accuracy can be considered to suppress the error propagation [7]. A typical NOMA based 5G network is illustrated in Figure 2.

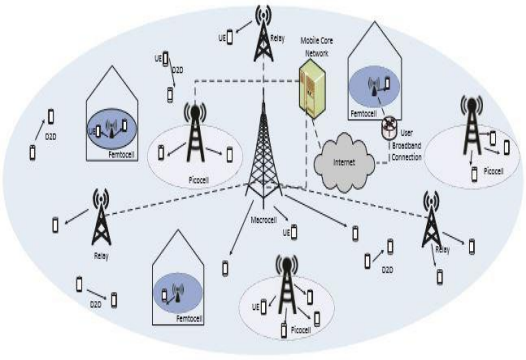

Figure 2: A proposed NOMA based multi-tier 5G mobile network.

II. REVIEW OF NOMA BASED INTERFERENCE MITIGATION SCHEMES

In [14] an uplink power control (PC) scheme for NOMA users was proposed, the scheme makes use of evolutionary game theory to dynamically adjust the transmitted power level of users which helps in mitigating user interference. The adaptive PC scheme was effective in increasing spectral and network efficiency but incurred higher complexity due to the SIC at the user end. In order to evaluate the outage performance of NOMA due to interference, [8] derived expressions for the ergodic sum rate and outage probability to demonstrate the effectiveness of NOMA with fixed power allocation. The fairness among multiple users in NOMA was considered by [17]. They developed low-complexity polynomial for adapting power allocation coefficients to control interfering users. The solution was only optimal with instantaneous and average CSI.

In [3] joint subcarrier and power allocation assignment in downlink NOMA was addressed. The solution uses matching theory by assuming equal power split and applying user subchannel matching algorithm that converges to a stable matching followed by a water-filling phase for power allocation. In order to strike a balance between computational complexity and optimality, [10] employed monotonic optimization to develop the optimal joint subcarrier and power allocation policy. Simulation results reveals the suboptimal algorithm achieves a close to optimal performance and provided substantial throughput improvement when compared to conventional multicarrier orthogonal multiple access (OMA). [9] assuming a perfect knowledge of CSI at the BS proposed a low complexity sub-optimal algorithm for energy efficient channel assignment and power proportional factors determination for subchannel multiplex users.

Using the channel gain difference among users in NOMA cluster, [2] derived the optimal power allocation policy that maximizes sum throughput per NOMA cluster and in turn maximizes the overall system throughput. Numerical compared the performance of NOMA over orthogonal multiple access and indicates significant improvement. In [8] an opportunistical user pairing model by statistically allocating transmission powers among NOMA users was proposed. Simulation results shows the scheme significantly improved system throughput when compared with conventional OMA.

In [19] multi-input multi-output (MIMO) technology with zero-forcing beamforming and minimum mean square error (MMSE) SIC scheme in NOMA to mitigate interference between clusters was applied. They proposed an interference predicted minimum mean square error (IPMMSE) SIC by modifying the MMSE weight factor using interference signals. The simulation results shows that the bit error rate (BER) is degraded putting into consideration the performance of practical SIC schemes. [21] investigated system level throughput performance of NOMA with minimum mean square error based linear filtering (MMSE-SIC) in the uplink NOMA. They employed a weighted proportional fair (PF)-based multiuser scheduling scheme to achieve a good tradeoff between total user throughput and cell-edge user throughput. The simulation results reveals significant enhancement in system level throughput compared to the orthogonal access which widely used in 3.9 and 4G mobile communication systems. [12] applied genetic algorithm (GA) for cluster user pairing and iterative gradient ascent method (IGAM) as an optimal power allocation technique for each user group in NOMA downlink systems. Simulation results shows that GA based NOMA achieves the same performance with the conventional exhaustive search methods with slightly lower complexity.

[19] developed a joint user association and power control optimization algorithm to determine the traffic load in energy corporation enabled Helnets. The algorithms achieved higher energy efficiency than existing OMA schemes but the computation complexity contributes to the overhead that may not be realizable for practical applications. [10] investigated zero-forcing beamforming and random beamforming making use of the imperfect CSI feedback with semi-orthogonal user selection algorithm to reduce the interference between NOMA users. Numerical results shows NOMA systems with limited CSI still gains larger rate over OMA schemes but only suitable with random beamforming which is not good in mitigating inter-beam interference. [20] proposed a novel receiver design for NOMA systems. The advantage of the receiver is that it has less complexity when compared with ideal SIC, although the complexity is still high for practical applications.

III. PROPOSED NOMA BASED INTERFERENCE MITIGATION SCHEMES

The proposed interference aware and mitigating schemes comprise algorithms that will be developed for a multi antenna zero-forcing beamforming technique at the transmitter to mitigate inter-cluster interference. A two user per cluster selection algorithm to reduce inter-user interference. An optimized power allocation method for the selected users in a cluster.

A. AMulti-Antenna Array Zeroforcing Beamforming (ZFBF)

In order to mitigate inter-cluster interference with the ZFBF in a two users per cluster NOMA based system, the stronger channel gain (h) user will be used to generate the BF vector. Assuming a perfect CSI, and based on channel matrix of the stronger user in the cluster the BF-vector (w_k) must satisfies the conditions in equation 7.

$$\frac{H_{n,1}}{|H_{n,1}|}.w_k = \{0, \text{ for } n \neq k1, \text{ for } n = k \quad (7)$$

Assume $H = [h_{1,1}{}^T \ldots h_{1,N}{}^T]^T$ where $(.)^T$ means transpose of a matrix.

Then

$$w = H^+ = H^*(HH^*)^{-1} \quad (8)$$

Where $(.)^{+}$ and $(.)^{*}$ are the pseudo-inverse and conjugate transpose of H

B. User Clustering Algorithm

In developing a user clustering algorithm, two users will be considered per cluster; a strong channel user k_1 and weak channel user k_2. Strong users in a cell will be distributed into different NOMA clusters. Key point of the proposed clustering algorithm is to pair highest channel gain user with lowest channel gain user in a cluster. Second highest channel gain user with second lowest channel gain user in the same cluster and so on. Based on these guidelines, users will be grouped into two sets: Group A and Group B, the users in group A denoted will have much higher channel gains compared to users in group B.

C. Optimized Power Allocation Algorithm

Based on the two user per cluster downlink NOMA, the channel gains of users k_1 and k_2 can be assumed to be γ_1 and γ_2 respectively. while $P_1$and P_2 are the transmission powers of γ_1 and γ_2 respectively. The NOMA principle gives higher power allocation to the weaker channel users, therefore an algorithm for optimal power allocation problem can be formulated by allocating $\frac{2}{3}$of total power P_t to the weak user.

$$\max \omega B \sum_{i=1}^{2} \log_2\left(1+\frac{P_i\gamma_i}{\sum_{j=1}^{i-1} P_j\gamma_i+\omega}\right) \quad (9)$$

Subject to: C_1: $\sum_{i=1}^{2} P_j = \frac{2}{3}P_t$

Where ω is the resource block each of bandwidth B allocated to a cluster.

IV. CONCLUSION

Although NOMA techniques is being proposed as a candidate for 5G network, its advantage of having very high spectrum efficiency can only be harnessed with careful interference aware resource allocation design. In this paper we reviewed some of the NOMA interference aware designs and proposed a multi antenna zero-forcing beamforming array with a two user cluster algorithm and an optimized power allocation scheme.

References

[1] G. A. Akpakwu, B. J. Silva, K. P. Hancke, and A. M. Abu-Mahfouz, "A Survey on 5G Network for Internet of Things: Communication Technologies and Challenges" IEEE ACCESS, vol.1, No.4, pp. 3619-3647, 2018.

[2] M. S. Ali, E. Hossain, M. J. Hossain, T. Tabassum, and D. I. Kim, "Non-orthogonal multiple access (NOMA) in cellular Uplink and Downlink: Challenges and Enabling Techniques" http://128.84.21.199/abs/1608.05783. 2016.

[3] L. S. Bayat, and Y. Li, "Radio Resource Allocation for Downlink Non-orthogonal Multiple Access (NOMA) Networks Using Matching Theory," IEEE Global Communication Conference, Vol 2. No.6, pp. 1205-1225, 2015.

[4] K. Benjebbour, K. Saito, A. Li, Y. Kishiyama, and T. Nakamura, "Non-orthogonal muiltiple access (NOMA): Concept Performance Evaluation and Experimental trials" IEEE International Conference on Wireless Networks and Mobile Communication, 2016.

[5] Y. Cai, Z. Qin, F. Cui, G. Ye Li, and J. McCann "Modulation and Multiple Access for 5G Networks" IEEE Survey and Tutorials Vol. 20 No.1 pp. 629-645, 2018.

[6] T. Dateki, H. Seki, and M. Minowa" From LTE -Advance to 5G : Mobile Access system in progress" Journal of fujitsu Science and Technology, Vol. 52 No.2 pp. 92-108, 2016.

[7] L. Dai, B. Wang, Y. Yuan, S. Hen, I. Chih-Lin and W. Zhaocheng "Non-orthogonal Multiple Access for 5G: Solutions, Challenges, Opportunities, and future Reseach" IEEE Communication Magazine, Vol. 9 No.53 pp. 74-81, 2015.

[8] Z. Ding, P. Fan, and H. V. Poor " Impact of User Pairing on 5G non orthogonal Multiple Access downli nk Trans mission" IEEE Transaction Vehicular Technology Vol. 65, No.8 pp. 1-12, (2014).

[9] F. Fang Z. Haijun, and C. M. Victor, "Energy Efficient Resource Allocation fpr Downlink Non-Orthogonal Multiple Access Network" IEEE Transactions on communications, Vol. 64, No. 9, 2016.

[10] S. Liu, and C. Zhang, "Non orthogonal Multiple Access in A Downlink Multiuser Beamforming system with Limited CSI Feedback" EURASIP Journal on communications and Networking, pp. 236, 2016.

[11] N. I. Mirikidis, and D. D. Vergados, " A Survey on Successive interference Cancellation Performabce frp Single-antenna and Multiple-antenna OFDMA systems" IEEE Communication surveys Tutorials Vol.15 No.1 pp. 312-335, 2013.

[12] F. G. Omer, K. Fatih, H. Ibrahim, and K. K. Gunes, "Resource Allocation for Downlin k NOMA System: Genetic Algorithm Approach" IEEE International Conference on Telecommunication and Signal Processing, **ISBN:** 978-1-5090-3982-1, 2017.

[13] S. M. Riazul Islam, N. Avazov, O. A. Dobre, and K. Kwak, "Power Domain Orthogonal Multiple Access (NOMA) in 5G Systems:Potentials and Challenges" IEEE communication Surveys and Tutorials, (2016) (2016) Vol. 19, No.2 pp.721-742, 2016.

[14] S. Riaz, and U. Park, " Power Control for Interference mitigation by evolutionary game theory in Uplink NOMA for 5G Networks" Journal of Chineese Institute of Engineers, Vol. 41, No.1 pp. 18-25, 2018.

[15] X. Su, , H. Yu, W. Kim, C. Choi, and D. Choi, " Interference Cancellation for Non –orthogonal Multiple access used in Future Wireless mobile Networks" Journal on wireless Communications and Networking, Issue 232 pp. 1-12, 2016.

[16] H. Tabassum, M. Shipon, E. Hossain, M. J. Hossain, D. I. Kim, "Non orthogonal Multiple Access (NOMA) in Uplink and Downlink: Challenges and Enabling Techniques" IEEE Transacions in Communications, Vol. 65, No.8 pp. 3555-3570, 2016.

[17] S. Timotheou and I. Krikidis "Fairness for Non-orthogonal Multiple Access in 5G Systems" IEEE Signal Processing Letters, Vol. 22 No.10 pp.1647-1651, 2015.

[18] S. Vanka, S. Srinivasa, Z. Gong, P. Vizi, K. Stamatiou, and M. Haenggi, "Superposition Coding Strategies: Design and Experimental Evaluation" IEEE Transaction on Wireless Communications, Vol.11, No.7, pp. 2628-2639 2012.

[19] B. Xu, Y. Chen, C. J. Riquena, and T. Zhang "Resource Allocation IN Energy Corporation Enabled Two- Tier

NOMA Helnets Towards Green 5G" IEEE Journal on Selected Areas in Communications, Vol. 35, No.12, pp. 2758-2770, 2017.

[20] C. Yan, A. Harada, A. Benjebbour, L. Yang, A. Li, and H. Jiang, "Receiver Design for Downlink Non orthogonal Multiple Access (NOMA)" IEEE 81st Vechicular Technology Conference (VTC Spring), **ISBN:** 978-1-4799-8088-8, 2015.

[21] E. Yuki, K. Yoshihita, and H. Kenichi "An Uplink Non orthogonal Access with MMSE-SIC in the Presence of Inter-cell interference" IEEE International Symposium on Wireless Communication Systems (ISWCS), **ISSN:** 2154-0225, 2012.

The Influence of Information and Communication Technology on Entrepreneur Skills Acquisition Among Business Education Students in Tertiary Institution in Zaria Metropolis

Mahmood Abdullahi
Department of Vocational and Technical Education
(ABU Zaria, Nigeria)
Email: saikomansur@gmail.com

A. A. Sadiq
Department of Communications Engineering
(ABU Zaria, Nigeria)
Email: aasadiq@abu.edu.ng

ABSTRACT— This research work carried out on the Influence of Information and Communication Technology on Entrepreneur Skills Acquisition among Business Education Students in Tertiary institution in Zaria. The researcher raised 4 objectives and 4 research Question, Among the objectives are; ascertain the nature of ICT tools used by lecturers and students in teaching and learning in Business Education Programme; Determine the uses of ICT tools in the development of business education students' entrepreneurial skills. The population of the study was 486 and 100 respondents were used as the sample size. The researcher employed survey method. Questionnaire was used as instrument for data collection. The researcher recommended that undergraduate students should be provided with necessary skill acquisition tools that will make them self-employed on graduation. These tools should be computer oriented as manual methods of doing things in the business world of today are fast being forgotten in our modern world of today; ICT tools like computers, projectors and internet facilities should be provided and made available to the department as the ones available at the moment are grossly inadequate and students have little or no access to them for their practical, thereby necessitating a theoretical or traditional system of teaching.

KEYWORDS: Entrepreneur, ICT, Tools, Acquisition and Vocation.

I. INTRODUCTION

The advent of Information and Communication Technology (ICT) has greatly impacted the development and growth of modern society. This impact could be felt in the field of science and technology, economy, marketing, medicine, and politics. Other fields that the impact of ICT has been felt are human interaction and communication, agriculture, engineering, aviation and education. Presently, there have been new dimensions to the use of ICT to create job and empower human to become self-reliant to the extent that they become not only job learners but job creators. Information and Communication Technology (ICTs) have become within a very short time, one of the basic building blocks of entrepreneurial and skills development in modern society. Many countries having understood the Impact of ICT which includes speed of business, dynamism in innovations, the creation of business and market opportunities with the wide range of links and market.

Information Communication Technology (ICT) tools have been developed to train and equip individuals with skills that are needed in their various field of human endeavor, (Oni 2007). The use of information and communication technology (ICT) is becoming an integral part of education in many parts of the globe. The dynamism in the use ICT application to education has enhances the delivery and access to knowledge, and improves the curriculum. It produces richer learning outcomes compared to education without ICT. It encourages critical thinking and offers unlimited means of achieving educational goals.

Education is the totality of life experience that man acquires and which enables him to cope with and derive satisfaction from living in the word. This is because it enables him to achieve social competence and optimum individual development (UNESCO, 2002). Business Education which is a subset of the general education can be seen as the development of person's head, heart and hands for his self fulfillment and optimum services to humanity and also empowers him economically. It is pertinent to note that education can be a means to an end. It can simply be a tool for securing employment and emancipation of people through the provision and acquiring of necessary knowledge and skills to make lives more flourishing.

Recent advancements in scientific discoveries have made the world a global village, changing tremendously the business world around us as a result of new technologies. The rapid technological changes are profoundly altering the business dynamics, redefining the shape of private firms, forcing not only companies that employ business education graduates to review and restructure how they communicate with their customers but also signal to the institutions that produce these students to review and restructure how to prepare the students by exposing them to technological tools that will equip them for entrepreneurial challenges. It is therefore important for business educators to educate, train and empower the students with knowledge and skills they need in their entrepreneurial endeavors after graduation. Toomey (2001) stated that integrating ICT in schools is intended to improve students' learning, to offer flexible learning opportunities and improve the efficiency of their business practices. According to Okoro (2009) "ICT has become a critical tool for vocational training. The sooner students know how to use products of ICT, the easier they can find their way in the ever-dynamic society like Nigeria."

Business education as a discipline has many options such as accounting, secretarial technology, and commerce as well as marketing/distributive education. Okolochaet. al., (2012) stated that Business Education trains her students in business skills and knowledge necessary for office career,

occupations and in management of personal business ventures using the services and ethics of business to modify attitudes and behaviours so as to achieve the objectives envisaged as office workers, entrepreneurs, producers of goods and services.

Ekpenyong and Ojo (2008) identified the goals of business education to include adopting the various business concepts, acquiring skills and competencies required for the performance of basic jobs such as handling minor administrative decisions, financial records and transactions, including playing productive roles in a free enterprise economy. Emphasizing on the objective of business education, Njoku (2006) opined that one of the goals of business education is to empower graduates with desired skills, knowledge and value to perform specific functions so as to become self-reliant. Hence, Business education as a field of study entrusted with the entrepreneurial skill development of undergraduates has been saddled with the responsibility to undertake this vanguard. Having recognized the demanding task of training, education and skill development in the modern time, synonymous to the need of the country as well as the graduates for employment and empowerment, ICT becomes the tools to embrace, adopt and use as the new tool to achieve this goal.

For many developing countries, entrepreneurship has been a powerful engine of economic growth and wealth creation, and is crucial for improving the quality, number and variety of employment opportunities for the poor. It has several multiplier effects on the economy, encourages innovation, and fosters investment in people, which is a better source of competitive advantage than other natural resources, which can be depleted, Oteh, (2009). Entrepreneurs create new enterprises, new commercial activities, and new economic sectors. They generate jobs for others; they produce goods and services for society; they introduce new technologies and improve or lower cost outputs; and they earn foreign exchange through export expansion or the substitution of imports.

In the words of Ngumbi (2004) educational institutions should provide more relevant forms of education designed to promote self-reliance and responsible entrepreneurial capacity for self-employment and community development to reduce unemployment and to revitalize national development. Entrepreneurial skills is in this light is aimed at providing vocational trainees with the skills necessary to make them self-employed in future.

The key to the success of establishing a culture of entrepreneurship in Nigeria is education. Apart from the educational impact of the home, the school can be regarded as the place where the most (holistic) profound impact can be brought about in the development of the youth. Economic growth in industrialized as well as developing countries remains a central issue and, as such, particular interest is focused on the role of entrepreneurship to achieve and maintain open and modern economies. In this regard, the importance of business education in our modern society as well as the growing demand for employment among our university graduates cannot be overemphasized. More so, entrepreneurial skill education should be the core area where business education which has been regarded as that aspect of education which provides the recipients with the basic knowledge and practical skills needed for entry into the world of work as employees or as self-employed must be inculcated into the life of its recipients (students). The essence of this, is to imbibe a more veritable and practicable system of economic empowerment on our youths and reduce dependence on the proverbial "white collar" job which is largely dependent on paper qualification than practical skills and knowledge, a dilemma which stares at us all and a source of concern to our educational system in particular and the government in general.

II. STATEMENT OF THE PROBLEM

Business Education graduates are among the proportion of students from numerous tertiary institutions in the country, who's after graduation engaged into the labour market. This accounts for approximately a high proportion of the new entrants into the Nigerian labour market every year. Due to the shrinking labour market, and slow growth of the industrial sector, this workforce cannot be entirely absorbed in the formal wage employment. The result of this scenario has been high unemployment among Business Education graduates with some opting to join self-employment which they are ill prepared.

It has been argued that entrepreneurial skills can be both learned and experientially acquired or they can be influenced considerably through strategic measures such as business education (European Commission, 2004), but this has not been the case as entrepreneurial skill which is considered a vital ingredient to training of a business student has been poorly embedded into the training system with some times no meaningful impact. This could be seen as an integral aspect which vocational education (Business Education) in our tertiary institution could explore to empower students primarily to learn business trade and skills that will be economically beneficial and self-sustaining to them after graduation.

However, we are witnessing an era where the basic infrastructures (ICT tools) needed to inculcate knowledge into the students are not readily available or at most times not provided to educational institutions of learning for onward impartation. This has made the students lagged behind when they go out to face the reality of the changing world, we live in. More so, the continual lag of the country is evident also in the system of education that places less emphasis on vocational learning and training of undergraduate with ICT skills. It is based on this premise that the researcher is researching on the Practical Application of ICT tools in the development of entrepreneurial skills of students through Business Education.

III. OBJECTIVES OF THE STUDY

The general objective of this study is to determine the influence of information technology on entrepreneur skills acquisition of business education students in tertiary institution while the specific objectives are to:

- ascertain the nature of ICT tools used by lecturers and students in teaching and learning in Business Education Programme.

- determine the uses of ICT tools in the development of business education students' entrepreneurial skills.
- determine the types of skills acquired by students in business education programme.
- ascertain the benefits on the use of ICT in the teaching and learning of Business Education Programme.

RESEARCH QUESTIONS

The study will be guided by the following research questions.

- What are the types ICT tools used in teaching and learning of business Education in Federal College of Education Zaria?
- To what extent has the teaching of ICT help in the development of Business Education studentsin Federal College of Education Zaria?
- What are the benefits of ICT in the teaching and learning of business education in Federal College of Education Zaria?
- What are the types of ICT tools bystudents in Business Education programmein Federal College of Education Zaria?

IV. LITERATURE REVIEW

Looking at the work of Musa (2008) title "Impact of ICT on Business Education programme: A case Study of Federal College of Education, Zaria" The objective of the study was to determine the systematic impact of ICT on business education programme and also examine the role played by business educators in integrating ICT into business education curriculum.

Data for this study was gathered through the distribution of questionnaires to both students and lecturers. Out of the total number of students and lecturers used in the study, which is 236, a sample population of 65 was used and the statistical tool used to interpret the data is the like scale. The study found that there is a non-challenge attitude towards to integration of ICT to Business Education, thereby making the students graduate without adequate knowledge of ICT. The study subsequently recommended that business educators should do everything possible to see that a comprehensive ICT and business education packages were incorporated into the curriculum contents of business education programme at the degree level.

The study was carried out on the Impact of ICT to Business Education thereby negating the specific roles ICT tools plays in the life of the Business Education students after school. The researcher used 65 as the sample size from a population of 236 which is short of the required percentage given by the scholar quoted in the work. Despite this, the research work is related to the current study because it looks at the significance of ICT to reaching and learning Business Education in Colleges of Education.

Leo (2010) in her study titled "The relevance of information technology on Business Education Programme in Federal College of Education, Zaria sought to know how information technology can be used to facilitate the acquisition and development of skills, competence, attitudes and attributes in business education which are necessary for efficiency in the economic system. The objective of the study includes;

- To determine the relevance of information technology devices in the Business Education Department of Federal College of Education, Zaria
- Assess the availability of information technology devices in the Business Education Department of Federal College of Education, Zaria
- Determine the academic qualification of lecturers in relation to information technology and business education
- Assess business students' interest in the use of information technology in the teaching and learning process in the business education programme in Federal College of Education, Zaria

The population of the study consists of a total of 12 lecturers and 57 students from Pre-NCE to NCE three(3) levels. Questionnaire was used in gathering data and the frequency distribution and percentages was used in analyzing the data. The study found that business student in FCE, Zaria perceive information technology as a new trend necessary for maximum performance and learning in their various career fields in the future and subsequently recommended that the curriculum should be readjusted to include the practical aspect of information technology at all levels of education so that students of business education can have the basic knowledge of information technology. The researcher finds this work valuable as a reference material for the completion of this work.

V. RESEARCH DESIGN

For the purpose of this study, the survey method will be employed for the conduct of this work. Surveys are used by behavioral scientist to describe people's opinion and attitudes (Adekoye, 2011). The survey method which is one of the categories of descriptive methods of research has been described also by Wimmer, R, D., and Dominick, J. R., (2011) as having the advantage of being an effective means of collecting data from a large number of sources and it is relatively inexpensive and takes short time. It is for this obvious reason that the researcher decided to employ a descriptive survey method as an appropriate means for the study to getting a great deal of specific information.

VI. POPULATION OF THE STUDY

Khan (2007) sees population "as the aggregate number from which a sample is taken; this population may be small or large. The population of this study is 486 NCE students of the Department of Business Education, Federal College of Education (FCE), Zaria.

The study covers the entire NCE Business Education students. The breakdown of the population is in Table 3.1 comprising NCE I, II, and III irrespective of gender.

Table 3.1: Population for the Study

S/N	LEVEL	NUMBER OF STUDENTS
1	NCE I	164
2	NCE II	187
3	NCE III	135
Total		486

Source: HOD Office, Business Education Department FCE, Zaria

VII. SAMPLING AND SAMPLING TECHNIQUE

The sample size of this study was based on the principle of Borg and Gail (1979) who said samples are representatives of the whole population in which generalization could be made using this principle, the researcher made use of 120 respondents conveniently drawn from the population of the study. The sample size was derived using the recommendations of Morgan and Krajcie (1970).

Sample size

Table 3.2 Population Distribution

Respondents	Population	Sample Size	Percentage (%)
Lecturers	5	3	1.68
100 L	23	12	10.08
200 L	76	30	25.21
300 L	82	35	29.41
400 L	74	40	33.61
	260	120	100

VIII. INSTRUMENT OF DATA COLLECTION

The instrument for data collection in this study was mainly the questionnaire. The Questionnaire was constructed using the four-point LIKERT format (Strongly agreed-SA, Agreed-A, Disagreed-D and Strongly disagreed-SD) to elicit respondents' degree of response necessary for meaningful interpretations. This focused specifications to get responses from given options to enable the study provide measurable answers to research questions. The researcher used questionnaire because questionnaire is seen as a very important instrument in research and can stand the test of time (Alamu, 2008).

The questionnaire was drawn in order to elicit response from respondents to answer the research questions earlier postulated in chapter one. The questionnaire comprised twenty-eight (28) question items generated from the four (4) research questions.

QUESTIONNAIRE RATING

The technique used in the rating of the questionnaire is the four (4) point scale of numerical values. In order to obtain the needed response, the researcher provided each questionnaire items with four (4) options from which the respondents choose. Each total response in any scale is multiplied by the numerical value before final calculation by percentage (%). This was an understanding of Tuckman (1979) who introduced the equal appearing interval scale. It was a four pointed scale in which the interval between each point on the scale was assumed to be equal. It was used to register the extent of agreement of disagreement with a particular statement of an attitude, belief or judgment. The items were constructed both in positive and negative directions. The scoring key for the positive and negative items will be as shown table 3.4

METHOD OF DATA COLLECTION

The researcher collected data with a view to answer the research questions. Data was personally distributed and collected by the researcher and with the assistance of some designated people in the Business Education Section, Department of Vocational and Technical Education, Faculty of Education Ahmadu Bello University, Zaria.

Method of Data Presentation

For the purpose of this study, the data collected will be grouped and analysed according to research questions and the percentage of the frequency of their agreement and disagreement represented in a tabular form for easy computation and understanding for the purpose of data analysis. Strongly agreed and Agreed formed the positive responses for the acceptance of the statement made, while disagreed and strongly disagreed formed the negative response for rejection accordingly. The result will be interpreted and the findings made at the concluding chapter will be used to make recommendations accordingly.

This formula will be used to calculate the agreed and disagreed percentages:

$$Agree = \frac{Totalagree}{Totalresponse} x \frac{100}{1} = \%Agree$$

$$Disagree = \frac{Totaldisagree}{Totalresponse} x \frac{100}{1} = \%Disagree$$

ANALYSIS OF DATA

Each of the items in the questionnaire was grouped in accordance with their relationship and analyzed using frequency distribution. The data were analyzed in four sections based on four research questions. Each section consists of respondent's response to each research question and presented in a tabular form and discussed as shown in the following tables below:

TYPES OF TOOLS USED IN TEACHING AND LEARNING BUSINESS EDUCATION IN FCE ZARIA

Table 4.2.1: All lecturers used ICT tools in teaching and learning in the department

Responses	Frequency	Percentage
Agreed	40	40%
Strongly agreed	10	10%
Disagreed	30	30%
Strongly disagreed	20	20%
Total	100	100%

The above table indicates that 40 respondents representing 40% agreed with the above statement, 30 respondents representing 30% disagreed, 20 respondents representing 20% strongly disagreed, while only 10 respondents representing 10% strongly agreed. This implies that majority of the respondents believe that all lecturers used ICT tools in teaching and learning in the Department.

Table 4.2.2: Lecturers make the use and application of ICT to improve your performance in teaching and learning

Responses	Frequency	Percentage%
Agreed	30	30
Strongly agreed	40	40
Disagreed	17	17
Strongly disagreed	13	13
Total	100	100

The above table shows that 30% of the respondent agrees with the statement that; lecturers make the use and application of ICT to improve their performance, 40 strongly agreed, 17% disagreed while only 13 n% strongly disagreed.

This implies that Lecturers make the use and application of ICT to improve their performance in teaching and learning

Table 4.2.3 All computers in computerlaboratory are connected withprinters

Responses	Frequency	Percentage %
Agreed	10	10
Strongly agreed	15	15
Disagreed	30	30
Strongly disagreed	45	45
Total	100	100

The table above shows that 10 respondents representing 10% agreed with the above statement, 15 respondents representing 15% strongly agreed, 30 respondents representing 30% disagreed, 45 respondents representing 45% strongly disagreed.This implies that most computers in computer laboratory are not connected with printers.

Table 4.2.4 Your Department is connected withinternet facilities

Responses	Frequency	Percentage %
Agreed	20	20
Strongly agreed	5	5
Disagreed	5	5
Strongly disagreed	70	70
Total	100	100

The above table reveals that 20 (20%) agreed with the above statement, 5(5%), 5(5%) disagreed and strongly agreed, 70(70%).

This shows that the department is not connected with internet facilities.

Table 4.2.5 Typewriters are used in Teaching and Learning in your Department

Responses	Frequency	Percentage %
Agreed	30	30
Strongly agreed	70	70
Disagreed	-	-
Strongly disagreed	-	-
Total	100	100

The table above shows that 30 respondents representing 30% agreed with the above statement, 70 respondents representing 70% strongly agreed.

TO WHAT EXTENT HAS ICT HELP IN DEVELOPMENT OF STUDENTS IN FCE ZARIA?

Knowledge of ICT helps students to perform better

Responses	Frequency	Percentage %
Agreed	30	30
Strongly agreed	70	70
Disagreed	-	-
Strongly disagreed	-	-
Total	100	100

The table above clearly shows that 30 respondents representing 30% agreed with the above statement, while 70 respondents representing 70% strongly agreed with the above statement.

This reveals that Knowledge of ICT helps students to perform better.

Table 4.3.2 Availability of ICT Facilities in your Department Motivate Student to Learn Faster

Responses	Frequency	Percentage%
Agreed	40	40
Strongly agreed	30	30
Disagreed	20	20
Strongly disagreed	10	10
Total	100	100

The table above shows that 40$ of the respondents believe that availability of ICT facilities in their department motivate students to learn faster, 30% of the respondents strongly agreed, 20% disagreed while only 10% strongly disagreed with the above statement.

This indicates that Availability of ICT Facilities in their Department Motivate Student to Learn Faster.

ICT saves time in teaching and learning word processing in Department

Responses	**Frequency**	**Percentage** %
Agreed	100	100
Strongly agreed	-	-
Disagreed	-	-
Strongly disagreed	-	-
Total	100	100

All the respondents agreed that ICT saves time in teaching and learning word processing in their department

Provision of ICT in your department increases the student' performance in learning word processing.

Responses	**Frequency**	**Percentage** %
Agreed	50	50%
Strongly agreed	30	30%
Disagreed	15	15%
Strongly disagreed	5	5%
Total	100	100%

The table above indicate that 50 respondents representing 50% agreed with the above statement, 30 respondents representing 30% strongly agreed, 15 respondents representing 15% disagreed, 5 respondents representing 5% strongly disagreed.

This implies that provision of ICT in their department increases the student' performance in learning word processing.

WHAT ARE THE SKILLS ACQUIRED BY STUDENTS IN BUSINESS EDUCATION PROGRAM IN FCE ZARIA?

Table 4.4.1: Most of the accounting students in your department have skills of self-reliance after graduation

Responses	**Frequency**	**Percentage** %
Agreed	40	40
Strongly agreed	60	60
Disagreed	-	-
Strongly disagreed	-	-
Total	100	100

Table 4.4.1 above indicates that 40 respondents representing 40% agreed with the above statement, 60 respondents representing 60% strongly agreed, while none of the respondents chooses disagreed or strongly disagreed as their opinion in regards to the question above.

This reveals that majority of the respondents strongly agreed that most accounting students in their department have skills of self reliance after graduation.

Table 4.4.2: Most of the marketing students have knowledge and skill of self reliance after graduation.

Responses	**Frequency**	**Percentage** %
Agreed	100	100
Strongly agreed	-	-
Disagreed	-	-
Strongly disagreed	-	-
Total	100	100

The table above implies that, all the 100 respondents representing 100% that responds to this questionnaire agreed that most of the marketing students have knowledge and skill of self reliance after graduation.

Table 4.4.3: The entrepreneur skills motivate students in teaching and learning in your department.

Responses	**Frequency**	**Percentage** %
Agreed	40	40
Strongly agreed	20	20
Disagreed	35	35
Strongly disagreed	5	5
Total	100	100

The above table shows that 40 respondents representing 40% agreed with the above statement, 20 respondents representing 20% strongly agreed, 35 respondents representing 35% disagreed, 5 respondents representing 5% strongly disagreed.

This reveals that majority of the respondents agrees with the fact that the entrepreneur skills motivate students in teaching and learning in the department.

Table 4.4.4: Administration skills give motivation in teaching and learning in the department.

Responses	**Frequency**	**Percentage** %
Agreed	20	20
Strongly agreed	30	30
Disagreed	40	40
Strongly disagreed	10	10
Total	100	100

Table 4.4.4 above shows that 20 respondents representing 20% agreed with the above statement, 30 respondents representing 30% strongly agreed, 40 respondents representing 40$ disagreed, while only 10 respondents representing 10% strongly disagreed.

This implies that majority of the respondents disagreed with the statement that Administration skills give motivation in teaching and learning in the department

BENEFITS OF I.C.T IN TEACHING AND LEARNING BUSINESS EDUCATION PROGRAM IN FCE ZARIA.

Table 4.5.1 The knowledge of ICT gives students motivation pertaining their education in teaching and learning.

Responses	**Frequency**	**Percentage** %
Agreed	30	30
Strongly agreed	20	20
Disagreed	25	25
Strongly disagreed	25	25
Total	100	100

The table above shows that 30(30%) agreed with the above statement, 20(20%) strongly agreed, 25(25%) disagreed, 25(25%) strongly disagreed. This implies that majority of the respondent believes that knowledge of ICT gives students motivation pertaining their education in teaching and learning.

Table 4.5.2: Knowledge of ICT makes students to understand what is taught them faster

Responses	**Frequency**	**Percentage** %
Agreed	40	40
Strongly agreed	30	30
Disagreed	25	25
Strongly disagreed	5	5
Total	100	100

The table above shows that 40 representing 40% agreed with the above statement, 30 respondents representing 30% strongly agreed, 25 respondents representing 25% disagreed, while only 5 respondents representing 5% strongly disagreed. This implies that knowledge of ICT makes students to understand what is taught them faster.

Table 5.5.3 ICT knowledge creates maximum relationship between teachers and the students in the department

Responses	**Frequency**	**Percentage** %
Agreed	40	40
Strongly agreed	20	20
Disagreed	17	17
Strongly disagreed	23	23
Total	100	100

Table 5.5.3 above shows that 40 respondents representing 40% agreed, 20 respondents representing 20% strongly agreed, 17 respondents representing 17% disagreed, 23 respondents representing 23% strongly disagreed with the above statement.

This implies that ICT knowledge creates maximum relationship between teachers and the students in the department.

Table 5.5.4 Knowledge of ICT makes staff and students to have more competence while performing their activities inyour department

Responses	**Frequency**	**Percentage**
Agreed	50	50%
Strongly agreed	30	30%
Disagreed	15	15%
Strongly disagreed	5	5%
Total	100	100%

The above table shows that 50 respondents representing 50% agreed with the above statement, 30 respondents representing 30% strongly agreed, 15 respondent 15% disagreed while only 5 respondents representing 5% strongly disagreed.

This implies that Knowledge of ICT makes staff and students to have more competence while performing their activities in your department.

SUMMARY

The study had four objectives and four research questions were raised to guide the study. The researcher adopted the descriptive survey research as the methodology for the study. The population of the study was 250 (for instance) and the sample was 100 (for instance) students taken from NCE 1,2, and NCE 3. Random selection as employed to determine the sample size of the study. A structural questionnaire was used as the instrument for data collection. The researcher personally administered the instrument, this process took one week. Data collection from respondents were analyzed using descriptive statistic and percentage.

The finding of this research reveals that Though ICT technologies are provided and being used in the Department for both teaching and learning by lecturers and students, it is grossly inadequate, thereby necessitating the inaccessibility by the students who are supposed to be beneficiaries.

Business Education lecturers do not make use of ICT tools in teaching and learning, which have impacted negatively in developing the entrepreneurial skill of Business Education students.

ICT tools are very much helpful and beneficial in improving teaching and learning of entrepreneurial skill among students of Business Education and will go a long to offer better job options to students after school

Furthermore, the challenges being faced in the adoption of ICT tools by business lecturers and students are amongst others to include; poor state of power, high cost of ICT tools, lack of qualified teachers, and also the inability of the Department to provide these tools.

CONCLUSION

In regard to the data analyzed and the major findings of this research work. The research wishes to draw the following conclusion.

ICT tools like computers, projectors and internet facilities in the department are insufficient and hinder the students from being effectively equipped for the world of work after graduation.

Business Education lecturers do not provide practical teaching and mastering of ICT technologies to students in the classroom.

Practical application of ICT tools will go a long way in providing and equipping individual students and potential business educators with basic skills, competencies, experiences and attitudes necessary for the world of work and saleable skills for job creation.

The prospects of ICT tools to the Business Education student surpass the challenges if only the right attitude will be cultivated by Business Educators.

Business Education students must be economically empowered through entrepreneurial skills and practical knowledge that will help them take advantage of the business opportunities which are bound out there after graduation.

RECOMMENDATION

It is recommended that undergraduates be provided with necessary skill acquisition tools that will make them self-employed on graduation. These tools should be computer oriented as manual methods of doing things in the business world of today are fast being forgotten in our modern world of today.

Government must pay more attention to vocational education and constitute a monitoring committee that will checkmate the activities of vocational schools and institutions running the programme. This is because skills acquisition which is the backbone of vocational education is in recent times being relegated to the background while emphases are being paid to traditional or theoretical system of imparting knowledge.

In view of the challenges encountered in the adoption of ICT tools to teaching and learning, it is recommended that qualified lecturers be employed, and the necessary tools needed for onward impartation to students should be made available to them to curtail these challenges.

ICT tools like computers, projectors and internet facilities should be provided and made available to the department as the ones available now are grossly inadequate and students have little or no access to them for their practical, thereby necessitating a theoretical or traditional system of teaching.

REFERENCES

Ajayi, I. A., Ekundayo, and Haastrup T. (2009), "The application of information and communication technology in Nigerian secondary schools." *International NGO Journal 4 (5), 281-286*

Ajibade, E. (2000), Information Technology and its Application for Curriculum Innovation. A Paper Presented at the 1st Annual Conference of Centre for Educational Technology (CET)

Akanwa, B., and C.N. Agu, (2005), Entrepreneurship: Theory and Practice in Nigeria. Owerri 1st Edn., Resources Development Centre

Akpomi, M.E. (2009), "Achieving Millennium Development Goals (MDGS) through Teaching Entrepreneurship Education in Nigeria Higher education Institution (HEIs)."*European Journal of Social Sciences*, 8(1): 152 – 159

Alamu J, F. (2008): Simplified Research Methodology: Principle and Practice. Zaria: Great glory.

Aliyu, M.M. (2006), "Integrating Information Technology into Business Education." *Business Education Journal*, 4(3)

Anderson (1984) in Aliyu (2006) Entrepreneurship and Entrepreneurial Education (EE): Strategy for Sustainable Development." *Asian Journal of Business Management* 3(3): 196-202.

Anyanwuocha, R. A. I. (2001), Fundamentals of Economics. Onitsha. Africana-FEP Publishers Ltd.

Azuka, E.B., Nwosu, B.O., Kanu, I.N., and Agomuo E.E. (2006), Foundation of Business Education.Oko,: Data-World Computer Academy.

Bandele SO (2006), "Development of modern ICT and internet system. *In Agagu AA (ed).* Information and communication technology and computer Applications." Abuja: Panof Press pp. 1 – 3.

Baran, S. J. and Davis, D. K. (2009), Mass Communication Theory: Foundation, Ferment and Future. 5th Edition. Boston, MA: Wadsworth Ceneage Learning.

Castells, M. (2001), "Lessons from the History of Internet", in "The Internet Galaxy", Ch. 1, pp 9–35. Oxford University Press.

Chukwurah C. C. (2011), "Strategies for global reforms in business teacher education towards self-reliance in Nigeria." *International Journal of Vocational and Technical Education* 3(4): 45-48, July.

Ewhrudjakpor, C. (2008), "Poverty and its alleviation: The Nigerian experience." *Journal of International social work*, 51(4) 519-531

Farstad (2002) Fundamental of Statistics and Research Methodology. Yaba, Lagos: Tummoh Service.

Garba, (2010) Spinning off an entrepreneurship culture among Nigerian university student; prospect and challenges. *African journal of Business Management*

Habila (2006) Automated Lighting: The Art and Science of Moving Light in Theatre, Live Performance, New Media, and Entertainment. New York: Focal Press.

Ibrahim and Soufani, 2002), The Perfect E-Storm. The Observatory on borderless higher education. Http://www.obhe.ac.uk/products/reports/publicaccesspdf/Bonk.pdf.

Ikelegbe (2009) the Nigerian National Policy for Information Technology (IT) Johns, 1999).

Kachian S. et al, (2000), "Re-thinking Higher Education Management for Poverty Reduction among the Youth in Africa." Paper Presented at the Third Regional Conference Higher Education for Youth Empowerment, Opportunities, Capabilities and Second Chance. Organized by Higher Education Research and Policy Network (NERPNET) at IITA, Ibadan, Oyo State. August 18-21.

Kamsah, Mokhtar and Yaakob, (2000) *Principles of Financial Accounting. Financial Accounting Series (12 ed.). Cengage Learning.*

Keister, (2005) Strategies for Effective Teaching of Entrepreneurship Education in Tertiary Institutions in Imo State and Anambra State. Business Education Journal, 8(1), 119-128

Leo (2010), Business Education in a Developing Economy: The Nigerian Case. Jos Binon Production:

Lowenthal, (2009). Entrepreneurship in Innovation, and Industrial Organization in Nigeria. Available at Chosen Navotama.

Milken (2003), Exchange on Education Technology, British Journal of Management. 28 (1): 3–13. doi:10.1111/1467-8551.12207. ISSN 1467-8551.

Mkpozi (1996) Information Fluency, Critical Examining IT Education. New Library world.

Musa (2008) Impact of ICT on Business Education programme:

Mwangi, (2011) *The promise of entrepreneurship as a field of research". Academy of Management Review. 25: 217–226.*

Nwite (2007) Information and Communication Technologies: Social Sciences Research and Training: A Report by the ESRC Programme on Information and Communication Technologies, ISBN 0-86226-179-1, 1986.

Ofodu (2007) "Impact and Management Research: Exploring Relationships between Temporality, Dialogue, Reflexivity and Praxis". British Journal of Management. 28 (1): 3–13. doi:10.1111/1467-8551.12207. ISSN 1467-8551.

Ogundele (2004))Alleviating Poverty through the use of Entrepreneurship Skill Acquisition in Kogi State, Nigeria. International Open Journal of Economics 1: 14-23

Ogunsola (2005) Entrepreneurship Training and Education as Strategic Tools for Poverty Alleviation in Nigeria. Adekunle Printing Press, Agbomosho

Okolocha, et al., (2012) Entrepreneurship in Innovation, and Industrial SOrganization in Nigeria. Available at Chosen Navotama

Oladunjoye L (2007) Foundation of Vocational Education: Social and Philosophical Concepts, Englewood Cliffs, New Jersey: Prentice-Hall, Inc

Olayemi .H (2004) Higher education for self-reliance: An imperative for the Nigerian Economy. NEAP publication pg. 1-8

Omole.Q (2011) Promoting entrepreneurship culture through vocational education In Nigerian universities. Journal of the institute of education, vol. 4 (1) pp117.

Osuwa A (2002) Creating More Opportunities for Young People Using Information and Communication Technology. The world summit on Information Societies, Geneva.

Pahad cited in Ibinola (2011) *Friends and Profits Don't Mix: The Performance Implications of Repeated Partnerships". Academy of Management Journal. **59** (2): 460*

Rosales H. (2006) Entrepreneurship education: Strategy for national development. Delta Business Education Journal 1: 113-183.

Shane H. (2003) Foundation of Vocational Education: Social and Philosophical Concepts, Englewood Cliffs, New Jersey: Prentice-Hall, Inc

Skinner, (1938), Teacher Controls the Instructional Process. University Press. Ibadan

Straubhaar and La Rose, (2004). Strategies for Sustainable Development of Entrepreneurship in Anambra State. Business Education Journal, 7(1): 95-111

The Oxford Advanced Learners Dictionary (2010) Edition.

Tinio, (2003) Factors influencing digital technology use in early childhood education. Computers & Education, 77, pp.82-90.

Toomey (2001) Information and Communication Technologies: Social Sciences Research and Training: A Report by the ESRC Programme on Information and Communication Technologies, ISBN 0-86226-179-1, 1986

Turow, (2009) "ICT Innovation and Entrepreneurship Strategy" International of Research in Entrepreneurship, 16(4) 446-463

Ubulum (2000) "ICT Innovation and Entrepreneurship Strategy" Technology Innovation and Entrepreneurship Centre.

Ubulum et al., (2011) "Youth Empowerment through ICT Entrepreneurial Involvement" *Journal of Social Enterprise Initiative*,2 (3): 61-83

Udonkang (2002) he Dynamics of Entrepreneurship in ICT, Case of Mobile Phones Services in Sub-Sahara Africa:" Journal of Entrepreneurship, 6 (1): 126-140.

Yusuf, (2000).The Role of Entrepreneurship Education in Poverty Alleviation. *Delta Business Education Journal* 2(1) 66-71.

Design of a Cell-Phone Based Monitoring and Controlling System for Poultry Incubator

M. J. Musa
Communications Engineering Department,
Ahmadu Bello University,
Zaria. Nigeria
mjmusa@abu.edu.ng

M. J. Saidu
Department of Agricultural and Bio-Environmental Engineering
Technology. College of Agriculture Jalingo,
Taraba
Msjauro2020@gmail.com

S. G. Zubairu
Institute of Computing & ICT, Ahmadu Bello University,
Zaria. Nigeria
sgzubairu@abu.edu.ng

I. Umar
Division of Agricultural colleges Ahmadu Bello University,
Zaria.Nigeria

A. Mohammed
Department of Physics, Kaduna State University,
Kaduna-Nigeria
mjmusa@abu.edu.ng

ABSTRACT—
The invention of fully automated artificial incubators brings about the production of large number of birds that are enough for day to day demands. But operating such automated incubators are labor intensive even though they are automated in nature, an operator must always be close to the machine for any malfunction. This research presents another approach to the design of a cell-phone monitoring and controlling of the poultry incubator from the comfort of your home. The control was executed Through Short Message Services (SMS) to the incubator, which in turn executes the exact command and provides a customized feedback message to the master's cell phone. The control was tested from ten different countries (Egypt, Ethiopia, Indonesia, Kenya, Malaysia, Nigeria, Saudi, Turkish, U.K, and U.S.A) with the based station at Ahmadu Bello University (ABU) Nigeria. The tested commands were stored in the EPROM of the micro used. GSM modem was used to initiate communication between the remote and the based station. Such communication was achieved through an algorithm, which utilized attention (AT) commands. The GSM modem was interfaced with the incubator and tested for 19 days of continuous operation in the laboratory. With the proposed control system installed in conventional incubator, the incubator was found to be responded to commands in addition to maintaining the necessary ambient temperature of 37^{0}C and humidity of 65.1%, which are ideal parameters for incubation. A communication success of 91.3% was recorded through SMS messages using 9mobile SIM due to its service reception at the base station. This result shows that the cell phone-based monitor and control unit has a failure of only 8.7%. The control system was made using locally available components and materials, which gives a low cost of only 16,000 naira for a control unit.

KEYWORDS—cell phone, control, monitoring system.

INTRODUCTION

Eggs incubation are done by the mother bird by sitting on the eggs and use its body to produce the required temperature and humidity for embryo development. To achieve large number of birds production that will met with the market requirement, artificial incubators are come into play for the view to solve the market demand. Manual incubators, semi-automatic incubators and automatic incubators were both invented to ease the market demand and reduce labor but with all in place the presence of human is mandatory to always check the functionality of the incubator [1, 2]. Hence the need to provide an efficient incubator control that can be control and monitor from all over the world. The control will have the means of commanding the incubator and to query for the incubator's status when necessary.

Section II of this paper describes the design of the circuitry for the cell phone interface. Section III provide the design of the relay board, section IV provide the design of the computer interface. Section V concludes on the presented results.

DESIGN OF CELL PHONE INTERFACE FOR INCUBATOR

Figure I show the GSM modem (SIMCOM 304Z) circuit diagram. Six pins namely V_{CC}, GND, power key, transmitting, receiving and network indicating pin were used from the available SIMCOM 304Z pins. Receiving (R_X) and transmitting (T_X) pins of the modem are interfaced with the transmitting (T_X) pin 15 and receiving (R_X) pin 14 of the ATmega16.

The network pin of the SIMCOM 304Z is connected to LED via resistor and transistor configuration to indicate presence of network for the SIM used [3]. R_7 is a current limiting resistor to Q_1. Due to common fluctuation; of power supply that may power off the SIMCOM 304Z modem the value of R_6 and C_9 were suggested to be 100 kΩ and 470 µF [3].

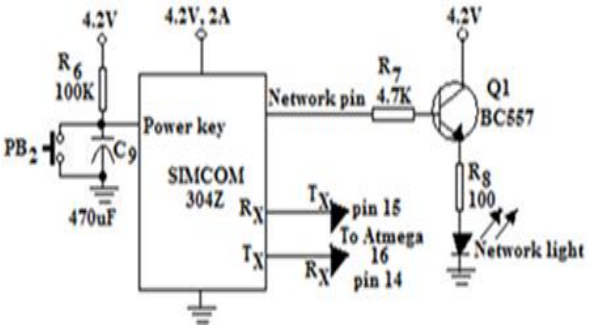

Figure V. Circuit Diagram of Cell Phone Control Interface

The resistor R_8 is a small emitter resistor for improving the noise immunity and its value can be arbitrarily selected from the range 100 Ω to 330 Ω as specified in the data sheet

of transistor Q_1 [4]. The smallest value in the range 100 Ω is used in this circuit.
The value of R_7 is obtained using equation (1) [4]:

$$R_7 = \frac{V_{CC} - V_{BE}}{I_B} \qquad (1)$$

The base current to the transistor Q_1 is the output current from the SIMCON 304Z (at network indicator pin) which can produce up to 800µA and V_{BE} = 0.7 V, VCC = 4.2 V.
Using the equation (1), the resistor R_7 is obtained as R_7 = 4375 Ω. But a standard resistor value of 4.7 kΩ ± 10% is used which satisfies the requirement.
A summary of the components required and used is shown in Table I

Table I. Components of the Cell Phone Interface

COMPONENT	CALCULATED VALUE (kΩ)	STANDARD VALUE
R_6	----------	100 kΩ
R_7	4.3	4.7 kΩ
R_8	----------	100 Ω
C_9	----------	470 µF, 25 V
Q_1	----------	BC 557

F. Design of Atmega16 External Interfaces with Incubator

Figure II shows the schematic diagram of the ATmega16 external interface to the incubator controls. LM35 is used as the precious integrated - circuit temperature sensor, whose output voltage is linearly proportional to the Celsius (Centigrade) temperature. The LM35 thus has an advantage over linear temperature sensors calibrated in Kelvin, because the subtraction of large constant voltage from its output to obtain convenient Centigrade scaling is not required.

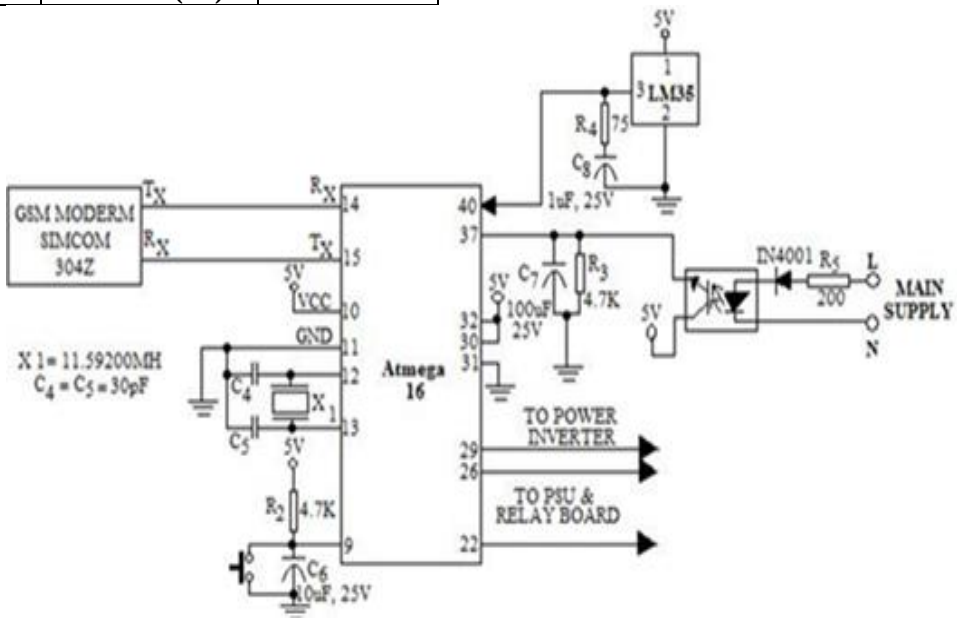

Figure VI. ATmega16 External Interfaces with Incubator

Since the LM35 is connected from the ATmega16 to the incubator chamber via a long conductor (wire), then a series or R-C damper of values 75 Ω (implemented as two parallel 150 Ω resistors) and 1 µF is connected from output pin 3 of the LM35 to ground pin 2. This temperature sensor is TTL compatible and is configured at Pin 40 of the ATmega16 (port A) ADC0. An opto-coupler is used to notify the ATmega16 the presence of mains supply from the utility company (PHCN). It isolates the AC from the ATmega16 pin 37 (PA3) port A. In the presence of the mains supply the photo transistor of the opto-coupler is activated and the ATmega16 sense it. Due to fluctuations of the mains supply that may occur, R-C combination (4.7 kΩ and 100 µF) in parallel from the output of the opto-coupler to ground is connected to act as a bleeder. Pin 27 (PC7) of port C goes to the power inverter to let it ON in absence of power supply and OFF in the presence of power supply. Pin 22 to 26 of ATmega16 goes to the PSU and relay board of Figure III through a driver UNL2003 which drives five (5) relays to control the incubator parameters.

R_2 and C_6 are 4.7 kΩ and 10 µF respectively, to hold pin 9 (Reset pin) always high in order to prevent unnecessary resetting of the microcontroller (ATmega16). Pin 13 (XTAL1) is the input to the inverting oscillator amplifier and input to the internal clock operating circuit while pin 12 (XTAL2) is the output from the inverting - oscillator amplifier. The crystal oscillator used is of value 11.59200 MHz. $\{X_1: \text{speed of microcontroller} \leq X_1\}$ and C_4 is C_5 is 30 ± 10 pF.
A summary of the components required and used is shown in Table II

Table II. Components of ATmega16 External Interfaces

DESIGN AND ANALYSIS OF RELAY BOARD WITH INCUBATOR

This This unit is made up of five (5) relays namely RL_1 to RL_5 which is used to control inductive loads, in this case they are used to control heater elements, incubator switch, egg tray turner, supply from inverter and that of PHCN as shown in Figure III. The relays are driven directly through the UNL 2003 which is a high-voltage, high-current Darlington arrays comprising of eight PNP Darlington pairs. Five (5) Darlington pairs are used.Diodes D_2 to D_6 are the freewheeling diodes used to prevent a reverse emf that may

COMPONENT	CALCULATED VALUE	STANDARD VALUE
X_1	----------	11.59200 MHz
C_4-C_5	----------	30 PF
C_6	----------	10 µF, 25 V
C_7	----------	100 µF, 25 V
C_8	----------	1 µF, 25 V
R_2	----------	4.7 kΩ
R_3	----------	75 Ω
R_4	----------	4.7 kΩ
R_5	----------	200 Ω

occur in the relays coil. RL_1 and RL_2 work simultaneously, i.e. they remain deactivated in the absence of PHCN and allow the inverter to feed the load (incubator) through the normally close terminals of the relays.

In the presence of power from PHCN RL_1 and RL_2 will energize and the normally - open closes, these results in eliminating the inverter supply to the incubator and permitting the PHCN to feed the incubator. Moreover, this can also be seen on the LCD display either:

PS* = *ne (power supply is NEPA) when it's on PHCN
Or
PS* = *in (power supply is inverter) when it's on inverter.
PS* = *ne (power supply is NEPA) when it's on PHCN
Or
PS* = *in (power supply is inverter) when it's on inverter.

Similarly, it can also be monitored on the master cell phone whenever the incubator status is demanded from any cell phone. A command ***'INCSTS'*** should be text to the incubator on MSISDN (Mobile Subscriber Integrated Services Digital Number): **07035027339** and an immediate feedback will be received on the master's MSISDN: **08065183151** on almost all the incubator status, such as:

STATUS

PWR: ne (i.e. if the incubator is powered from the mains supply),
Or
PWR: in (i.e. if the incubator is powered by the inverter).

RL3 is connected to the egg turner tray and is by default deactivated which turns the egg trays in a clockwise direction (CW). The trays remain in that position until a command is received from a cell phone to turn the egg trays in a counter clockwise direction. Moreover, this can also be seen on the LCD display, either:

TR = CW (tray is clockwise) when the egg trays are turned clockwise or
TR = ACW (tray is anticlockwise) when the egg trays are turned anticlockwise.

Similarly, a command can be sent through SMS to turn the egg trays from any cell phone and receive a feedback on the master cell phone.

A command '***TETCKW***' should be sent to the incubator to turn the incubator CW
Or
'***TETACW***' to turn the incubator tray anticlockwise (ACW) direction and an immediate feedback will be received on the master cell phone as explained, such as:

STATUS

Turning the Tray in the anti-clockwise direction was successful
Or
Turning the Tray in the clockwise direction was successful.

The feedback depends on the command sent.

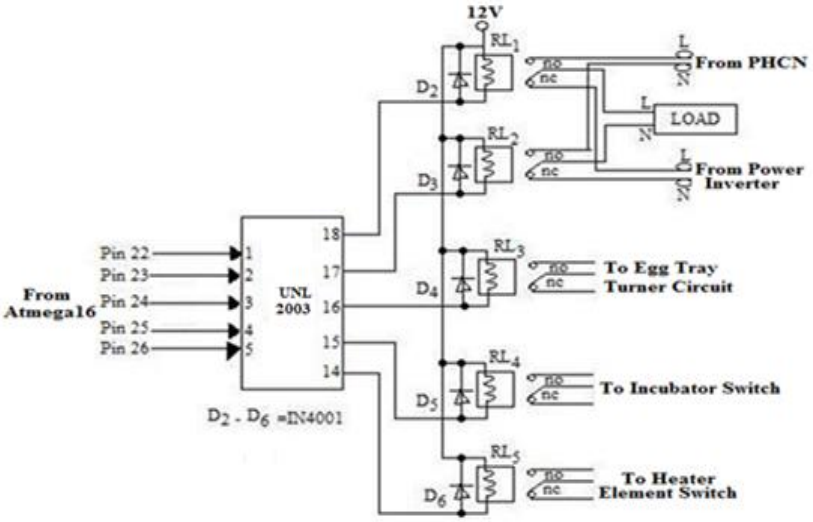

Figure VII. Relay Board Interface with Incubator

RL_4 is connected to the incubator mains power switch which is OFF by default and remains in that OFF position until it receives a command from a cell phone to switch it ON. This can also be seen on the LCD display which displays:

"IC = of" (incubator is OFF)

Or

"IC = on" (incubator is ON).

This depends on the deactivation or activation of the RL_4 respectively.

Similarly, it can be monitored on the master cell phone whenever the incubator status is demanded via an SMS command to the incubator:

"OFMYIN" (i.e. OFF my incubator)

Or

"ONMYIN" (i.e. switch ON my incubator)

An immediate feedback will be received on the master cell phone, i.e.:

"Switching the incubator OFF was successful" (i.e. when the incubator is switched OFF)

Or

"Switching the incubator ON was successful" (i.e. when the incubator is switched ON).

It can also be monitored when requesting for the overall incubator status by sending ***"INCSTS"*** via SMS to the incubator and receiving:

STATUS

INC: of (incubator is OFF),

INC: on (incubator is ON).

The feedback depends on the command sent to the incubator.

RL_5 is connected to the heater elements switch and it can only be activated when the temperature of the elements used is less than or equal to 38^0C. The relay RL_5 will be deactivated when the temperature is above 38^0C. In this design a temperature of 38^0C which is the most suitable incubating temperature required for chicken egg was achieved [3].

Moreover, this can also be seen on the LCD display, either:

HT = on (heater is ON)

Or

HT = of (heater is OFF).

This depends on the deactivation or activation of the RL_5 respectively.

Similarly, it can also be monitored on the master cell phone whenever the incubator status is demanded. A command ***'INCSTS'*** should be sent to the incubator and an immediate feedback will be received on the master cell phone as explained, such as:

STATUS

HTR: on (i.e. heater is ON),

Or

HTR: of (i.e. heater is OFF).

The feedback depends on the RL_5 energizing or de-energizing state.

DESIGN AND ANALYSIS OF COMPUTER (PC) INTERFACE CIRCUIT

The complete circuit diagram is as shown in Figure IV. The logged data can also be accessed by a PC through a PC interfaced to the main microcontroller. Because of voltage level differences of the devices, a MAX232 was used to provide voltage matching for the different types of logic used in the microcontroller and those in the PC. The MAX232 (RS232 to TTL converter) is a 16-pin dip integrated circuit (IC) that converts signals from an RS-232 serial port to signals suitable for use in TTL compatible digital logic circuits. This makes it useful for implementing RS-232 in devices that otherwise do not need any voltages outside the 0 V to +5 V range, as power supply design does not need to be made more complicated just for driving the RS-232.

The PC interface is accomplished through a serial RS 232 connector as recommended in the datasheet of MAX232 application note.

The device is powered from the 5 V stabilized DC to pin 16 and with pin 15 to ground. It is recommended in the data sheet that $C_{10} = C_{11} = C_{12} = C_{13}$ ($1\ \mu F \leq C_{10} \leq 10\ \mu F$).

Terminal 9 is the receiving terminal while data transmission is accomplished through the transmitting pin 10 of the MAX232 device. The computer is expected to transmit instruction for request of data from the main microcontroller [5].

The microcontroller then copies the data from the EEPROM registers and transfers it to the PC for display [5]. The receiver of the MAX232 is connected to the transmitter of the microcontroller while the transmitting terminal of the MAX232 is connected to the receiving pin of the microcontroller.

The values of C_{14} and R_9 are within the range of $10\ \mu F \geq C_{14} \geq 1\ \mu F$ and $8.2\ K\Omega \geq R_9 \geq 4.7\ k\Omega$ respectively [5]. Hence C_{14} was selected as 10 µF and 4.7 kΩ was adopted asR_9.

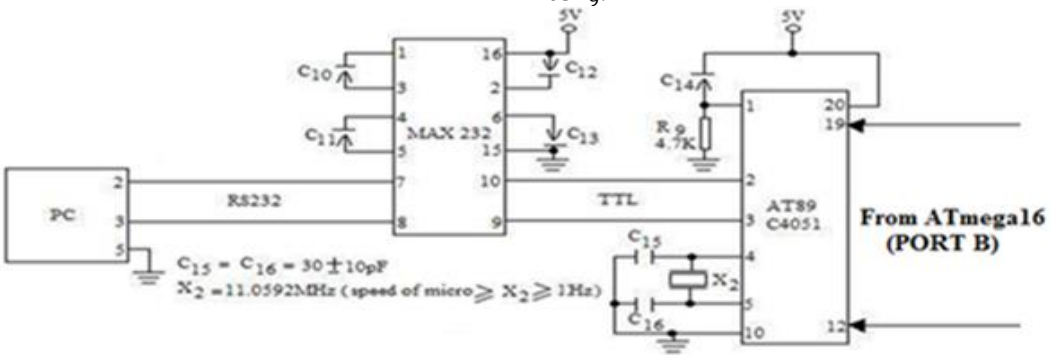

Figure VIII. PC Interface with the Incubator

A summary of the components required and used is shown in Table III

Table III. Component of the Computer (PC) Interface

RESULTS

The cell phone control-based incubator was implemented and tested through SMS from ten different countries (Egypt, Ethiopia, Indonesia, Kenya, Malaysia, Nigeria, Saudi, Turkish, U.K, and U.S.A). 91.3% success was recorded when different commands and queries were sent from different countries and 8.7% of failure was observed. The computer interface was also tested, and no failure was recorded.

CONCLUSION

The proposed cell phone incubator control was implemented and tested from ten different countries. The finding shows that the proposed system is of about 91% efficiency. With this achievement it can be concluded that the proposed method of cell phone control for incubator is encourage to the used by incubator builders to provide flexibility in the control and monitoring and to minimize labor.

COMPONENT	**CALCULATED VALUE**	**STANDARD VALUE**
X_1	----------	11.0592 MHz
C_{10}–C_{14}	----------	1 µF
C_{15}-C_{16}	----------	10 pF
R_9	----------	4.7 kΩ

REFERENCES

[7] A. Mohammad, M. J. Musa; K. Ahmad, S. Garba and M.D. Almustapha "Design and Performance of HEFINC840 Micro-controller Based Incubator" NIAE International Conference, University of Uyo, Nigeria. October 21-24, 2013, p. 685-692, 2013

[8] A. B. Umar, K. Lawal, M. Mukhtar and M. S. Adamu "Construction of an Electrically-OperatedEgg Incubator" International Journal of Modern Engineering Sciences, vol. 5, issue 1, Florida, USA. p. 1-18, 2016

[9] Z. N. Oriolowo; F. A. Maude; A. Raji and M. J. Musa "Design and Construction of an Automatic Electric Incubator for Hatching Chicken Eggs" 8th international Conference Gold in Nigeria Agricultural Engineering and the Millennium Development, 28th January – 1st February 2008, Yola, p. 215-220, 2007.

[10] U. F. Abdu-Aguye, S. Garba, M. J. Musa, K. Ahmad, and A.M.S. Tekanyi "Development of an Embedded Light Activated Remote for fan Regulator" Proceedings of Academia Industry Conference. Faculty of Engineering, Bayero University Kano 9th-11th December 2014.

M. J. Musa; K. Ahmad; S. Garba; Y. A. Sha'aban and A. S. Musa "Microcontroller-Based Patient Temperature Monitoring System" Zaria Journal of Electrical Engineering Technology, Department of Electrical and Computer Engineering, Ahmadu Bello University, Zaria,vol. 2, issue 2, p. 1-15, 2013.

Measurement and Analysis on the Health Effect of Electromagnetic Radiation from Telecommunication Masts in Some Selected Areas in Kaduna Metropolis

Abubakar Kabir, Elvis Obi, Aminu Yerima Musa
Communications Engineering
Ahmadu Bello UniversityZaria, Nigeria
aakabeer9@gmail.com, elvisobi72@gmail.com, aminuyerima@yahoo.com

ABSTRACT— this study presents the practical analysis on the electromagnetic exposure emitted by telecommunications mast on the human body in some selected areas in Kaduna metropolis, Kaduna State. In this study electromagnetic radiation from base station antennas installed for various wireless communication purposes was investigated based on the electric field strength E, magnetic field strength H and power density S, at some distances from telecommunication masts owned by the four network providers, namely Airtel, Etisalat, Glo and MTN Nigeria. Five base stations/ masts from each service provider were selected making a sum total of twenty base stations that were surveyed. The EMF Strength meter was used for the measurement then compared the Electromagnetic field (EMF) emission with the International Commission on Non ionizing Radiation Protection (ICNIRP), Federal Communication Commission (FCC) and Institute of electrical and electronic engineers (IEEE) limits to know if the service provider did adopt the precautionary majors. The all measured power density of the Service provider falls low from 60m to 100m as such it is safe to adequately install a telecommunication masts from 100m away from a residential or public buildings and the percentage ratio of the maximum power density is 1.3034% and 1.0687% observed high at Airtel Mast whereas the least is 0.0308% and 0.0252% obtained at Etisalat mast and said did not exceed the limit.

KEYWORDS— Electromagnetic Radiation, Base Station Antenna, Electric field, Magnetic field, Power density

INTRODUCTION

Since the introduction of wireless telecommunication in the 1990s, there has been unending argument, whether telephone networks emit electromagnetic radiation, EMR, which pollutes cities and rural areas. With multiple sources of mobile communication technology, people fear that it could result in exposure of people and wide-life to microwaves that can have intense adverse health effects. Expectedly, the effect of telecommunications equipment, such as masts, have been a subject of interest and concern to people worldwide, given the speed of mobile phone penetration in both developed and developing nations. However, the Nigerian Communications Commission (NCC) had, on various occasions, dismissed the fear that radiation from telecom masts could have negative health implications, insisting that no known study has proved so. Meanwhile the National Environmental Standard, Regulatory and Enforcement Agency, NESREA, appears to be stoking fire on the debate. Director General of the agency, Dr Lawrence Anukam, in a television interview recently, called for caution in sitting telecom masts around living areas, admitting that there have been conflicting reports about the level of radiation coming from telecom masts. (Vanguardngr, 2017).

Radiation has also been linked in a host of researches to brain tumours, depression, miscarriage, Alzheimer's disease, and other deadly illnesses. Children are said to be at the greatest risk because of their special vulnerability during periods of development before and after birth. Over 100 physicians and scientists at Harvard and Boston University Schools of Public Health have called cell towers a radiation hazard while 33 delegate physicians from seven countries have declared cell phone towers a 'public health emergency'.(Gerald et at., 2011).

A base station and its transmitting power are designed in such a way that mobile phones should be able to transmit and receive enough signal for proper communication up to a few kilometers. Majority of these towers are mounted near the residential and office buildings to provide good mobile phone coverage to the users. These cell towers transmit radiation every second, so people living within tens of meters from the tower will receive 10,000 to 10,000,000 times stronger signal than required for mobile communication. Buildings located at certain distances from cell towers are found to absorb high power densities which are dangerous to humans. The Base Stations, The mobile and wireless communication networks transmit radiations through antennas mounted on the base station. (ICNIRP, 2009).

COMPONENTS OF ELECTROMAGNETIC FIELD

Radio frequency gives rise to electric field and magnetic fields which can directly couple into people inducing fields and currents in their bodies. Electric fields are associated only with the presence of electric charges and exert forces on the electric charge, whereas magnetic fields are associated with the physical movement of charges and exert physical forces on the electric charges only when the charges are in motion (ICNIRP, 1996). Electric field strength, E, is defined as the force, F, per unit charge q, on infinitesimally small charge at any given point in space and its unit is volt per meter (V/m). It is given as

$$E=F/Q \quad (1)$$

The force on a charge q, places in electric field, is then

$$F=qE \quad (2)$$

Ma**g**netic Field Strength, **H** is equal to magnetic flux density, **B** divided by the permeability of the medium, given as

$$H=B/\mu \quad (3)$$

Its Unit is ampere per meter (A/m). Magnetic flux density is a vector force field defined as the force ($\mathbf{F}_m$) per unit charge on as infinitesimal moving charge q_v, at a given point in space. Its unit is Tesla (T) and it is given as:

$$B = F_m/q_v \quad (4)$$

The force $\mathbf{F}_m$ exerted on q by **B** is always perpendicular to both the velocity of the particle and the direction of **B.** The force is given as

$$F=q(v\times\mathbf{B}) \quad (5)$$

(NCRP, 1993).

A magnetic field can be expressed as a magnetic flux density **B**, or as Magnetic field strength, H. The both are related by

$$B=\mu H \quad (6)$$

Why μ is the constant of proportionality called the magnetic materials permeability, given as 4×10^{-7}H/m in air, vacuum and non magnetic materials (ICNIRP, 1996).

Another component of Electromagnetic field that is used to quantify Radiofrequency for health hazard assessment is the power density. Power density S, is the power per unit area to the direction of propagation. Power density is obtained from Poynting's theorem which relates the rate of absorption in an object to the incident fields. The theorem is a statement of conservation of energy, if A is any enclosed surface and V is the volume inside A, then

$$\frac{\delta}{\delta t}\int_v (w_c + \varepsilon E.E + \mu H.H)dV + \oint_A E\times H.da = 0 \quad (7)$$

$$\frac{\delta}{\delta t}\int_v (w_c + \varepsilon E.E + \mu H.H)dV + \oint_A E\times H.da = 0$$

$$\frac{\delta}{\delta t}\int_v (w_c + \varepsilon E.E + \mu H.H)dV + \oint_A E\times H.da = 0$$

$$\frac{\delta}{\delta t}\int_v (w_c + \varepsilon E.E + \mu H.H)dV + \oint_A E\times H.da = 0$$

$$\frac{\delta}{\delta t}\int_v (w_c + \varepsilon E.E + \mu H.H)dV + \oint_A E\times H.da = 0 \quad (7)$$

Where: w_c is the energy per unit volume possessed by charged particles at a given point in the volume $\varepsilon E.E.\varepsilon E.E$, is the energy per unit volume stored in the electric field at a given point in the volume, $\mu H.H\ \mu H.H$ is the energy per unit volume stored in the magnetic field at a given point in the volume, da is a differential surface elements of A.

Since a closed surface is any surface that completely encloses a volume, the volume integral corresponds to summing the terms in the integrand over all points inside the volume. Then, the integral over the volume corresponds to the total energy possessed by all charged particles within the volume plus the energy stored in the electric and magnetic fields. The integral on the left is the time rate of change of the total energy within the volume and is equal to the total power. The term on the right of the equation is an integral over the closed surface enclosing the volume. The equation (7) becomes

$$S= E\times H \quad (8)$$

Where S is called the Poynting vector with W/m^2 and is interpreted as power density. The direction of the cross product of E and H is perpendicular to both E and H and the vector dot product of E × H with **da** selects the component of E × H that is parallel **da.** So S.da is the power d**p** passing out through the differential surface element da and the surface integral is the sum of the power passing through each surface element over the entire surface A, which is equal to the total power passing out through A.

Extensive studies have nevertheless been done to critically investigate the effect of EM Radiation from mobile and wireless telecommunication masts in various cities all over the world (e.g. Manteuffel et. al., 2002; Hirata et. al., 2003; Adilza et. al., 2011; Michael et al, 2013). In Nigeria, there have been reports on the cities of ikeja Area of Lagos Akinyemi et al, 2014, P. Enyinna and G. Avwir, 2010, In Aba, Asiegbu, A. and O. Ogunlaja, 2010, among probably many others.

MATERIALS AND METHODS FOR THE MEASUREMENT

This includes calibration of the equipment, data collection from the surveyed masts of the UMTS service providers. The data collected was used to calculate the power density beamed out from the masts at different distances.

The Equipment and Calibration: The instrument for the study was the RF EMF Strength meter, model 480836. The RF EMF strength meter is a broadband isotropic instrument. It is designed to measure electric, magnetic field strength and power density of EMF of frequency of 50 MHz to 3.5GHz with specified frequency of 900MHz, 1800MHz and 2.7GHz. (Aliyu and Ali 2012). The unit of measurement and the measurement types are expressed in units of electrical and magnetic field strength and power density given as mV/m, V/m, μA/m, mA/m, $\mu W/m^2$, W/m^2, $\mu W/cm^2$, mW/cm^2. The instrument displays instantaneous measured values, maximum values, average values and maximum average values. The display resolution is 0.1mV/m, 0.1μA/m, $0.1\mu W/m^2$, and $0.001\mu W/cm^2$. The setting is typically 1second. The absolute error at 1V/m and 50MHz is ±1.0dB. The instrument was calibrated with a factor of 1.00 based on the manufacturer's instruction.

MEASUREMENTS OF ELECTRIC FIELD, MAGNETIC FIELD, AND POWER DENSITY

Measurements were taken at 0, 20, 40, 60, 80, and 100 away from the masts, starting from 100m to 0m. The base of the fence served as the origin of the measurement, since the study focuses on the safety of the general public who lie or spend a lot of time around the mast, we felt that it may not be necessary to struggle to gain access into masts bases.

Measurements were taken at this six position starting from 100m to 0m. At each of these points, the values of the electric field strength, magnetic field strength and power density were measured while the equipment was in maximum mode. The instrument used for the study at the point of measurement was held at 1.5m height above ground level which is the standard height of an average man.

ANALYSIS OF THE RESULTS

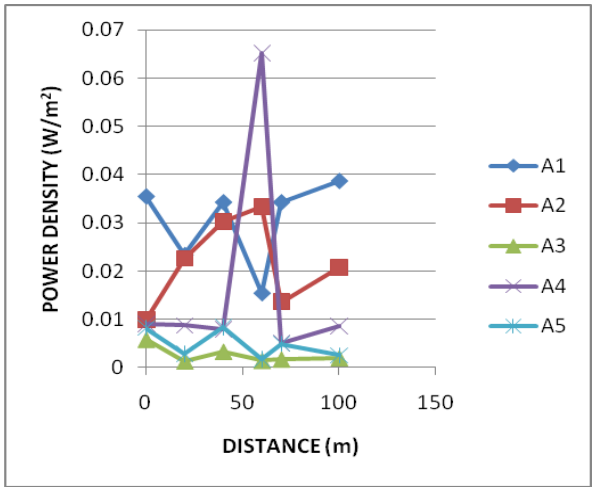

Fig. 1: A Plot of Power density (W/m^2) against Distance (m) for the measured Aitel Service provider, the graph depicted that the maximum value of S measured is 0.06517W/m^2 at 60m and the minimum value of S measured is 0.00133W/m^2 at 20m

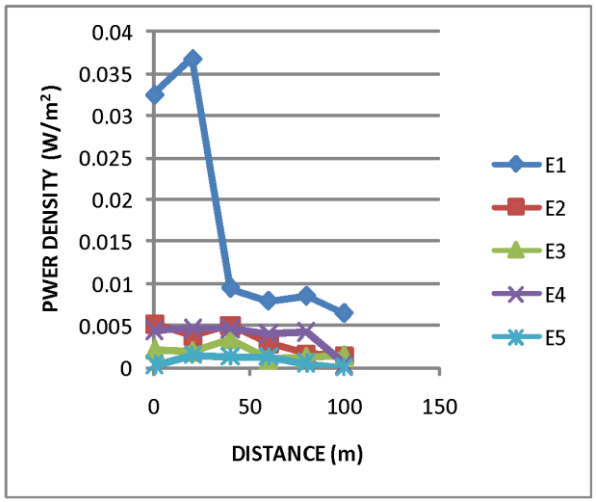

Fig. 2: A Plot of Power density (W/m^2) against Distance (m) for the measured Etisalat Service provider, the graph depicted that the maximum value of S measured is 0.03677W/m^2 at 20m and the minimum value of S measured is 0.00008W/m^2 at 100m

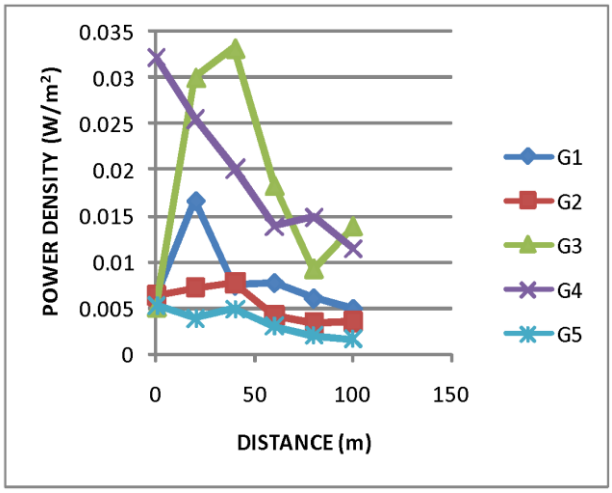

Fig. 3: A Plot of Power density (W/m^2) against Distance (m) for the measured Glo Service provider, the graph depicted that the maximum value of S measured is 0.03321W/m^2 at 40m and the minimum value of S measured is 0.0.00163W/m^2 at 100m.

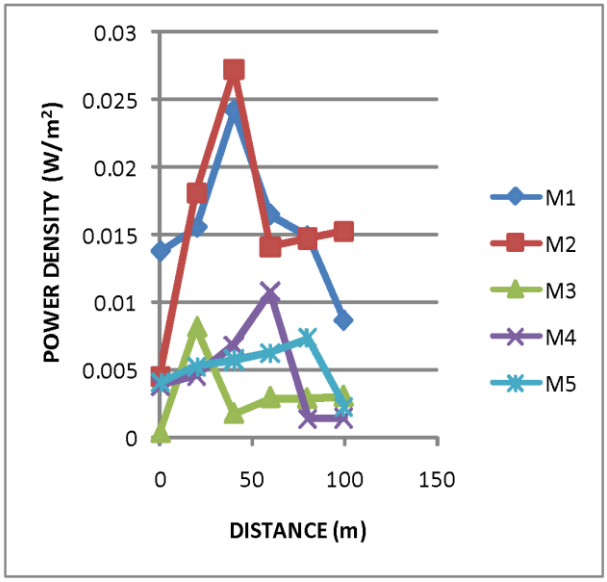

Fig. 4: A Plot of Power density (W/m^2) against Distance (m) for the measured MTN Service provider, the graph depicted that the maximum value of S measured is 0.02723W/m^2 at 40m and the minimum value of S measured is 0.00033W/m^2 at 0m.

The pattern of the measured values of Power density S is as expected. The mode or pattern of increase, decrease, increase and decrease of the values of Power density S are due to interference of the radiofrequencies resulting in wave crests and troughs. The graph depicted that from 0m to 40m the power density is high, but still falls within the limit, the all measured power density of the service provider falls low from 60m to 100m, except for Airtel service provider which falls low from 80m to 100m as such it is safe to adequately install a telecommunication masts from 100m away from a residential or public buildings.

To compare the measured power density of each service provider to the ICNIRP, FCC and IEEE power density limits where calculated. From the results the highest percentage ratio was 2.96% and 3.62% observed at Airtel Mast whereas the least was 1.00% and 1.21 observed at MTN masts while 1.76% and 2.15% observed at Etisalat masts and 1.40% and 1.70% observed at Glo masts falls in between the highest and the least percentage ratio, This confirms that all audited sites comply with the standards of the ICNIRP, IEEE and FCC in terms of the amount of EMFs that the base station is radiating.

CONCLUSION

In conclusion, this study was based on Measurement and Analysis on the Health Effect of Electromagnetic Radiation from Telecommunication Masts in Some Selected Areas in Kaduna Metropolis, Nigeria. it is adequately advisable that telecommunication masts are installed at 100m away from residential or public building and that the radiofrequency emission from the measured mast are low and falls within the exposure limits set by the International Commission on Non-Ionizing Radiation Protection, Federal Communication Commission and Institute of Electrical Electronics Engineers and a good agreement was obtained therefore, people around these vicinity are safe to live, work, or transact.

ACKNOWLEDGMENT

We are very much grateful to Dr Haruna Ali of the department of Physics, Nigerian Defense Academy, Kaduna and Isah Ahmad for their helpful contributions to the success of this work.

REFERENCES

[1] A.D. Asiegbu, and O.O. Ogunlaja. “Preliminary Investigation of RF Exposure levels from Mobile Telephone Base Stations in Abia,south east Nigeria”, International Journal of Current Research, vol. 11, pp 47-53, 2010.

[2] A. Hirata, M. Morita, and T. Shiozawa, “Temperature increase in the human head due to a dipole antenna at microwave frequencies”, IEEE Trans. Electromagn. Compat., Vol. 45, No. 1, pp. 109-116, 2003.

[3] Akinyemi, L.A. Shoewu, O. Pinponsu, O.A. Emagbetere, J.O and Edeko, F.O, ‘‘Effects of Base Transceiver Station (BTS) on Humans in Ikeja Area of Lagos State’’, Pacific Journal of Science and Technology, vol. 3, Issue 8, pp 28-34, 2014.

[4] A.O. Michael., B.E. Nnaemeka, and T.O. Matthew, (2013): Locational Effect of GSM Mast on Neighbouring Residential Properties' Rental Values in Akure, Nigeria. Academic Journal of Interdisciplinary Studies Vol. 2 No 3, November 2013. MCSER Publishing, Rome-Italy.

[5] A.O.M Ibrahim, A. Hamdallah (2012). Analysis of Electromagnetic Pollution due to high Voltage Transmission Lines. Journal of Energy Technologies and Policy. ISSN 2224-3232, volume 2, number 7.

[6] D. Adilza, L. Monica, T. Francisco, G. Antonio, D. Daiana, D. Michael, M. Cristina, C. Vania, A. Claudia and C. Waleska, "Mortality by neoplasia and cellular telephone 28 base stations in the Belo Horizonte municipality minas Gerais state, Brazil", Science of the Total Environment, Vol. 409, No. 19, pp. 3649–3665, 2011.

[7] D. Manteuff, A. Bahr,, C. Bornkessel,, F. Gustrau, and I. Wolff, "Fundamental aspects for the design of low-SAR mobile phones", IEEE Technical Seminar on Antenna Measurement and SAR, Loughborough UK, pp. 25/1-25/5, 2002.

[8] ICNIRP (1996) International Commission on Non Ionizing Radiation Protection.

[9] ICNRIP (2009). Exposure to high Frequency Electromagnetic Fields, Biological Effects and Health Consequences (100 kHz – 300GHz). 85764 Oerschlebheim, Germany. IEEE (1999). IEEE Standard for Safty Levels with Respect to Human Exposure to Radiop Frequency Electromagnetic Fields, 3kHz to 300GHz.

[10] J.W. Gerald, and E.G. Jessica (2011) Current State of Research on Biological Effects of Terahertz Radiation, Journal of Infrared, Millimeter, and Terahertz Waves, Volume 32, Issue 10, pp 1074-1122

[11] NCRP (1993): A practical guide to the determination of human exposure to Radiofrequncy Fields. National Council on Radiation Protection and Measurement.

[12] P.I. Enyinna, and G.O. Avwir, “Characterization of the Radiofrequency Radiation Potential of Alakahia and Choba Communities, Nigeria”, Working and Living Environmental protection, vol. 7, pp 25-31, 2010.

Automatic Body Mass Index Measurement Device

Shehu Keri, Ismail K. Musa, Musa Mamman, Mayo Zion O. & Tanko Aquila Nuhu
Department of Communications Engineering,
Ahmadu Bello University Zaria, Nigeria.
swazkeri@gmail.com, Ismkmusa1@gmail.com, musamamman@yahoo.com, mayozion@gmail.com, tankoaquila@gmail.com

ABSTRACT— Body fat composition is a function of the BMI. The BMI is used for screening the health of the general population due to the strong correlation between being overweight or obese and having health problems, chronic disease and premature death. People who are overweight or obese have an increased risk of hypertension, coronary heart disease, and stroke, type 2 diabetes, osteoarthritis, respiratory problems and so on. An increase in BMI happens so subtle that one may not take notice of it quickly. And since one is not ready to go through the stress of measuring his/her height and weight every day, we have decided to develop a device that will automatically calculate the BMI of a person in lessthan seconds. To achieve this, we used the ultrasonic sensor and the weight cell. This projectis achieved by using Ultrasonic sensor, 200kg weight cell, ATMega328p Microcontroller and 2004 LCD display. At the completion of the project, the test was carried out. The test result demonstrates suitability for an Automatic Basic Mass Index Measurement Booth.

INTRODUCTION

The higher risk of death resulting from excess adiposity may be attenuated by physical activity (PA). However, the theoretical number of deaths reduced by eliminating physical inactivity compared with overall and abdominal obesity remains unclear. **(Ekelund et al., 2018).**
The Body Mass Index (BMI) is a simple tool that estimates body fatness using a mathematical formula. The only instruments necessary to measure your BMI are a scale, a tape measure to determine your height and a calculator.

Why the BMI Measurement is Important

Once you know your BMI number, you'll want to know what it means. BMI is divided into weight status categories. Your health risk depends on the category you fall into.

A BMI of 18.5 or less is considered underweight, while a value between 18.5 and 24.9 is considered a normal weight. A BMI between 25 and 29.9 is overweight and 30 or greater is considered obese. For good health, you want to fall into the normal weight category. A higher BMI increases your risk of developing a chronic illness such as heart disease, diabetes or cancer. And having a BMI that's too low may pose a different set of health risks **(Manios, 2012).**

Determining a person's health based on weight and height squared was first developed in the early 19th century, according to a 2006 article about BMI published in the Archives of Disease in Children. But it wasn't until the 1980s that it was used more regularly by healthcare professionals as a means to assess health, and this was only because researchers were finding a correlation between the number calculated and health risk, according to a 2014 article published in Today's Dietitian.

Your BMI is determined by plugging your weight and height into a mathematical formula:

For example,
1.1 A 5-foot, 10-inch person weighing 210 pounds has a BMI of 30.1. This is because

A good scale, an accurate height measurement and a calculator are all that's necessary to estimate your BMI, making it easy to measure.

BMI Compared to Other Fat-Measuring Techniques

A number of other techniques are used to measure body fat, including underwater weighing, dual-energy X-ray absorptiometry, skinfold measurements and bioelectric impedance. But most of these require a special machine and/or a trained professional for accurate testing. While BMI is not a perfect tool, it's been compared to these other forms of measuring body fat and stands up fairly well on its own **(Sara Police, 2017).**

Dual-energy X-ray absorptiometry, or DXA, is considered one of the most accurate ways to measure body fatness and health risk. But because of the expense and complexity, the test is used primarily by those in research facilities.

BMI is a simple, easy-to-calculate tool that can be used anywhere and may be just as good as the more complicated body fat measurements. In fact, BMI measurements compare favorably to DXA measurements, according to a 2005 cohort study published in the International Journal of Obesity. This study compared the use of DXA against BMI, skinfold measurements of body fatness and risk of heart disease in a group of adolescents. The researchers found that both BMI and skinfold measurement correlated well with DXA for assessing health **(International Atomic Energy Agency., 2010).**

METHODOLOGY

The methodology implemented in the accomplishment of this research work includes the following;

1. Identification of components and tools to be used for the research work.
2. Documentation andobtaining of the required components.
3. Implementation of the components on a bread board for testing.
4. Programming of the microcontroller.
5. Powering of the setup circuit to see if it meets desire results.
6. Transferring of the circuit to a Vero board.
7. Implementation of the design.

REVIEW OF FUNDAMENTAL CONCEPTS

Load Cell

Load cells are transducers used to convert weight (Mass x Acceleration) into an electrical signal.
This signal can come in a number of different formats, such as a voltage change, current change or frequency change, while the majority of devices are based on the fundamental principle of change

of resistance in response to an applied load. Typically, a load cell consists of four strain gauges in a Wheatstone bridge configuration, while one strain gauge (Quarter Bridge) or two strain gauges (half bridge) are also available. A number of different options are available, including hydraulic load cells, pneumatic load cells and strain gauge load cells.

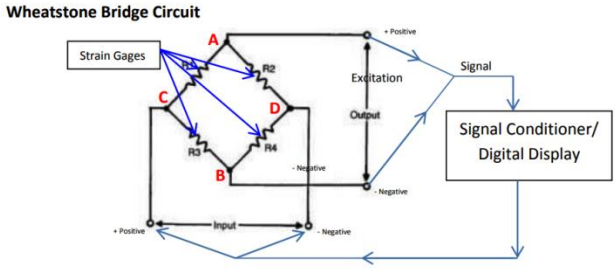

Figure 1: Diagram of a Wheatstone bridge circuit (**Dunnicliff, 1988)**

Strain gauge-based load cells

Strain-gauge load cells have become increasingly popular within the industry; in part because of the highly-precise and linear measurements they are capable of giving. Moreover, temperature changes do not have a big impact on their operations, while they are smaller in size when compared with other load cell options. Because of the lack of operating parts in the device, it has a relatively long operating life and it is very easy to produce **(Dunnicliff, 1988**).

For example**:** The KR high power load cell is specified for industrial applications such as tanks, silos and weighing bridge. It is operational for force and traction loads up to 30tonnes and comes with the protection class IP65. Boasting accuracy of 0.2%, it has an operating temperature of between -15ºC and 75ºC. Featuring a DMS strain-bridge (shear-beam device) for industrial applications, the SB8 Martens load cell with ATEX option is available as standard or with alterations made. Its maximum overload is 200% and a breaking load of 300%.

Ultrasonic Sensor

Ultrasonic sensors are used around the world, indoors and outdoors in the harshest conditions, for a variety of applications. Our ultrasonic sensors, made with piezoelectric crystals, use high-frequency sound waves to resonate the desired frequency and convert electric energy into acoustic energy, and vice versa. Sound waves are transmitted to and reflected from the target back to the transducer. Targets can have any reflective form, even round. Certain variables, such as the target surface angle, changes in temperature and humidity, and reflective surface roughness, can affect the operation of the sensors **(Migatron Corp., n.d.)**.

There are two types of ultrasonic sensors

a. **Proximity Detection:** An object passing within the preset range will be detected and generate an output signal. The detect point is independent of target size, material or reflectivity.

b. **Ranging Measurement:** Precise distance(s) of an object moving to and from the sensor are measured via time intervals between transmitted and reflected bursts of ultrasonic sound. Distance change is continuously calculated and outputted.

Microcontroller

A microcontroller is a computer present in a single integrated circuit which is dedicated to perform one task and execute one specific application.

It contains memory, programmable input/output peripherals as well a processor. Microcontrollers are mostly designed for embedded applications and are heavily used in automatically controlled electronic devices such as cell phones, cameras, microwave ovens, washing machines, etc.**(Lipovski, 2004).**

MATERIALS AND METHODS

HX711 Based on Avia Semiconductor's patented technology, HX711 is a precision 24-bit analog-to-digital converter (ADC) designed for weigh scales and industrial control applications to interface directly with a bridge sensor. The input multiplexer selects either Channel A or B differential input to the low-noise programmable gain amplifier (PGA). Channel A can be programmed with a gain of 128 or 64, corresponding to a full-scale differential input voltage of ±20mV or ±40mV respectively, when a 5V supply is connected to AV_{DD} analog power supply pin. Channel B has a fixed gain of 32. On chip power supply regulator eliminates the need for an external supply regulator to provide analog power for the ADC and the sensor. Clock input is flexible. It can be from an external clock source, a crystal, or the on-chip oscillator that does not require any external component. On-chip power on -reset circuitry simplifies digital interface initialization. There is no programming needed for the internal registers. All controls to the HX711 are through the pins.

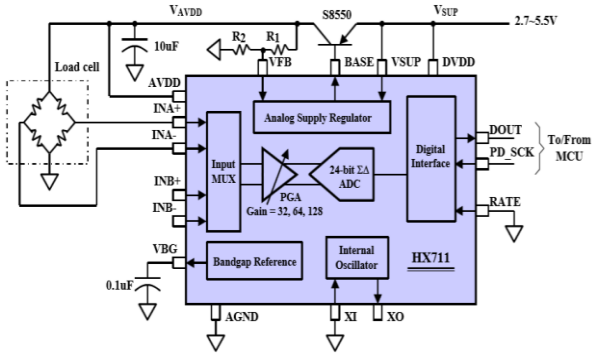

Figure 2: Application of the Hx711**(Avia Semiconductor, 2016)**

50kg load cell

This single disc load cell (sometimes called a strain gauge) can translate up to 50kg of pressure (force) into an electrical signal. Each load cell is able to measure the electrical resistance that changes in response to, and proportional of, the strain (e.g. pressure or force) applied to the disc. With this gauge you will be able to tell just how heavy an object is, if an object's weight changes over time, or if you simply need to sense the presence of an object by measuring strain or load applied to a surface.

Figure 3: 50 kg load cell **(SparkFun, 2018).**

Disc load cells are a bit easier to mount than bar-style load cells, making them more straightforward to implement into a design.

Each load cell is made from a steel-alloy and is capable of reading a capacity of 50kg. These load cells have four strain gauges that are hooked up in a Wheatstone bridge formation. The color code on the wiring is as follows: red = E+, green = O+, black = E-, and white = O-. Additionally, these load cells offer an IP66 protection rating.

***Ultrasonic sensor* HC-SR04 Ultrasonic sensor** is a 4 pin module, whose pin names are Vcc, Trigger, Echo and Ground respectively. This sensor is a very popular sensor used in many applications where measuring distance or sensing objects are required. The module has two eyes like embeded in the front which forms the Ultrasonic transmitter and Receiver. The sensor works with the simple high school formula that

The Ultrasonic transmitter transmits an ultrasonic wave, this wave travels in air and when it gets objected by any material it gets reflected back toward the sensor this reflected wave is observed by the Ultrasonic receiver module as shown in the Fig. 3.3 below

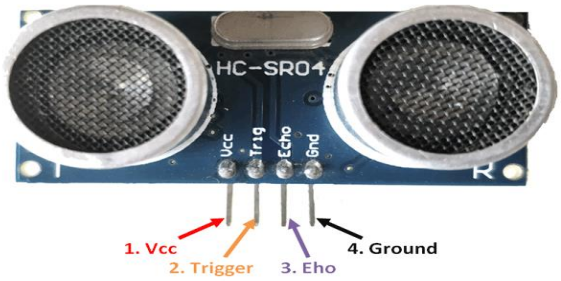

Figure 4: HC-SR04 Ultrasonic sensor (Borschbach, 2017)

Now, to calculate the distance using the above formulae, we should know the Speed and time. Since we are using the Ultrasonic wave we know the universal speed of US wave at room conditions which is 330m/s. The circuitry inbuilt on the module will calculate the time taken for the US wave to come back and turns on the echo pin high for that same particular amount of time, this way we can also know the time taken. Now simply calculate the distance using a microcontroller or microprocessor

ATMEGA328P

The high-performance Microchip 8-bit AVR RISC-based microcontroller combines 32KB ISP flash memory with read-while-write capabilities, 1KB EEPROM, 2KB SRAM, 23 general purpose I/O lines, 32 general purpose working registers, three flexible timer/counters with compare modes, internal and external interrupts,serial programmable USART, a byte-oriented 2-wire serial interface, SPI serial port, 6-channel 10-bit A/D converter (8-channels in TQFP and QFN/MLF packages), programmable watchdog timer with internal oscillator, and five software selectable power saving modes. The device operates between 1.8-5.5 volts.

For this design work, the Atmega328 was chosen because of its simplicity and the available pins needed for the connection of the design components as show below:

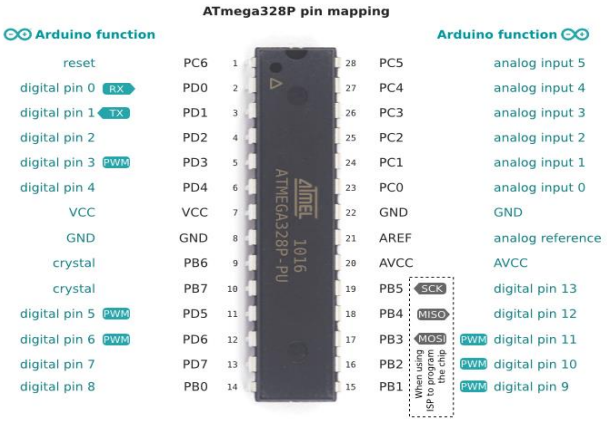

Figure 5: ATmega328P pin mapping **(Jordan, 2016)**

Hardware

The schematic diagram was drawn and the circuit was setup on breadboard and tested. As the testing gave a positive result, the circuit was transferred finally to a veroboard.

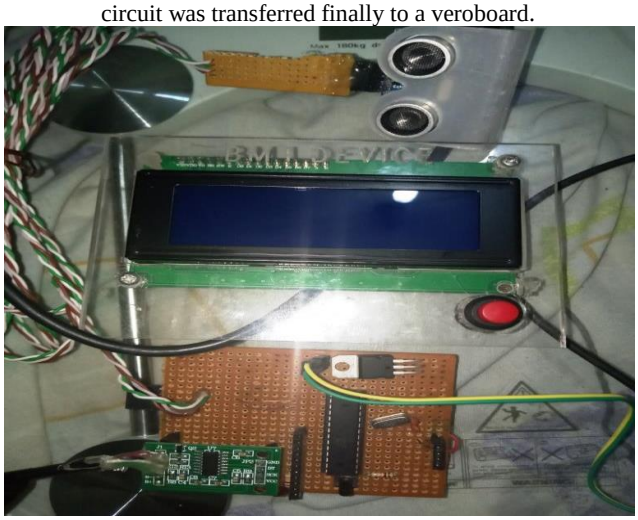

Figure 6: The Picture of the BMI Device

Software

The coding of the Atmega328 microcontroller was done using arduino IDE which is C++. Then the code was then transfer to the MCU controller with the help off Arduino Uno board show in plate I below

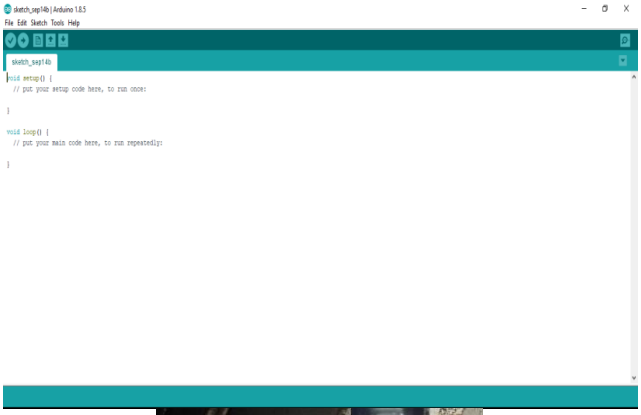

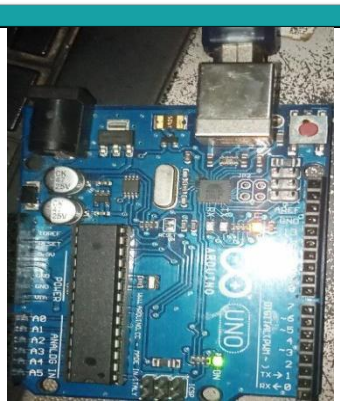

Figure 7: Arduino IDE and Uno Programmer in use.

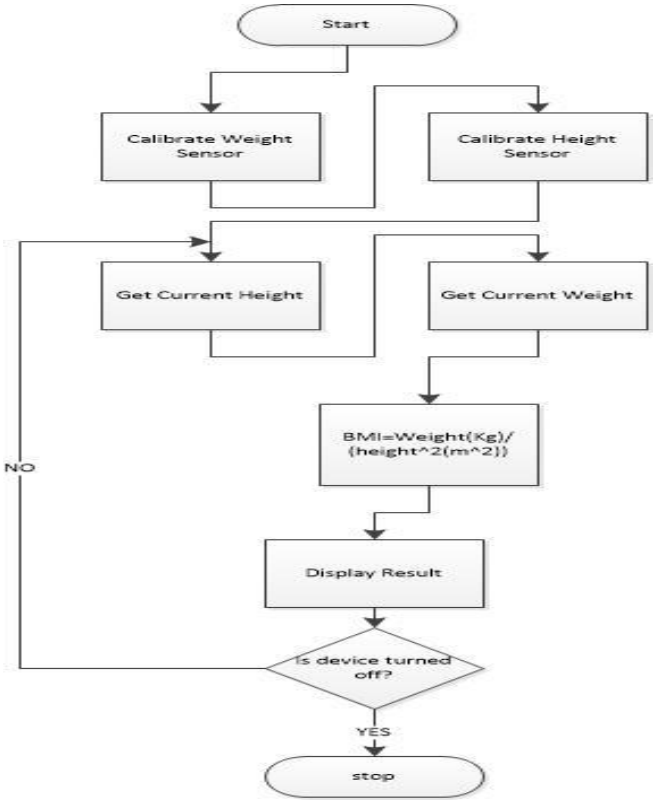

Figure 8: Flow Chart of Automatic Body Mass Index Measurement Device

I. RESULTS ANALYSIS AND DISCUSSION

During Setup, the height between the surface of the weight scale and ultrasonic sensor, SH is measured and stored as show in Plate III. When a subject climbs on it, the distance between the subjects head and the sensor is taken as SHH. The height of the subject; MH, is measured by subtracting SHH from SH i.e.

…… (4.1)

The weight (Kg) of the subject is simultaneously taken as the height is taken. Then the BMI is calculatedas shown in plate V and VI using equation (ii) below

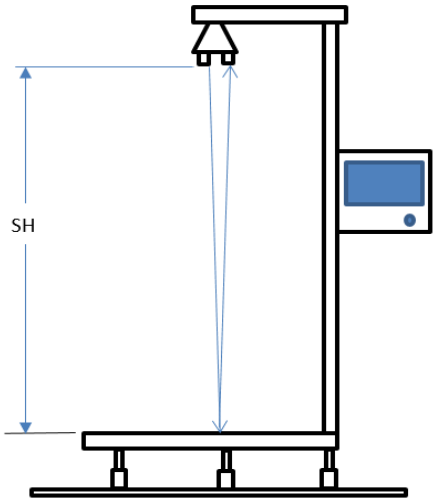

Figure 9: Setup or idle State

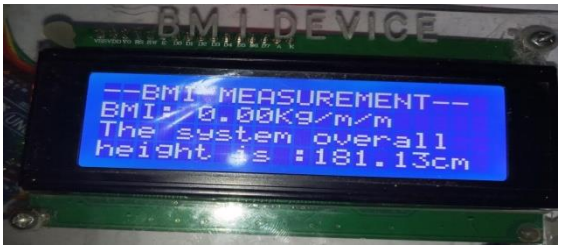

Figure 10: The Figure Show The Device In Idle Mode

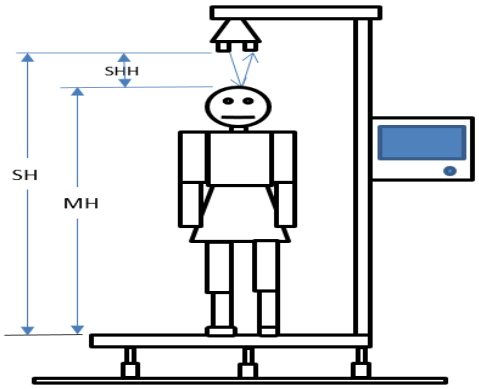

Figure 11: Demonstrates the device in Service

Figure 12: Device display the BMI, Height and Weight of the subject been measured.

COST OF MATERIAL

The table below shows the cost of material used for this design.

Table 1: Shows the list and cost of material used for the embedded system

Item	Cost	Quantity	total
Atmega328	1200	1	1200
LCD 2004 Display	2000	1	2000
50kg load cell	500	4	2000
Crystal Oscillator	50	1	50
0.22 uF capacitor	10	2	20
Button	20	2	40
10k resistor	10	2	20
LED	10	1	10
Casing	1500	1	1500
Total cost			**6,840**

CONCLUSION

This project has developed a system which automatically measures the body mass index of a person at a price relative cheaper than taking a Magnetic Resonance Imaging (MRI) scan. The objective function is achieved by using the microcontroller technology. The system is constructed using a load cell sensor to measure weight, ultrasonic to measure height, a microcontroller to process data received and LCD display to display the result in Kg/m^2.
The result achieved is faster and cheaper when compared to an MRI scan. The efficiency of the proposed system will improve the efficiency of the BMI system by reducing the time it takes to get a result at a very low cost.

REFERENCES

[1] Amin, N., & Borschbach, M. (2017). Quality of obstacle distance measurement using Ultrasonic sensor and precision of two Computer Vision-based obstacle detection approaches. *International Conference on Smart Sensors and Systems*, 1–4. https://doi.org/10.1109/SMARTSENS.2015.7873595[2] Avia Semiconductor. (2016). 24-Bit Analog-to-Digital Converter (ADC) for Weigh Scales. *Hx711*, *9530*(592), 1–9. Retrieved from https://www.mouser.com/ds/2/813/hx711 _english-1022875.pdf%0Ahttps://cdn.sparkfun.com/datasheets/Sensors/ForceFlex/hx711_english.pdf

[3] Dunnicliff, J. (1988). *Geotechnical Instrumentation for Monitoring Field Performance*. John Wiley & Sons, New York.

[4] Ekelund, U., Ward, H. A., Norat, T., Luan, J., May, A. M., Weiderpass, E., … Riboli, E. (2018). Physical activity and all-cause mortality across levels of overall and abdominal adiposity in European men and women : the European Prospective Investigation into Cancer and Nutrition Study (EPIC) 1 – 6 The EPIC cohort, (July), 1–6. https://doi.org/10.3945/ajcn.114.100065.weight

[5] Gəşpəresc, G., & Gontean, A. (2015). Performance evaluation of ultrasonic sensors accuracy in distance measurement. *2014 11th International Symposium on Electronics and Telecommunications, ISETC 2014 - Conference Proceedings*, 0–3. https://doi.org/10.1109/ISETC.2014.7010761

[6] International Atomic Energy Agency. (2010). Dual energy X ray absorptiometry for bone mineral density and body composition assessment. *IAEA Human Health Series No. 15*, 132. Retrieved from http://www.iaea.org/Publications/index.html

[7] Jordan, R. (2016). Arduino to AVR-C Reference Guide – Jordan Réjaud – Medium. Retrieved September 17, 2018, from https://medium.com/@jrejaud/arduino-to-avr-c-reference-guide-7d113b4309f7

[8] Lipovski, G. J. (2004). Introduction to Microcontrollers. *Introduction to Microcontrollers*, 379–414. https://doi.org/10.1016/B978-012451838-4/50016-9

[9] Manios, Y. (2012). The 'ToyBox-study' obesity prevention programme in early childhood: an introduction. *Obesity Reviews*, *13*, 1–2. https://doi.org/10.1111/j.1467-789X.2011.00977.x

[10] Marty, B. (1990). *Practical Switching Power Supply Design*. Academic Press.

[11] Migatron Corp. (n.d.). Applications for Ultrasonic Sensors. Retrieved July 23, 2018, from https://www.migatron.com/ultrasonic-detections-and-control-applications/

[12] Sara Police. (2017). How Does a Handheld BMI Machine Work? Retrieved July 9, 2018, from https://www.livestrong.com/article/558509-how-does-a-handheld-bmi-machine-work/

[13] Shin, S., Kim, M. H., & Choi, S. B. (2017). Improving efficiency of ultrasonic distance sensors using pulse interval modulation. *Proceedings of IEEE Sensors*, 5–7. https://doi.org/10.1109/ICSENS.2016.7808766

[14] Singh, N. A., & Borschbach, M. (2017). Effect of External Factors on Accuracy of Distance Measurement using Ultrasonic Sensors, 266–271.

[15] Siregar, B., Seniman, Fadhillah, D., Andayani, U., Pranoto, H., & Fahmi, F. (2017). Simulation of waste transport monitoring based on garbage load capacity using load cell. *2017 International Conference on ICT For Smart Society (ICISS)*, 1–7. https://doi.org/10.1109/ICTSS.2017.8288883

[16] SparkFun. (2018). Load Cell - 50kg, Disc (TAS606) - SEN-13331 - SparkFun Electronics. Retrieved September 17, 2018, from https://www.sparkfun.com/products/1333

Coexistence of 5Gwith Fixed Services

S. A. Mikail, I. K. Musa
Department of Communications Engineering,
Ahmadu Bello University Zaria, Nigeria
[1]samikail@abu.edu.ng
ismkmusa1@gmail.com

ABSTRACT—Fifth generation (5G) network is a promising technology to support massive connectivity, improves quality of experience as well as supports sophisticated applications. Feasibility studies for deployment of 5G on higher frequency bands up to 86GHz have been recommended during world radio communication conference held in 2015 (WRC-15). Since such frequency band, especially 70GHz, have already been allocated to fixed service (FS) by spectrum regulatory bodies, 5G need to coexist with the incumbent system. This paper investigated feasibility of existence of a terrestrial 5G BS with FS terminal at 70GHz band considering interference from the FS terminal into the terrestrial 5G BS. The study considered a single FS terminal at different positions with respect to the 5G BS and evaluated signal to interference plus noise ratio at each sector of the 3-sector cell terrestrial 5G BS, considering immobile users at the edge of the 5G cell. The results suggested that terrestrial 5G BS can coexist with the FS terminal provided the deployment parameters of the former are carefully chosen.

KEYWORDS—5G, FS, coexistence, mmWave band.

INTRODUCTION

5G network is expected to provide minimum end-to-end latency; improvement in quality of experience; efficiency in utilization of resources; reduction in capital and operational expenditure (CAPEX and OPEX) through flattening the network architecture; and supporting versatile applications via software define networks [1]. These could only be achieved by deployment of 5G on a band with huge bandwidth. With the advancement in multiple-input-multiple - output (MIMO) technology, the factors that used to hinder deployment of mobile networks on high frequency can be mitigated [2]. As a result, spectrum operators recommended deployment of 5G network on high frequency bands.

The world radio communication conference of 2015 (WRC-15) have recommended frequency up to 86GHz for feasibility studies towards deployment of 5G network [3]. 70GHz band is a suitable for this purpose. However, International Telecommunication Union (ITU) Radio Regulation and Nigerian Communications Commission (NCC) have already allocated 71 to 74GHz band to fixed service (FS), fixed satellite services (FSS) and mobile services [4]. But, based on National Frequency Allocation Table (NFTA) [1], 71 to 74GHz band had already been allocate to FS. So, 5G need to coordinate with the incumbent FS. Figure 1 depicts the ITU allocation and the corresponding Nigeria allocation based on NFTA. Based on Figure 1, 5G network needs to coexist with FS.

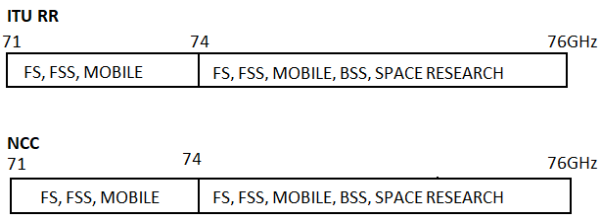

Figure 1: ITU and ECC allocation on 71-76GHz band

Recent studies on coexistence feasibility of different networks are include data base approach had been used in EU FP7 European research work cognitive radio (CoRaSat) to investigate feasibility of coexistence of FSS systems with incumbent fixed service (FS) systems on Ka-band [5]. The work found under-utilized spectrum allocated to FS systems within the Europe for additional deployment of FSS systems carriers. Moreover, the concept of cognitive radio (CR) has been used in coexistence studies of Ka-band satellite systems with terrestrial systems [6]. The cognitive user, FSS, is provided with intelligence based on its location, gain pattern and path loss awareness models. The information enables estimation of the interference it is generating to the incumbent FS system. Based on such information, the cognitive user is able to reduce the interference to an acceptable level that can be tolerated by the FS system. The research also found a limit to the number of uniformly distributed FSS terminals in an area that guaranteed an $\frac{I}{N}$ threshold of -10dB at the FS terminal.

Different from the existing relevant literatures, this paper investigates coexistence feasibility of terrestrial 5G BS with the incumbent FS system on 70GHz band, considering only co-channel interference form an FS terminal into a terrestrial 5G BS. The research uses a threshold signal to interference plus noise ratio (SINR) as a protection parameter for the 5G system. The threshold SINR of -8.266db had been found, prior to this study, at 5G innovation center of University of Surrey, United Kingdom via a link level simulation for different modulation and code rate schemes allowing a maximum block error rate (BLER) of 10% as

Table SEQ Table * ARABIC 1: SINR requirement for different code rates and modulation schemes performed at the 5G Innovation Centre of the University of Surrey.

and modulation schemes performed at the 5G Innovation Centre of the University of Surrey. Deployment distances of the terrestrial 5G BS were investigated such that the SINR on all sectors of a 3-sector cell 5G BS do not degrade below the required thresholds. At the end, it will be shown that 5G can coexist with the incumbent FS provided the deployment parameters of the former are carefully chosen.

SYSTEM MODELLING

This study considered 71 GHz, frequency of point-to-point link in Nigeria. The scenario as depicted in Figure 2 consists of a terrestrial 5G BS with immobile users at the edge of their corresponding cells. Each user is assumed to be schedule by a single sector. The link between the sectors and their users are depicted with black lines. The incumbent interference from the FS terminal is depicted with red lines.

The signals on each of the sectors, on the assumption that there is power control such that users transmit equal power [8] is given by:

$$S_j = P_{UE} + G_{UE} - PL_{BU} + G_{BUj}(\theta_2, \varphi_2) \quad (1)$$

S_j, *is* the useful signal on sector j from user j, P_{UE} is the transmit power of UE j and $G_{UE}$is the gain of UE j antenna. Also, PL_{BU} is the Path loss between the sector j and user j and $G_{BUj(\theta_2,\varphi_2)}$ is the gain of sector j towards UE j.

The interference on each of the sectors based on [8] is given by:

$$I_j = P_{FS} + G_{\phi_f} - PL_{BF} + G_{BEj}(\theta_2, \varphi_2) \quad (2)$$

P_{FS} is the a transmit power of the FS terminal with a gain of G_{ϕ_f} towards the terrestrial 5G BS. Also, $G_{BEj(\theta_2,\varphi_2)}$ is the gain of sector j of the terrestrial 5G BS towards the FS terminal and PL_{BF} is the path loss between the terrestrial 5G BS and the FS terminal.
So, the signal to interference ratio (SIR) on each of the sectors is given by:

The thermal noise of a sector with noise Figure of N_F, at an average temperature of T, based on [9] is given by:

$$N = N_F + 10KT \quad (3)$$

where K is the Boltmann constant.

The SINR at each of the sector is then obtained by combining the presented equations as:

$$SINR_j = 10\left[\left(10^{(SNR_j/10)}\right)^{-1} + \left(10^{(SIR_j/10)}\right)^{-1}\right]^{-1} \quad (4)$$

Where SIR and SNR are the signal to interference and signal to noise ratio in decibels respectively.

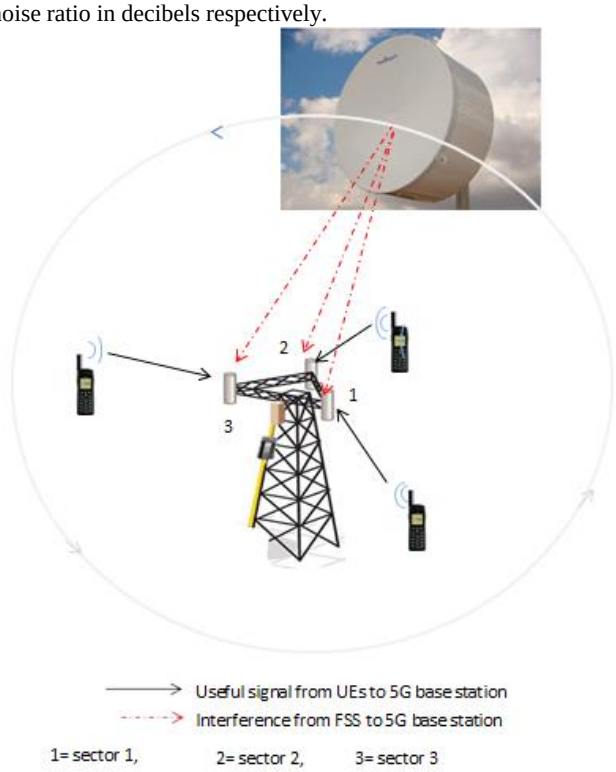

Figure 2: 3-sector cell base station with schedule user terminals around an FS terminal

The FS antenna gain for a point-to-point link, a function of off-axis angle (ϕ_s), depends on the heights of the FS and 5G terminals, relative azimuth angle between them. The off-axis according [6] is;

$$\phi_f = (cos\ cos(E_s)\ cos\ cos(\varepsilon)\ cos\ cos(\alpha) + sin\ sin(\varepsilon)\ sin\ sin(E_s)) \quad (5)$$

Where ε is the elevation angle, in degrees, of the radio wave at the FSS terminal given by:

$$\varepsilon = \left(\frac{(z_b - z_a)*10^{-3}}{d} - \frac{d}{2r}\right) * \frac{180^o}{\pi} \quad (6)$$

$r = 8500Km$ is the effective earth radius. z_a, z_b and d are the height of the FS terminal, height of the 5G terrestrial BS and the distance between them respectively. The gain of an FS terminal of diameter, D, according to [6] is given by:

$$G_{\phi_f} = \{G_{max} - 25 * 10^{-3\left(\frac{D}{\lambda}\phi_s\right)^2} \quad 0^0 < \phi_s \leq x_{t1} G_1, \quad x_{t1} < \phi_s \leq x_{t2} 52 - 10\left(\frac{D}{\lambda}\right) - 25(|\phi_s|), \quad x_{t2} < \phi_s \leq 48^o 10 - 10\left(\frac{D}{\lambda}\right), \quad 48^o < \phi_s \leq 180^o \quad (7)$$

A model recently released by 3GPP s used for the estimation of path loss between both the users and the FS terminal to the terrestrial BS. Figure depicts a configuration with user of height h_{UE} and 5G BS o height, h_{BS}, for path loss estimation.

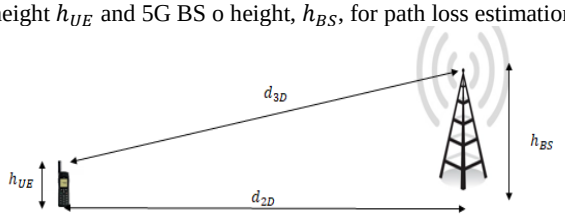

Figure 3: User terminal to 5G terrestrial BS configuration

According to [10], the relationship between d_{3D} and d_{2D} is:

$$d_{3D} = \sqrt{(d_{2D})^2 + (h_{BS} - h_{UE})^2} \quad (8)$$

The non-line of sight pathlos between the UE and the 5G BS according to 3GPP recommendation [10] is given by:

$$PL_{BU} = max\ ((PL_{UMI-LOS},\ PL'_{UMI-NLOS})) \quad (9)$$

Where,

$$PL_{UMI-LOS} = \{PL1, \quad 10 \leq d_{2D} \leq d'_{BP} \quad PL2, \quad d'_{BP} \leq d_{2D} \leq 5km \quad (10)$$

With

$$PL1 = 32.4 + 20d_{3D} + 20f \quad (11)$$

And

$$PL2 = 32.4 + 40d_{3D} + 20f - 9.5[(d'_{BP})^2 + (h_{BS} - h_{UE})^2] \quad (12)$$

Also,

$$PL'_{(UMI-NLOS)} = 35.5d_{3D} + 22.4 + 21.3f - 0.3(h_{UE} - 1.5) \quad (13)$$

With,

$$d'_{BP} = 4 * h'_{BS} * h'_{UE} * \left(\frac{f*10^9}{c}\right) \quad (14)$$

Where,

$$h'_{UE} = h_{UE} - 1 \quad (15)$$
$$h'_{BS} = h_{BS} - 1 \quad (16)$$

C is the speed of light (in m/s) and f is frequency of operation (in GHz).

The path loss between the terrestrial 5G BS and an FS terminal is obtained by replacing h_{UE} with h_{FS} in equations (12), (13), (14) and (15) above.

The antenna pattern of the 5G terrestrial BS also follows a 3GPP model in [11]. Each sector consists of a uniformly rectangular array. But for this analysis, only a single antenna element was considered per sector. The gain of the 5G antenna element depends on two off-axes angles: vertical off-axis angle, θ_2, and horizontal off-axis angle, φ_2. The gain of a 5G antenna element is given by:

$$G_{BE}(\theta_2, \varphi_2) = G_{BE,max} + RP_{BE}(\theta_2, \varphi_2) \quad (17)$$
$$= 8 + RP_{BE}(\theta_2, \varphi_2) \quad (18)$$

where, $G_{BE,max}$, the maximum gain of the antenna element having a value of 8dB. $RP_{BE}(\theta_2, \varphi_2)$ is the antenna element radiation pattern as a fuction of the two off-axes angles, θ_2 *and* φ_2 and:

$$RP_{BE}(\theta_2, \varphi_2) = -\left\{-\left(RP_{BE,V}(\theta_2) + RP_{BE,H}(\varphi_2)\right), 30\right\} \quad (19)$$

With,

$$RP_{BE,V}(\theta_2) = -\left\{12\left(\frac{\theta_2 - 90}{65}\right)^2, 30\right\} \quad (20)$$

And

$$RP_{BE,H}(\varphi_2) = -\left\{12\left(\frac{\varphi_2}{65}\right)^2, 30\right\} \quad (21)$$

The off-axes angles were calculated by assuming the origin of the global coordinate system was shifted to the position of the 5G terrestrial BS.
With the 5G terrestrial BS assumed to be pointing in a direction with angle α^o away from the positive x-axis and down tilted by an angle of β^o with slant angle of γ^o,the spherical coordinate of the FS terminal within the local coordinate system of the 5G terrestrial BS is$(\rho_2, \theta_2, \varphi_2)$. The transformation method of [11] was used to obtain the expessions for θ_2 and φ_2 as:

$$\theta_2 = \Big(cos\,cos(\beta)\,cos\,cos(\gamma)\,cos\,cos(\theta_1) + \left[sin\,sin(\beta)\,cos\,cos(\gamma)\,cos\,cos(\varphi_1 - \alpha) - sin\,sin(\gamma)\,sin\,sin(\varphi_1 - \alpha)\right] sin\,sin(\theta_1)\Big) \quad (22)$$

$$\varphi_2 = \arg\left(j\left[\begin{matrix}[\cos(\beta)\sin(\theta_1)\cos(\varphi_1-\alpha) - \sin(\beta)\cos(\theta_1)] + \\ \cos(\beta)\sin(\gamma)\cos(\theta_1) \\ +\{\sin(\beta)\sin(\gamma)\cos(\varphi_1-\alpha) + \cos(\gamma)\sin(\varphi_1-\alpha)\}\sin(\theta_1)\end{matrix}\right]\right) \quad (23)$$

Assuming the terrestrial 5G BS is pointing along the positive x-axis (=0) for sector 1, =120 for sector 2 and =20 for sector 3. In practical deployment, sectors are usually tilted by certain angle so as to reduce interference to neighboring cells. However, since we intend to evaluate maximum interference, all the sectors are assumed to be unstilted such that down tilt angle $\beta = 0°$, and slantangle $\gamma = 0°$.

Table 1: Parameters used in the study

Parametr	5G	FS

Carier frequency	73.5GHz		
Bandwidth	1GHz		
Pathloss model	UMi		
	BS	UE	FS
Maximum gain	8dBi per element	0 dBi	50dBi
Tranmit power		13dBm/MHz	19dBm/MHz
Antenna height	10m	1.5m	25m
temperature	300K		
Noise Figure	7dB		
Number of element	1		

In the scenario considered, 5G terrestrial BS was assumed to be at coordinate (0, 0) around a single FS terminal. Since high frequency signal transmission suffers from huge propagation losses, a cell size of 200m was assumed for the 5G terrestrial BS. The users are assumed to be immobile and placed at the edges of their respective cells. Other parameters used in the study are in Table 1. The FS terminal is then placed at different distances and relative azimuth angle to the 5G BS. The FS is deployed on r-θ coordinate with r=0:50:5000 and θ=0: π/50:2π. The Available SINR on each of the 5G sectors is evaluated, using MATLAB 2016a, as a function of distance and relative azimuth angles to the 5G BS.

.PERFORMANCE EVALUATION

The deployment of 5G micro BS parameters coexisting with FS terminal were investigated. Assuming the relative azimuth angle from the FS terminal to the 5G BS is 0^oalong the direction of the first sector ($\alpha = 0^o$). The 3D plot of the SINR availble on sectors 1,2 and 3 are as depicted in Figures 4,5 and 5 Respectively.

The minimum deployment distances for sector 1 are the points where the -8.266dB plane (grey in colour) cut the SINR 3D plot. Based this, when the relative azimuth angle are within a range of0^o *to* 3.6^0 *and* 0^o *to* -3.6^o, the sector has to be at a minimum of 1250m away from the FS terminal. Moreover, if the relative azimuth angle to the FS terminal is between 10^o *to* 35^o *and* -10^o *to* -35^o,the sector need to be atleast at a distance of 700m away from the FS terminal. In addition, within realtiv azimuth angle of 50^o *to* 280^o, only a minimu of 100m is required for the deployment of this sector such that the minimum SINR threshold of -8.266dB is always guaranteed.

Based on SINR available on sector 2, when the FS terminal is at relativce azimuth angle of 0 t0 70, a minimum deployment distance of about 100m ie needed. The lagest deployment distnace of about 20m needed by the 5G BS occures when the relative azimuth angle is between 100 to 126.

For sector 3, 200m is also required by the 5G Bs irrespective of the relative azimuth angle to the FS terminal.

As a result, sector is the most critical and determines the overall deployment distance of the terrestrial BS. Hence, 5G terrestrial BS requires a minimum distance of about 1.25km away for an FS backhaul terminal.

Since sector 1 determines the deployment distance of the 5G terrestrial BS, a 2D plot of minimum deployment distance of the 5G BS for different transmit powers of the FSS terminal at elevation angle commonly used in Nigeriaria so that a minimum SINR of -8.2dB is always guranteed on sector 1 is depicted in Figure 7. The

minimum 5G terrestrial BS deployment distances required based on FSS transmit powers (Po) and elevation angles are as reported in Table 1.

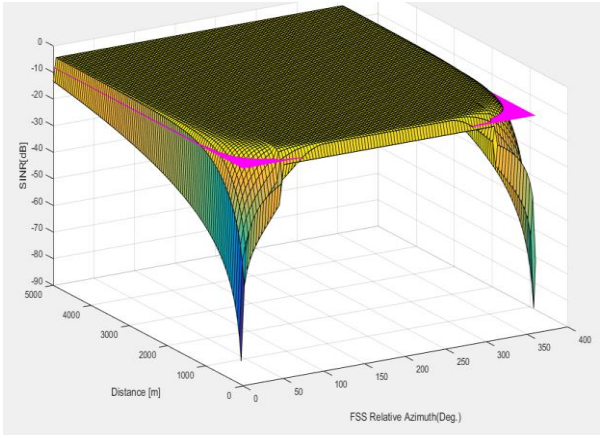

Figure 4: SINR on sector 1

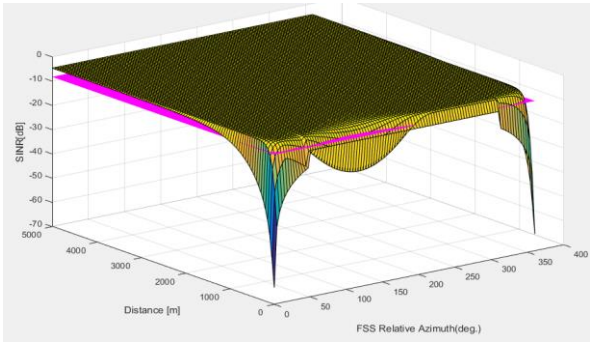

Figure 5: SINR on sector 2

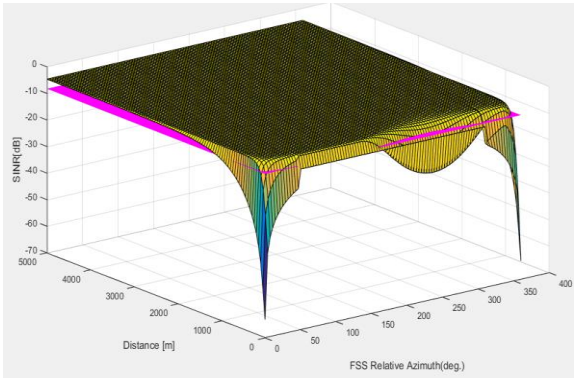

Figure 6: SINR on sector 3

CONCLUSION AND FUTURE WORK

Coexistence of a terrestrial 5G BS with an Fs terminal for a backhaul link at 73.5GHz. the study is highly impotant towards world radiocommunication conference to be held in 2019 (WRC-19), where final decision will be made regarding allocation to 5G system allocation. The research considered only interference from he Fs terminak into the 5G terretrial BS. The research also used singnal to intefernce plus noise ration as the protection parameter of the 5G system. A threshold of -8.266dB, obtained via link level simulation (performed prior to this research) performed at the 5g innovation centre of the universty of surrey. Using recently released 5G antenna gain and pathloss models, a FS terminal at different positions to the terrestrial 5G BS and evalauted the SINR at each sector of the 3sector 5G BS. It has been found that a minimum distance of about 1.25km away from the FS terminal is reqired by the terrestrial 5G BS.

However, the study is not exhaustive as the users were considered immobile, contrary to real live scenation where users mostly move. As a result further study considering this is needed.

REFERENCES

[1] X. Huang, R. Yu, J. Kang, Y. He, and Y. Zhang, "Emerging Technology for 5G Enabled Vehicular Networks; Exploring Mobile Edge Computing for 5G-enabled Software Defined Vehicular Networks," *IEEE Wirel. Commun.*, no. December, pp. 55–63, 2017.

[2] M. Gul, E. Ohlmer, A. Aziz, W. McCoy, and Y. Rao, "Millimeter Waves for 5G: From Theory To Practice," in *Signal Processing for 5G: Algorithms and Implementations*, 2016, pp. 321–353.

[3] O. UK, "Spectrum above 6 GHz for future mobile communications," *UK, Ofcom*, no. January 16, p. 62, 2015.

[4] Nigeria Frequency Management Council (NFMC), "National Frequency Allocation Table," no. October, p. 188, 2014.

[5] K. Liolis *et al.*, "Cognitive Radio Scenarios for Satellite Communications: The CoRaSat Approach," pp. 1–10, 2013.

[6] A. Mohamed, M. López-benítez, and B. Evans, "Ka-Band Satellite Terrestrial Co-Existence : a Statistical Modelling Approach," no. October, 2014.

[7] 3GPP, "TS 36.211 version 10.0.0 Release 10; Evolved Universal Terrestrial Radio Access (E-UTRA); Physical channels and modulation," *Tech. Specif.*, vol. 0, p. 9, 2011.

[8] F. Guidolin, M. Nekovee, L. Badia, and M. Zorzi, "A study on the coexistence of fixed satellite service and cellular networks in a mmWave scenario," *IEEE Int. Conf. Commun.*, vol. 2015–Septe, pp. 2444–2449, 2015.

[9] S. Kim, E. Visotsky, P. Moorut, K. Bechta, A. Ghosh, and C. Dietrich, "Coexistence of 5G with the incumbents in the 28 and 70 GHz bands," *IEEE J. Sel. Areas Commun.*, vol. 35, no. 6, pp. 1254–1268, 2017.

[10] "38900-e10." .

[11] "38802-003."

Optimal Overcurrent Relay Protection Coordination in Distribution Network Based on a Simulated Annealing Inertia Weight Particle Swarm Optimization Technique

Mohammed Kabir
Department. of Electrical Engineering
Kaduna Polytechnic
Kaduna, Nigeria
kabirjb@gmail.com

Aliyu D. Usman
Dept. of Communications Engineering
ABU Zaria
Kaduna, Nigeria
adusman@abu.edu.ng

Boyi Jimoh
Department of Electrical Engineering
ABU Zaria
Kaduna, Nigeria
jboyi@abu.edu.ng

ABSTRACT— The coordination of overcurrent relays in a power system is to ensure that only the faulted section of the system is isolated when an abnormal operating state occurs. Large numbers of relay tripping and mis-coordination are due to improper or inadequate settings rather than to genuine faults. A Modified Particle Swarm Optimization (MPSO) techniques which is based on an adaptive simulated annealing inertia weight was used to solve the problem of overcurrent relay coordination. The objective function is the minimization of the operation time of the protective relays in the IEEE 15 and 30 bus networks. The Time of Operation (T_{op}) and Coordination Time Interval (CTI) were used as the performance metrics of the research. The obtained operating time of the IEEE 15 bus is 23.22 seconds. The simulation time of the 15 bus network is 11.22 seconds. Relay no. 11 and 21 with CTI values of 0.0863 seconds and 0.0940 seconds violated the CTI constraints. The result obtained for the IEEE 15 bus was validated and an improvement of 11.3288% was observed in terms of reduction in the operating time of the relays in the system. The obtained T_{op} and CTI settings of the relays in the system show the effectiveness of the proposed MPSO technique.

KEYWORDS - Relays, Optimal Coordination, Plug Setting, Time Multiplier Setting, Coordination Time Interval.

INTRODUCTION

This The primary objective of all power systems is to maintain a very high level of continuity of service, and when intolerable conditions occur, to minimize the extent and time of the outage. However, because it is impossible, as well as impractical, to avoid the consequences of natural events, physical accidents or equipment failure owing to human error, many of these will result in faults [1, 2].

Since 1960s, a great effort has been devoted for solving this problem by computational tools [3]. The methods, which are used for performing this task can be classified into three classes: trial and error method, topological analysis method, and Heuristic optimization method [3, 4]. Furthermore, due to the complexity of the power system network, trial and error approach and topological analysis are time consuming and not optimal [5].

Several optimization techniques and artificial intelligence methods have been deployed in solving relay coordination problem, methods such as Harmony Search Algorithm (IHSA) to solve relay coordination problem with three different cases on IEEE 14-bus and IEEE 30-bus systems [6], Cuckoo Search Algorithm [7]. Variants of PSO and its hybrids have also been deployed in optimal relay coordination [8-12].

The optimal coordination of over current relays poses serious problems in the modern complex power system networks, which are interconnected, because of that, they are protected by directional over current relays, which are standalone devices and strategically placed throughout the system [4, 5].

According to statistical evidence, a large number of relay tripping and mis-coordination are due to improper or inadequate settings rather than to genuine faults [5]. Overcurrent relay coordination has been worked upon by many researchers and the challenge was mainly on how to design an optimal relay coordination system. The relay coordination is not an exact science, but in fact an Art that involves some degree of uncertainty due to its complexity and nonlinearity [5, 6], hence it is difficult to claim that a global optimal result has been yielded

Thus, this work seeks to improve the solution of the coordination problem by using a modified particle swarm optimization technique for reaching the global optimum value with less computational time. Simulated Annealing Inertia Weight is used to modify the conventional PSO to develop an efficient model for solving the relay coordination problem was based on the outcome of experiments where several inertia weight strategies were subjected to optimization test functions. The Simulated Annealing Inertia Weight strategy gave an outstanding performance when the average error, average number of iteration and minimum error were used as the criteria for comparison.

COORDINATION PROBLEM FORMULATION

The coordination problem and constraints for optimum relay coordination are formulated in this section.

A. Objective Function (OF) Formulation

First, The objective function of the optimization problem is therefore, the minimization of the operation time of the associated relays. After considering all these criteria, the objective function (OF) can be formulated mathematically as given in equation 1.

$$\text{OF} = \min \sum_{i=1}^{n} w_1 \times T_{op_i} \quad (1)$$

Where n is the number of relays in the network, is a coefficient usually set to 1, it indicates the probability of the occurrence of a fault and is the operating time of relay.

All relays are assumed to be identical and have IDMT characteristic, the operating time is given by equation 2 [1, 3, 5, 7, 9, 11-13].

$$T_{op} = \frac{\lambda \times TMS}{\left(\frac{I_f}{PS \times CT}\right)^{\eta} - 1} + L \quad (2)$$

Where TMS is the Time Multiplier Setting, PS is the Plug Setting, I_f is the fault current, CT is the current transformer ratio and $i = 1, 2, ...n$.

There are several characteristics of overcurrent relays as shown in Table I. The standard Inverse overcurrent relay is the relay of choice for this paper.

Table I: Characteristics of DOCRs [6]

Type of Characteristic	K	A	L
Short Time Inverse	0.05	0.04	0
Standard Inverse	0.14	0.02	0
Very Inverse	13.5	1	0
Extremely Inverse	80	2	0
Long Time Inverse	120	1	0
Moderately Inverse	0.0515	0.02	0.114
Very Inverse	19.61	2	0.491
Extremely Inverse	28.2	2	0.1217

In equation (3), λ, η and L are the characteristic constants of the relays while I_f is the fault current through the relay operating coil. For standard inverse definite minimum time (IDMT) relays λ = 0.14, η = 0.02 and L = 0 [4, 7, 8, 10, 11-13].

$$T_{op,i} = \frac{0.14 \times TMS_i}{\left(\frac{I_{f,i}}{PS_i \times CT}\right)^{0.02} - 1} \quad (3)$$

B. Constraints Formulation

For the objectives of optimum relay coordination to be achieved, the coordination and boundary constraints must be satisfied. The lower and upper bounds of TMS and PS of each DOCR are given by equations 4

$$TMS_{i_{\min}} \le TMS_i \le TMS_{i_{\max}}$$
$$PS_{i_{\min}} \le PS_i \le PS_{i_{\max}} \quad (4)$$

Based on the Standard Inverse relay characteristic used in this work, the TMS and PS are the decision variables of the optimization problem, their limits are outlined in equations (5), (6) and (7). The values of the limit are adopted from [9] for the purpose of validation.

$$0.1 \le TMS \le 1.1 \quad (5)$$

$$0.5 \le PS \le 2.5 \quad (6)$$

$$0.1 \le T_{op} \le 4s \quad (7)$$

I. C. Coordination Time Interval (CTI)

Coordination time interval (CTI) is the criteria to be considered for coordination. It's a predefined time delay and it depends on the type of relays. For electromagnetic relays, CTI has a minimum value of 0.2 s, while for a microprocessor based relay, it is of the order of 0.1 to 0.2 s [9, 15]. The sample network of two directional overcurrent relays is shown in Figure 1, where R_b and R_p are in order of backup and primary relays for close in fault to R_p at location *F* [6, 8, 13, 15].

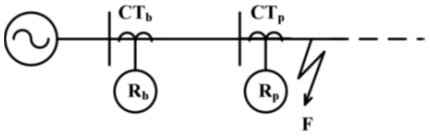

Figure 1: Illustrative diagram for P/B relay pair [6, 13]

In this case, R_p should trip as quickly as possible, whereas R_b should operate after time period required for preserving selectivity between P/B protections known as CTIexpressed by 8.

$$T_b - T_p \ge CTI \quad (8)$$

Where T_b and T_p are operating time of backup relay (R_b) and primary relay (R_p) respectively. The *CTI* depends on the types of relays, circuit breaker operating time, relay error and safety margin [9, 14].

II. SIMULATED ANNEALING INERTIA WEIGHT PARTICLE SWARM OPTIMIZATION

This research work employed an adaptive behavior based simulated annealing inertial weight for selecting the appropriate inertia weight for the PSO as the algorithm swarm towards the optimum solution. This is given in equation (9)

$$w_k = w_{\min} + \left(w_{\max} - w_{\min}\right) \times \lambda^{(k-1)} \quad (9)$$

Where w_k is the inertial weight at current generation, w_{min} is a randomly generated number within an interval of 0 and 1, w_{max} is a randomly generated number within an interval of 0 and 1, k is the current iteration number.

In this work, the value of lambda shall be determined using equation (10)

$$\lambda = \left(\frac{ITR\max - ITR}{ITR\max} \right)^n \quad (10)$$

Where ITR_{max} is the maximum value of iteration which is defined by the user, ITR is the current value of iteration, n is the total number of particle defined by the user.

The lambda in equation (10) serves as the dynamic parameter for the inertia weight which is selected adaptively during the optimization process. Figure 2 shows the flowchart modified PSO. The shaded portion in the flowchart indicates the application of the simulated annealing inertia weight.

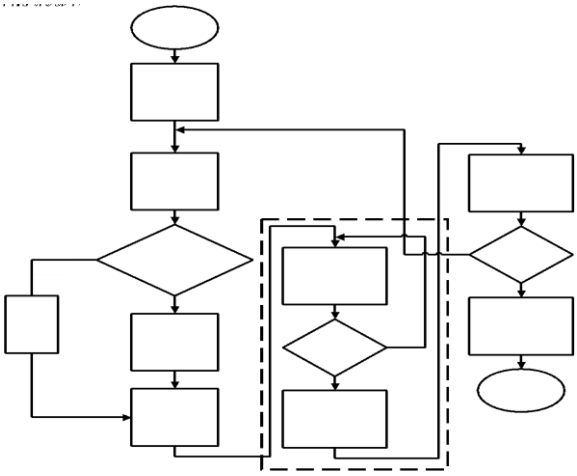

Figure 2: PSO flowchart showing the Simulated Annealing Inertia Weight

III. IEEE 15-BUS SYSTEM

The IEEE 15 bus radial test system is used in this work to validate the performance of the proposed solution. The data and parameters used are based on the work of [9]. The test system is shown in Figure 3. The system is widely used as a case for conducting various studies such as relay coordination, interconnected grid problems etc.

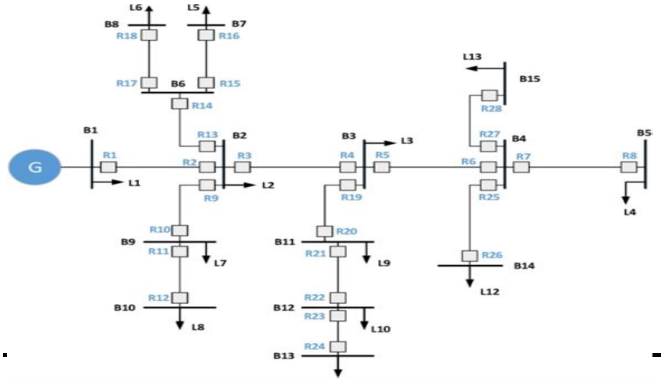

Figure 3: IEEE 15-Bus Radial network

All the relays in the network are considered Directional Overcurrent Relays (DOCR) with standard Inverse Definite Minimum Time (IDMT) characteristics and have their tripping direction away from the bus. The fault currents values given in Table II are based on International Electrotechnical Commission standard for the IEEE 15 bus 3-ϕ bolted faults simulated at the near end.

Table II: Fault Current Values of the Relays for IEEE 15-Bus Radial System

Relay No.	Fault Currents (A)	Relay No.	Fault Currents (A)
1	22778	15	7710
2	11532	16	5790
3	11509	17	7700
4	7710	18	5790
5	7700	19	7700
6	5790	20	5790
7	5785	21	5785
8	4636	22	4636
9	11509	23	4632
10	7710	24	3866
11	7700	25	5785
12	5790	26	4636
13	11509	27	5785
14	7710	28	4636

IV. SIMULATION

V. A. MATLAB Simulation Software

The professional software package MATLAB software is used to develop the optimal relay coordination model. For the purpose of this research MATLAB version R2017a was used. When the program is run, the Matlab Graphical User Interface prompts the user to select which of models will be evaluated, either 1 or 2 (1 = the developed algorithm; 2 = the standard PSO). MATLAB's flexibility and user-friendly environment made it a choice for this research.

B. Computer System

All the simulations carried out in this research were done on an Acer laptop computer system. The specification of the computer is given in Table III.

Table III: Computer Specification

Items	Specification
Operating System	Windows 8 Professional
RAM	4.00GB
System Type	64-bit Operating System
Processor	Core i5-243M @ 2.40GHz
Rating	4.0
Video Graphics	32MB

C. PSO Parameters

A set of initialization parameters has to be declared for the PSO algorithm to work effectively. The values in Table 4 were selected based on [9] for ease of validation. Subsequently, the N_{pop} and number of iterations will be varied in order to see their effect on the optimality of the decision variables.

Table 4: PSO Parameters Settings

Initialization Parameters	Values
Learning coefficient C_1&C_2	2.0
Maximum inertia weight (w_{max})	0.9
Minimum inertia weight (w_{min})	0.4
Damping Ratio	0.99
Number of population (N_{pop})	60
Number of iterations	100

VI. VI. RESULTS AND DISCUSSION

In this section, the performance of the optimal relay coordination using the MPSO is evaluated. The operating time of the IEEE 15 bus test system is presented.

A. Convergence on the IEEE 15-Bus System

After the developed MPSO is run for 100 iteration using the IEEE 15 data, the plot in Figure 4 is obtained. The figure shows the fitness evolution in the developed model.

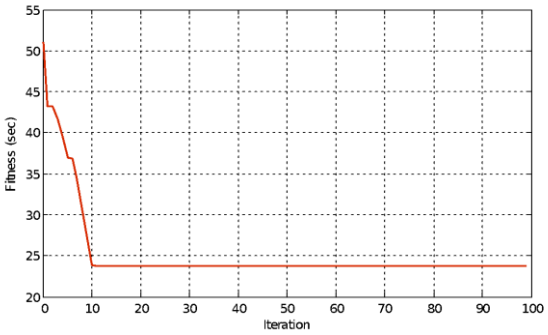

Figure 4: Fitness function evolution of the IEEE 15 Bus using MPSO

It is observed from Figure 4 that the optimal operating time of the relays in the system converged at 23.2221secs after 10 iterations, the optimal time remained constant through the 100th iteration.

B. Simulation Result on IEEE 15-Bus System

The optimal values of the Time Multiplier Settings (TMS) and Plug Settings of the IEEE 15 bus test system is shown in Table 5, the table also shows the optimal operating times of the relays in the network. The results in Table 5 are obtained using the set of 28 fault currents values given in chapter three. A fixed CT Ratio of 500:1 in used for the simulation.

The results of the optimized TMS, PS and T_{op} of the entire primary relays obtained by the MPSO is shown in Table 5. The objective function value obtained is $\sum T_{op} = 23.2221 \text{secs}$ and is the summation of the individual operating time of the relays in the system. This value represents optimal operating time of the relays in the network and is obtained after the algorithm determines the set of optimal values of TMS and PS which it used to compute the time of operation of the relay.

Table 5: Optimized PS, TMS and T_{op} for the IEEE 15-bus

Relay No.	PS	TMS	T_{op}
1	0.6612	0.6612	1.3223
2	0.4307	0.4307	0.8189
3	0.3987	0.3987	0.8181
4	0.3126	0.3126	0.5220
5	0.5566	0.5566	1.4473
6	0.1948	0.1948	0.4960
7	0.2042	0.2042	0.5036
8	0.4567	0.4567	1.0909
9	0.3409	0.3409	0.7582
10	0.2350	0.2350	0.5055
11	0.2263	0.2263	0.4546
12	0.2103	0.2103	0.5405
13	0.7773	0.7773	1.4967
14	0.4189	0.4189	0.9242
15	0.4749	0.4749	0.9402
16	0.462	0.462	0.7627
17	0.4087	0.4087	0.9459
18	0.2597	0.2597	0.6271
19	0.2512	0.2512	0.5581
20	0.1709	0.1709	0.3883
21	0.5222	0.5222	1.2783
22	0.2441	0.2441	0.5792
23	0.5544	0.5544	1.4856
24	0.2053	0.2053	0.4712
25	0.4069	0.4069	0.9957
26	0.2420	0.2420	0.6885
27	0.3541	0.3541	0.8744
28	0.3694	0.3694	0.9281

VALIDATION

To validate the result of the research, the result obtained using the proposed model is compared with that obtained in [9] which is the base research work used.

Table 7: Comparison of Results for the IEEE 15-Bus

A. *Comparison of the TMS, PS and T_{op}*

The summation of the optimized time of operation of the individual relays in the IEEE 15 bus system which is equal to the objective function value is compared as shown in Table 7.

Relay No.	Proposed			[9]		
	PS	TMS	T_{op}	PS	TMS	T_{op}
1	0.8136	0.3126	0.5220	0.5499	0.7439	1.1277
2	0.6609	0.4307	0.8189	1.2551	0.3222	0.7523
3	0.7812	0.6612	1.3223	1.5153	0.3416	0.8552
4	0.5686	0.3987	0.8181	2.4141	0.5525	2.0470
5	0.7974	0.2053	0.4712	0.6086	0.3634	0.7622
6	0.7596	0.1948	0.4960	1.0805	0.4309	1.2418
7	0.7318	0.2042	0.5036	1.2611	0.1119	0.3456
8	0.5375	0.4567	1.0909	1.8220	0.2726	1.1538
9	0.7927	0.2263	0.4546	1.1148	0.4539	1.0181
10	0.6592	0.2350	0.5055	1.3933	0.1536	0.4366
11	0.7277	0.3409	0.7582	0.5009	0.3213	0.6344
12	0.8165	0.2103	0.5405	2.4727	0.2642	1.1793
13	0.6887	0.7773	1.4967	1.9075	0.3209	0.8796
14	0.7113	0.4189	0.9242	2.1497	0.7389	2.5740
15	0.5057	0.4749	0.9402	0.7922	0.4263	0.9762
16	0.5319	0.3462	0.7627	0.6784	0.5439	1.3043
17	0.8170	0.4087	0.9459	0.6199	0.2179	0.4598
18	0.6917	0.2597	0.6271	1.1896	0.1204	0.3619
19	0.7255	0.2512	0.5581	0.6667	0.3199	0.6912
20	0.5826	0.1709	0.3883	1.1323	0.5657	1.6638
21	0.7172	0.5222	1.2783	0.6075	0.2638	0.6083
22	0.5276	0.2441	0.5792	1.8741	0.1431	0.6167
23	0.7260	0.5544	1.4856	0.7978	0.1249	0.3481
24	0.5617	0.5566	1.4473	1.3848	0.5530	2.2124
25	0.7166	0.4069	0.9957	0.6553	0.2225	0.5271
26	0.8396	0.2420	0.6885	1.6316	0.2904	1.1498
27	0.7342	0.3541	0.8744	0.7789	0.1347	0.3401
28	0.6161	0.3694	0.9281	2.4925	0.1028	0.5404
			$\sum T_{op}$=23.222s			$\sum T_{op}$=23.222s

The objective function value of the developed MPSO is 23.2221s, while that obtained by [9] is 26.189s as shown in Table 7. This shows that the total operating time of the relays in the IEEE 15 bus has reduced significantly by 2.967s which translate to a reduction of 11.3288%.

B. *Conergence Response Comparison*

The developed MPSO and that of the work of [9] are run using the same set of parameters, i.e. iterations, number of particles and same boundary conditions, both are then plotted on the same figure. Figure 6 shows the fitness evolution of both developed algorithms.

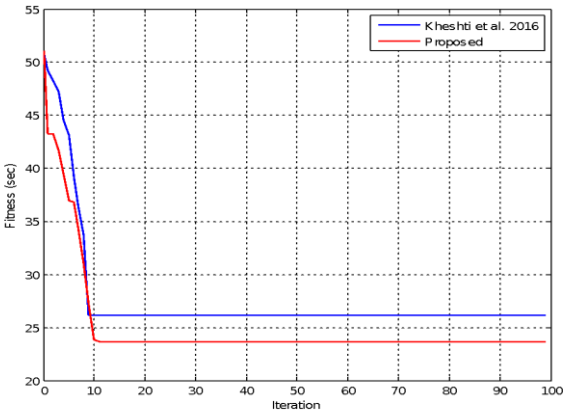

Figure 6: Fitness function evolution comparison of MPSO and [10]

It is observed from Figure 6 that the fitness function of the MPSO converges at 23.222s, while that of [9] converges at 26.189s. MPSO converges after 10 iterations while [9] converges before the 10th iteration. This shows that the minimal operating time of the relays in the IEEE 15 bus network is achieved using the MPSO.

CONCLUSION

The research developed an Optimal Overcurrent Protection Relay Coordination for distribution system using a Modified Particle Swarm Optimization Technique. The modification is based on a Simulated Annealing Inertia Weigh. The objective function is the minimization of the operation time of the protective relays. The optimality and Coordination Time Interval (CTI) were used as the performance metrics of the research. The result obtained an optimum solution with a good convergence when implemented on IEEE 15-bus network. When the result of the research was validated with that of [9], an improvement of 11.3288% is observed in terms of optimality and the CTI violations was reduced to two when compared to five recorded in [9]. The effectual result obtained for the relay coordination problem shows that the method is a viable one.

REFERENCES

[1] M. Zellagui, R. Benabid, M. Boudour, and A. Chaghi, "Mixed integer optimization of IDMT overcurrent relays in the presence of wind energy farms using PSO algorithm," *Periodica Polytechnica. Electrical Engineering and Computer Science*, vol. 59, p. 9, 2015.

[2] M. Y. Shih, A. C. Enríquez, T.-Y. Hsiao, and L. M. T. Treviño, "Enhanced differential evolution algorithm for coordination of directional overcurrent relays," *Electric Power Systems Research*, vol. 143, pp. 365-375, 2017.

[3] S. Raza, T. Mahmood, and S. Bukhari, "Optimum overcurrent relay coordination: A review," *Nucleus*, vol. 51, pp. 37-49, 2014.

[4] D. Vijayakumar and R. Nema, "A novel optimal setting for directional over current relay coordination using particle swarm optimization," *International Journal of Electrical Power and Energy Systems Engineering*, vol. 1, 2008.

[5] M. Hussain, S. Rahim, and I. Musirin, "Optimal overcurrent relay coordination: a review," *Procedia Engineering*, vol. 53, pp. 332-336, 2013.

[6] V. N. Rajput and K. S. Pandya, "On 8-bus test system for solving challenges in relay coordination," in *Power Systems (ICPS), 2016 IEEE 6th International Conference on*, 2016, pp. 1-5.

[7] E. Dehghanpour, H. Karegar, R. Kheirollahi, and T. Soleymani, "Optimal Coordination of Directional Overcurrent Relays in Microgrids by Using Cuckoo-Linear Optimization Algorithm and Fault Current Limiter," *IEEE Transactions on Smart Grid*, 2016.

[8] M. Zellagui, R. Benabid, M. Boudour, and A. Chaghi, "Mixed integer optimization of IDMT overcurrent relays in the presence of wind energy farms using PSO algorithm," *Periodica Polytechnica. Electrical Engineering and Computer Science*, vol. 59, p. 9, 2015.

[9] M. Kheshti, B. S. Tekpeti, and X. Kang, "The optimal coordination of over-current relay protection in radial network based on Particle Swarm Optimization," in *Power and Energy Engineering Conference (APPEEC), 2016 IEEE PES Asia-Pacific*, 2016, pp. 604-608.

[10] F. Namdari and S. Samadinasab, "A New Method for Optimal Coordination of Overcurrent Relays Considering the Communication Channels Constraints," *Indonesian Journal of Electrical Engineering and Computer Science*, vol. 1, pp. 17-30, 2016.

[11] A. R. Al-Roomi and M. E. El-Hawary, "Optimal coordination of directional overcurrent relays using hybrid BBO/DE algorithm and considering double primary relays strategy," in *Electrical Power and Energy Conference (EPEC), 2016 IEEE*, 2016, pp. 1-7.

[12] H. Bouchekara, M. Zellagui, and M. Abido, "Optimal coordination of directional overcurrent relays using a modified electromagnetic field optimization algorithm," *Applied Soft Computing*, vol. 54, pp. 267-283, 2017.

[13] V. N. Rajput and K. S. Pandya, "On 8-bus test system for solving challenges in relay coordination," in *Power Systems (ICPS), 2016 IEEE 6th International Conference on*, 2016, pp. 1-5.

[14] M. Abdel-Salam, A. Abdallah, R. Kamel, and M. Hashem, "Improvement of Protection Coordination for a Distribution System Connected to a Microgrid using Unidirectional Fault Current Limiter," *Ain Shams Engineering Journal*, 2015.

[15] A. Rathinam, D. Sattianadan, and K. Vijayakumar, "Optimal coordination of directional overcurrent relays using particle swarm optimization technique," *International Journal of Computer Applications*, vol. 10, pp. 43-47, 2010.

[16] H. Zeineldin, E. El-Saadany, and M. Salama, "Optimal coordination of overcurrent relays using a modified particle swarm optimization," *Electric Power Systems Research*, vol. 76, pp. 988-995, 2006.

Design and Construction of British Siren Triggered by Heat Operated Switch

A. D. Usman, U.F. Abdul Aguye, Isa Umar
Department of Communications Engineering
Ahmadu Bello University Zaria, Nigeria
adusman@abu.edu.ng, isaumar442@gmail.com

ABSTRACT-Fire outbreak is a common accident in homes and businesses and industrial areas. In our community fire alarms are mostly not used in our houses and shops to give early warning of fire outbreak for possible control. Therefore, in this design we intent to design and develop a fire alarm device made from easy to find components such as 555 timer and thermistor to sound an alarm based on British siren triggered by heat operated switch, for early warnings. The significant of the design is to develop a device that will be able to sense fire outbreak and alarm the fire fighters using alarm. Also, the aim of the design is to develop a circuit that will be able to alarm the environs in the case of fire outbreak. Finally, the significant of the design work is to reduce the level of fire accident.

***KEYWORDS*—Diodes, fire, alarm, thermistor**.

INTRODUCTION

A transducer is a device that converts energy from one form to another. Usually a transducer converts a signal in one form of energy to a signal in another. Transducers are often employed at the boundaries of automation, measurement, and control systems, where electrical signals are converted to and from other physical quantities (energy, force, torque, light, motion, position, etc.). The process of converting one form of energy to another is known as transduction. A thermistor is the transducer used for this design. A thermistor used here is as a transducer is also a resistor, the value of which changes with its temperature rise. It is known as a negative-temperature-coefficient (N.T.C) thermistor. The appearance of these thermistors is shown below;

METHODOLOGY

The research work has started on the desired components. The methodology adopted are described in the following steps:

1)Assembling of electronic components.

a) Analysing the circuit

b) Get the required component,

c) Assembly of components is done on design board (breadboard).

d) Assembly of components is done on design board (breadboard).

2) Testing the circuit

a) A multi meter is used to check for continuity and open circuit of the constructed circuit.

b) The design is powered by a 12Vdc supply to check the desired and intended result.

c) At the entrance, a proximity sensor is mounted on the case of construction.

d) A proximity sensor is mounted at each room or location within a building.

e) At each slot, a proximity sensor is installed to sense the presence of fire outbreak.

II. Components use

B. TH1VA1098(*Thermistor*)

1) A thermistor is a type of resistor whose resistance is dependent on temperature, more so than in standard resistors. The word is a portmanteau of thermal and resistor. Thermistors are widely used as inrush current limiters, temperature sensors (negative temperature coefficient or NTC type typically), self-resetting overcurrent protectors, and self-regulating heating elements (positive temperature coefficient or PTC type typically).

C. BC108, 2N3702 (*Transistor*)

2) The three transistors use are made from very pure silicon or germanium, but certain other semiconductor materials can also be used. A transistor may have only one kind of charge carrier, in a field effect transistor, or may have two kinds of charge carriers in bipolar junction transistor.

3) IN4001(*Diode*) A diode is a two-terminal electronic component that conducts current primarily in one direction (asymmetric conductance); it has low (ideally zero) resistance in one direction, and high (ideally infinite) resistance in the other. A vacuum tube diode utilizes thermionic emission of electrons and unidirectional conduction between the cathode and plate. A semiconductor diode, the most common type today, is a crystalline piece of semiconductor material with a p–n junction connected to two electrical terminals. Semiconductor diodes were the first semiconductor electronic devices.

The Circuit Diagram

The design circuit diagram was designed with the aid of the software called multism. The diagram below shows the circuit diagram of the heat operated switch trigger by British siren.

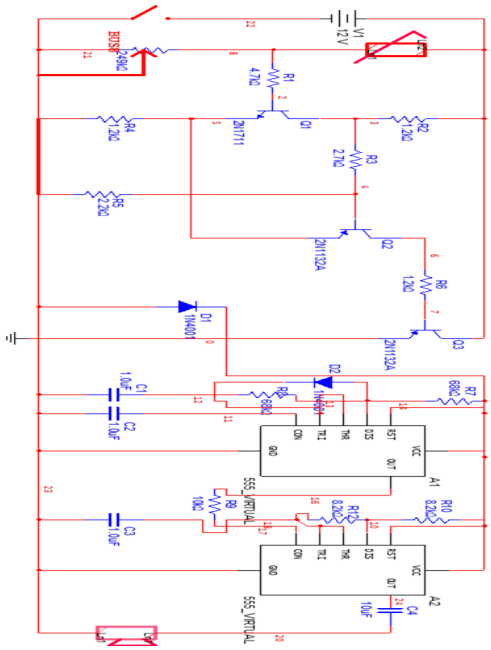

Fig. 1. Circuit Diagram of the heat operated switch

B. NE555TIMER(*IC555TIMER*)

The Complete circuit diagram of the alarm system is shown in Fig 2.1. The 555 timer in the trigger unit gets activated whenever pin 2 senses a smaller potential that is less than1/3 the supply voltage. When activated it sounds for duration of time determined by R3 and C1, this also determines how long the alarm will sound before going off.

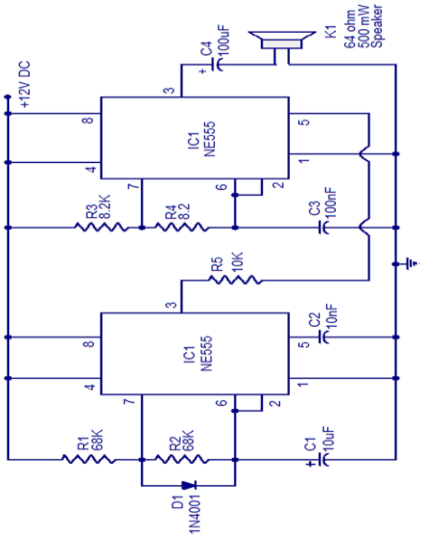

Fig.2. The British siren circuit

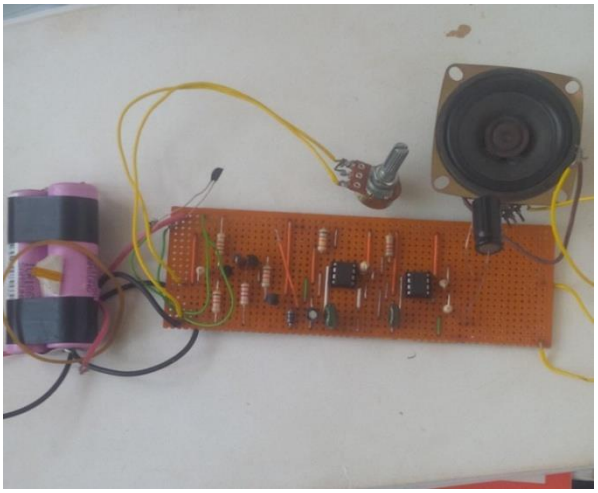

Fig.3. S-Dec layout of a heat operated switch

CONCLUSIONS

Hence electronic circuits can be designed for the fire based alarms and they provide very high efficiency and can be used for the security reasons. Early fire detection is best achieved by the installation and maintenance of fire detection equipment in all rooms and areas of the house or building.

Overall the design was successful. The performance of the design met the original technical problem, which was to build a circuit that would sound an alarm when the heat in the atmosphere reach a hazardous temperature. Also the design was well under the overall design cost designed, making the design a good product since the application was successfully demonstrated and the circuit price was reasona

REFERENCES

[1] Bird, John (2010). Electrical and Electronic Principles and Technology. Routledge.ISBN 9780080890562

[2] Duff, Wilmer (1908–1916). A Text-Book of Physics (4th ed.); Philadelphia: P. Blakiston's Son & Co.

[3] Devices (7th ed.). Upper Saddle River, NJ: Pearson Education. p. 10. ISBN 0-13-127827-4

[4] Farago, P.S. (1961). An Introduction to Linear Network Analysis, The English Universities Press Ltd.

[5] Floyd, Thomas (1984–2005). Field Effect Semiconductor Device Concepts Patented. *Computer History Museum*, Archived *from the original on March 22, 2016*

[6] General Semiconductors (2010) Physical Explanation
[7] Harder Douglas Wilhelm, (2014). Resistors: A Motor with a Constant Force (Force Source).Thesis, Department of Electrical and Computer Engineering, University of Waterloo.
[8] Milestones: Invention of the First Transistor at Bell Telephone Laboratories, Inc., (2014)*;IEEE Global History Network. IEEE.* Archived *from the original on November 21, 2014*.
[9] NTC Thermistors (2010). Micro-chip Technologies
[10] Shorthouse,D. (1980). Basic Electronics. Burton Street, Nottingham 4BU: Hodder and Strughton - Educational division
[11] The Constituents of Semiconductor Components (2010). Archived from the original on 2011-07-10.
[12] The Nobel Prize in Physics 1956. *Nobelprize.org. Nobel Media AB (2014).*Archived *from the original on December 16, 2014*
[13] Wu, F. Y. (2004). "Theory of resistor networks: The two-point resistance". Journal of Physics A: Mathematical and General. 37 (26): 6653.
[14] Wu, FaYueh; Yang, Chen Ning (2009). Exactly Solved Models: A Journey in Statistical Mechanics: Selected Papers (15)with Commentaries (1963–2008). World Scientific. –. ISBN 978-981-281-388-6.
[15] www.alibaba.com s2018, Thermistor, (Accessed, July 2018)

Development of a Wireless Interactive Communication Application using Android and Windows PC Platform

Pindar Ibrahim, Elvis Obi, Gabriel Inaku
Department of Communications
Ahmadu Bello University, Zaria, Nigeria
pindahi12@gmail.com; elvisobi72@gmail.com; inakugabriel@gmail.com

ABSTRACT—This paper presents the development of a wireless interactive communication system using android and Windows PC platform. The goal is to ensure the deployment of a wireless interactive communication system chat app via Bluetooth and Wi-Fi in an ad-hoc environment, to enables multiple users to chat without internet/data bundles. This app will function as Whatsapp, WeChat, Hangouts etc without the use of data/internet at a range of up to 100M. This Chatting Application is based on a research titled "Bluetooth Chat Application: Bluz by Aishwarya, et al., (2015) which is limited to Bluetooth range of 10M. The proposed improvement is on the Bluetooth Chat Application in terms of long-range communication, using both Bluetooth and Wi-Fi connection without the need of any internet service from a provider. The Bluetooth chat app was first developed for Android devices and it worked perfectly through Bluetooth without the use of data. The Bluetooth chat app was then replicated for Windows PC. Then the app was improved by incorporating Wi-Fi as alternate path which has a range of up to 100M. The performance of this application was evaluated in terms of range coverage. Result shows that integrating Wi-Fi as alternate route in the app improved the distance between users by 90%.

INTRODUCTION

The Android platform support for the Bluetooth network stack. It allows a device to wirelessly exchange data with other Bluetooth devices. The new vitality to the mobile space has injected because of the release of Android smart platform (Aishwarya, 2015).

Android is an operating system based on Linux kernel. It is designed for the touch screen mobile devices. The user interface of Android is based on direct manipulation. The Android system provides many Bluetooth APIs for developers to call (Farkade *et al*., 2015)

Bluetooth technology allows users to exchange voice and data transmission between two or more devices. It is basically a wireless communication technology. Bluetooth technology is reflected in the low price, easy to control and non-visual distance limitations. Bluetooth is integrated into the android platform as an android mobile network communication module. BlueZ is used to connect the Android phones into a local area network. It helps to communicate with each other (Aishwarya *et al*., 2015).

Bluetooth does not need a license around the globe for the working frequency band. In the connection initialization phase, firstly, it starts the application and searches the Bluetooth devices. Second, it sends the signals to the server class. After this it can run, pause and stop the application. Third, it shows alert using set Alert function on every changing. Server goes active and sends the signals to other devices (Aishwarya, 2015). Client class works to respond the other Bluetooth device server. This allows a two-way chat over Bluetooth. No GSM or Wi-Fi connection required. In addition to the person-to-person chat, chat rooms can be used to gather more than two persons at a time (Ishupreet *et al*., 2018)

Analysis of the Existing System

During a personal interview from student who are the most user of chatting applications, it was deduced that the current applications runs at highly cost for the user and the high-power consumption is another setback. Users would have to register and get connected online before the user can communicate with one another.

A. Weakness of the existing Chatting Applications

The notable weaknesses of the existing system are:

i. High power consumption

ii. Costly

iii. Must be connected to the internet Unable to chat with community

iv. Short range connectivity

B. Analysis of the proposed System.

This wireless interactive communication application is developed in two ways; one for mobile device and the other for PC, in both case you can connect and send messages from one android or PC device using Bluetooth or wireless to other compatible devices around you. No GSM data connection is required, all you need is a Bluetooth or Wi-Fi compatible android device or PC in range of each other and you can text, send Audio, Video, Image and send all kind of Document the through the App.

METHODOLOGY

The research work has both hardware and software components. The methodology adopted are described in the following steps:

The interface design is a milestone in this application development. Starting by the developing simple buttons, text boxes and warning messages. Next, preparing the protocols needed for the application to use Bluetooth/Wi-Fi and Client/Server codes.

The work has been divided into two phases. First phase involves designing a Windows application and in next phase designing an Android application. Messenger Application in Microsoft Windows Environment: Using the Visual studio.net. The Bluetooth package of a client and a server program were written in Java programming Language.

The server and client program was design in order to exchange messages, in this case perform chatting with each other. The server is also capable of interacting with several clients at the same time, using the concept of piconet. A piconet is an ad hoc network that links a wireless user group of devices using Bluetooth technology protocols. A piconet consists of two or more devices occupying the same physical channel (synchronized to a common clock and hopping sequence). It allows one master device to interconnect with several active slave devices.

System Design

System design is the process of defining the architecture, modules, interfaces, and data for a system to satisfy specified requirements.

Mobile APP design steps (Android environment setup)

Whether you are building an Android application in unity or programming it from scratch, you must set up the Android Software Development Kit (SDK) before you can build and run any code on your Android device.

Step 1: Install the Java Development Kit
The Java Development Kit (JDK) was downloaded and installed.
Step 2: Download the Android SDK
The Android SDK was installed using command line tools and through Android Studio.
Step 3: Install the Android SDK using the command line tools
The Android SDK was installed or unpacks. After installing, open the Android SDK Manager and add: at least one Android SDK Platform.
Step 4: Install the SDK using Android Studio
Install Android studio from the Android developer portal. The Android developer portal provides detailed installation instructions.
Step 5: Enable USB debugging on your device
To enable USB debugging, you must enable Developer options on your device.
Step 6: Configure the Android SDK path in Unity
The first time you create a Project for Android (or if Unity later fails to locate the SDK), Unity asks you to locate the folder in which you installed the Android SDK.
Step 7: Download and set up the Android NDK
If you are using the IL2CPP

Scripting backend

For Android, you need the Android Native Development Kit (NDK). It contains the toolchains (such as compiler and linker) needed to build the necessary libraries, and finally produce the output package (APK). If you are not targeting the IL2CPP back end, you can skip this step.

Window APP design Steps

Whenever an application is need to be developed, it includes many steps to identify the features provide by the app. This was planned according to SRS (Software requirement Specification)

Step 1:Install visual studio.net on your PC
Microsoft Visual Studio is an integrated development environment (IDE) from Microsoft
Step 2: Launch the application.
Locate and open the folder on your system from the control panel or systems settings.
Step 3: Draw your Labels and control
This step is to create a graphical control element which displays text on a form. It is usually a dynamic control; having an interactivity.
Step 4: Code each label and control
This is a step where a code was written that will drive each label and control.

Step 5: Text Run and Deploy
This is the step describes how to deploy and run the application as shown in figure 3.5.

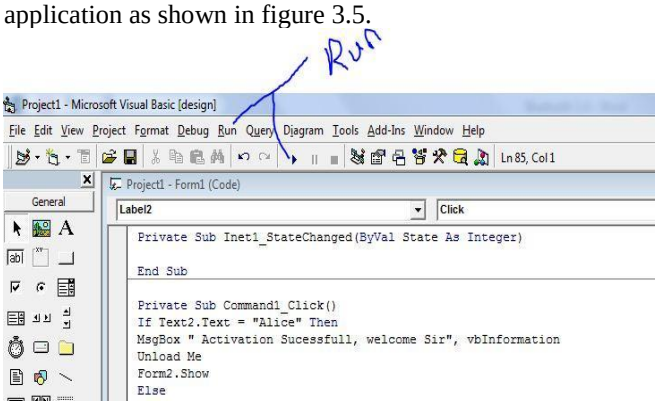

Figure 1. Run and Deploy screen shot

System Requirement

System requirement are the resources used for building a system. It varies from application to application due to system configuration. The most important requirement from this wireless link is that there should be a universal frame work that offers means to access information across a divers set of devices (mobile). This consists of the hardware, software as detailed below.

II. Software Requirement

A software requirement is a description of a software system to be developed. The following software was use in this project:
i. Operating system: window 7 or higher
ii. Coding Language: Java1.6and Xml
iii. Tool kit: Android 3.0
iv. IDE: Eclipse
v. Visual studio.net

Hardware Requirement

This is the hardware required for developing this chat app. The following Android phone hardware was use in this project.

i. 1GB Ram
ii. 2GM Rom
iii. Bluetooth
iv. Wireless Device

The following Laptop Computer hardware was use in this project.

i. System: Pentium IV 2.4GHZ or higher
ii. Hard disk: 80GB or higher
iii. Ram: 1G or higher
iv. Bluetooth Device
v. Wireless Device

Program Lunch

The following steps are taking in lunching the chat app:
Step1: Double click the program icon
Step2: confirm to turn on Bluetooth/Wi-Fi
Step3: click yes to turn on Bluetooth/Wi-Fi
Step4: click menu
Step5: select "make device discoverable"
Step6: select "connect to a device" to get connected
Step7: on available device list, select a device to chat with
Step8: click back to terminate the application
Step9: exist

Server Flowchart

This provides a visual representation of basic flowchart of the server in showing the sequence of process steps.

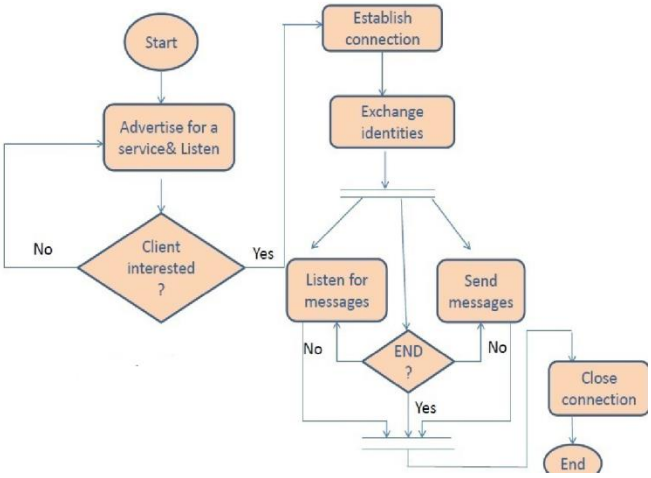

Figure 2 Server Flowchart

Client Flowchart

This provides a visual representation of basic flowchart of the client in showing the sequence of process steps.

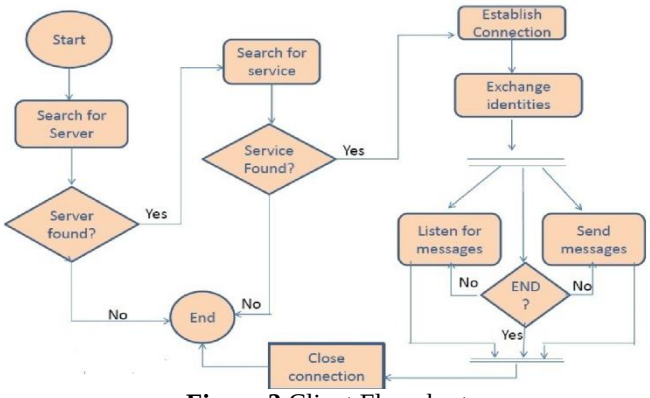

Figure 3 Client Flowchart

RESULT AND DISCUSSIONS

Program Development

The purpose of the application is to provide a long range (up to 100M) wireless link capable of transmitting messages among personal mobile devices (supported by android) and Windows PC. This program (wireless interactive communication application using Android and windows PC platform) also intends to eliminate the high-power consumption on internet chatting. The proposed improve system was developed using windows 8, java1.6, Android 23.0 toolkit and Eclipse IDE for interface design and integration of the modules.

System Performance

This is the process of checking the performance of the system alongside with the desired requirement. This has to do with testing the designed system and see if it evaluates. The improved application has been tested using different data to validate its functionalities, accuracy, speed and reliability.

The result of the application after the lunching it on Laptop PC and on Android phone is shown in screenshot below:

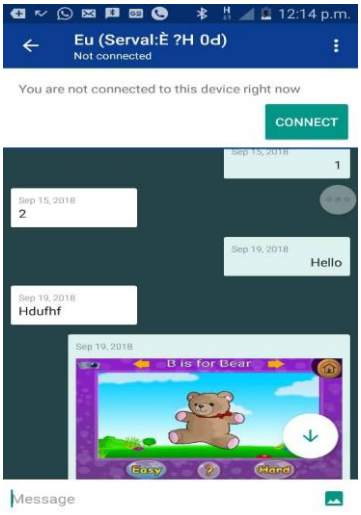

Figure 4 screen shot of the android mobile app

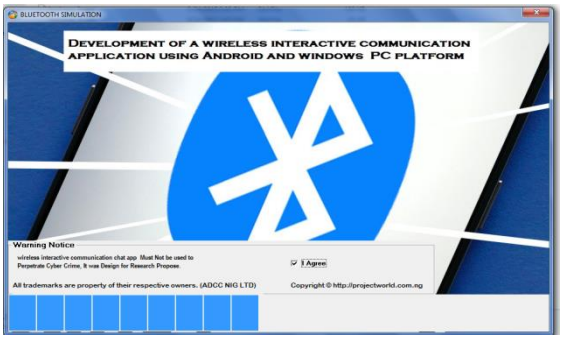

Figure 5 First Screen shot of the app

Figure 6 Screen shot of the app home page

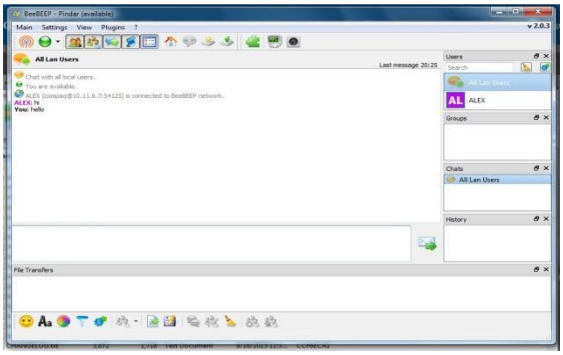

Figure 7 Windows PC chat box.

III. Summary

The messenger application using wireless technology was successfully completed in Android and Windows PC platform.

a) Bluetooth consumes low power as compared to Wi-technology and on the other hand Wi-Fi has a range (100M) of almost ten times to that of Bluetooth (10M). In order to account for the limitations in range, I incorporate Wi-communication in the application. Whenever a client application finds that server is not within range, the client may start scanning for the server using Wi-Fi. This will ensure the range limitations do not arise.

b) In a piconet at most 7 clients can connect with the server. In order to connect with more number of devices a client itself need to act as a server.

Java programming language and XML (Extended Markup Language) was chosen as the application development via Android Studio to its effectiveness had being efficient; Eclipse IDE was used for the development of the mobile application; Android virtual machine was used as emulator to demonstrate its workability, while visual studio.net was used to develop the system application.

IV. Limitation

Fig. 1. The limitations of this project work is that; this project work did not consider the possibility of the android device app to communicate with the PC app

CONCLUSIONS

The improved Bluetooth Chat app (wireless interactive communication application using Android and windows PC platform) was successfully developed by incorporating Wi-Fi technology into the conventional Bluetooth Chat app. The improved Chat app was compared with the conventional Bluetooth Chat app. Results showed that the Wi-Fi improved the Bluetooth Chat app better because it increased the range of connectivity by 90% and improved the delivery probability. These results obtained from this application conformed that using Wi-Fi is the preferred medium of connection than Bluetooth for the chat app considered in this project.

REFERENCES

[1] Aishwarya S *at el.*, (2015) *Bluetooth Chat Application: Bluez International Journal of Engineering and Computer Science ISSN:2319-7242 Volume 4 Issue 3 March 2015, Page No. 10674-10679.*

[2] Amrita D and Swarnabha S, '*Bluetooth Messenger: an Android Messenger app based on Bluetooth Connectivity', IOSR Journal of Computer Engineering (IOSR-JCE) e-ISSN: 2278-0661, p-ISSN: 2278- 8727Volume 16, Issue 3, Ver. III (May-Jun. 2014), PP 61-66 www.iosrjournals.org.*

[3] Android Platform [online] 27 March 2015, *URL: http://developer.android.com/guide/basics/what-is-android.html Accessed 12 May 2010.*

[4] Andrew D, David C, DongHer S, (2004) *Bluetooth technology: an exploratory study of the analysis and implementation frameworks', Department of DSC and MIS, Miami University, Oxford, OH 45056, USA.*

[5] Bettstetter C, (2003) "Topology Properties of Ad Hoc Networks with Random Waypoint Mobility," *ACM SIGMOBILE Mobile Computing and Communications Review*, Vol. 7, Issue 3, pages 50-52, July 2003.

[6] Brian P, *et al.*, (1997), "IEEE 802.11 Wireless Local Area Networks", *IEEE Communications Magazine*, pages 116-126, September 1997.

[7] Corson S and Macker J, (1999) "Mobile Ad Hoc Networking (MANET): Routing Protocol Performance Issues and Evaluation Considerations," IETF RFC 2501.

[8] David B. and David A., (1996) "Dynamic Source Routing in Ad Hoc Wireless Networks," *Mobile Computing*, edited by Tomasz Imielinski and Hank Korth, Chapter 5, pages 153–181. Kluwer Academic Publishers, 1996

[9] Garcia-Luna-Aceves J. and Marcelo S, (1999) "Source-Tree Routing in Wireless Networks," *Proceedings of the Seventh Annual International Conference on Network Protocols*, pages 273, October 31- November 03, 1999.

[10] Han C, Liang Q, *The Bluetooth Special Interest Group, Bluetooth Specification Core v4.0 (2009-02)., 'Principles and development points of the Android system', Publishing House of Electronics industry, 2010.*

[11] Ing-Ray C, *et al.*, (2002) "Wireless Ad Hoc Messenger," Microsoft Research Grant, Virginia Polytechnic and State University, Microsoft RFP, Section 2: Mobile and Wireless, 2002.

[12] Jackquet P, *et al.*, (2001) "Optimized Link State Routing Protocol for Ad Hoc Network," *IEEE INMIC*, Pakistan, 2001. [Jiang2001] Hong Jiang and J.J. Garcia-Luna-Aceves, "Performance Comparison of Three Routing Protocols for Ad Hoc Networks," *Tenth International Conference on Computer Communications and Networks*, pages 547-554, 2001

[13] Joseph D, *Mastering JXTA: Building Java P2P Applications, USA: John Wiley&Sons: Wiley Publishing Inc; 2002*.

[14] Jin-Hee C, (2016), *Design and Implementation of Ad-hoc Communication and Application on Mobile Phone Terminals: Proc. IEEE ICASP, pp. 2029-2032 (2016).*

[15] Leung, R., *et al.*, (2001) "MP-DSR: a QoSaware multi-path dynamic source routing protocol for wireless ad-hoc networks," *Local Computer Networks, Proceedings of the 26th Annual IEEE Conference*, pages 132-141, November 2001

[16] Mandar L and Pravin R, '*Bluetooth Chat Application: Bluez: International Journal of Engineering and Computer Science ISSN:2319-7242 Volume 4 Issue 3 March 2015, Page No. 10674-10679.*

[17] Nikita M and Garima V, "*Design of Chatting Application Based on Android Bluetooth, International Journal of Computer Science and Mobile Computing, Vol.3 Issue.3, March- 2014, pg. 712-717 © 2014, IJCSMC All Rights Reserved 712.*

[18] Rahul V, *at el.*, (2015) *A Complete Study of Chatting Room System based on Android Bluetooth', Moradabad Institute of Technology, Moradabad, International Conference on Advanced Developments in Engineering and Technology (ICADET-14), INDIA.*

[19] Sung-Ju L, William S and Mario G, (2000) "On-Demand Multicast Routing Protocol (ODMRP) for Ad Hoc Networks," *IETF MANET Working Group*, Internet-draft, 2000.

[20] Tracy C, *et al.*, (2002), "Performance Comparison of Two Location Based Routing Protocols for Ad Hoc Networks," *Proceedings of the 21st Annual Joint Conference of the IEEE Computer and Communications Societies (INFOCOM 2002)*, pages 1678-1687. 2002.

[21] Tracy C, *et al.*, (2002) "A Survey of Mobility Models for Ad Hoc Network Research," *Wireless Communication & Mobile Computing (WCMC): Special Issue on Mobile Ad Hoc Networking: Research, Trends and Applications*, Vol.2, No.5, pp.483502, 2002.

[22] Yujin N and Hidetoshi Y, (2016), *Design and Implementation of Ad-hoc Communication and Application on Mobile Phone Terminals: Thesis submitted to the Faculty of the Virginia Polytechnic Institute and State University.*

Performance Evaluation of Empirical Path loss Models of GSM Signal in Kaduna Metropolis

Abdullahi Z. M.
Dept. of Communications Engineering
Ahmadu Bello University
Zaria, Nigeria.
amzanna@gmail.com

Okpo U.Okereke ,Jibrin Danladi Jiya, Elijah Ehiagwina Omezigba
Dept. of Computer & Comms. Eng'g
Abubakar Tafawa Balewa University
Bauchi, Nigeria
Ouokereke@gmail.com, Jibjiya27@gmail.com, omezigbaee@gmail.com

***ABSTRACT*— In this work, comparison was made for some of the most popular empirical propagation models for path loss prediction in order to find a good radio frequency propagation prediction model for GSM 900 and 1800 MHz frequencies bands of Kaduna metropolis. Empirical prediction models used for this work are Free Space Path Loss (FSPL),Electronic Communication Committee-33 (ECC-33), Ericsson 9999 and Stanford University Interim (SUI). Hence, the FSPL showed better prediction for Kaduna metropolis than all the other models under review, a good path loss prediction will improve network optimization which leads to improved received signal for the GSM subscriber**.

KEYWORDS—Path Loss, Propagation, Frequency and Data.

INTRODUCTION

Propagation path loss is the loss in signal power as the signal travels from the transmitter to the receiver. Path loss is measured in different areas (rural, urban, and suburban) and propagation path loss models are used for prediction of the path loss. There are mainly three categories of these models; empirical, deterministic and stochastic. The empirical models are models obtained by observations and measurements only and are generally used to predict the path loss. The deterministic models are models that require a complete 3-D map of the propagation environment. Whereas, Stochastic models are the models that usually model the environment as series of random variables, these models are the least accurate but require the least information about the environment and use much less processing power to generate predictions. Empirical models can be split into two subcategories namely, time dispersive and non-time dispersive [2].

Path loss models are necessary in mobile radio systems for the purposes of proper planning, estimation of interference, assigning of frequency and cell parameters which are vital for the processes of network planning [1].

Propagation of radio wave cannot be mentioned without considering the simple fact that is a function of frequency; this brings us to the electromagnetic wave described by Maxwell's equation as they carry energy in the direction of propagation. While the basics of free space propagation are consistent for all frequencies, real world channel often shows considerable sensitivity to frequency, hence, practical propagation models are frequency dependent since the designer may be required to address different phenomena at different frequency bands. The electromagnetic spectrum is loosely divided into frequency ranges; mobile Communications are mostly within the VHF (30- 300 MHz) and UHF (300 MHz - 3 GHz) bands due to the reasonable antenna sizes, minimal sensitivity to weather and moderate building penetration [5].

EMPIRICAL PATH LOSS MODELS

a). Free Space Path Loss Model

In this model, the received power is a function of transmitted power, antenna gain and distance between the transmitter and the receiver. The basic idea is that the received power decreases as the square of the distance between the transmitter and the receiver subjected to the assumption that there is one single path between the transmitter and the receiver. The received signal power in a free space at a distance *'d'* in meters from the transmitter is given in equation (1), the ratio of transmit to received signal powers in equation (2) and the path loss (L in dB) in equation (3).

$$P_R = P_T G_T G_R (\lambda/4\pi d)^2 \quad (1)$$

Where P_T – Transmitted signal power,
P_R – Received signal power,
G_T – Transmitter antenna Gain,
G_R – Receiver Antenna Gain and
λ – is the wavelength.

$G_T = G_R = 1$ (for Isotropic antenna)

$$P_T/P_R = (4\pi d/\lambda)^2 = (4\pi d f/c)^2 \quad (2)$$

$$L = 10\log(P_T/P_R) = 10\log(4\pi d f/c)^2$$

$$= -147.56 + 20 \log d + 20 \log f \quad (3)$$

Where the frequency, f is in hertz [6].

b). Stanford University Interim (SUI) Model

This model is categorized into three types of terrains, namely A, B and C. Type A is associated with maximum path loss and is appropriate for hilly terrain with moderate to heavy foliage densities. Type B is characterised with either mostly flat terrains with moderate to heavy tree densities or hilly terrains with light tree densities. Type C is associated with minimum path loss and applies to flat terrain with light tree densities. The basic path loss equation with correction factors is given in equation (4) [4].

$$L = A + 10\gamma \log_{10}(d/d_0) + X_f + X_h + s \text{ for, } d > d_0 \quad (4)$$

Where, d is the distance between the access point (AP) and the customer premises equipment (CPE) antennas in metres, d_0 = 100 m and s is a *log* normally distributed factor that is used to account for the shadow fading owing to trees and other clutter and ranges between 8.2 − 10.6 dB.

The other parameters are defined as in equations (5) and (6).

$$A = 20 \log_{10}(4\pi d_0/\lambda) \quad (5)$$

$$\gamma = a - bh_b + c/h_b \quad (6)$$

Where, the parameter h_b is the base station height above ground in metres and should be between 10 m and 80 m.

For terrain A, the constants a, b(m^{-1})and c (m) are 4.6, 0.0075, 12.6 respectively; for terrain B, are 4.0, 0.0067, 17.1 respectively and for terrain C, are 3.6, 0.005, 20 respectively. The parameter γ in equation (6) is equal to the path loss exponent. For a given terrain type the path loss exponent is determined by h_b.

Correction factors for the operating frequency and CPE antenna height for the model are expressed in equations (7) and (8).

$$X_f = 6.0 \log_{10}(f/2000) \quad (7)$$

$$X_h = -10.8\log_{10}(h_r/2000) \text{ for terrain A and B}$$

$$= -20.0\log_{10}(h_r/2000) \text{ for terrain C} \quad (8)$$

Where, f is the frequency in MHz and h_r is the CPE antenna height above ground in metres.

The SUI model is used to predict the path loss in all three environments, namely rural suburban and urban.

c). ECC-33 Path Loss Model

The original Okumura experimental data were gathered in the suburbs of Tokyo which has the characteristics of a highly built-up area that are quite different to those found in typical European suburban areas. A different approach was taken which extrapolated the original measurements by Okumura and modified its assumptions so that it more closely represents a Fixed Wireless Access (FWA) system by the Electronic Communication Committee (ECC) within the European Conference of Postal and Telecommunications Administration (CEPT) in their Technical Report (ECC Report 33) of May 2003. The path loss model presented is referred to as the ECC-33 model and defined as in equation (9) [3].

$$L = A_{fs} + A_{bm} - G_b - G_r \quad (9)$$

Where A_{fs}, A_{bm}, G_b, G_r are the free space attenuation, the basic median path loss, the BS height gain factor and the terminal CPE height gain factor are individually defined in equations (10), (11), (12) and (13) respectively;

$$A_{fs} = 92.4 + 20\log_{10}(d) + 20\log_{10}(f) \quad (10)$$

$$A_{bm} = 20.4 + 9.83\log_{10}(d) + 7.894\log_{10}(f) + 9.5[\log 1\ 0(f)]^2 \quad (11)$$

$$G_b = \log_{10}(h_b/200)\{13.958 + 5.8[\log_{10}(d)]^2\} \quad (12)$$

and for medium city environments;

$$G_r = [42.57 + 13.7\log_{10}(f)][\log_{10}(h_r) - 0.585] \quad (13)$$

Where, f is the frequency in GHz, d is the distance between AP and CPE in km, h_b is the base station (BS) antenna height in meters and h_r is the CPE antenna height in meters.

d). Ericsson 9999 Model

This model is implemented by Ericsson as an extension of the Hata model. Hata model is used for frequencies up to 1900 MHz. In this model, the parameters can be adjusted according to the given scenario. The path loss as evaluated by this model is described as in equation (14).

$$L = a_0 + a_1\log(d) + a_2\log(h_b) + a_3\log(h_b)\log(d) - 3.2(\log(11.75))^2 + g(f) \quad (14)$$

Where, $g(f) = 44.49\log(f) - 4.78(\log(f))^2$ (15)

The parameter $g(f)$ is calculated as in equation (15). The values of a_0, a_1, a_2 and a_3 are constant but can be changed according to environment. The defaults values given by the Ericsson model are a_0= 36.2, a_1= 30.2, a_2= –12.0 and a_3 = 0.1. The parameter f, represents the frequency [7].

METHODOLOGY

This work is actually for Kaduna metropolis base on the data collected from live networks. The following steps was taken for realization of this research work.

a. The base stations (BSs) were identified and their location determined.
b. The BSs parameters obtained from the network service provider.
c. The test routes and points were mapped out using GPS.
d. Received signal strength were measured at every test point using net-monitor.
e. Some of the popular empirical path loss prediction models that have their frequency ranges between the area of interest (above 800 MHz to about 1900 MHz) and their ranges of distance is from 200 m and above were validated for these locations.

IV. RESULTS AND DISCUSSION

Figures 1 to 12 shows the comparisons between the measured data and the values of the empirical predicted propagation path loss models which are FSPL, ECC-33, Ericsson 9999 and SUI for all the routes, for 900 MHz and 1800 MHz frequencies.

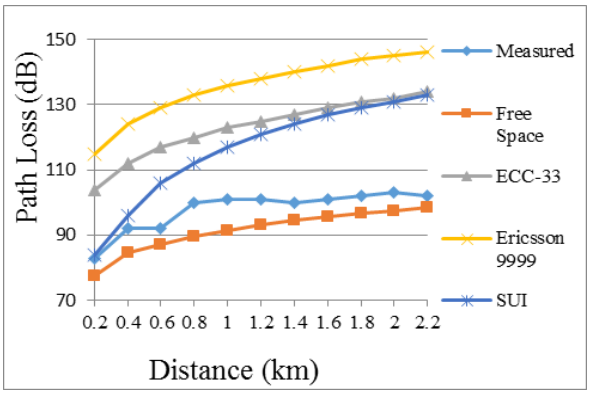

Figure 1: Path loss models for BS 1 900MHz.

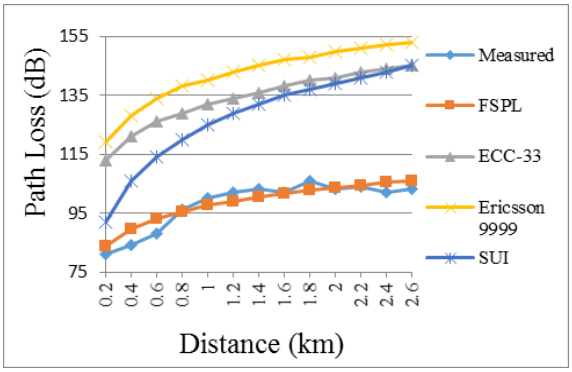

Figure 2: Path loss models for BS 1 1800MHz.

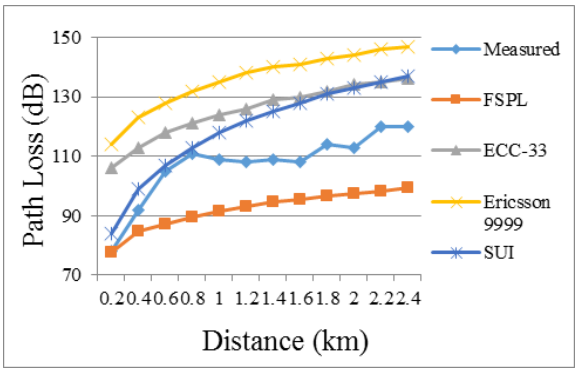

Figure 3: Path loss models for BS2 900MHz.

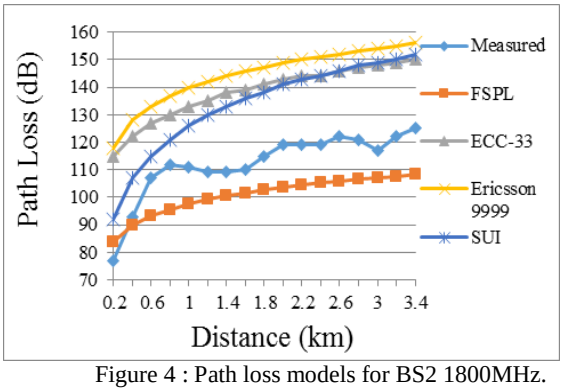

Figure 4 : Path loss models for BS2 1800MHz.

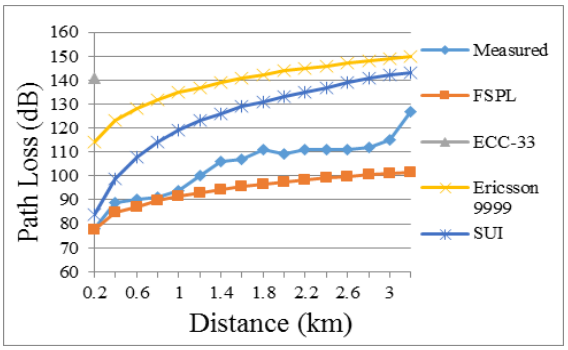

Figure 5: Path loss models for BS 3 900 MHz.

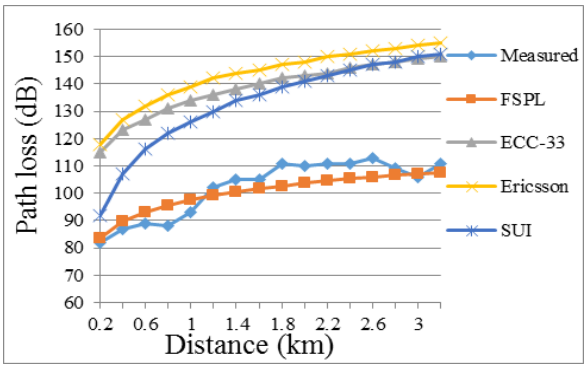

Figure 6: Path loss models for BS 3 1800MHz.

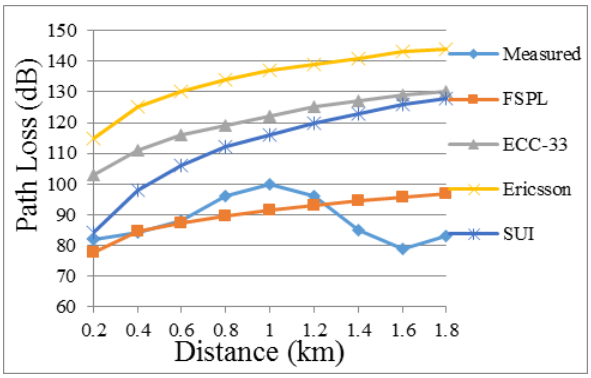

Figure 7: Path loss comparison, BS 4 900 MHz.

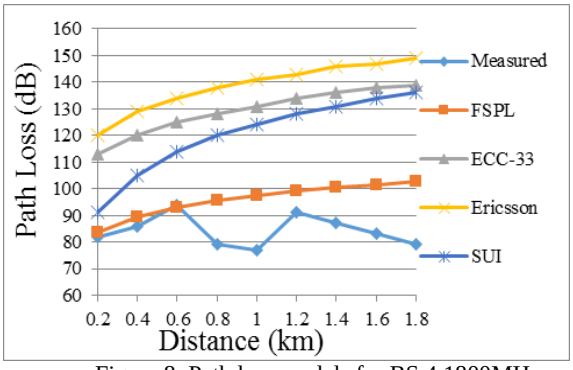

Figure 8: Path loss models for BS 4 1800MHz.

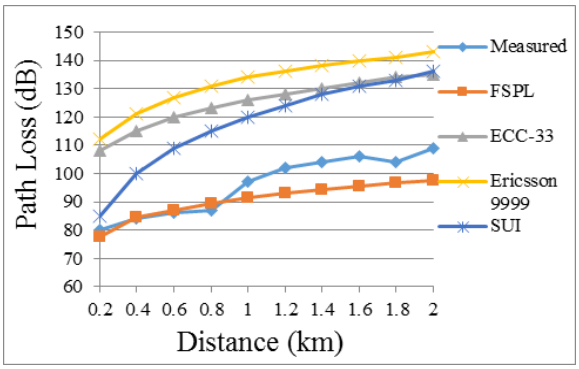

Figure 9: Path loss models for BS 5 900 MHz.

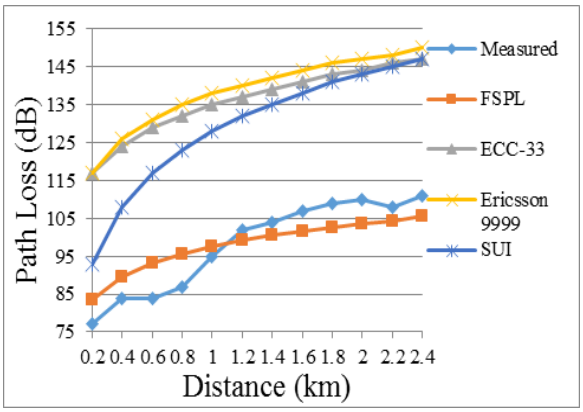

Figure 10: Path loss models for BS 5 1800MHz

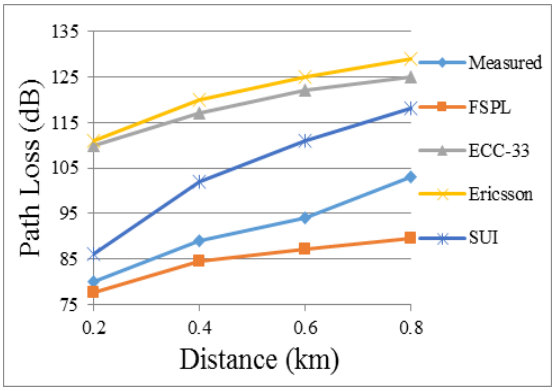

Figure 11: Path loss models for BS 6 900MHz.

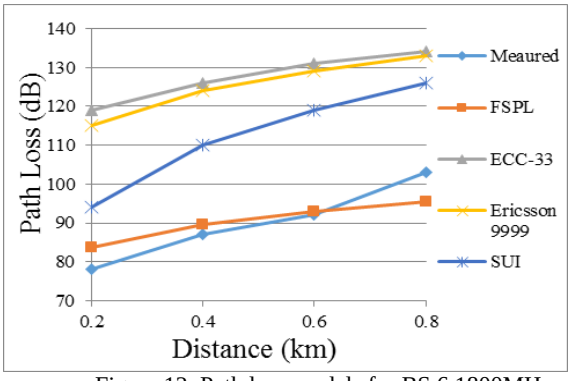

Figure 12: Path loss models for BS 6 1800MHz

The empirical predicted models performances were evaluated by the following statistical performance evaluations; (i) Mean Absolute

Error (μ), (ii) Standard Deviation (σ), (iii) Root Mean Square Error (*RMSE*) and (iv) R^2.

$\mu$is an average of the absolute errors, σ is the measure of the dispersion of a set of data from its mean, *RMSE*determine the average deviation of the predicted path loss values from the measured values and$R^2$is a measure of how well the predicted values fit the measured data set or simply the measure of the correlation between the actual response and the predicted response.

A model with lowest values of μ, σ and *RMSE* and higher value of R^2 is adjudged a better prediction model for the environment.

Tables 1, shows the results of μ, σ, *RMSE*, and R^2 for the empirical predicted path loss propagation models at 900 MHz.

For BS 1, FSPL model showed low values of μ, σ and *RMSE at* 6.436, 6.354 and 6.742 respectively as compared to ECC-33 with 25.182, 9.214 and 25.486 respectively, Ericsson 9999 with 37.727, 9.709 and 37.953 respectively and SUI with 18.455, 15.597 and 20.756 respectively. For BS 3, BS 4 and BS 5 the trend is the same with BS 1. But in the case of BS 2, FSPL model showed low values only in σ while SUI model showed low values in μ and *RMSE* as compared to the other models, the values of μ, σ and *RMSE* for FSPL model are15.1256, 6.466 and 16.228 respectively, ECC-33 are 18.083, 9.355 and 18.648 respectively, Ericsson 9999 are 28.667, 10.059 and 28.954 respectively and SUI are 12.083, 16.763 and 13.629 respectively.

As for R^2, values for BS 1 for the FSPL, ECC-33, Ericsson and SUI are 0.892, 0.864, 0.891 and 0.884 respectively, these values are high as they tend towards 1 they showed very good correlation and all the four values show minimal variations from each other. BS 2, BS 3, BS 5 and BS 6 show same pattern with BS 1. For BS 4 the values are 0.110, 0.006, 0.017 and 0.013 respectively showing fair correlation and minimum variations.

Hence, Free Space Path Loss showed better prediction for Kaduna metropolis than all the other models under review for the 900 MHz frequency.

Table 1: μ, σ, *RMSE* and R^2 for Empirical Prediction Models at 900 MHz.

Model	μ	σ	*RMSE*	R^2
FSPL BS1	6.436	6.354	6.742	0.892
ECC-33 BS1	25.182	9.214	25.486	0.864
Ericsson BS1	37.727	9.709	37.953	0.891
SUI BS1	18.455	15.597	20.756	0.884
FSPL BS2	15.125	6.466	16.228	0.875
ECC-33 BS2	18.083	9.355	18.648	0.852
Ericsson BS2	28.667	10.059	28.954	0.876
SUI BS2	12.083	16.763	13.629	0.875
FSPL BS3	9.588	6.764	11.37	0.914
ECC-33 BS3	25.438	10.111	25.726	0.921
Ericsson BS3	34.875	10.195	35.103	0.909
SUI BS3	21.313	16.798	22.171	0.902
FSPL BS4	7.067	6.116	8.796	0.011
ECC-33 BS4	32.111	8.983	33.798	0.006
Ericsson BS4	46.111	9.497	47.316	0.017
SUI BS4	24.444	14.432	28.461	0.013
FSPL BS5	5.98	6.244	7.12	0.882
ECC-33 BS5	28.2	8.711	29.397	0.903
Ericsson BS5	36.4	9.821	36.568	0.88
SUI BS5	22.2	16.196	23.191	0.893
FSPL BS6	6.775	5.17	7.942	0.937
ECC-33 BS6	27	6.557	27.166	0.958
Ericsson BS6	29.75	7.762	29.829	0.962
SUI BS6	12.75	13.817	13.407	0.961

Tables 2, shows the results of μ, σ, *RMSE*, and R^2 for the empirical predicted path loss propagation models at 1800 MHz.

For BS 1, FSPL model showed low values of μ, σ and *RMSE at* 2.877, 6.516 and 3.348 respectively as compared to ECC-33 with 36.000, 9.618 and 36.171 respectively, Ericsson 9999 with 44.154, 10.189 and 44.300 respectively and SUI with 29.539, 15.804 and 30.649 respectively. For BS 2, BS 3, BS 4 BS 5 and BS 6 the trend is the same, FSPL model showed low values as compared to the ECC-33, Ericsson 9999 and SUI models.

Table 2: μ, σ, *RMSE* and R^2 for Empirical Prediction Models at 1800 MHz.

Model	μ	σ	*RMSE*	R^2
FSPL BS1	2.877	6.516	3.348	0.838
ECC-33 BS1	36	9.618	36.171	0.861
Ericsson BS1	44.154	10.189	44.3	0.882
SUI BS1	29.539	15.804	30.649	0.886
FSPL BS2	12.582	6.927	13.277	0.832
ECC-33 BS2	26.118	10.061	26.48	0.864
Ericsson BS2	32.235	10.465	32.458	0.896
SUI BS2	21.412	16.763	22.413	0.888
FSPL BS3	4.881	6.844	5.649	0.798

ECC-33 BS3	36.25	10.111	36.435	0.871
Ericsson BS3	41.25	10.556	41.416	0.873
SUI BS3	30.875	16.759	31.818	0.867
FSPL BS4	11.911	6.244	14.421	0.011
ECC-33 BS4	41.111	8.746	46.272	0.009
Ericsson BS4	54.333	9.475	55.429	0.013
SUI BS4	36.111	14.807	39.281	0.009
FSPL BS5	6.008	6.364	6.614	0.832
ECC-33 BS5	38	9.243	38.197	0.932
Ericsson BS5	40.5	9.921	40.663	0.924
SUI BS5	31	16.414	31.499	0.922
FSPL BS6	4.175	5.202	4.85	0.931
ECC-33 BS6	37.5	6.557	37.7	0.932
Ericsson 9999 BS6	35.25	7.762	35.38	0.937
SUI BS6	22.25	13.817	22.6	0.936

As for R^2, values for BS 1 for the FSPL, ECC-33, Ericsson and SUI are 0.838, 0.861, 0.882 and 0.886 respectively, these values are high as they tend towards 1 they showed very good correlation and all the four values show minimal variations from each other. BS 2, BS 3, BS 5 and BS 6 show same pattern with BS 1. For BS 4, the values are 0.110, 0.009, 0.013 and 0.009 respectively showing fair correlation and minimum variations.
Hence, FSPL showed better prediction for Kaduna metropolis than all the other models under review for the 1800 MHz frequency.

CONCLUSION

The importance of path loss prediction using the empirical models and comparing them cannot be overemphasized, as regular path loss prediction and performance analysis gives the best model to be used. This improves network optimization which leads to improved received signal for the GSM subscriber, this analysis will surely give the operators the aspect of their KPI to work on and improve upon. The FSPL model showed a good performance on one BS and outstanding performance on the other five BSs. Hence, the best choice to be used for path loss prediction for Kaduna Metropolis

REFERENCE

[1] Alim, M. A., Rahman, M. M., Hossain, M. M. & Al-Nahid A. **(2010).** "Analysis of Large-Scale Propagation Models for Mobile Communications in Urban Area". International Journal of Computer Science and Information Security (IJCSIS), Vol. 7, No. 1.

[2] Bouzera, N. and Kheirddine, A. **(2012).** "Comparison of Propagation Models for Small Urban Cells in GSM Network". International Journal of Communication and Networking System Volume: 01 Issue: 01 January- June 2012. ISSN: 2278-2427.

[3] Electronic Communication Committee (ECC) within the European Conference of Postal and Telecommunications Administration (CEPT) **(2003).** "The analysis of the coexistence of FWA cells in the 3.4 - 3.8 GHz band". Tech. Rep., ECC Report 33, May.

[4] Erceg, V., Hara, K. V. S. **(2001).** "Channel Models for Fixed Wireless Applications" Technical Report IEEE 802.16 Broadband Wireless Access Working Group, January.

[5] John, S. S. **(2005).** "Introduction to RF Propagation". John Wiley and Sons, Inc. Hoboken, New Jersey.

[6] Rappaport, T. S. **(2002).** "Wireless Communication: Principles and Practice". 2nd Ed., pp.31-48, New Delhi: Prentice Hall.

[7] Shabbir, N., Sadiq, M. T., Kashif, H. and Rizwan Ullah**(2011).** "Comparison of Radio"

An Intelligent Digital Door Security System with Password Recovery

Bakut Yabvo, Abdullahi, Z. M. Aminu Yerima
Department of Communications Engineering,
Ahmadu Bello University Zaria, Nigeria
pauloskyakaat@yahoo.com, Zanna@gmail.com, aminuyerima@yahoo.com

ABSTRACT— This research implements an Intelligent Digital Door Security System with Password Recovery. The security system is designed on the principle of accessibility by a password code and provides an extended and user-friendly security features to security interfaces. Many door security systems have been proposed and implemented by different system designers but fails to proffer integrated combinations of security features to help beat security breaches. Here presented in this research work is a system that has a door sensor, a customized keypad with special keys, password recovery capability, alarm system, password change and a proximity sensor to flicker the LCD back to life as someone approaches. It is expected that the microcontroller unit scans the keypad continuously for a four-digit numeric string. When the ENTER button is pressed, the microcontroller unit compares it with the predetermined code saved in the EEPROM, if it corresponds, access is granted else access is denied and an SMS alert reading: "Illegal Entry Attempt" is sent to the facility owner. After three consecutive attempts, the screen of the LCD is frozen and the alarm system is activated. It will blare continuously until a master override code is entered. When access is granted and the door is not pushed open, it locks up after ten (10) seconds.

KEYWORDS—password, GSM module, microcontroller, stepper motor

INTRODUCTION

Optimum security of life and property has been man's major challenge in his existence. Right from time immemorial, man has employed diverse means of protecting himself and his valuables. Traditional techniques of bolts, chains, padlock etc, were employed in the past.

An Electronic Security System refers to any electronic equipment that can perform security operations like surveillance, alarming, or controlling access to a particular facility or an area. Depending upon the area to be protected and possible threats associated with it, security systems may be classified into Access Control Systems and Surveillance Systems [1].

The security sector is experiencing diversification as it has never seen before. This has brought about the need to review the reliability of already existing systems and look into the possibility of creating better systems that are smarter and more secure [2]. Presently, embedded systems are used to design security systems due to advanced technologies in microcontrollers' architectures and breakthrough in GSM applications.

An access control for security interfaces forms a key link in a security chain. The microcontroller based digital lock for doors is an access control system that allows only authorized persons to access a restricted area. An electronic lock or digital lock is a device that has an electronic assembly attached to it and are provided with access control.

I. WORKING CONCEPT OF THE PROPOSED SYSTEM

1. When the system is powered, it activates the door sensor to determine whether the door is closed or opened. If the door is open, the LCD displays "DOOR OPEN" and no further activity is carried out by the door. If the door is closed, the LCD displays "DOOR CLOSED" it delays for ten (10) seconds then the intelligent unit activates the stepper motor controller and instructs it to rotate forward to lock the door then followed by a display "DOOR LOCKED". After a while the screen clears and control shifts to the keypad awaiting any input.

2. The keypad continuously scans through the keys for key press. If a numeric key is pressed it enters a string which takes a maximum of four characters and is displayed on the LCD screen. When the maximum is reached, no any number can be inputted. The string is only processed when the ENTER key is stroke. After pressing ENTER, the inputted string is compared with the stored password, if it is correct: door is unlocked and the LCD screen displays "WELCOME: ACCESS GRANTED". The system waits for ten (10) seconds, if the door is pushed open, LCD screen displays "DOOR OPEN" and remains open. If the door is not pushed open, the intelligent unit activates the stepper motor controller and instructs it to rotate forward to lock the door then followed by a display "DOOR LOCKED". Then control shifts to the keypad awaiting any input. If the comparison is not correct: an SMS that reads "ILLEGAL ENTRY ATTEMPT" is sent to the home or facility owner and the LCD displays "WRONG PASSWORD: ACCESS DENIED".

3. Same sequence of actions is taken each time an attempt is made and control returns to the keypad awaiting any input. On the third attempt, an alarm system is activated by the intelligence unit and it keeps blaring until a master override code is entered by the home or facility owner.

4. Now, if instead of the numeric key the MENU key is pressed, the LCD screen displays four (4) options: 1: NEW PASSWORD, 2: GET PASSWORD, 3: FREEZE, 4: EXIT. If 1 is selected, LCD screen displays "ENTER OLD PASSWORD". The typed string is compared with the old password and if it is correct, LCD screen displays "ENTER NEW PASSWORD". The four-digit string typed and entered is now stored as the new password, the LCD screen displays "PASSWORD CHANGED" and an SMS containing the new password is sent to the home or facility owner the control is shifted to the keypad awaiting any input. In this case, if the

comparison is not correct: an SMS that reads "ILLEGAL ENTRY ATTEMPT" is sent to the home or facility owner and the LCD displays "WRONG PASSWORD: ACCESS DENIED". Same sequence of actions is taken each time an attempt is made and control returns to the keypad awaiting any input. On the third attempt, an alarm system is activated by the intelligence unit and it keeps blaring until a master override code is entered by the home or facility owner. If 2 is selected, the stored password is sent to the home or facility owner, and the LCD screen displays "CHECK YOUR PHONE". Then control is shifted to the keypad awaiting any input. If 3 is selected, the LCD screen is frozen, only a master code can bring it back up. If 4 is selected, control returns to the keypad awaiting any input.

II. BLOCK DIAGRAM AND UNIT DESCRIPTION

Figure 1.1 shows the block diagram of the door security system.

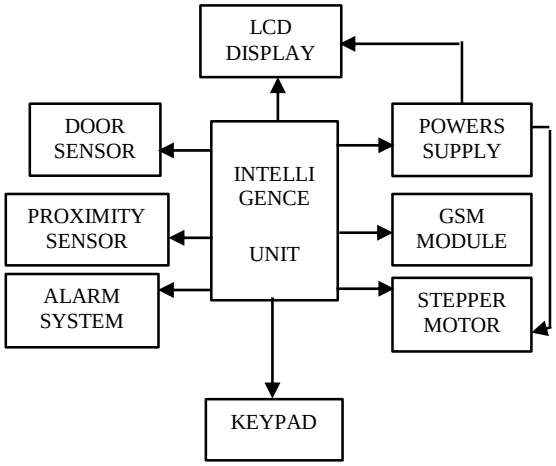

Figure 1.1: Block Diagram of the System

A. Power Supply Unit

The power supply supplies variable voltages to different parts of the circuit. It functions in two modes: AC mode and DC mode. In the AC mode, the AC volyage is stepped down to 12V and is rectified with the aid of diodes. A capacitor is used to filter out the ripples. The filtered output is further stepped down and conditioned to 5Vusing a voltage regulator 7805, for the intelligence and GSM Module. In the DC mode, the +12V from the battery is fed directly into the unit and is regulated at the second stage into +5V.

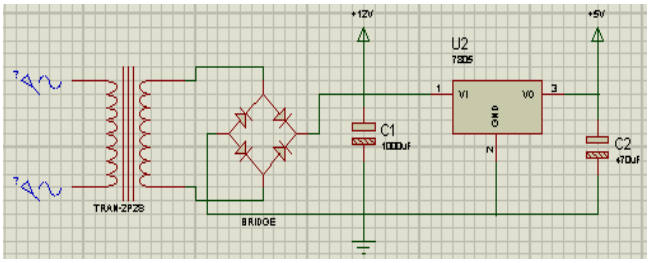

Figure 1.2: Power Supply Circuit Diagram

B. Intelligence Unit

The main component of this unit is the ATmega 32 microcontroller which controls the logic flow of the program. The ATmega16 provides the following features: 16 Kbytes of In-System Programmable Flash Program memory with Read-While-Write capabilities, 512 bytes EEPROM, 1 Kbyte SRAM, 32general purpose I/O lines, 32 general purpose working registers, a JTAG interface for Boundary scan, On-chip Debugging support and programming, three flexible Timer/Counters with compare modes, Internal and External Interrupts, a serial programmable USART, a byte oriented Two-wire Serial Interface, an 8-channel, 10-bit ADC with optional differential input stage with programmable gain (TQFP package only), a programmable Watchdog Timer with Internal Oscillator, an SPI serial port, and six software selectable power saving modes[3].The microcontroller contains the hex file in a flash memory and stores the password and authorized phone number.

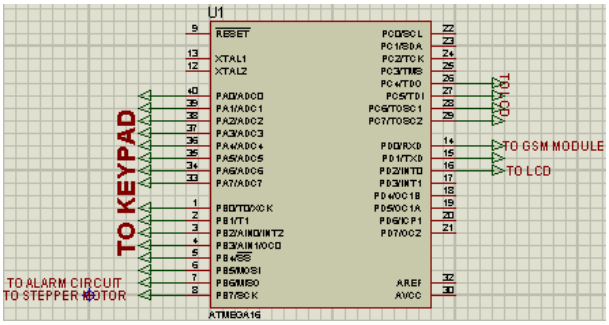

Figure 1.3: Intelligence Unit Circuit Diagram

C. Door Sensor

This is fixed to the door and senses when the door is closed or pushed open. Whatever the status of the door, it sends signal to the intelligence unit for appropriate action.

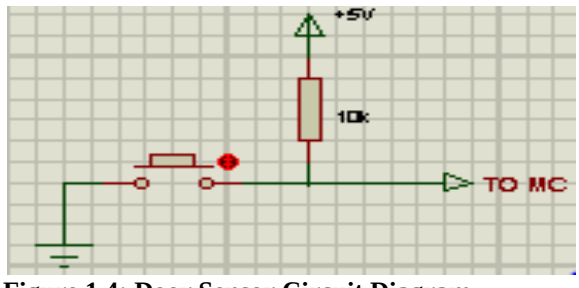

Figure 1.4: Door Sensor Circuit Diagram

D. Proximity Sensor

This senses the presence of a person within range and wakes up the system from sleep. The system goes to sleep immediately the door locked and the person is outside the range.

Figure 1.5: Proximity Sensor[4]

E. Alarm System

This unit is responsible for blaring sound continuously whenever there is a security breach. It consists of a speaker connected to and controlled by the intelligence unit.

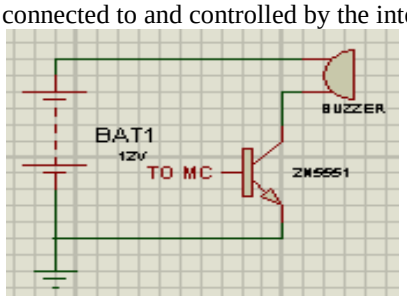

Figure 1.6: Alarm System Circuit Diagram

F. Customized Keypad

This is a non matrix keypad which primarily serves as an interfacial input to the intelligent door lock security system. It consist of 13 keys altogether, 0 – 9 and three special function keys: enter, delete and menu. It is customized in the sense that it has a specific number of functional keys to serve the purpose of this project.

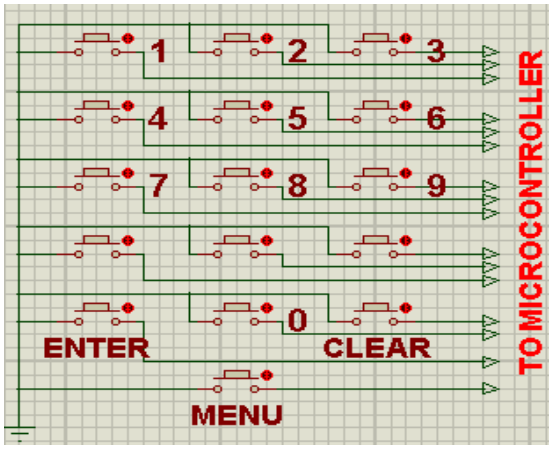

Figure 1.7: Keypad Circuit Diagram

G. Stepper Motor

This engine that provides mechanical motion to the bolt. It makes calculated motion at a determined speed. Depending on instruction received, it either moves the bolt forward to lock or backwards to unlock.

Figure 1.8: Stepper Motor[5]

H. GSM SIM800L

SIM800L is a quad-band GSM/GPRS module, that works on frequencies GSM850MHz EGSM900MHz, DCS1800MHZ and PCS1900MHz. SIM800L features GPRS multi-slot class 12/class 10 (optional) and support the GPRS coding schemes CS-1, CS-2, CS-3 and CS-4. Other features include:

- Real Time Clock
- Power voltage 3.4 ~ 4.4V DC
- Supports 2.8 to 5V logic level
- Supports 5 x 5 x 2 keypad
- One full modem serial port, user can configure two serial ports
- One USB, the USB interfaces can debug, download software
- Audio channels which includes two microphone input, a receiver output and a speaker output
- Programmable general purpose input and output
- A SIM card interface
- Support FM
- Support PWM[6]

GSM Module constitutes the secondary interface of the intelligent door lock security system. It permits a two-way communication between the home or facility owner and the Security Lock system. The GSM Module is responsible for sending real-time SMS alerts to the owner, in the event of an unauthorized attempt to access the device.

Figure 1.9: GSM SIM800L[6]

III. HARDWARE AND SOFTWARE INTEGRATION

The circuit schematic is designed and will be simulated on proteus while the source code will be written in Atmel studio environment. After the construction and coupling of the various blocks that makes up the project, the hex file of the source code will be loaded on the microcontroller unit using FlyPro software, tested and cased. Figure 1.9 shows the overall circuit diagram.

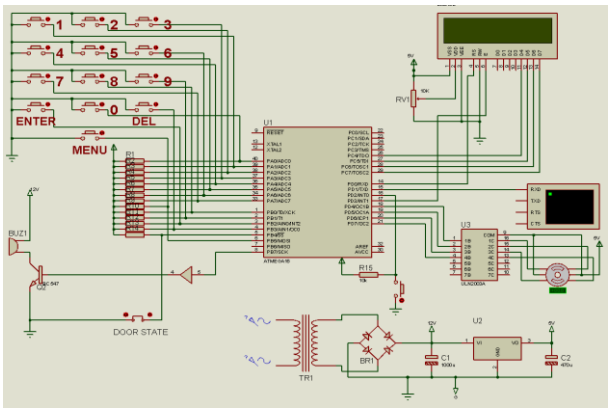

Figure 1.10: Circuit Diagram

V. RESULTS AND DISCUSSION

1. Computer Simulation

When the over all circuit was designed on proteus and the source code was written in Atmel Studio. Then it was simulated and it succeeded with no warnings. Figure 1.10 shows a screen shot of the simulation result.

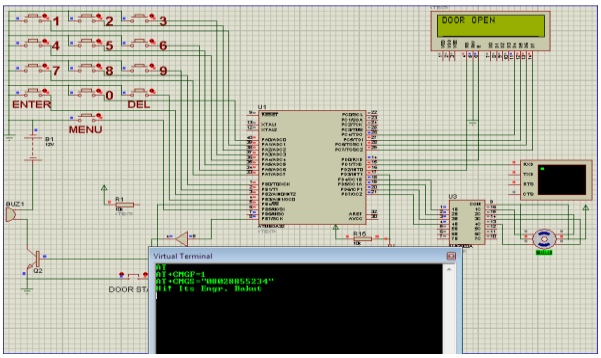

Figure 1.11: Simulated Result

2. Temporary Construction

The power supply unit was first of all constructed on a bread board. Two outputs are supplied by the power supply unit: +12V and regulated +5V.

3. Permanent Construction

The permanent construction was done on a Vero Board. All the units were constructed in modular form and connected together by header connectors. Figure 1.11 shows the final construction.

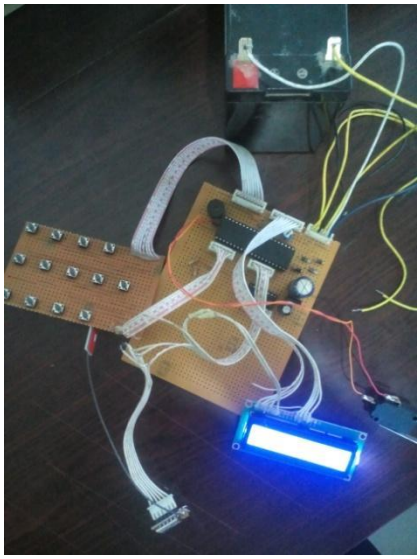

Figure 1.12: Final Construction

VI. CONCLUSION AND RECOMMENDATIONS

The prototype of an intelligent digital door security system was designed, constructed and implemented successfully. All the components and modules that make up the entire project are working well.

This design gives the flexibility of changing the password in situations where the initial password is compromised.

In instances where a wrong character or characters is or are entered during typing of the password, a special button can be used to delete these characters.

The beeping unit provides continues blaring of sound in a case where a wrong password is entered more than three times. This is to notify neighbours of an illegal entry attempt on a nearby facility.

The GSM module sends the desired message irrespective of whether GLO, MTN or AIRTEL is been used in the module. The GSM module also makes the recovery of password possible by sending the current password as a text to the facility owner only on demand.

RECOMMENDATION

The design and simulation of this project uses only one destination phone number, future work can add more destination phone numbers so that more people can receive text message of an illegal entry.

This project can further be enhanced by including bio-metrics security features. This increases the security features but it comes with an increased cost.

Also, a camera can be integrated in the design to give a facial identification of people accessing the facility.

REFERENCES

[1] [1]]Mitu Raj (2017) "GSM Based Smart Security Lock for Access Control Applications". International Journal of Electronics and Communication Technology (IJECT) – Volume 8, Issue 1, Jan – Mar, 2017, 2230-7109

[2] [2]Chaitanya Rane (2015) "Password Based Door Locking System Using GSM". International Journal of Engineering Trends and Applications (IJETA) – Volume 2, Issue 4, July-Aug 2015, 2393 – 9516

[3] https://www.atmel.com/Literature

[4] www.alselecto.com

[5] www.sparkfun.com

[6] www.sim.com/wm

A Survey of the Evolution and Application of Mobile Edge Computing

Mohammed Auwal Ahmed,Nahuru Ado
Dept. of Computer Science
Kaduna Polytechnic, Kaduna, Nigeria
horare10@gmail.com, nahuru5@yahoo.com

Abdulsalam Y. Gital
Dept. of Mathematical Science
Abubakar Tafawa Balewa University, Bauchi, Nigeria

ABSTRACT— It is difficult to estimate the number of devices connected to the internet. Informed estimates range from 20billion to 50billion by the year 2020. The implication of this is that the sheer number of smart devices trying to communicate on the internet would render the model upon which the concept of Cloud Computing is built, ineffective. The proliferation of Real-time and other resource-intensive applications owing to the advent of Internet of Things and Big Data, as well as the constraints of mobile devices in terms of processing capability and battery life has made computational offloading necessary if Quality of Service and Quality of Experience are to be met. Offloading to Data Centers at the core of the network would reduce but not eliminate delays as latency would still be significantly high. Mobile Edge Computing is a technology that provides a solution to this problem by relocating computational power from the core of the network to the edge. This reduces the distance between mobile equipment and data centers because in most instances user equipment is just a hop away from datacenters. Hence reducing latency significantly and improving both QoS and QoE. This paper surveys the evolution of Mobile Edge Computing and looks at some application areas.

KEYWORDS—Mobile Edge Computing, Cloudlets, Cloud Computing, Fog Computing, IoT

INTRODUCTION

There are over two billion smartphones in the world today and the advent of the Internet of Things would see to the addition of many more billions of smart devices into the communication ecosystem. By some estimates smart devices would number up to 20 billion by the year 2020 [1]. The direct consequence of this proliferation of smart devices is the overstretching of mobile networks and the internet backbone itself. This becomes even more pertinent with Big Data and the computation intensive applications that handle such data because mobile devices have major limitations in terms of computational capacity, battery life, and storage space. Because of these constraints, smart devices make extensive use of the Cloud to offload computation-intensive tasks.

In spite of the apparent advantages of offloading onto the Cloud, there is an associated cost in terms of latency and Quality of Service. The time it takes for data to travel to the core of the network where Cloud servers are located and back is usually too long to make the execution of real-time applications feasible [2]. This forms the core of the argument for shifting computational power from the core of the network to the edge. Hence the birth of Edge Computing.

I. EVOLUTION OF MOBILE EDGE TECHNOLOGY

The widening gap between the demand for complex applications that require high computational capacity and huge storage space such as video processing, object recognition, or 3D navigation systems, and the availability of these resources in mobile devices have created a niche for Mobile Cloud Computing. Mobile Cloud Computing is a technology that is based on the idea of Offloading complex applications that demand huge resources (in terms of computation and storage) to Cloud servers that have an abundance of these resources.

Offloading, as argued by [3], is different from other similar computing architectures like Client/Server or Grid computing. In both Client/Server and Grid Computing process migration occurs typically within the same computing environment – the Grid for Grid computing and the Local Area Network for Client/Server. Computational Offloading on the other hand involves migrating programs to servers outside of the immediate computing environment.

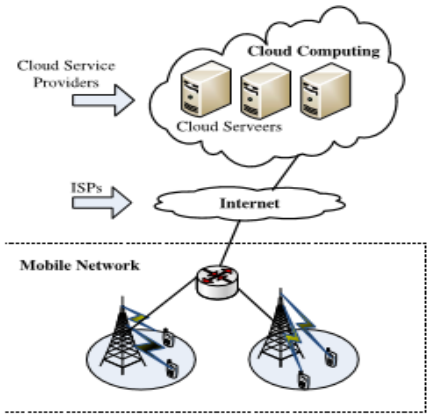

FIGURE 1. Architecture of mobile cloud computing.

The figure above shows the typical architecture of Mobile Cloud Computing. Mobile user equipment connectto the Mobile network via base stations and subsequently use the internet infrastructure to connect to Cloud Servers through Cloud Service Providers.

This architecture however has a lot of latency inherent in it. This is largely due to the fact that it is WAN dependent and delay and jitter are parameters that are difficult to control in WANs [4]. An early solution to the issue of latency in Mobile Cloud Computing is the concept of Cloudlets.

A. *Cloudlets*

Cloudlets are viewed as an implementation of Mobile Cloud Computing but conceptually they are more similar to Mobile Edge Computing (MEC). The difference being that in MEC servers are owned and managed by mobile infrastructure

providers while Cloudlets are owned and managed by end-users. [5].

Cloudlets are perhaps the first step in the evolution towards Mobile Edge Computing. Basically, a Cloudlet is just a high capacity computer (or cluster of computers) that is deployed within the vicinity of mobile devices in order to provide computation and storage services to mobile user equipment [4]. The Cloudlet is usually a single hop away from User Equipment and resource demanding applications can be offloaded and results sent back at incredibly low latencies.

The design architecture of Cloudlets is such that mobile devices switch from mobile networks to WIFI in order to access the Cloudlet services [5].

The major improvement that Cloudlets brought over the concept of Mobile Cloud Computing is in the reduction of latency. Latency hurts usability by degrading the crispness of crispness of system response thereby making deeply immersive and computation intensive tasks jerky to the point of distraction [6].

A cloudlet typically has a 3-layered architecture; the component level, the node level and the cloudlet level [7]. They also classified Cloudlets as adhoc and elastic. With adhoc Cloudlets, nodes are discovered dynamically as opposed to elastic Cloudlets whose entire infrastructure is visualized using a virtual machine.

B. Fog Computing

In spite of the apparent advantages of MCC and Cloudlets, they still do not meet the needs of some mobile devices especially IoT. This is due to the fact that IoT applications usually require in addition to low latency, mobility support, geo-distribution, and location-awareness [8].

Fog computing is proposed to enable computing directly at the edge of the network, those devices that provide these services are called Fog nodes [8]. Unlike in Cloudlets, Fog nodes do not have to be resource rich [9] because conceptually, fog nodes are a huge number of heterogeneous (wireless and sometimes autonomous) ubiquitous and decentralised devices communicate and potentially cooperate among them and with the network to perform storage and processing tasks without the intervention of third parties [8].

C. Mobile Edge Computing

In the article "Challenges and Opportunities in Edge Computing" [10] explored the research space in Edge Computing. Interestingly they didn't identify any difference between Edge Computing, Fog Computing, and Cloudlets. They identified them as terms used to describe the same phenomenon.

Their paper discussed the motivations, the opportunities, and the challenges in Edge Computing. Figure 2 summarizes their findings.

Basically, Mobile Edge Computing (MEC) is a computing paradigm in which the vast amounts of idle computation power and storage space distributed at network edges is harnessed in such a way that resource-constrained mobile devices can perform computation-intensive and latency-critical tasks [11].

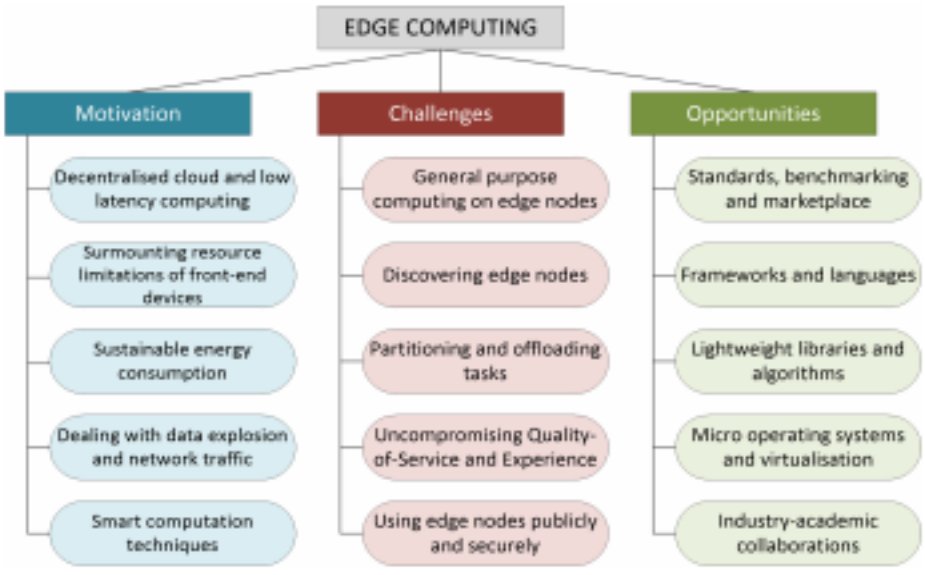

Fig. 2. Motivation, challenges and opportunities in edge computing

APPLICATIONS OF MOBILE EDGE COMPUTING

The proliferation of mobile devices and the exponential growth we are currently witnessing in the number of the active mobile devices that are being coopted into the communication ecosystem has seen to the unprecedented success of Cloud and Cloud-related services. Amazon and Dropbox readily come to mind [11].

Edge Computing is still at its very infancy yet a lot of research has been done to highlight some of its key areas of application.

When mobile networks supporting high data rates and low latency computation are deployed, new application areas emerge [12]. Augmented Reality which is an interaction paradigm that superimposes a computer-generated environment to a real-life environment, is one such application area.

Other areas highlighted by [12] are Intelligent Video Acceleration, connected cars, and Internet of Things.

Big Data analytics is also an application area of immense importance. A significant proportion of the devices that make up the Internet of Things are video cameras or camera-enabled sensors [13]. Analytics of the massive video content being generated at the Edge of networks is an area with a lot of applications in smart cities, surveillance, and in fighting crime.

RESEARCH AREAS

As with any emerging field, Standardization and Benchmarking is needed in order for the technology to become established and ultimately become ubiquitous as is the target with Mobile Edge Computing.

Currently, organizations such as National Institutes of Standards and Technology (NIST), IEEE Standards Association, International Standards Organisation (ISO), Cloud Standards Customer Council (CSCC) and the International Telecommunication Union (ITU) are actively engaged in research about standards and benchmarking [10].

Another area of research is in software mechanisms and algorithms needed for the collective control and sharing of cloudlets and in computational offloading [14].

The work of [11] categorizes the research areas in Mobile Edge Computing into five as depicted in figure 3.

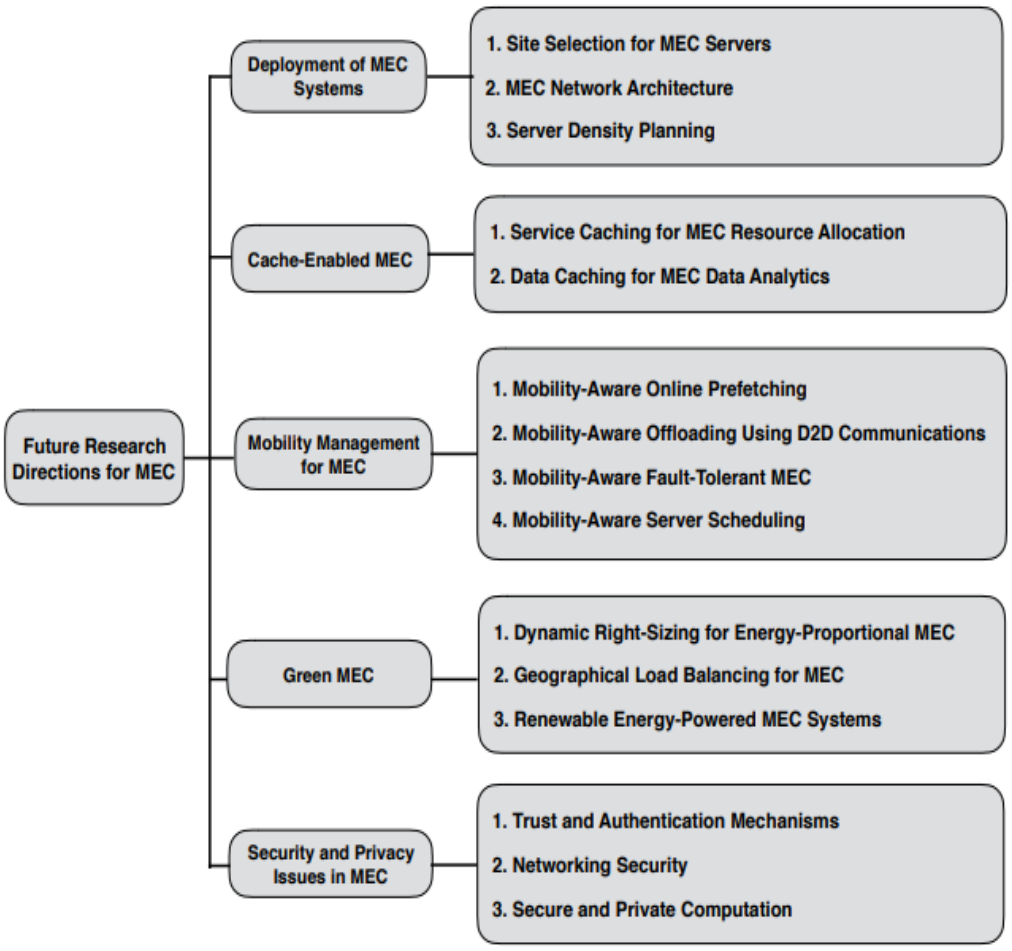

Figure 3: Research Areas in Mobile Edge Computing

CONCLUSION

The speed with which the sizes of data sets are growing and the accompanying high computation capacities required to process these big data sets is not matched by advances in speeds of processors of mobile devices and battery life. Mobile Edge Computing bridges that gap. Smart phones have made the dream of ubiquitous computing a reality and the Internet of Things would further entrench this reality in the years to come. Mobile Edge Computing is the glue that holds all of that together. The field is at its infancy but already has numerous areas of application. Its numerous active research areas would only just further widen this area of application.

REFERENCES

[1] Gubbi, J., Buyya, R., Marusi, S., & Palaniswami, M. (2013). Internet of Things (IoT): A Vision, Architectural Elements, and Future Directions. *Future Generation Computer Systems, 29(7),* 1645-1660.J. Clerk Maxwell, A Treatise on Electricity and Magnetism, 3rd ed., vol. 2. Oxford: Clarendon, 1892, pp.68–73.

[2] Pavel, M., & Zdenic, B. (2017). Mobile Edge Computing: A Survey on Architecture and Computation Offloading. *arXiv preprint arXiv:1702.05309*.

[3] Kumar, K., Liu, J., Lu, Y.-H., & Bhargava, B. (2012). A Survey of Computation Offloading for Mobile Systems.

[4] Pavel, M., & Zdenic, B. (2017). Mobile Edge Computing: A Survey on Architecture and Computation Offloading. *arXiv preprint arXiv:1702.05309*.

[5] Beck, M. T., Werner, M., Feld, S., & Schimper , T. (2014). MobileEdgeComputing: A Taxonomy. *The Sixth International Conference on Advances in Future Internet.* Munich.

[6] Satyanarayanan, M., Bahl, P., Caceres, R., & Davies, N. (2009). The Case for VM-based Cloudlets in Mobile Computing. *IEEE Pervasive Computing*.

[7] Verbelen, T., Simoens, P., De Turck, F., & Dhoedt, B. (2012). Cloudlets: Bringing the cloud to the mobile user. *Verbelen, Tim, et al. "Cloudlets: Bringing the clouProceedings of the third ACM workshop on Mobile cloud computing and services.* (pp. 29-36). ACM.

[8] Yi, S., Li, C., & Li, Q. (2015). A Survey of Fog Computing: Concepts, Applications, and Issues. *Proceedings of the 2015 workshop on mobile big data* (pp. 37-42). ACM.

[9] Willis, D., Arkodeb, D., & Suman, B. (2014). ParaDrop: a multi-tenant platform to dynamically install third party services on wireless gateways. *Proceedings of the 9th ACM workshop on Mobility in the evolving internet architecture* (pp. 43-48). ACM.

[10] Varghese, B., Wang, N., Barbhuiya, S., Kilpatrick, P., & Nikolopoulos, D. (2016). Challenges and Opportunities in Edge Computing. *arXiv preprint arXiv:1609.01967*.

[11] Mao, Y., You, C., Zhang, J., Huang, K., & Letaief, K. (2017). *A Survey on Mobile Edge Computing: The Communication Perspective.* IEEE.

[12] Hu, Y. C., Patel, M., Sabella, D., Sprecher, N., & Young, V. (2015). *Mobile Edge Computing A key technology towards 5G.* Sophia Antipolis: European Telecommunications Standards Institute.

[13] Satyanarayanan, M., Simoens, P., Xiao, Y., Pillai, P., Chen, Z., Ha, K., . . . Amos, B. (2015). Edge Analytics in the Internet of Things. *IEEE Pervasive Computing*, 24-31.

Satyanarayanan, M. (2017). *The Emergence of Edge Computing.* IEEE Computer Society.

Intelligent Image-Processing for Crack Detection on Rail Surface

I. I. Danfillo and M. T. Kabir[1]
Department of Electrical and Computer Engineering, Ahmadu Bello University, Zaria- Nigeria.

ABSTRACT- Rail inspection is an essential task in railway maintenance. It is periodically needed for preventing dangerous situations and ensuring safety in railways. Currently, most of the inspections are manual and are conducted visually by railroad track inspectors. Inspections include detecting defects on rail. This work presents a vision-based technique to automatically detect the presence of a defect on rail surface. The system uses acquired digital images of rail. An intelligent image-processing algorithm capable of detecting defect on rail surface is the used to achieve hig performance automated detection. Various algorithms related to morphological operations, edge detection, thresholding, segmentation and feature extraction are applied for processing the images of rail surface defect and cracks. For better speed and accuracy, the algorithm was implemented on Matlab.
KEYWORD: Rolling contact Fatique, Visual Inspection System, SR.

INTRODUCTION

Railway networks are among the major ways to release traffic congestion in urban areas. Though, due to effects such as aging, thermal expansion and contraction, human damage, and topographic change, railway tracks suffer from breaks in their surfaces and internal structures. These split and slender defects are generally known as cracks, which reflect on the health of the railway tracks. Appropriate and accurate management of railway tracks is essential for the maintenance of the rail structures and stoppage of accidents. An additional important motivation of carrying out inspections and detections on railways is to lower the infrastructure and rolling stock maintenance costs that still form a main fraction of the total operation cost of the rail transformation systems. The massive reductions that occurred over some years back in many countries has really contributed to their economy which largely made inspection and detection systems more powerful and useful. Also, decrease in maintenance budgets in some countries of railways has led to the growth of the frequency of hazardous defects and that will cost them much more when trying to maintain the hazardous defects.

Based on Magel et al (2005), the problem of rolling contact fatigue (RCF) in rail that comprises of head checks, shelling, squats on the rail surface and deep-seated shell on subsurface developed both domestically and internationally around the 1990s, and came to worldwide notice through the loss of life in the Hatfield (UK) derailment that occurred in 2000. From FRA statistics, within eight years from 1995 to 2002, rolling contact fatigue (RCF) was powerfully involved in 122 derailments, and may have added 160 more. Network rail describes that certain parts of track rail steel are subjected to bending moments and impact forces, while rail head material is governed by compressive loading and sliding forces within a comparatively small contact patch known to result in wear and rolling contact fatigue (RCF) damage.

Martin and Tosunoglu, (2000) said that in some few decades back, experienced inspectors have done inspection of cracks on rails manually, which is not adequately accurate. Consequently, the development of an automatic crack detection and classification technique is the only way to solve this problem, which uses image-processing techniques. To be efficient, image-processing techniques used should be able to provide high detection rate and accurateness. Some of the image-processing techniques that are suitable in detection of cracks in rail are: Morphological image processing technique, image thresholding, segmentation technique, feature extraction technique, color based processing technique, shape based processing technique, edge detection technique, etc. the implementation of machine vision and image processing algorithms are succeeded using a very competent and dependable computer software packages (platforms), which are MATLAB, OpenCV library in C/C++, etc.

LITERATURE REVIEW

Bello et al (2016) proposed a paper on the development of an intelligent image-processing algorithm capable of detecting fatigue defects from image of the rail surface. The algorithm generates statistical data such as total number of defects per image. Adaptive histogram equalization was used for the local contrast enhancement so the defect regions are clearly visible. Then an adaptive thresholding was applied to segment the defects.

A more robust visual inspection system (VIS) was described by Quingyoung et al (2012), it focused on the local contrast enhancement in addition to segmentation by thresholding algorithm. However, feature extraction of detected defects was not investigated.

Jyoth, and Gimy, (2014) presented a paper on VIS based contrast enhancement, projection profile of the mean intensity of each transversal and longitudinal line pair forming a suspect rectangle (SR) was described. Defects were segmented using threshloding algorithm. The method is capable of only extracting the longitudinal and transverse positions of defected defects.

Muhammad, et al (2001) proposed a paper on defects inspection method based on computer vision system on railroad tracks, work that centers on the analysis of railroad track surface to detect diverse kinds of problems to avoid any kind of possible accidents. The paper centers on detecting defects on railroad tracks, which are:

i. Crack detection
ii. Object detection
iii. Detection of rail head spalling

The images of the railroad track surface were taken by CCD camera in a very high frame rate then the image was processed using different softwares to remove the defects

and also parameter computation. The diverse image processing algorithms that was applied in the images of the railroad track defects and cracks are de-noising, filtering, thresholding segmentation and feature extraction which is regularly implemented on computer. These were developed on diverse embedded platforms like MATLAB and C++, which use the openCV library.

Liu (2010) proposed a rail surface defects inspection method centered on automated machine vision system. The main focus of the paper was on two different types of defects on rail surface, which are spalling of the railhead and cracks in the surface. The image processing algorithms used for the processing of images of rail surface defects are de-noising, image segmentation and feature extraction. Then dynamic thresholding and feature matching were applied to extract and recognize region of defect correctly. At the end, percentage of wear of railhead and length of cracks in the rail surface were calculated. The adaptability of algorithm required to be proved by processing more images next.

Zhang (2014) wrote a paper that emphasis on automatic crack detection and classification method for subway tunnel safety monitoring. General cracks are a fundamental indicator for the safety status of an infrastructure. Based on the paper, high-speed complementary metal-oxide-semiconductor (CMOS) industrial camera was utilized to capture and store the tunnel surface. Then morphological techniques of image processing and thresholding operations are used to segment the local dark areas with potential crack defects from the original gray-scale images. In the feature extraction process, a distance histogram based shape detector is used to define the shape difference amid cracks and other irrelevant objects. And it is developed for achieving high performance in the subsequent aspects, detection rate, and detection accuracy and detection efficiency.

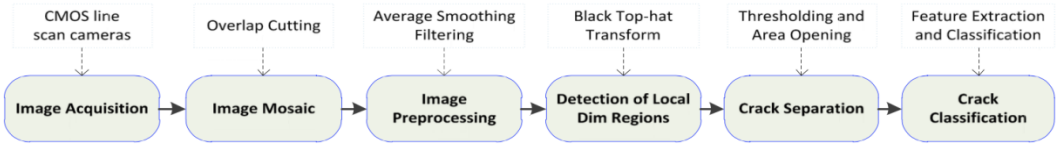

Figure 1: flowchart of the proposed approach (Zhang W. 2014)

Deutschi (2004) proposed a new vison-based inspection technique for rail surface defects. This method really can substitute visual inspections with an automatic inspection system. Color line-scan cameras and a special image acquisition method, which is usually called Spectral Image Differencing

Procedure (SIDP) permit the automatic 3D detection of defects on rail surfaces for example crack, break-offs, flakes, grooves by the methods of image processing. Image enhancement with more emphasis on illumination method is made on shading correction computed based on nonlinear differential function, scale enables differentiating among cavity or elevation type of defects.

I. DEVELOPMENT OF IMAGE PROCESSING ALGORITHMS FOR CRACK DETECTION ON RAIL

The image proposes to be used in this paper is shown in the Figure below.

Figure 2: shows the image of the cracked rail to be used for the analysis

METHODOLOGY

The Image Processing Techniques used for designing the algorithm for crack detection and length measurement on rail are:

Cheng, et al (2010) presents a paper for visualization of damaged rail, in which the damage has been recognized using wavelet transform. The paper focuses on general identification of rail damage. The paper follows the method of finite element analysis (FEA) simulation of intact and damaged rail, to identify displacement mode difference. Wavelet transform applied to the displacement mode difference and wavelet coefficients are used to specify damage. The damage detection results are visualized through volume visualization method.

Description and Justification of the Image-Processing Algorithm (Methodology)

RGB to gray scale image:

Based on Kanan and Cottrell, (2012) the reason for applying this function is to convert the true color image, which is the RGB image to a gray scale intensity image, the function of this is to eliminate the hue and saturation information on the image while retaining the illuminance.

Gray scale to black and white image:

The reason for applying this function is in order to find the region of interest, the portions of the image that is of interest for further processing. The intension is binary; "yes" means the pixel is of interest while "no" means the pixel is not of interest.

Edge detection (prewitt):

Based on Maini and Aggarwal, 2009, and Maar and Hildreth (1980), we decided to apply edge detection (prewitt) to the black and white image because edge detection is regarded as

the initial step in object recognition. Edge detection refers to the process of identifying and locating sharp discontinuities in an image. Discontinuities are abrupt changes in pixel intensity, which characterize the boundaries of objects in a scene.

$$M(x,y) = \sqrt{I_x^1}(x,y)^2 + I_y^1(x,y)^2 \quad (1)$$

The Infinite Symmetric Exponential Filter uses another optimization function to find the edge in an image and it can be written as follows:

$$C_N^2 = \frac{4\int_0^\infty f^2(x)dx.\int_0^\infty f'^2(x)dx}{f^4(0)} \quad (2)$$

C_N will be reduced with an optimal smoothing filter for an edge detector. It can be called symmetric exponential filter (ISEF):

$$f(x) = \frac{P}{2}e^{-p|x|} \quad 1D \quad (3)$$

$$f(x,y) = a.e^{-p(|x|+|y|)} \quad 2D \quad (4)$$

The filter from the ISEF Edge Detector is given as one-dimensional recursive filter. By assuming the 2D-filter function real and continuous, it can be given as below:

$$f[i,j] = \frac{(1-b)b^{|x|+|y|}}{1+b} \quad (5)$$

Using recursive filter speeds up the convolution. b Can be entered by the user.

Morphological operation dilation:

Based on Ledda, (2007), I decided to apply morphological operator dilation after the edge detection basically to gradually enlarge the boundaries of the foreground pixels that is the white pixels. Thus are area of the white pixels grow in size while holes within those regions becomes smaller.

Morphological operation dilation is defined as follows;

$$A \oplus B = \{c = a + b \ for\ some\ a \in b \in B\} \quad (6)$$

Dilation is also associtive and also commutative

$$(A \oplus B) \oplus C = A \oplus (B \oplus C) \quad (7)$$

Morphological operation erosion:

Based on Ledda, (2007), we then applied morphological operator erosion so that the function erosion will shrink the enlarged boundaries of the foreground pixels, which are the white pixels. That makes the boundaries slimmer which is more accurate. The whole idea from the application of morphological operators' dilation and erosion is to improve the quality of the edge detection, which was done and a better result was achieved.

Morphological erosion can be defined as given below:

$$A \ominus B = \{x + b \in A\ for\ every\ b \in B\} \quad (8)$$

Unlike dilation, erosion is not commutative. Much like how addition is commutative whereas subtractive is not. And again, also unlike dilation, erosion is not associative.

$$(A \ominus B) \ominus C = A \ominus (B \ominus C) \quad (9)$$

Implementation of the Developed Algorithm on Matlab to Analyze Cracks on Rail Surface

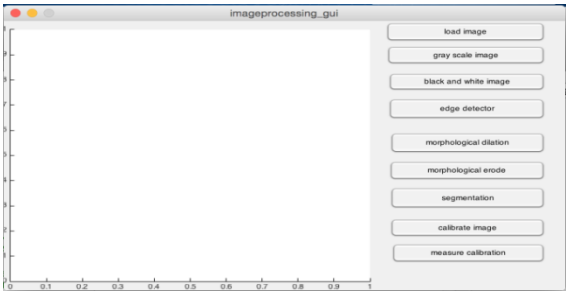

Figure 3: A blank GUI before loading an image

Step 1: Load an image into the workspace.

This step involves using the imread command to load an image into the workspace. It reads the rail crack image stored in the toolbox as shown in the Figure below.

Segmentation:

Image segmentation technique is applied in order to divide the image into regions or categories, which correspond to different parts of the image. Every pixel in the same category have similar greyscale of multivariate values and form a connected region, while neighboring pixels which are in a different category have dissimilar value, which also form a connected region as well.

Calibrating image:

The main aim is to calculate the length of the crack in millimeter, but Matlab gives measured length in pixels. The length of the railhead in millimeter is known which is 72mm while the length of the railhead in pixel can easily be measured on Matlab, which I did. Using mathematics, I related the two to find my unknown, which is the length of the crack in millimeter.

Measure calibration:

The length of the crack in length is calculated in millimeter and also displayed on the screen.

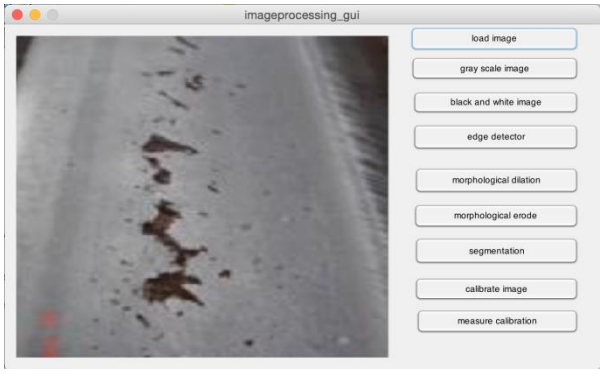

Figure 4: An image loaded on the GUI

Step 2: conversion from RGB to grayscale image.

A grayscale image sometimes called gray-scale, gray scale, or gray-level is a data matrix whose values represent intensities within some certain range. MATLAB saves a grayscale image as an individual matrix,

and every element of the matrix corresponding to one image pixel, as shown in the Figure below.

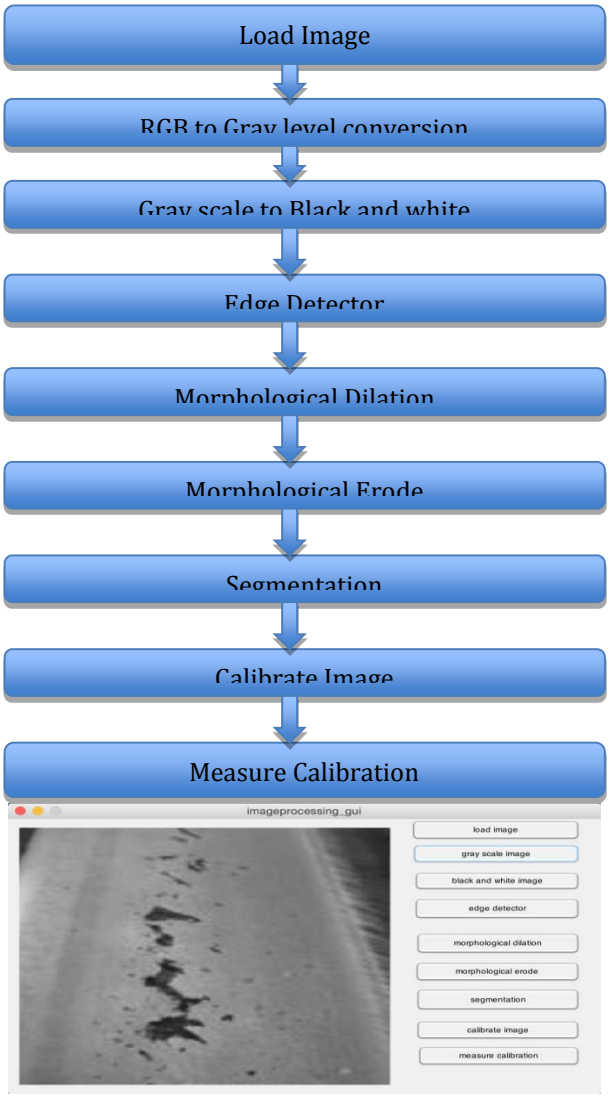

Figure 5: A grayscale image

Step 3: Conversion of the processed image to binary image (black and white).

Creating a binary version of the processed image so toolbox function for analysis is been used, as shown in the Figure below.

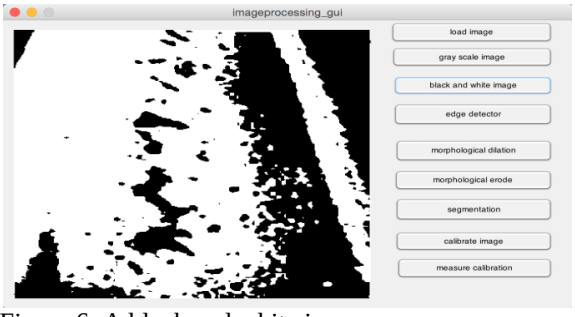

Figure 6: A black and white image

Step 4: Applying edge detector to the processed binary image (black and white).

In an image, an edge is said to be a curve that follows a path of quick change in image intensity. Edges are normally associated with the boundaries of objects in a scene. Edge detection is utilized to locate the edges in an image, as shown in the Figure below.

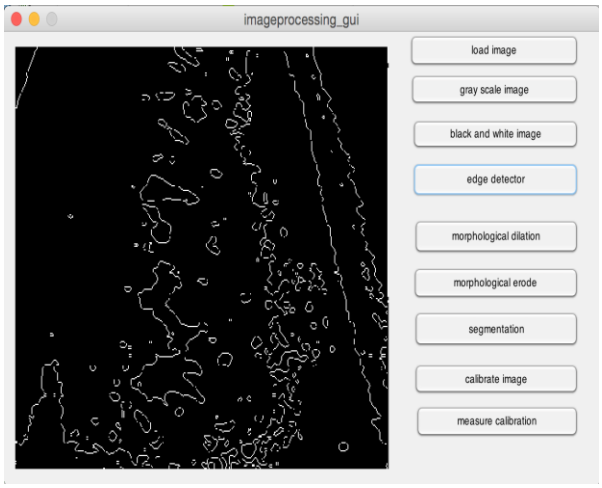

Figure 7: An edge detector applied to the image

Step 5: Applying morphological dilation to the edge-detected image.

Dilation involves the addition of pixels to the boundaries of the objects in the image, as shown in the Figure below.

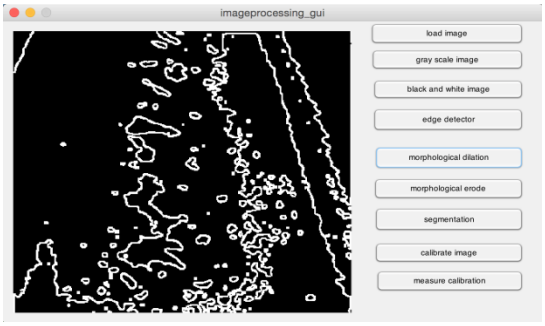

Figure 8: A morphological dilation applied to the image

Step 6: Applying morphological erosion (erode) to the edge-detected image.

While in the other hand erosion involves the removal of pixels on the object boundaries of the image, as shown in the Figure below.

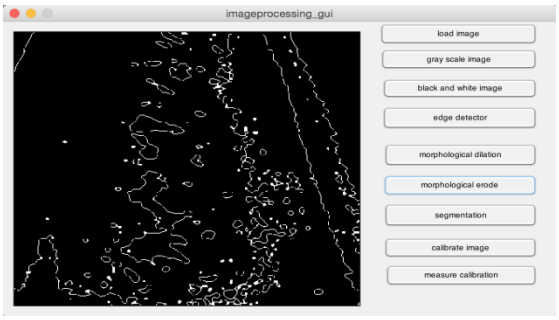

Figure 9: A morphological erode applied to an image

Step 7: Applying segmentation to the eroded image.

Image segmentation is the process of dividing an image into 2 different parts or regions. This division into two parts is often

based on the characteristics of the pixels in the image, as shown in the Figure10.

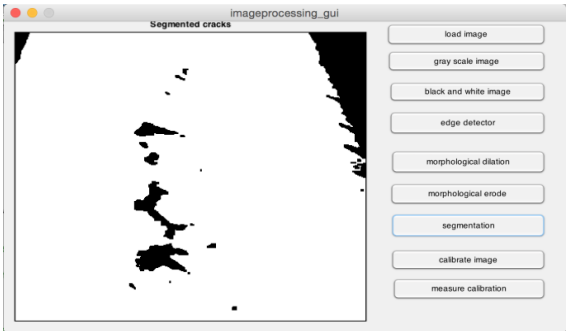

Figure 10: A segmentation done on the image

Step 8: Calibration of the image
Cropping.
To remove a rectangular portion of an image, the imcrop function is used. Using imcrop, the crop region can be specified interactively using the mouse or programmatically by identifying the size and position of the crop area, as shown in the Figure11.

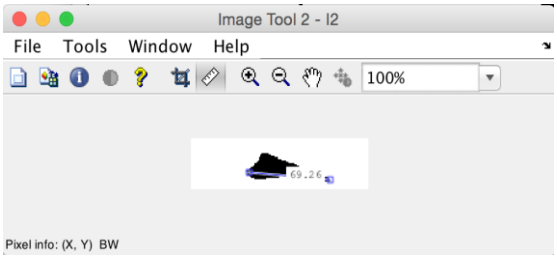

Figure 11: An image calibration

Step 9: Measuring the image in pixels.
The length of the crack of interest is measured to be 69.26 pixels, as shown in the Figure below.

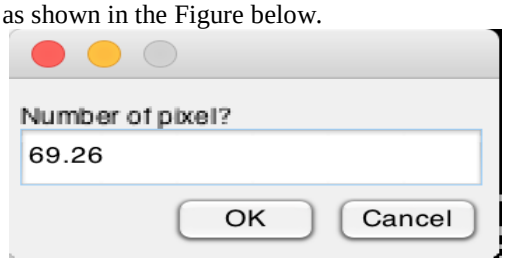

Figure 12: Measured crack length in pixel
Step 10: Converting the measured length in pixels to millimeter (mm).
The measured length in pixels is then converted to millimeter (mm), as shown in the Figure13.

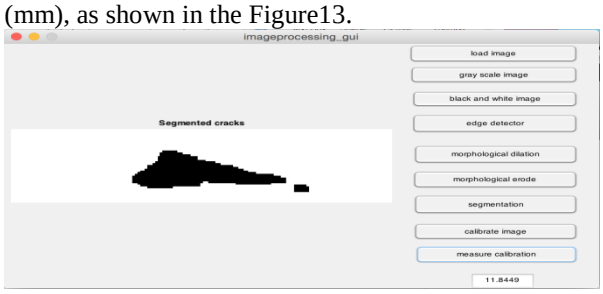

Figure 13: Measured crack length in millimeter (mm)

CONCLUSION

The aim of this paper has been achieved which involves developing an intelligent image processing technique that is able to detect fatigue defects on the image of a rail surface and thereby measuring the length of the detected defect.
In this paper, a surface rail defect has been considered for the detection because most of the rail incidents that occur are due to bad condition of the rail surface defects. In doing so, based on the wide literature review on the different image-processing techniques used for defect detection on general surface and also on rail surface, an intelligent image processing algorithm was developed capable of detecting defects on rail surface, some of the image processing techniques used are edge detection technique, morphological operations (dilation and erosion) techniques, segmentation techniques etc.

REFERENCE

[1] B. Sambo, A. Bevan, C. Pislaru (2016). A novel application of image processing for the detection of rail surface rcf damage and incorporation in a crack growth model, institiue of railway research, university of huddersfield, UK.
[2] Magel, E., Sroba, P., Sawley, K., & Kalousek, J. (2005). Control of Rolling Contact Fatigue of Rails, centre for surface transportation technology, National Research Council Canada,
[3] Martin, A. & Tosunoglu, S. (2000). Image Processing Techniques for Machine Vision, Florida International University, Department of Mechanical Engineering
[4] Zhang, W., Zhang, Z., Qi, D., & Liu, Y. (2014) Automatic Crack Detection and Classification Method for Subway Tunnel Safety Monitoring, 19307-19328.
[5] Kanan, C. & Cottrell, G.W. (2012). Color-to-Grayscale: Does the Method Matter in Image Recognition, 7, 50-70.
[6] Ledda, A. (2007). Mathematische morfologie in de beeldverwerking Mathematical Morphology in Image Processing, 983-965.
[7] Cheng Liangyan, Li Guilin, Nie Zhenhua, & Ma Hongwei (2010). Visualization research of damage detection in rail . Paper presented at the 502-505.
[8] Maar, D. & Hildreth E., (1980) "Theory of edge detection", Proceedings Royal Soc. London, vol. 207, 187-217,
[9] Quingyong Li, & shengwei Ren. (2012), A Visual Detection System for Rail Surface Defects, In Systems, Man, and Cybernetics, Part C: Applications and Reviews, IEEE
[10] Muhammed F, & Aviash, G K, (2013). Computer-Vision Based Visual Inspection and Crack Detection of Railroad Tracks, In IEEE 5th Int. Conf on Soft computing and pattern recognition, vol 1, no 1 pp. 228-236
[11] Jyoth, R.L. Gimy, J. (2014)"A real Time VIS for Rail Flaw detection. In Int Journal of Scientific Research and Publication,vol 4, no 8.
[12] Gimmy, J. Hyfa, N. Remya, K. "Rail flaw detection using image processing concepts-A review". In Int Journal of Engineering and Technology, vol 3, no 4, 2014.
Transactions, vol 42, no 6, pp. 1531-1542.

Data Rate-based Sleep Mode in LTE Hetnet

Abubakar Ahmed, Kabiru Abubilal, Suleiman Sani
Department of communications engineering
Ahmadu Bello University Zaria, Nigeria
habusadik@gmail.com, kb.ahmad74@gmail.com, smsani_2@yahoo.com

ABSTRACT*—Base stations significantly contribute to power consumption in cellular networks. This is a factor which needs to be addressed when modelling cellular networks. This is due to the fact that high power consumption will result in high operational cost. Several energy saving algorithms have been proposed to save energy in heterogeneous networks. This paper therefore introduces a Data Rate-Based Sleep Mode Algorithm for energy savings for a pico evolved NodeB (eNodeB) cell in a Long-Term Evolution (LTE) heterogeneous network (HetNet). The algorithm switched the operating state of some pico eNodeB cells to sleep mode (inactive state) at low traffic and medium traffic during which the users are offloaded to other pico eNodeB and macro eNodeB cells to save overall energy consumption in the network. As traffic increased and the average user data rate of the overall network reduced (less than 2Mbps), the pico eNodeB cells return to active state to ensure service delivery was not obstructed. The work considers temporal fluctuations of traffic with a view to achieving higher energy savings.

***KEYWORDS*—base station, cellular networks, heterogeneous network (*HetNet*), sleep mode, evolved NodeB (*eNodeB*), Long Term Evolution (*LTE*), pico, macro, average user data rate**

INTRODUCTION

The number of subscribers and the demand for cellular traffic has increased. Hence, mobile operators find meeting these new demands in wireless cellular networks inevitable, while they save to keep their costs minimum [1]. In a wireless network, base stations (BSs) consume about two-third of total network power consumption and are logically responsible for 70% of CO2 emission from the entire network. For this reason, management of energy consumption of wireless base station has become an essential topic of discussion in the research society [2].

Increase in the number of small cell base stations in HetNets as well as their power consumption has made energy savings an important topic for research. Sleep mode technique helps in the reduction of power consumption in HetNets. Most researches implemented sleep mode focusing on base station transmit power, constant data rate, number of users, signal-to-interference-and-noise ratio (SINR) and traffic load. These factors do not efficiently represent realistic traffic load conditions. This paper considers average user data rate as a metric for sleeping pico evolved NodeB (eNodeB) cells in a Long-Term Evolution (LTE) HetNet.

A traffic model, data rate model and a power consumption model were used to implement the sleep mode in the LTE HetNet. The traffic model was based on Round Robin resource allocation, the data rate model was based on SINR link adaption mapping, and the power consumption model was based on power consumption parameters of the pico eNodeB cells.

PROBLEM DEFINITION

It has been found out that little or no investigation has been made on the effect of average user data rate on sleeping pico eNodeB cells. However, setting a pico eNodeB cells into sleep mode could lead to poor service delivery. Therefore, there is a need to consider the realistic average user data rate of 2Mbps [3] when implementing sleep mode for LTE HetNets.

A. LTE Network Architecture

The Long-Term Evolution (LTE) encompasses the evolution of the Universal Mobile Telecommunications radio access through Evolved Universal Mobile Telecommunications System Terrestrial Radio Access Network (E-UTRAN). It is accompanied by an evolution of the non-radio aspects under the term System Architecture Evolution (SAE) which includes the Evolved Packet Core (EPC) network. Together LTE and SAE comprise the Evolved Packet System (EPS). The access network of LTE, E-UTRAN, simply consists of a network of eNodeBs as illustrated in Fig. 1. For normal user traffic (as opposed to broadcast), there is no centralized controller in E-UTRAN; hence the E-UTRAN architecture is said to be flat [4].

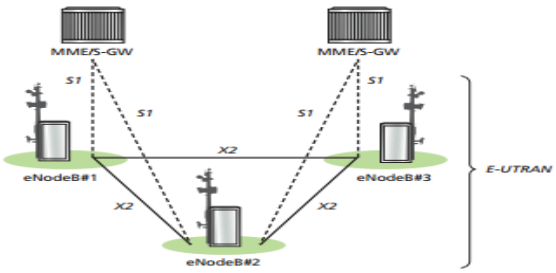

Fig. 1. Overall E-UTRAN Architecture. [4]

B. LTE Network Architecture

A macrocell base station consists of six power consuming components as discussed hereunder [5]:

1) *Rectifier:* Converts alternating current (AC) to direct current (DC), also known as a AC-DC converter.
2) *Digital Signal processing:* This is concerned with the conversion of the signal to a sequence of bits or symbols and the processing of these signals.
3) *Transceiver:* This is responsible for transmitting and receiving the signals.

4) *Power Amplifier:* This converts the DC input power into a significant radio-frequency (RF) signal.
5) *Air Conditioning:* Regulates the temperature in the base station cabin.
6) *Micowave Link:* This is responsible for the communication with the backhaul network.

The total power consumption of the base station is a sum of the power consumption of all the above-named components. The power consumption of these components should be multiplied by their number of occurrences to determine the base station power consumption. Some of the components depend on the number of sectors, n_{sector} and the number of transmitting antennas, n_{tx}. The n_{sector} determines the number of rectifiers, digital signal processing, transceivers and power amplifiers. Each sector requires one rectifier, one digital signal processing unit, one transceiver and one power amplifier. Therefore, the power consumption of these components should be multiplied by n_{sector}. The n_{tx} determines the number of transceivers and power amplifier. For each transmitting antenna, one transceiver and one power amplifier are needed. This means that the power consumption of the transceiver and the power amplifier should not only be multiplied by n_{sector} but also by the number of transmitting antennas n_{tx}. Taken this into account, the power consumption per macrocell base station for High Speed Packet Access (HSPA) and LTE (Advanced) is up to about 1672.6W [5].

The same components used for a macrocell base station are used for a microcell base station except for the backhauling. The backhauling of a microcell base station is typically established through the overlaying macrocell base station. A microcell base station supports only one sector covered by one antenna. This results in a power consumption of 376.6W per microcell base station. The size of a femtocell base station is much smaller than that of a macrocell and microcell base station and is comparable to that of a Wireless Fidelity (WiFi) access point. Therefore, the power consuming components are different from those of a macrocell and microcell base station. The femtocell base station consists of a microprocessor, a transceiver and a power amplifier. Femtocell base station power consumption is 12W per base station [5].

C. Energy Savings in Base Stations

Power consumption for each base station is about 1400 watts and energy cost per BS is about $3200 per annum with a carbon emission of 11 tons of CO2. The radio network itself adds up to 80% of the total network energy consumption. Therefore, BS equipment manufacturers have begun to offer a number of eco-friendly solutions to reduce power demands of base stations. A typical cellular network consists of three main elements; a core network that takes care of switching, base stations providing radio frequency interface, and mobile terminals for making voice or data connections [1].

There are different ways to reduce energy consumption in base stations, such as [6]:

Employing power saving protocols such as base station sleeping which enables an inactive operation mode for base stations under load conditions.

Improved power amplifier technology which makes the hardware design of a typical base station more energy efficient.

Cell size adjustment schemes such as cell-breathing and cell-zooming where different cells adapt their size depending on the received interference or traffic load conditions.

Deployment of relays (e.g. amplify-forward) improves the power reduction with reduced complexity at an increased cost for deployment of infrastructure.

D. Heterogeneous Networks for LTE-Advanced

LTE-Advanced (LTE-A) networks were developed to offer considerably high data rates than the existing 3rd Generation (3G) networks. In order to meet the requirements of LTE-A (e.g. peak data rates up to 1Gbps), more spectrum bands are needed. Besides the existing carriers for 3G networks, spectrum bands located at 450– 470 MHZ, 698–790 MHZ and 2.3–2.4 GHZ, and 3.4–3.6 GHZ can be used for the deployment of LTE and LTE-A networks. LTE-A has been designed to support scalable carrier bandwidth exceeding 20 MHZ, potentially up to 100 MHZ. The LTE-A consists of eNodeBs that are interconnected with each other by means of X2 interface. The eNodeBs are connected through the S1 interface to the core network [7].

Network coverage and high data rate requirements in hotspot and indoor environments have brought new challenges to LTE systems. In order to improve the system capacity and energy efficiency for hotspot and indoor environments, HetNets and their enhancements have been proposed. The architecture of a HetNet for an LTE-A system is shown in Fig. 2. Among the different technologies that have been proposed and studied in 3GPP HetNet, small cell (pico cell) enhancement is one of the major techniques.

The benefits of using pico cell enhancements include [7]

Flexible pico cell deployment according to users and traffic distributions.

Optimized pico cell mobility by reducing Radio Access Network (RAN) to core network signalling.
Increased data rates by using macro and pico cells together.

Energy saving by using dynamic pico cell sleeping.

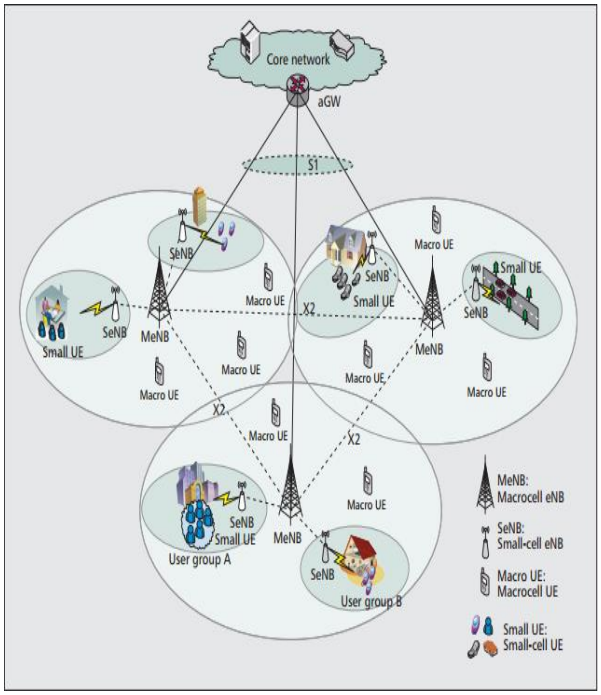

Fig. 2. Architecture of HetNet for LTE-Advanced Systems. [7]

E. 3GPP Heterogeneous Network Topologies

Two heterogeneous network topologies are supported in the LTE system level simulator toolbox developed by Wireless Systems Research Lab, Hitachi America Ltd. These topologies are in line with the standard 3GPP specifications that are widely used in industrial simulations. They are used for evaluating performance metrics such as coupling loss (link gain) and geometry (received SINR) distributions [8].

Reference [9] specified the heterogeneous network scenarios as follows

1) HetNet Configuration 1: 3GPP specified HetNet Configuration 1. Reference [8] implemented the configuration in the system level simulator Toolbox in MATLAB to illustrate the pictorial representation of the topology. In this configuration, small cells (Pico eNodeB cells) are overlaid in the macro area coverage with uniform density. The macro and small cells serve both indoor and outdoor users that are uniformly located in the macro coverage area as shown in Fig. 3.

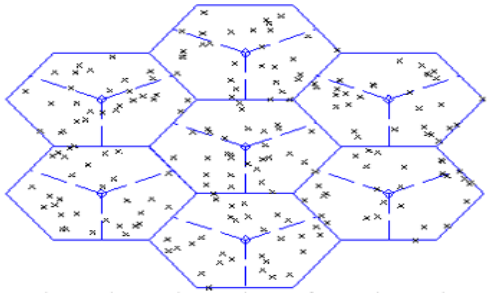

Fig. 3. Schematic Diagram of HetNet Configuration 1. [8]

2) HetNet Configuration 4b: 3GPP specified HetNet Configuration 4b. Reference [8] implemented the configuration in the system level simulator Toolbox in MATLAB. It comprises urban area with small cells overlaid in macro coverage area with uniform density. The macro and small cells serve both indoor and outdoor users, a fraction of whom are clustered around the Pico eNodeB cells modeling a hot-spot scenario as shown in Fig. 4.

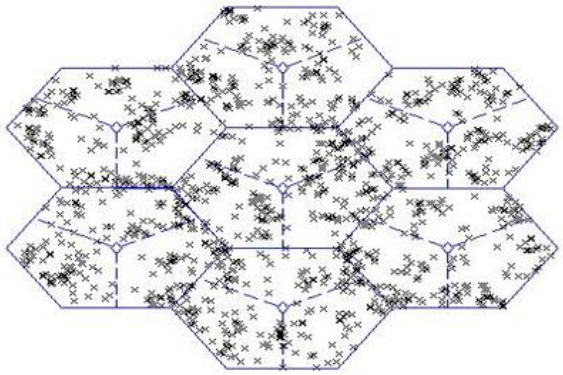

Fig. 4. Schematic Diagram of HetNet Configuration 4b. [8]

F. Base Station Sleep Mode Algorithms

Whenever a base station is working in sleep mode, the other energy consuming equipment such as air-conditioner have to be switched off. The energy consumption of cellular network can be largely reduced when the base station is sleeping. However, in such a case the cell with base station working in sleep mode will be zoomed in to zero and its neighbouring cell will zoom out to guarantee coverage [10].

The idea of sleep mode activation in pico base stations is the introduction of a low-power state in the hardware, referred to as the SLEEP state. Pico cells are in one of the following states at any given time [11]:

1) Ready State (RE): In this state, all hardware components in the pico base station are fully switched on. This can also be referred to as the ACTIVE state.

2) Sleep State (SL): In this state, some of the hardware components in the pico cells are either completely switched off or operated in low-power modes. The base station is correspondingly said to be in SLEEP mode. The exact components to be switched off are a function of the specific hardware architecture and the particular energy saving algorithm. During SLEEP mode, it is assumed that the power consumption is 0W.

METHODOLOGY

Three models were used to achieve the sleep mode in this research work; the traffic model, data rate model and power consumption model.

G. Traffic Model

Round robin resource allocation was used. The simulations were based on fair scheduling of resources. Thus, all the available resources are scheduled among all the users

and the users are utilizing all the allocated resources. In order to efficiently allocate equal number of resource blocks to users, the Number of Resource Blocks (NRB) was divided by the number of UE in the eNodeB cell. Thus, the number of resource blocks allocated to a user at distance, d, from an eNodeB cell per transmission time interval according to [12] is expressed in (1), as in:

$$NRB(d) = (NRB / TTI) / NumUEperCell \quad (1)$$

Where: *NRB(d)* is the number of resource blocks per eNodeB cell, *NumUEperCell* is the number of UE per eNodeB cell, and *TTI* is the transmission time interval (1ms).

H. Data Rate Model

The Data rate model was based on Signal-to-Interference and Noise Ratio (SINR) mapping for link adaptation to accurately estimate individual user data rate. Equation (2) gives the expression for the SINR which was adopted in this research work. For a UE placed at distance, d, from the eNodeB (eNB), the average Signal-to-Interference and Noise Ratio (SINR) at the UE is given by [13] as in:

$$SINR(d) = P_{TX} + G_{TX} + G_{RX} - N - I - SF(d) - PL(d) - PLN \quad (2)$$

Where: P_{TX} is the eNB transmission power (per cell sector) in dB; G_{TX} and G_{RX} are the eNB and UE antenna gains respectively. N and I are the noise and the inter-cell-interference (ICI) power from all the interfering eNBs at the UE location respectively. *PLN* is the wall penetration loss for signals received by indoor UE. Finally *PL(d)* and *SF(d)* are the path loss and shadow loss in dB respectively measured at different UE position [13].

Depending on the SINR(d) at the user equipment (UE) calculated using (2), and the intervals of CQI state, the data rate *R(i)* at the UE is expressed according to [13] by (3) as in:

$$R(i) = [TBS(i) \times NRB(i)] / TTI \times [1 - BLER(i)] \quad (3)$$

Where: *TBS(i)* is the physical transmission block information capacity in bits, and *BLER(i)* is the average Block Error Rate (BLER) for the CQI state i, *TTI* is the transmission time interval and *NRB(i)* is the number of resource blocks allocated to UE *i*.

Three modulation levels of Quadrature Phase Shift Keying (QPSK), 16-Quadrature Amplitude Modulation (16-QAM) and 64-QAM are supported according to the LTE specification in [14] with 26 Modulation and Coding Schemes (MCSs), this implies that there are 26 Channel Quality Indicator (CQI). The SINR to TBS mapping for these MCSs, assuming a Block Error Rate (BLER) target of 10% was established is expressed in (4):

$$SINReff(d) = max\{SINR(d), SINRthreshold\} \quad (4)$$

Where: *SINReff (d)* is the effective SINR of a UE for mapping to corresponding CQI and TBS. *SINR(d)* is the SINR as a result of the UE's instantaneous channel conditions. And *SINRthreshold* is the SINR value corresponding to the 26 MCSs level.

Using the SINR value allocated to the UE, the mapping of the SINR to TBS was obtained in the system level simulator in MATLAB. Substituting for *SINReff(d)* obtained from (4) is expressed in (5), as in:

$$TBS(d) = TBS\{ SINReff(d)\} \quad (5)$$

Where: *TBS(d)* is the *TBS* in bits allocated to UE based on *SINReff (d)*.

Therefore, to obtain the average user data rate (realistic data rate of a user) of a single UE, the overall data rate of the HetNet was divided by the total number of user equipment as in (6):

$$Average\ UE\ Data\ Rate = RtotalUE / NumUE \quad (6)$$

Where: *Average UE Data Rate* is the average user data rate, *RtotalUE* is the total data rate in a macro area coverage, and *NumUE* is the total number of UE.

I. Power Consumption Model

The power consumption equation for a base station of [15] was adopted and expressed as in (7):

$$P_{C(i)} = N_{SEC} \times N_{ANT} (A_i P_{TX} + B_i) \quad (7)$$

Where: N_{SEC} and N_{ANT} denote the number of sectors of the eNBs and the number of antennas per sector, respectively. $P_{C(i)}$ is the average total power per base station in Watts and P_{TX} is the power fed to the antenna. The coefficient A_i accounts for the part of the power consumption in Watts that is proportional to the transmitted power, which includes radio frequency amplifier power and feeder losses. While B_i denotes the power that is consumed in Watts independent of the average transmit power which includes signal processing and site cooling [16]. The values for A_i and B_i are given in Table 1.

TABLE I. POWER CONSUMPTION PARAMETERS [16]

Base Station	Power Coefficients	
	A_i (W)	B_i(W)
Macro	21.45	354.44
Pico	5.5	38.0

[a]

RESULTS AND DISCUSSIONS

In order to validate the model developed in this research, it was compared with the standard 3rd Generation Partnership Project (3GPP) Always-On Scheme. The results for the power consumption of the various nodes [pico eNodeBs (PeNB), macro eNodeBs (MeNB) and all the eNodeBs in the HetNet (AlleNB)] is presented below.

Low Traffic Power Consumption

It is observed from Fig. 5 that the Developed sleep mode algorithm performed better than the Always-on scheme, because 63 pico cells are in sleep mode, with only 21 active PeNB cells while 84 PeNB are active for always-on. This implies, there is only 1 active pico cell per macro cell coverage, and 3 sleeping pico cells per macro cell coverage. The Developed sleep mode algorithm was able to determine the required number of active pico cells by considering the

average user data rate. With this low traffic, the power consumption of the MeNB remained the same for both algorithms because the sleep mode was only implemented for the PeNB cells. There was a decrease in power consumption for the overall HetNet (AlleNB) as a result of the PeNB power consumption improvement during low traffic.

Fig. 5. Low Traffic Power Consumption in Configuration 1.

J. Medium Traffic Power Consumption

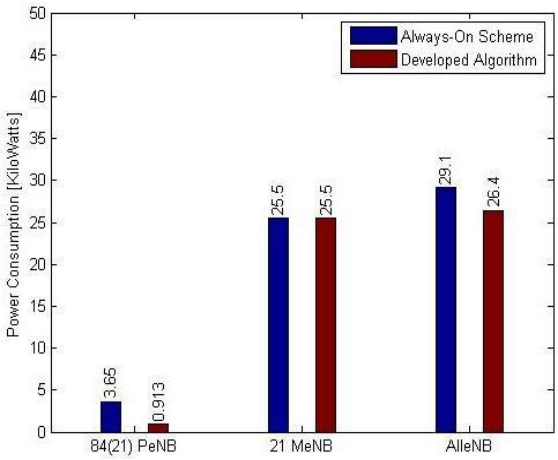

From Fig. 6, as the number of user equipment increased, it is observed that the power consumption for the developed sleep mode algorithm is lower than the always-on scheme because 42 PeNB (two pico cells per macro cell coverage) are active while the other 42 PeNB cells are in sleep mode to save energy. The MeNB power consumption is still constant with an improvement in the overall HetNet (AlleNB) power consumption.

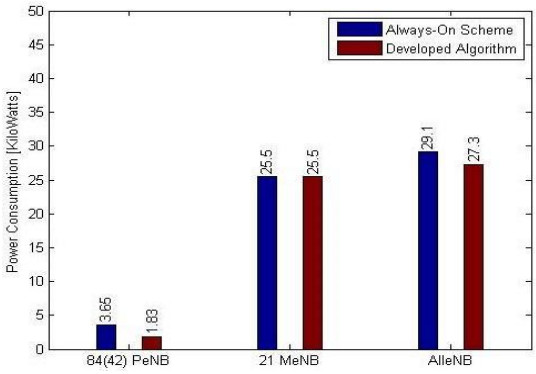

Fig. 6. Medium Traffic Power Consumption in Configuration 1.

K. Configuration 1 HetNet Power Consumption

In HetNet Configuration 1, the Developed algorithm achieved a reduction in power consumption for low (5UE per cell) and medium traffic (12 UE per cell) in the pico eNodeB cells of about 75% and 50% respectively. On the other hand, 9.28% and 6.19% reduction were achieved for the overall HetNet for low and medium traffic respectively.

In terms of power consumption reduction, the Developed sleep mode algorithm performed better up to about 20UE per cell than the Always-on scheme as shown in Fig. 7. The power consumption increases with increase in the number of users and becomes maximum at high traffic.

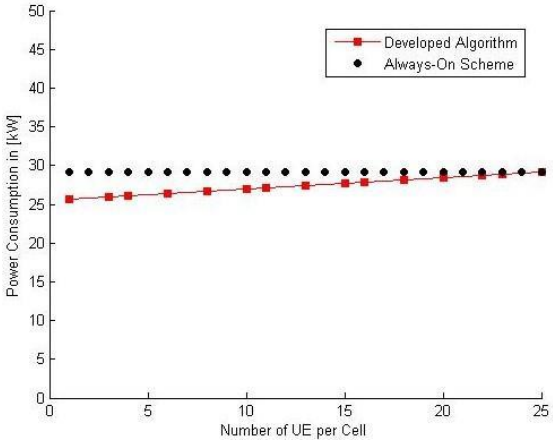

Fig. 7. Power Consumption in HetNet Configuration 1.

L. Configuration 4b HetNet Power Consumption

Similarly, in HetNet Configuration 4b, the Developed algorithm achieved a power consumption improvement for low (5 UE per cell) and medium traffic (20 UE per cell) of about 75% and 50% respectively in the pico eNodeB cells as shown in Fig. 8. About 9.28% and 6.19% was achieved with the developed algorithm for the overall HetNet al low and medium traffic respectively. The Developed sleep mode algorithm performed better than the Always-on Scheme up to about 50UE per cell.

Fig. 8. Power Consumption in HetNet Configuration 4b.

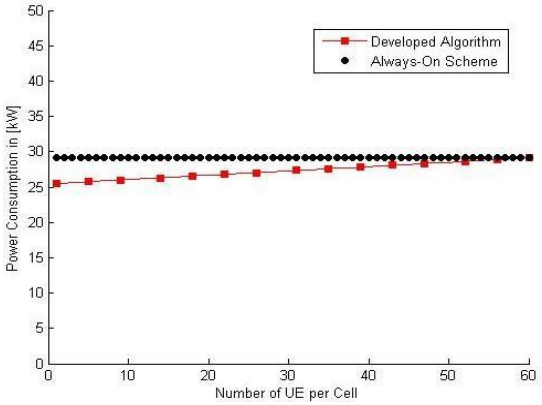

CONCLUSION

A data rate-based sleep mode algorithm for energy savings for a pico eNodeB in LTE-Advanced HetNet has been proposed and implemented. The algorithm is a function of traffic situations, data rate and power consumption in the system. Simulations were carried out to evaluate the system level performance of the developed data rate-based sleep mode algorithm. The algorithm performed better in terms of energy savings when compared with the 3GPP Always-on scheme. However, the Developed algorithm did not consider

the effect of interference. Interference management could further improve the service delivery and energy savings.

REFERENCES

[1] Z. Hassan, H. Boostanimehr, and V. K. Bhargava, "Green cellular network: A survey, some research issues and challenges," IEEE Communications Surveys & Tutorials, vol. 13, pp. 1–16, 2011.

[2] K. C. Tun, and K. Kunavut, "An overview of cell zooming algorithms and power saving capabilities in wireless networks," KMUTNB: International Journal of Applied Science and Technology. Vol. 7, No.3, pp. 1–13, 2014.

[3] Motrolla White Paper, Realistic LTE performance: from peak rate to subscriber experience, White Paper. www.motorola.com, 2009.

[4] LTE Alcatel White Paper. The LTE network architecture, Strategic White Paper, www.alcatel-lucent.com, 2009.

[5] M. Deruyck et al., "Reducing the power consumption in wireless access networks: overview and recommendations," Progress in Electromagnetics Research, pp. 2230–2235, 2012.

[6] A. R. Ekti, M. Z. Shakir, E. Serpedin, and K. A. Qaraqe, "Downlink power consumption of hetnets based on the probabilistic traffic model of mobile users," IEEE 24th Annual International Symposium on Personal Indoor and Mobile Radion Communications (PIMRC), pp. 2812–2817, 2013.

[7] X. Zhang, Y. Zhang, R. Yu, W. Wang, and M. Guizani, "Enhancing spectral efficiency for LTE-Advanced heterogeneous networks: a users' social pattern perspective," IEEE Wireless Communications, vol. 48, pp. 10–17, 2014.

[8] J. Acharya, L. Gao, and S. Gaur, Heterogeneous Network in LTE-Advanced, 2014.

[9] Technical Report 36.814 v9.0.0, Technical Specification Group Radio Access Network, Further Advancements for E-UTRA Physical Layer Aspects, 3GPP Release 9, March 2010.

[10] P. S. Gundawar, P. D. Dorge, and C. S. Gode, "Optimization of base station power using cell zooming technique, " International Journal of Advent Research in Computer and Electronics (IJARCE), vol. 2, no. 1, pp. 16–21, 2015.

[11] I. Ashraff, F. Boccardi, and L., Ho, "Sleep mode techniques for small cell deployments, " IEEE Commun. Mag., vol. 49, no.8, pp. 72–79, 2011.

[12] A. Ambrosy et al., "Definition and parameterization of reference systems and scenarios," EARTH Project Report, Deliverable D2.2 pp. 1-87, 2012.

[13] C. Khirallah, D. Rastovac, D. Vukobratovic, and J. Thompson, "Energy Efficient Multimedia Delivery Services over LTE/LTE-A," IEICE Transactions on Communications, 97(8): pp. 1504–1513, 2014.

[14] Technical Report 36.931, 3GPP Evolved Universal Terrestrial Radio Access (E-UTRA); Radio Frequency (RF) requirements for LTE Pico NodeB, 2011.

[15] F. Richter, A. Fehske, and G. Fettweis, "Energy efficiency aspects of base station deployment strategies for cellular networks," In Proc. of IEEE Vehic. Technol. Conf. (VTC Fall), Anchorage, USA. pp. 1–5, 2009.

A. Abdulkafi et al., "Modeling of energy efficiency in heterogeneous network," Research Journal of Applied Sciences, Engineering and Technology 6(17), pp. 3193–3201, 2013

Development of an Improved Altitude Estimation Technique for a Minimum Configuration Multilateration System

Abdulmalik Shehu Yaro, Muhammad Surajo and Isiyaku Yau
Department of Communications Engineering, Ahmadu Bello University, Zaria
yaroabdulmalik@yahoo.com,smdgw2002@gmail.com,ishaaqyau@gmail.com

ABSTRACT— Multilateration (MLAT) system is known to have high altitude estimation error limiting its application in 3-dimensional (3-D) aircraft surveillance. This paper proposed a technique based on vector polynomial addition of the second-order time difference of arrival (TDOA) quadratic equations aimed at reducing thealtitude estimation error of a 3-D minimum configuration MLAT system. The proposed technique is validated at some randomly selected aircraft positions at different flight level (FL)s by comparing with the conventional technique. Monte Carlo simulation result shows a reduction in the altitude root mean square error (RMSE) by at least 50% using the proposed technique based on a square ground sensor (GS) configuration. Furthermore, the proposed technique enables for the implementation of the minimum configuration MLAT system in a 3-D scenario having an altitude RMSE in compliance with the reduced vertical separation minimum (RVSM) initiative.

KEYWORDS—multilateration, TDOA, altitude estimation, polynomial addition, RVSM

INTRODUCTION

Multilateration (MLAT) system is a type of wireless positioning system used by the air navigation service provider (ANSP) for surveillance purposes [1]. The aircraft position estimation (PE) process of the system is in two stages [2, 3]: (1) time difference of arrival (TDOA) estimation and; (2) localization with a lateration algorithm. The TDOAs are estimated from the aircraft transponder emission detected at spatially located ground sensor (GS) pairs [1, 4, 5]. The TDOA estimates are used with the lateration algorithm to estimate the aircraft position which is displayed on the screen at the air traffic control (ATC) center [1].

Aircraft altitude estimation above 29,000 ft. is critical as the Vertical Separation Minima (VSM) between two consecutive flight level (FL)s is reduced from 2,000 ft. to 1,000 ft. [6]. This is one of the initiatives by the International Civil Aviation Organization (ICAO) to increase airspace capacity to meet up with current and future global air traffic demands [7]. MLAT systems are known to have high aircraft altitude estimation error [8, 9]. With a 300 ft. maximum allowed system altitude report error for all FLs set by the International Civil Aviation Organization (ICAO) in accordance with the Reduced VSM (RVSM) initiative [6], it is difficult to implement the system for 3-D surveillance purposes. Several techniques have been proposed to able the implementation of MLAT system in 3-D scenario [8, 10, 11]. It was suggested in [8] that altitude information of an aircraft should be obtained from other sources such as Mode C of secondary surveillance radar (SSR) interrogator reply and then incorporated in the MLAT system PE process. The Mode C altitude information has been shown to be an actual measure of pressure and is not always accurate as it varies with time and place [12]. In [13, 14], a 3-D minimum configuration MLAT system closed-form lateration algorithm is developed. The MLAT system consist of four spatially located GSs each connected to a central processing station (CPS) [1]. This paper presents a technique to improve the altitude estimation accuracy of the lateration algorithm. Monte Carlo (MC) simulation is used to determine the improvement in the altitude estimation process at some randomly selected aircraft positions.

The rest of the paper is organized as follows. Section II presents the mathematical derivation of the MLAT system PE methodology and the conventional technique for altitude estimation. The proposed altitude estimation technique is presented in section IIIwhich is followed by simulation result and discussion in section IV Finally, the conclusion is presented in section V.

MLAT System Position Estimation Methodology

This section first gives a summary of the closed-form approach to the development of the 3-D minimum configuration reference pair lateration algorithm as presented in [14]. This is followed by the conventional technique to the estimation of altitude based on the minimum configuration closed-form lateration algorithm.

Closed-Form Reference Pair Lateration Algorithm Development

Let $\mathbf{x}_e = (x, y, z)$ be the coordinate of an aircraft in the 3-D Euclidean space while $\mathbf{s}_i = (x_i, y_i, z_i)$, $\mathbf{s}_j = (x_j, y_j, z_j)$, $\mathbf{s}_k = (x_k, y_k, z_k)$ and $\mathbf{s}_l = (x_l, y_l, z_l)$ respectively be the coordinate of the *i*-th, *j*-th, *k*-th and *l*-th ground sensors. Using the *i*-th and *j*-th GS are reference for TDOA estimation, four TDOA hyperbolic equations are obtained as follows [14]:

$$\tau_{ik} = \frac{1}{c}\left(\|\mathbf{x}-\mathbf{s}_i\| - \|\mathbf{x}-\mathbf{s}_k\|\right) \quad (1)$$

$$\tau_{il} = \frac{1}{c}\left(\|\mathbf{x}-\mathbf{s}_i\| - \|\mathbf{x}-\mathbf{s}_l\|\right) \quad (2)$$

$$\tau_{jk} = \frac{1}{c}\left(\|\mathbf{x}-\mathbf{s}_j\| - \|\mathbf{x}-\mathbf{s}_k\|\right) \quad (3)$$

$$\tau_{jl} = \frac{1}{c}\left(\|\mathbf{x}-\mathbf{s}_j\| - \|\mathbf{x}-\mathbf{s}_l\|\right) \quad (4)$$

Where: c = 3×10^8 m/s, $\hat{\tau}_{ik}$ and $\hat{\tau}_{il}$ are respectively the TDOA measurements obtained using the *i*-th reference GS with the *k*-th and *l*-th non-reference GS while $\hat{\tau}_{jk}$and$\hat{\tau}_{jl}$ are respectively the TDOA measurements obtained using the *j*-th reference GS

with the *k*-th and *l*-th non-reference GS. The symbol ‖ ‖ denotes the 2-norm operator.

In practical application, the TDOA measurements in (1) to (4) are obtained with error. By modelling the TDOA error as zero mean Gaussian random variable with a normal probability density function [15], the estimated TDOAs in (1) to (4) respectively are:

$$\hat{\tau}_{ik} = \tau_{ik} + N(0,\sigma) \quad (5)$$

$$\hat{\tau}_{il} = \tau_{il} + N(0,\sigma) \quad (6)$$

$$\hat{\tau}_{jk} = \tau_{jk} + N(0,\sigma) \quad (7)$$

$$\hat{\tau}_{jl} = \tau_{jl} + N(0,\sigma) \quad (8)$$

Where:σ is the TDOA error standard deviation (SD) with typical values ranges from 0 nsec to 20 nsec [1, 16]. The TDOA error is assumed to include error due to noise in the signal, GS clock synchronization error, and quantization error.

Algebraically manipulatingEq. (1) to Eq. (4) as previously done in [13, 14] results in a pair of 3-D plane equation in the form [14]:

$$A_{i,k,l} = xB_{i,k,l} + yC_{i,k,l} + zD_{i,k,l} \quad (9)$$

$$A_{j,k,l} = xB_{j,k,l} + yC_{j,k,l} + zD_{j,k,l} \quad (10)$$

Where: the coefficients of Eq. (9) and Eq. (10) are functions of the TDOA measurements and GS coordinate which can be found in [14]. The detailed derivation of Eq. (9) and Eq. (10) from Eq. (1) to Eq. (4) is not within the scope of this work but can be found in [13, 14].

Conventional Technique to Altitude Estimation

The conventional technique to obtain the altitude of the aircraft using Eq. (9) and Eq. (10) as previously done in [13, 14] involves first expressing the horizontal coordinates of the aircraft (x, y) as a function of its altitude (z) as shown in Eq. (11) and Eq. (12).

$$x = K - zI \quad (11)$$

$$y = I - zJ \quad (12)$$

This is followed by substituting Eq. (11) and Eq. (12) into Eq.(1) to obtain a second-order quadratic equation as follows [13]:

$$Q_{ik} z^2 + 2P_{ik} z + Q_{ik} = 0 \quad (13)$$

Where: the coefficients of Eq. (11) to Eq. (13) can be found in [13].

Lastly, the solution to z in (13) is obtained as:

$$z = \frac{-P_{ik}}{2O_{ik}} \pm \frac{\sqrt{P_{ik}^2 - 4O_{ik}P_{ik}}}{2O_{ik}} \quad (14)$$

Since the altitude of the aircraft cannot be a negative value, the estimated altitude is:

$$\hat{z} = \frac{-P_{ik}}{2O_{ik}} + \frac{\sqrt{P_{ik}^2 - 4O_{ik}P_{ik}}}{2O_{ik}} \quad (15)$$

Eq. (15) is the conventional technique to estimating the altitude of the aircraft for the minimum configuration MLAT system lateration algorithm.

PROPOSED ALTITUDE ESTIMATION TECHNIQUE DEVELOPMENT

In this section, the technique to improve the altitude estimation of the minimum configuration multilateration system is presented. The use of a single TDOA measurement to solve for the aircraft altitude is not optimum. An improvement in the altitude estimation can be achieved by using all the four TDOA measurements that is using Eq. (2) to Eq. (4) in addition to Eq. (1). The remainder of the second-order quadratic equations obtained using the TDOA measurements in Eq. (2) to Eq. (4) respectively are:

$$Q_{il} z^2 + 2P_{il} z + Q_{il} = 0 \quad (16)$$

$$Q_{jk} z^2 + 2P_{jk} z + Q_{jk} = 0 \quad (17)$$

$$Q_{jl} z^2 + 2P_{jl} z + Q_{jl} = 0 \quad (18)$$

Vector polynomial addition of Eq. (13), Eq. (16) to Eq. (18) results in another second-order quadratic equation expressed as follows:

$$O_{ijkl}\, z^2 + 2P_{ijkl}\, z + Q_{ijkl} = 0 \quad (19)$$

Where: the coefficients of (19) are:

$$O_{ijkl} = O_{ik} + O_{il} + O_{jk} + O_{jl} \quad (20a)$$

$$P_{ijkl} = P_{ik} + P_{il} + P_{jk} + P_{jl} \quad (20b)$$

$$Q_{ijkl} = Q_{ik} + Q_{il} + Q_{jk} + Q_{jl} \quad (20c)$$

Thus, the estimated altitude of the aircraft by solving for z using Eq. (19) is:

$$\hat{z} = \frac{-P_{ijkl}}{2O_{ijkl}} + \frac{\sqrt{P_{ijkl}^2 - 4O_{ijkl}P_{ijkl}}}{2O_{ijkl}} \quad (21)$$

Eq. (21) is the proposed altitude estimation technique and will result in less altitude error due to the averaging effect as shown in Eq. (15).

SIMULATION RESULT AND DISCUSSION

In this section of the paper, the improvement in the altitude estimation using the proposed technique based on Eq. (21) is determined by comparing with the conventional technique based on Eq. (15) as previously done in [13, 14] is presented. The altitude root mean square error (RMSE) is used as the performance measure for comparison and is mathematically expressed as follows:

$$Alt_{rmse} = \sqrt{\frac{1}{500}\sum_{n=1}^{500}\left(\hat{z}_n - z\right)^2} \qquad (22)$$

Where: z is the known altitude of the aircraft and $\hat{z}_n$ is the estimated altitude at the n-th MC simulation realization.

For the analysis, aircraft at six randomly selected positions are considered each at a different FLs as shown in Table 1.

TABLE I: POSITION OF AIRCRAFT FOR ALTITUDE ESTIMATION IMPROVEMENT

Aircraft location	**Coordinates**		
	x ***(km)***	***y*** ***(km)***	***z*** ***(ft.)***
A	50	80	29,000
B			31,000
C	80	50	33,000
D			35,000
E	100	30	37,000
F			39,000

By varying the TDOA error SD from 0 nsec to 5 nsec, the relationship between the TDOA error SD and the altitude RMSE at each of the selected aircraft positions with coordinate defined in Table I is determined for both the conventional and proposed technique. Fig. 1 shows the relation between the TDOA error SD and altitude RMSE at the selected aircraft positions defined in Table I. Irrespective of the aircraft position, the altitude RMSE increases with the TDOA error SD from 0 nsec to 5 nsec. At a fixed TDOA error SD, the altitude RMSE varies with aircraft position. Comparison between the two techniques at each of the selected aircraft positions shows an improvement in the altitude estimation accuracy by the proposed technique through the reduction in the altitude RMSE. Table II shows the altitude RMSE comparison between the conventional and proposed technique at different aircraft positions using a receiver with TDOA error SD of 1 nsec [16]. At aircraft position A, the altitude RMSE obtained using the conventional and proposed techniques are 196 ft. and 82 ft. respectively. The absolute difference in the altitude RMSE is about 114 ft. which is about 58% of the error obtained using the conventional technique. This means that, the proposed technique reduced the altitude RMSE of the aircraft at position A by about 58% compared to the conventional technique.

TABLE II. ALTITUDE RMSE COMPARISON AT TDOA ERROR SD OF 1 NSEC

Aircraft location	**Altitude RMSE (ft.)**		**Altitude RMSE Reduction (ft.)**
	Conventional technique	***Proposed technique***	
A	196	82	114
B	181	79	102
C	219	75	144
D	199	71	128
E	996	264	732
F	893	250	643

Extending the analysis to the remaining aircraft positions, the absolute altitude RMSE differences at aircraft positions B, C, D, E, and F are 102 ft., 144 ft., 128 ft., 732 ft, and 643 ft. respectively. The percentage reduction in the altitude RMSE obtained using the proposed technique compared to the conventional technique at these aircraft positions are ~56%, ~65%, ~64%, ~73% and ~72% respectively. On the average, based on the selected aircraft position, there is about 60% reduction in the altitude RMSE using the proposed technique based on Eq. (21) compared to using the conventional technique based on Eq. (15).

As earlier mentioned, the maximum allowed altitude RMSE for compliance with the ICAO RVSM at all FLs in 300 ft. At aircraft positions E and F, the altitude RMSE values using the conventional technique respectively are 996 ft. and 893 ft. which are 696 ft. and 593 ft. above the approved ICAO

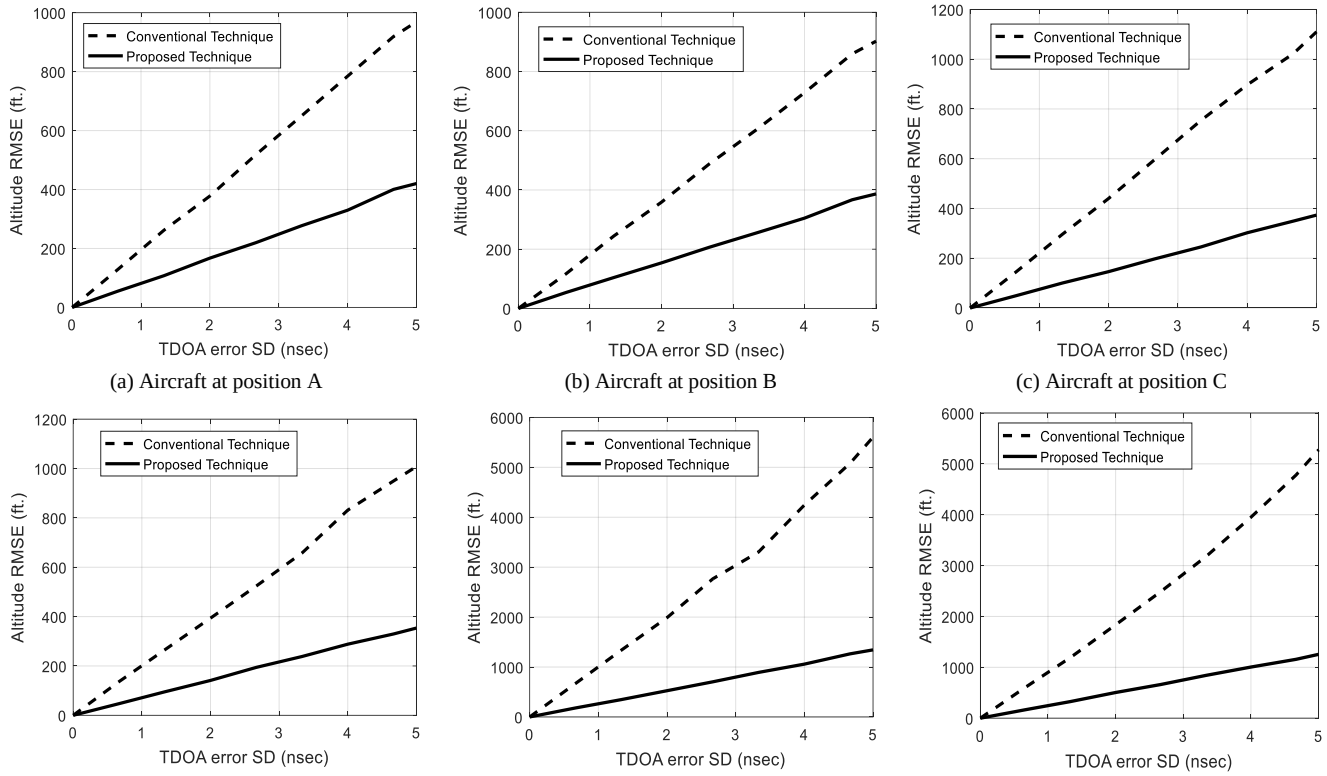

(a) Aircraft at position A (b) Aircraft at position B (c) Aircraft at position C

(d) Aircraft at position D (e) Aircraft at position E (f) Aircraft at position F

Fig. 1. Altitude RMSE versus TDOA error SD comparison at some selected aircraft positions.

RVSM standard thus, not acceptable. Using the proposed technique, the altitude RMSE at these selected aircraft positions are 264 ft. and 250 ft., which are below the 300 ft. maximum, approve standard. This means that the proposed technique reduced the altitude RMSE at these selected aircraft positions to be within approved standard set for the ICAO RVSM initiative making it possible for implementation in 3-D aircraft position estimation scenarios.

CONCLUSION

In this paper, a technique to improve the altitude estimation accuracy of a 3-D minimum configuration MLAT system is suggested. The proposed technique is validated by comparing it with the conventional technique at some selected aircraft position using MC simulation. Simulation result shows the proposed technique improved the altitude estimation accuracy through a reduction in the altitude RMSE by at least 50% compared to the conventional technique. Compliance verification with the ICAO RSVM standard for 3-D implementation shows that the altitude RMSE obtained using the proposed technique is less than the 300 ft. maximum error. With the use of the proposed technique, MLAT system can be implemented in a 3-D scenario and the altitude RMSE obtained will be within the proved set standard.

REFERENCE

[1] W. H. L. Neven, T. J. Quilter, R. Weedo, and R. A. Hogendoorn, "Wide Area Multilateration (WAM)," Eurocontrol, Report on EATMP TRS 131/04 Version 1.1, 2005.

[2] I. A. Mantilla-Gaviria, M. Leonardi, G. Galati, and J. V. Balbastre-Tejedor, "Localization Algorithms for Multilateration (MLAT) Systems in Airport Surface Surveillance," Signal, Image and Video Processing, vol. 9, no. 7, pp. 1549–1558, 2015.

[3] H. C. So, "Source Localization: Algorithms and Analysis," in Handbook of Position Location: Theory, Practice, and Advances, 1st ed., B. R. Michael, Ed. John Wiley & Sons, Inc., 2012, pp. 25–66.

[4] H. Shi, H. Zhang, and X. Wang, "A TDOA Technique with Super-resolution based on the Volume Cross-correlation Function," IEEE Transactions on Signal Processing, vol. 64, no. 21, pp. 5682–5695, 2016.

[5] R. Kaune, C. Steffes, S. Rau, W. Konle, and J. Pagel, "Wide area multilateration using ADS-B transponder signals," in Proc. of FUSION'12 - 15th IEEE International Conference on Information Fusion, 2012, pp. 727–734.

[6] FAA, "Advisory Circular AC91-4: Reduced Vertical Separation Minimum (RVSM)," 2014.

[7] ICAO, "Doc 9574: Manual on Implementation of a 300 m (1000 ft.) Vertical Separation Minimum Between FL 290 and FL 410 Inclusive," Montréal, Quebec, Canada, 2001.

[8] M. A. Garcia, R. Mueller, E. Innis, and B. Veytsman, "An Enhanced Altitude Correction Technique for Improvement of WAM Position Accuracy," in

Integrated Communications, Navigation and Surveillance Conference (ICNS), 2012, pp. 4–9.

[9] T. M. R. Costa, "Analysis of Aircraft Accuracy Location in Aeronautcal Multilateration Systems," Electrical and Computer Engineering, Instituto Superior Técnico, University of Lisbon, 2017.

[10] K. C. Ho and Y. T. Chan, "Geolocation of a Known Altitude Object from TDOA and FDOA Measurements," IEEE Transactions on Aerospace and Electronic Systems, vol. 33, no. 3, pp. 770–783, 1997.

[11] Y. Cao, L. Peng, J. Li, L. Yang, and F. Guo, "A New Iterative Algorithm For Geolocating a Known Altitude Target using TDOA and FDOA Measurements in the Presence of Satellite Location Uncertainty," Chinese Journal of Aeronautics, vol. 28, no. 5, pp. 1510–1518, Oct. 2015.

[12] P. Cabalkova and R. Plsek, "Comparison of Target Detections from Active MSPSR Aystem with Outputs of MLAT System," in 2016 17th International Radar Symposium (IRS), 2016, pp. 1–6.

[13] R. Bucher and D. Misra, "A Synthesizable VHDL Model of the Exact Solution for Three-dimensional Hyperbolic Positioning System," VLSI Design, vol. 15, no. 2, pp. 507–520, 2002.

[14] A. S. Yaro, A. Z. Sha'ameri, and N. Kamel, "Ground Receiving Station Reference Pair Selection Technique for a Minimum Configuration 3D Emitter Position Estimation Multilateration System," Advances in Electrical and Electronic Engineering, vol. 15, no. 3, pp. 391–399, Oct. 2017.

[15] G. Galati, M. Leonardi, J. V. Balbastre-Tejedor, and I. I. A. Mantilla-Gaviria, "Time-difference-of-arrival Regularised Location Estimator for Multilateration Systems," IET Radar, Sonar & Navigation, vol. 8, no. 5, pp. 479–489, 2014.

[16] INDRA, "Wide Area Multilateration System," 2017. [Online]. Available: https://www.indracompany.com/.../indra-indra_wide_area_multilateration_system.pdf. [Accessed: 01-Apr-2018]

Development of an affordable Smart Home Energy Management System Opereting via SMS using Arduinouno

Aminu, Abubakar Sambo
Communication Engineering Department
Ahmadu Bello University
Zaria, Nigeria
asaik56@yahoo.co.uk

Engr. I.K. Musa
Communication Engineering Department
Ahmadu Bello University
Zaria, Nigeria
ismkmusa1@gmail.com

Tanko, Aquila
Communication Engineering Department
Ahmadu Bello University, Zaria, Nigeria
tankoaquila@gmail.com

ABSTRACT*: Energy can neither be created nor destroyed but can be mismanaged which can lead to financial and safety consequences. This work propose a device, using arduino microcontroller, a relay, a GSM module, to develop a remote control in switching on and off of home appliances such as bulbs, air conditions, heaters other energy consuming appliances. In this paper we are using ATmega8 embedded microcontroller with a dedicated port for future reprogramming in implementing this technique in homes. These appliances like fridge, bulb, fan, television, air conditions, heaters etc. are connected to the microcontroller through the relay. We can switch ON and OFF the appliances by using switches whenever we need. The power consumed by the appliances is measured, the consumption of power by the appliances is measured by the sensing unit. The power used is calculated with the help of current transformer. The reading of the consumed energy will be displayed on an LED display. The GSM module will send and receive command using text massaging. The main significance of this project is to remotely control (ON and OFF) home appliances via text massaging. The device is developed using cost effective and affordable materials.

***KEYWORDS: AtMega8 microcontroller, relay, voltage and current sensors, GSM module*.**

INTRODUCTION

An energy management system (EMS) is any computer-aided tool or tools used mostly by electric utility grid operators to monitor, optimize, and control the performance of a generating and/or transmitting system. it is also used in micro grids**.**

As wireless communication is gaining ground day by day. It made it easy for us to use mobile phones to remotely control household appliances and to receive alert via SMS about the energy consumption in the house. In this paper we describe a remote appliance control system which can control different household appliances by sending an SMS from a mobile phone and monitor the energy consumption in the house just by a SMS remotely. This controller is extremely handy when we are away at places where we cannot monitor or control the energy consumption in the house manually, we can use this device to monitor and control the ON and OFF switching of the appliances as no wired connection is required between the switch and the home appliances as it can be controlled from any place in this world with a GSM service. The microcontroller would then control the home appliances based on the information given to it and send a feedback. The proposed solution is easy to use, it is simple, secure, and robust.

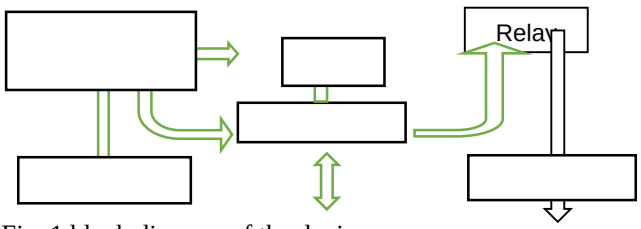

Fig. 1 block diagram of the device.

This system consist of two parts, the hardware which consist of embedded system that is based on 8-bit microcontroller (ATMega8), a GSM handset with GSM Modem (SIM900), relay module, voltage and current sensors. The software part consists of programming an arduinouno microcontroller. The GSM modem provides the medium of communication between the home owner and the system via short message service (SMS).

METHODOLOGY

This device is developed to help households in monitoring and controlling remotely high consuming home appliances. The microcontroller (AtMega8), the relay and display are powered by a power source. The arduino which is the microcontroller is connected to the display and the GSM modem where one is an output device and the other serve as both input and output device. The microcontroller is also connected to the relay which serve as an electric switch, the relay is connected to the loads to be managed. The sensors both voltage and current are input devices attached to the AtMega8 to provide voltage and current consumption of the home appliances. The microcontroller is programmed to calculate the power consumed by this appliances with the GSM module serving as clock. At a certain set amount of power consumed, the microcontroller command the module to send an SMS alert to the programmed number of the owner's GSM handset. The owner then can send an SMS command (if he wishes so) to be executed, this SMS is sent to the GSM modem via the GSM public networks as a text message with a definite predefined format, the commands sent will be executed by the microcontroller. The system will interpret the commands and turn the appropriate appliance/s ON/OFF accordingly via the relay which serve as the switching module.

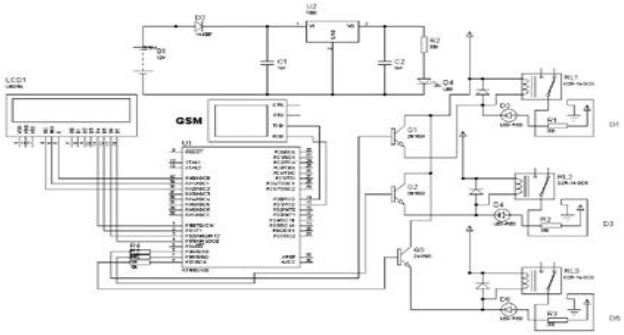

ACKNOWLEDGMENT

All praise and veneration to Allah the beneficent the merciful God that bestowed His abundant blessing of knowledge to humans, peace and blessings be upon his last messenger Muhammad bin Abdullahi the prophet of mercy and compassion.

To my supervisor, colleagues, lecturers, family, friends and all well-wishers that either directly or indirectly render assistance in the formulation of this work. I say thank you all.

REFERENCES

[1] Mahmud, Khizir; Town, Graham E. (June 2016). "A review of computer tools for modeling electric vehicle energy requirements and their impact on power distribution networks". Applied Energy. 172: 337–359. doi:10.1016/j.apenergy.2016.03.100.

[2] Curry, Edward. 2012. "System of Systems Information Interoperability Using a Linked Dataspace." In IEEE 7th International Conference on System of Systems Engineering (SOSE 2012), 101–106.

[3] International Journal of Advanced Research in Computer and Communication Engineering Vol. 4, Issue 1, January 2015.

[4] Alkar, A. Z., &Buhur, U. (2005). An Internet Based Wireless Home Automation System for Multifunctional Device IEEE Consumer electronics,51(4),1169-1174. Retrieved fromhttp://www.thaieei.com/embedded/pdf/Automation /2002 2.pdf

[5] Uhuegbu, C.C. , and Ayara W.A. , "Delay Timer (Relay driver) for home electrical appliances", Archives of Physics Research, 2011, ISSN : 0976-0970

[6] ZulkifliOthman,RohaidaHusin,Mohd Faisal Saari ,"Automatic Street Lighting System for Energy Efficiency Based on Low Cost microcontroller", ISSN: 1473-804, January 2005

[7] Hari CharanTadimeti, ManasPulipati, "Overview of Automation Systems and Home Appliances Control using PC and Microcontroller", Volume 2 Issue 4, April 2013

[8] SajidullahS.Khan, AnujaKhoduskar, Dr. N.A,Koli,"Home automation system", IJAET/Vol.II/April-June,2011/129-132

[9] Stevens,Tim, "The smart office", ISBN 0965708101(1994)

[10] Subashri P, et al. (2016), "An Advanced Energy Management System Facilitated by GSM with Automated Power Scheduling", GRD Journals, Volume 1 Issue 7, June 2016 ISSN: 2455-5703

[11] Atul V. Kamble, Sandeep S. Bidwai, Varsha B. Chougule, "AUTOMATION AND POWER SAVING OF HOME USING ANDROID MOBILE", IJRET, eISSN: 2319-1163 | pISSN: 2321-7308.

[12] S.Nagalakshmi's et al, (2017), "Design and Implementation of Aurdino Based Smart Home Energy Management System Using Renewable Energy Resources", ISSN: 0974-4290, Vol 10 No.6, pp 696-701.

[13] Huurdeman, A. A., (2003).The Worldwide History of Telecommunications. John Wiley & Sons: pages 529.

[14] Shibu, K. V., (2009). Intro to Embedded Systems 1E. Tata McGraw-Hill Education: pages 709.

[15] K.N Ramli et al, (2014) "Development of Home Energy Management System Using Arduino" ISBN: 978-0-9891305-4-7

[16] C S Kudarihal and P M Menghal (2010) "Smart and Intelligent Energy Management System Using GSM Technology" IDAEPSC.

[17] SnehaChaudhari, PurvangRathod, Ashfaque Shaikh (2017) "Smart Energy Meter Using Arduino" Malaysia, 86400 Parit Raja, BatuPahat, Johor. ISBN: 978-0-9891305-4-7

[18]http://www.edgefxkits.com/media/wysiwyg/Integrated_Energy_Management_System_based_on_GSM_with_User_Programmable_Number_Featuresand_acknowledgement_features_Block_Diagran.JPG

[19]]https://www.bing.com/images/search?view=detailV2&ccid=1oOETyg%2b&id=CCBEADBCD60B8185CD81281E8244633D7F6C29D4&thid=OIP.1oOETyg-f1l8TV--#54HowHaED&mediaurl=https%3a%2f%2fcircuitdigest.com%2fsites%2fdefault%2ffiles%2fcircuitdiagram_mic%2fIR-Remote-Controlled-Home-Automation-circuit-diagram.gif&exph=622&expw=1138&q=printed+circuitboard+diagram+of+energy+management+system+with+programmable+numbers+using+gsm&simid=607986291545146957&selectedIndex=0&ajaxhist=0

Wireless Power Transfer and Charging System: System Overview and Development Trends

Francis E. Chinda, Aliyu N. Shuaibu, Danjuma D. Dajab
Department of Electrical and Electronics Engineering, University of Jos, Plateau State, Nigeria

ABSTRACT—Strong coupled magnetic resonance wireless power transfer is proposed by researchers at Qi in 2007, and attracted the world's attention by virtue of its mid-range, non- radioactive and high-efficiency power transfer. In this article, current developments and research progress in the technology of WPT are presented. Advantage of WPT are analysed by comparing it with other wireless power transfer (WPT) technologies and different analytic principles of WPT are elaborated in depth and further compared. The hot research spots, including system architectural analysis, frequency splitting phenomena, impedance matching and optimization designs are classified and elaborated. Finally, current research directions and development trends of WPT are discussed and the simulation results are presented.

KEYWORDS—WPT, Frequency, Impedance and Optimization

INTRODUCTION

Due to globalization, power transfer efficiency is an important objective in designing wireless power transfer (WPT) system [1]. Wireless Power Transfer (WPT) [2] or wireless power transmission is the process of transmission of electrical power source to the consuming device without the use of solid wires or conductors, this is a generic term that refers to the number of different form of power transmission technologies that use time varying electromagnetic fields [3]. Wireless transmission is very useful to power electrical devices in cases where interconnecting wires are inconvenient, hazardous or completely not possible. In wireless power transfer process, a transmitter device is connected to a power source such as mains power line, transmits power using electromagnetic field across all the intervening space to one or more receiver devices, where it will be converted back to electrical power for utilization. These will be similar to how Wi-Fi and Bluetooth become globally very standardized by implementing this work, users can forget about the use of different chargers anymore for a different portable electrical devices in the feature and be able to use wireless means to aid their charging efficiently.

The theory and the idea of wireless power transfer and charging system started long time ago by Nicola Tesla who began demonstrating wireless broadcasting and power transmission in early 1900s. He could able to power lights in the ground at his Colorado Springs experiment station remotely [4]. Michael Faraday formulated the law of electromagnetic induction whereby is now possible to transfer energy from one environment to another using Electromagnetic waves. All contributed to enhanced efficient wireless charging. At present wireless charging has already been developed for low-power devices that can powered up to 5W such as mobile phones and wireless powered access card. In the year 2000, Professor Shu Yuen Hui from The City University of Hong Kong invented a planar wireless charging pad that can able to charge several electronic loads simultaneously. Also in the year 2007, MIT researchers demonstrated an efficient wireless power transmission based on a strong coupled magnetic resonance and was successfully powered a 60W light bulb with 40% efficiency remotely at 2 meters [4]. In the subsequent year, Intel successfully lighted an electric bulb with 70% efficiency at 1 m distance.

Generally, wireless charging is multidisciplinary field that includes power electronic circuits, coils and a control circuitry. Comparing to wired topology, wireless charging has lower efficiency due to added losses on coupling and power conversion units. This will increase resistive heating losses and causes overheating on battery which will reduce its life time. Thus this article addresses the efficiency issues which is the main concern on wireless charging technology using the most advanced solutions, the coupling efficiency can achieve 85% and the overall system efficiency can achieve up to 75% [5].

So many other research work has been conducted to extend the possibility and the efficiency of wireless charging to 2-ways and 4-ways radios but the limitations is that must of the 2-ways and 4-ways radios required only 7.5V battery for its operations and the efficiency of the wireless charging was considerably low compared to the traditional wired charging. This work basically is to make improvement on the efficiency of the RF Wireless Power Transfer and Charging System already on ground and to extend the charging voltage up to 8.5 V and 12V and the transmitter toemit a low- power radio wave at a frequency of 500-900MHz.

TYPES OF RF WIRELESS POWER TRANSFER

Radio Charging: This charges low- power electronic devices within a distance of 10 meters from the transmitter which sent out low-power radio wave to the receiver which converts the signal to energy. This could activate advanced RFID (radio frequency identification) chips through a considerable enhanced induction.

Inductive Charging: This is the most important method of transferring energy wirelessly through and inductive coupling. It is used for near field power transmission. The power transmission takes place between two conductive materials through the mutual inductance. The typical example of inductive coupling transmission is a transformer.

Resonance Charging: this applies the concepts of resonance whereby both the transmitter and the receiver coils are turn to the same electromagnetic frequency. At resonance,

the receiver coil can pick up the signal when energy at resonant frequency is applied.

An inductive charging method will be the technique to be used in implementing this project for it is the commonly used method for electronic devices. This will ease the use for both the consumers and the developers, Wireless Power Consortium (WPC) has established Qi as the global standard for wireless power system with the output power of up to 5W to create interoperability between the transmitter and the receiver [6]. Under WPC standard, the type of inductive coupling and communication protocol are always defined.

Wireless charging system consists of two distinguishable devices:

a) The wireless power transmitter coil section: the wireless transmitter section converts the DC power from an oscillator to a high frequency AC power signal. This high frequency alternating current, which is linked with the wireless transmitting power, would create an alternating magnetic field in the coil due to induction to transmit energy.

b) Wireless power receiver section: in this section the receiver coils receives the energy as induced alternating voltage (due to induction) in its coil and rectifier in the wireless power receiver converts the AC voltage to a DC voltage. Finally the rectified DC voltage would be feed to the load through the voltage controller section. That means the main function of a wireless receiver section is to charge a low-power devices through an inductive coupling.

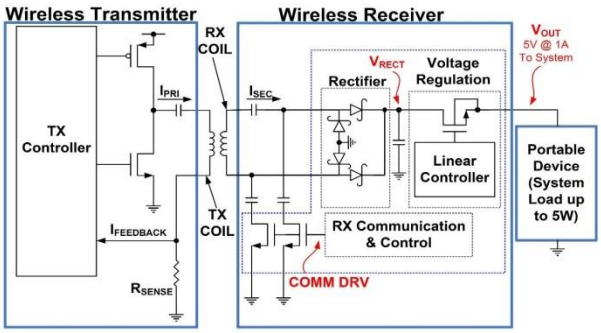

Fig. 1. Qi- Complaint Wireless Power System [7]

I. DESIGN FLOW AND OPTIMIZATION

Generally the design process for an inductor coil is very complicated as the physical and electrical parameters that affect the performance of the coil are interrelated where by any change in one of the parameters will have an effect on another. Thus, a design flow for the coils is developed to model the inductor coils based on the design of solenoid shaped coil and PSC where the performance is compared between the two designs. The ultimate goal of this design flow is to optimize the power transfer efficiency between two coils while meeting the design specifications and constraints as per the application system requirements. The design flow for the inductor coil is described systematically as shown below first by explaining the parameters and good shape and size of the coil used.

In wireless power transfer, charging coil is formed by winding a conducting wire to a certain configuration. This tends to concentrate the magnetic field by coil, hence improving the induced voltage collected. This will also improves the inductive coupling between coils. The Printed Circuit Board (PCB) gives an easier concept in designing a Printed Spiral Coil (PSC) because it can be manufactured using PCB process, which is term as a standard process for manufacturing PSC. This also can be integrated in the receiver circuit, which reduces the size of the receiver. The coil area and the number of layers are limited by PCB where higher self-inductance is very difficult to be achieved. Accurate inductance has to be calculated as it cannot be modified once the PCB is fabricated [8]. Commonly used structures for wireless charging are, Helical coil, planar spiral coil and printed spiral coil as shown in the Fig. 2.

The structure of a helical coil is similar to an inductor and can easily be constructed compared to a planar coil. This gives a better magnetic field with longer wavelength but this does not have advantage to short range charging [9]. Helical coil occupies more space to obtain a desired inductance compare to a planar coil. Helical coil produces a horizontal magnetic flux as shown in figure. Both the coils are required to be positioned perpendicular to each other in order to allow capturing of magnetic flux, which is not suitable for a slim design of portable devices.

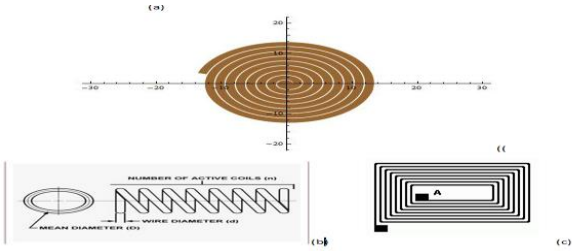

Fig. 2. Different Ty pes of Winding Structures on WCC, (A) Spiral Coil (B)Helical Coil (C) Planar Spiral Coil

Planar coils generate vertical flux where both charging coils can be positioned in parallel position to each other. Hence, it is more suitable for implementation in wireless charging application [10]. The inductance and the design of coil can be easily modified with a planar spiral coil configuration. Planar Spiral Coil (PCB) is commonly made up of Litzwire which tends to increase the impedance of a conductor caused by eddy current effects as discussed in the previous chapter. For this article, Planar Spiral Coil is the targeted coil design to be implemented as it tend to give higher efficiency with Litz wire and is allows for slim design at higher frequency.

The shape of coil will also affect the magnetic properties, as such, the choice of better shape of coil will lead to an efficient power transfer between the transmitter and the receiver coils. Hence, the typical coil shapes available includes circular, square and rectangular structure [11]. Segmented shape, which splits the rectangular area into two parallel-connected

coils, is also considered. The shape of the coil also affects the coupling factor (K) as in figure .In all the four shapes of coil circular shape gives the highest coupling factor [12], in other hand, the coil with higher area has higher coupling factor .for the purpose of this design circular coil will be used based on it advantage as discussed and shown in Fig. 3.

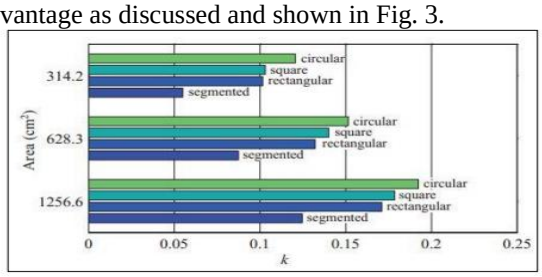

Fig. 3. Areas against Coupling Factor of Different Coil Shapes and Area

Computer Simulation Technology (CST) Microwave Studio was used to carry out the design process it has the ability to simulate 3D electromagnetic coil at high frequency using frequency domain solver and provides full circuit simulation tools and present results in 3D electromagnetic form. The CST software also have many features such as; parameter sweep , mesh properties and mini-match to match the two port of transmitter and receiver coils, it also provides other features for optimisation and model construction to enhance efficient wireless communications within the circuit.

TABLE I. ENVIRONMENT SETTING IN CST MICROWAVE STUDIO

Frequency level	High Frequency
Setup Solver	Frequency Domain Solver
Mesh Type	Tetrahedral
Frequency Range	650MHz -750MHz
Surrounding Space Diameter	300mm

Basically to start with, 3D model type of inductive coils are constructed for transmitter and receiver sections of wireless power transfer in CST Microwave Studio using FEM behavioural approach for the 3D and circuit combination study. The settings in Table 1 are maintained in the simulation environment for the coils model. As in Table 1, for wireless power transfer and charging, the commonly used applications on CST microwave studio are frequency domain solver with tetrahedral meshing. The air domain for model surrounding is represented by normal background material which is 300mm apart for this project.

Listed in Table 1, are the design specifications for transmitter and receiver modelled coils shown in Fig. 4. To reduce the complexity of the coil design and simulations in CST MWS, a single core copper wire is used for the modelling for coils instead of earlier proposed Litz wire in the literature review. All the parameters of transmitter section are kept constant during the modelling with modification on the outer radius of the receiver coil section and changing the distance between. Other parameters are kept constant to meet the design specifications and to enhance energy transfer within the coils. This will results in given a better coupling performance within the coils with the separation Gap of 50mm.

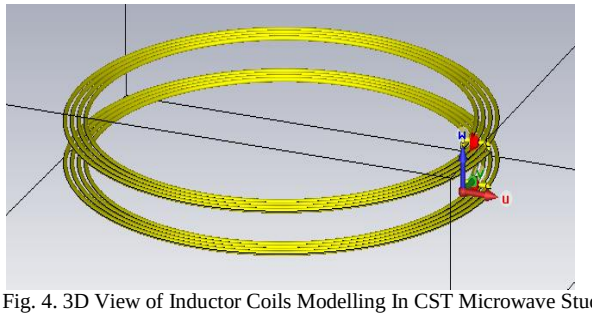

Fig. 4. 3D View of Inductor Coils Modelling In CST Microwave Studio

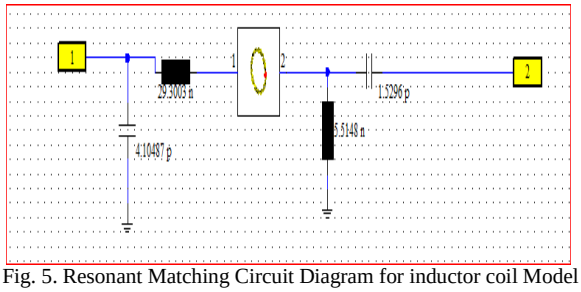

Fig. 5. Resonant Matching Circuit Diagram for inductor coil Model

For the receiver coil, the capacitor in the inductive loop ofone coil model is simultaneously altered until the surface coil is turned to 700MHz called the resonance frequency at the resonance frequency the magnitude of S_{11} S_{11} is at minimum. The voltage and current through the inductive loop should be close to the maximum. Once the coil has been turned, the turning capacitors and inductors are noted. The basic reason for this is to allow the implanted coil to be turned to 700MHz while still being inductively coupled to the surface coil; this is to avoid frequency splitting during the energy transfer. Shown in Fig. 5 is the designed matching circuit for this work that resonate the frequency at 700MHz alongside the component value of resonant circuit matching presented in Table 2.

TABLE II COMPONENTS VALUE OF RESONANT CIRCUIT MATCHING

Components		Value
Transmitter Capacitor	C1	4.104 $pFpF$
Receiver Capacitor	C2	1.529. $pFpF$
Transmitter Inductor	L1	29.300 $nHnH$
Receiver Inductor	L2	45.51 $nHnH$

RESULTS FROM RESONANT CIRCUIT DESIGN ON CST

Initially, simulation is carried out for the weak inductively coupled transmitter and receiver coils in CST for coupling performance study. The s-parameters results are obtained for power transmission analysis in coils as shown in Fig. 6 (a). In s-parameters, S21 represents the transmitted power from transmitter coil to receiver coil while the S11 and S22 represent the reflected power in between two coils.

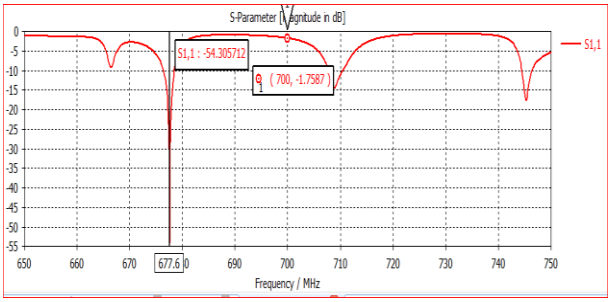

(a) With Matching

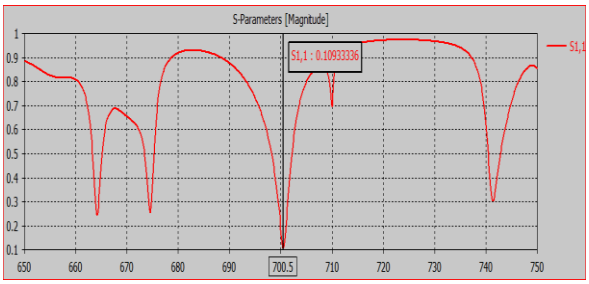

(b) Without Matching

Fig. 6. S-Parameter S11 With and Without Matching

At operating frequency of 700 MHz, the power transmission efficiency obtained for the coils model is 0.321 % with S21 of -24.935 dB. Therefore, wireless power transfer in the coils model is impossible with almost no coupling between coils. After matching the resonant circuit the resulting resonant efficiency was enhanced as shown in Fig. 7.

From Fig. 7 the coils model is matched at resonant frequency of 700MHz with maximum amount of power transfer and minimum amount of power reflection. This gives the maximum power transmission efficiency between coils of 93.1 % for the inductor coils with separation gap of 50mm at operating frequency of 700MHz.

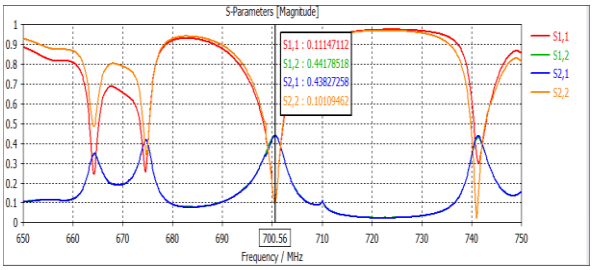

Fig. 7. Combined S-Parameter Results after Matching

CONCLUSION

In conclusion, the proposed coils model meets the design specifications. It is capable of providing efficient wireless power transfer to portable charging devices through resonant inductive coupling method with maximum power transmission efficiency of 93%. Furthermore, it passes the coils performance evaluation test that is subjected to different external factors in real situation. The additional adjusting freedoms existing in CST systems architectural design are beneficial for optimizing system transfer characteristics. The global optimization design and regulations methods by considering multi-effects factors are also valuable for its engineering applications.

In real practice, a certain rated power is required but this MHz resonant frequency may bring a great challenge to some portable electronics components, for example the circuit rectifier, MOSFET driver and so on. Fortunately with the rapid development of semiconductor and material industry this will overcome these challenges. Generally, WPT actually belongs to a marginal discipline between physics and electronics as such it needs the efforts from different research fields. The simulations of high frequency range WPT need a super speed for its simulations process in order to obtain high efficiency and high quality factor.

REFERENCES

[1] B. Johns, "An introduction to the Wireless Power Consortium standard and TI ' s compliant solutions (sylt401)," *Analog Appl. J.*, 2011.

[2] A. O. Hariri, A. Berzoy, A. A. S. Mohamed, S. Members, O. A. Mohammed, and F. Ieee, "Performance Evaluation of a Wireless Power Transfer System using Coupled 3D Finite Element-Circuit Model," pp. 7–10, 2015.

[3] D. Kurschner, C. Rathge, and U. Jumar, "Design Methodology for High Efficient Inductive Power Transfer Systems With High Coil Positioning Flexibility," *Ind. Electron. IEEE Trans.*, vol. 60, no. 1, pp. 372–381, 2013.

[4] J. Agbinya, "Investigation of Near Field Inductive Communication System Models, Channels and Experiments.," *Prog. Electromagn. Res. B*, vol. 49, no. February, pp. 129–153, 2013.

[5] Anuradha Menon and A. Menon, *Intel's Wireless Power Technology Demonstrated*. The Future of Things e-magazine, 2008.

[6] H. J. Choi, E. H. Ahn, S. Y. Park, and J. R. Choi, "Portable battery charging circuits for enhanced magnetic resonance Wireless Power Transfer (WPT) system," *Conf. Proc. - 9th Conf. Ph. D. Res. Microelectron. Electron. PRIME 2013*, pp. 273–276, 2013.

[7] "WiTricity Corporation." [Online]. Available: http://www.witricity.com/assets/highly-resonant-power-transfer-kesler-witricity-2013.pdf. [Accessed: 26-Jul-2015].

[8] S. Davis, "Wireless power minimizes interconnection problems," *Power Electron. Technol.*, pp. 10 – 14, 2011.

[9] A. K. Sah, A. Christ, M. G. Douglas, J. M. Roman, E. B. Cooper, A. P. Sample, B. H. Waters, J. R. Smith, N. Kuster, and R. M. Cano, "Evaluation of Wireless Resonant Power Transfer Systems With Human Electromagnetic Exposure Limits," *IEEE Trans. Electromagn. Compat.*, no. 1, pp. 1–10, 2012.

[10] S. Y. Hui, "Planar wireless charging technology for portable electronic products and Qi," *Proc. IEEE*, vol. 101, no. 6, pp. 1290–1301, 2013.

[11] P. Grover and A. Sahai, "Shannon meets tesla: Wireless information and power transfer," *IEEE Int. Symp. Inf. Theory - Proc.*, pp. 2363–2367, 2010.

J.-P. Curty, M. Declercq, C. Dehollain, and N. Joehl, *Design and Optimization of Passive UHF RFID Systems*. Springer, 2006.

A Novel Model for Network Anomaly Detection based on Naïve Bayes using Wrapper Approach

John OcheOnah and Shafi'i Muhammad Abdulhamid,
Department of Cyber Security Science, Federal University of Technology Minna, Nigeria.
jhonchekzy@gmail.com, shafii.abdulhamid@futminna.edu.ng

ABSTRACT—The drastic increase in network attack has been a major concern in cyber security especially now that internet usage and connectivity is at high demand. In a way of combating some of these network attacks, data mining technique for network anomaly detection and network event classification attack has proven efficient and accurate. This research presents a novel feature selection approach that eliminates extraneous features to minimise time complexity as well as building an improved model that predict result with a higher accuracy based on wrapper approach for intrusion detection. Attack types are predicted based on Naïve Bayes - the base classifier. From the experiment, our proposed model demonstrates a higher overall performance of 99.73% accuracy, keeping the false positive rate as low as 0.006. Our model performed better than models like as Markov chain, K-Nearest Neighbors (KNN), Hidden Naïve Bayes (HNB) and Boosted Decision Tree (DT). The NSL-KDD is used in experimental setup as benchmark data set using Weka library functions.

KEYWORDS—component, formatting, style, styling, insert (*key words****)***

INTRODUCTION

Recently, they have been a high increase in the computer network intrusion incidents and network hacking tools due to the increase in technology and computer networks vulnerabilities. As threats on networks keep increasing, there is an urgent need to develop more accurate and sensitive intrusion detection system that will reduced these threats. Intrusion detection system is usually designed and installed on networks in other to protect the network and systems on the network form known and unknown vulnerabilities, threats and malicious attacks. Based on the nature of attacks on a network, Intrusion detection can be categorised in two (2) major forms, namely; anomaly detection and misuse(signature-based) detection [1]. Patterns of normal network behaviour and usage are used to pinpoint various anomalies or attacks as in the case of anomaly detection approach [13] whereas, patterns and behaviours of known attacks are used to detect attack types that are already known as in the case of signature-based misuse detection. Various approaches of identifying anomaly and misuse of a system are achieved through the application of various techniques of data mining and machine learning methods that involve single classifier [5][22] and ensemble classifiers [16] have been widely used by researchers. Researchers have been using different classifiers to identify pattern-based attacks but the degree of accuracy of these classifiers which is based on the various algorithms and how they are been trained have been a major concern. In other to reduce the learning run time and accuracy of the algorithm, best features must be selected for the feature vector of the algorithm [1].

Feature selection is an essential criterion in dataset training as it removes irreverent features and reduce dimensionality and thereby improves the predictive accuracy [25]. It is very useful in the field of intrusion detection, pattern recognition, data mining, image processing and machine learning, as it maps out only useful features (subset of features) for data and pattern. It thereby builds a high accuracy model since its eliminate inappropriate features and reduces time complexity. Levent*et al.,* (2012) [12] classified feature selection model into Filter, Wrapper and Embedded method.

Classification on the other hand, is a data mining technique where each instance in a dataset is assigned to a particular class. Important data classes are defined to extract data models and these models are called as classifiers. In this technique learning and classification are two steps for data classification. In the learning step a classifier is formed and the class labels for the data are predicted by using this classifier. In the classification technique every data in the dataset has an attribute value that defines class and all the classes are predefined so that the analyst has a prior knowledge [1]. Classification can also be used to label every record in the data set and the records can be classified in predetermined set.

I. BRIEF DESCRIPTION OF GENETIC ALGORITHM AND NAÏVE BAYES

A. Genetic Algorithm

Genetic algorithm is derived from the theory of Darwin on natural selection [17]. It is an optimization algorithm which comprise of genetic information known as chromosome for optimizing the problem set by encoding the solution of the candidate (i.e. individuals). Genetic information is represented by binary strings such as 0's or 1's and the problem set solution is encoded with sets of bits. The two major operators involved in genetic algorithm are crossover and mutation that are applied on the individuals for the next generation. The selected strings of bit from the parent are duplicated by the crossover operator producing two posterity strings. While on the other hand, mutation arbitrarily alters the value of string bits. The increased in the probability of a single bit survival is guaranteed by fitness function increased throughout the evolutionary process [4]. Genetic algorithm is more effective and has huge space for searching with a small probability of achieving local optimal solution as compared to other algorithms. Genetic algorithms work productively to select subset of features with a less computational prerequisite for classification using stochastic optimization strategy [11].

B. Naïve Bayes

In data mining, Naïve Bayes algorithm as an effective inductive learning algorithm is a straightforward type of classifier derived from classical statistical theory "Bayes

theorem." The "naïve" is established on Bayes Rule which shows that the features are conditionally independent from each other with respect to the class [3]. In the literature, the Naïve Bayes algorithm has demonstrated its adequacy in different spaces, for example text classification [6], improving search engine quality [10], image processing [27][23], and medical diagnoses [2].

The working of Naive Bayes classifier is as follows: let X be a vector of random variables representing the observed attribute values in the training set $X = [x_1, x_1, \ldots x_n]$ to certain class label c in the training set. The probability of each class given the vector of observed values for the predictive attributes can be computed using the following formula [8]:

$$P(c/x) = \frac{P(x/c)\ P(c)}{P(x)}$$

$$P(c/X) = P(x_1/c) \times P(x_2/c) \times \ldots \times P(x_n/c) \times p(c)$$

Where:

P(c/x) is the posterior possibility of class (target) given predicator (attribute)

P(c) is the prior possibility of class.

P(x/c) is the possibility which is the probability of predicator given class.

P(x) is the prior possibility

Adequacy of Naïve Bayes algorithm in classification and learning is ascribed to several attributes, for example.

High computational effectiveness when contrasted with other wrapper strategies since it is economical, it is viewed as linear time complexity classifier.

Low variance due to less searching.

Incremental taking in light of the fact that NB functions work from estimate of low-order probabilities that are derived from the training data. Thus, these can be quickly updated as new training data are obtained.

i. High ability to deal with noise in the dataset.

ii. High ability to deal with missing values in the dataset.

In addition, Naïve Bayes implementation has no required adjusting parameters or domain knowledge. The real downside of NB just lies in the assumption of features independence. Despite this, Naïve Bayes often delivers competitive classification accuracy and is broadly applied in practice especially as benchmark results.

II. RELATED STUDIES

A list of research has been done on enhancing the performance of intrusion detection system in order to beat the impediment of old-fashioned systems by consolidating machine learning techniques with different detection approaches.

Muniyandi et al., (2012) [14] combined k-means clustering and C.45 decision tree method for classification method called Cascading developed to ease the dominating of k-means technique and forced assignment. The k-means breakdown the training dataset into k-subsets then C.45 is created for the broken-down subsets. Also, Natesan et al (2012) [15] in their work proposed an improved single weak classifier using AdaBoost. Bayes Net, Naïve Bayes and Decision Tree (DT) were used as weak performed better than those with AdaBoost. However, the major problem is that, it lacks mechanism for detecting novel attacks that have signature similar to known attacks leading to low detection possibly.

Keep your text and graphic files separate until after the text has been formatted and styled. Do not use hard tabs, and limit use of hard returns to only one return at the end of a paragraph. Do not add any kind of pagination anywhere in the paper. Do not number text heads-the template will do that for you.

Govindarajan and Chandrasekaran [9] introduced a hybrid-based detection architecture-entailing ensemble and base classifiers for detection system. The ensemble module was built using the result of both Radial Basis function (RBF) neural networks and Multilayer Perceptron (MLP). This experiment result showed this hybrid architecture was better than the individual RBF and MLP classification model in terms of performance. However, the drawback hybridising the classification models is overhead since each connection is examined by the individual classifier models.

A cuttlefish optimization-based algorithm (CFA) was proposed by [1] for optimally selecting from KDD cup 99 dataset, subset features with an accuracy of 91.986 %. Another feature selection framework was put forward by (Yang and M. T, 2011) [24]. Their approach involves combing genetic algorithm and K-nearest neighbour for optimal feature selection and weighting. Originally during the training step, 35 features were weighted and in light of their weight the top ones were picked for the testing stage implementation. 19 features were considered and give an accuracy of 97.42% for known attacks, actually, accuracy rate of 78% was recorded when 28 features were considered for obscure attacks.

Ranker based Boosted model was proposed by Yung-TsungHou (2010) [26] with an accuracy of 96.14%. whileLevent et al. (2012) [12] carried out the Hidden Naïve with accuracy of 93.72% in intrusion detection system though suffers from dimensionality. Shun-Sheng [21] in 2011 came up with a ranker search based Adaptive Response Theory on SVM with accuracy of 95.13% accuracy in intrusion detection system. A Markov chain intrusion detection system having an accuracy of 90.0% is proposed by Seongjun (2013) [19] based on advance probabilistic approach.

An adaptive and hybrid neurofuzzy system ensemble (NFBoost algorithm) was proposed by Selvakumar and Kumar P. A. Raj [18] in their research to identify both known and novel attacks of DDoS, it reduces total error thereby improving the accuracy of the detection. They developed the base classifier using Neuro-Fuzzy Inference System (ANFIS). The final classification conclusion or decision is gotten by the

combination of the ensemble classifier's output and Neyman Pearson cost minimization strategy.

FC-ANN IDS as a proposed work of Gang Wang et al. [7] is a final product of Fuzzy Clustering (FC) and Artificial Neural Network (ANN). The Fuzzy Clustering method is part of FC-ANN that split training dataset into several similar subsets. This simplify each training subset by decreasing the complexity and improving the detection performance. It means, while the Fussy Clustering technique splits the training dataset, diverse ANN Classifier are trainedby the generated training subset trains the Produced preparing subsets. Fuzzy aggregator, at last is employed to integrate the outputs of individual classifiers into a unified one for final prediction.

its six subcategories; Averaged One-Dependence Estimators (AODE), DTNB, Weightily AODE (WAODE), Tree-Augmented Naïve Bayesian (TAN), Decision Tree (NBTree), Hidden Naïve Bayesian (HNB) as regards to DDoS attacks. The results demonstrated the high accuracy rate of HNB using proportion K-Interval discretization method as regars to the other variants experimented with.

Shi-Jinn Horng et al. [20] designed an IDS combining hierarchical clustering and Support Vector Machine (SVM). The hierarchical clustering algorithm part transformed the training dataset to a reasonable sizable dataset for SVM to train large dataset with reduced time. This transformed dataset is partitioned into five categories which is used for training

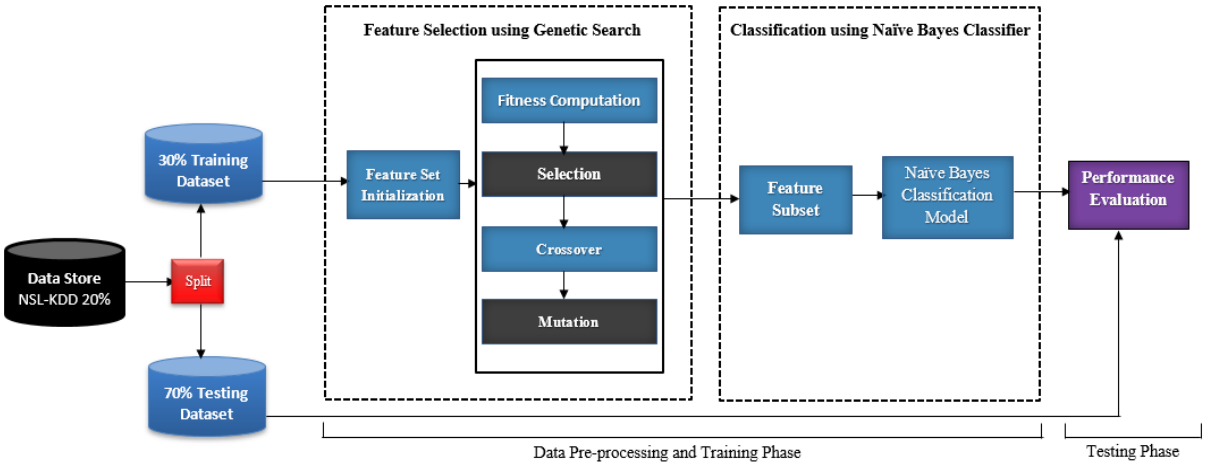

Fig. 1 Proposed Wrapper-Based Naïve Bayes Classification Framework

Levent et al. [12] carried out experiments on KDD99 dataset to ascertain the accuracy of Naïve Bayesian (NB) and four SVM classifiers. The final result is the outputs of the merged classifiers.

III. PROPOSED FRAMEWORK

The operation of this proposed framework is in two stages. Stage 1 involves the feature selection process using a wrapper approach with Genetic Search algorithm while stage 2 is about the classification of Test instances using Naïve Bayes.

Process involved in stage 1 is screening and removing redundant features and a wrapper feature selection is proposed for the purpose of getting a better accuracy. Genetic search as the search algorithm used for searching through the space of possible features and Naïve Bayes based model employed on each subset for evaluation. At the end, feature subset is been selected based on the performance while, stage 2 entails building a classification model using a Naïve Bayes

algorithm. Finally, an instance of a test is by the new Naïve Bayes based built classification model as shown by Fig. 1 followed by the algorithm.

Algorithm: Proposed Wrapper Based Naïve Bayes Attack Detector (WBNAD)

Input: Dataset

Output: Class labelled test instance

Step 1: Generate randomly, an initial population, *P*.

Step 2: Compute *e(x)* for each member $x \in P$.

Step 3: Define a probability distribution *p* over the member of *P* where $p(x) \propto e(x)$.

Step 4: Select two population members *x* and *y* with respect to *p*.

Step 5: Apply crossover to *x* and *y* to produce new population members *x'* and *y'*.

Step 6: Apply mutation to *x'* and *y'*.

Step 7: Insert *x'* and *y'* into *P'* // *The next generation.*

Step 8: if $|P'| < |P|$, goto 4

Step 9: Let $P \leftarrow P'$

Step 10: if there are generations to still process, goto 2.

Step 11: Return $x \in P$ where *e(x)* is highest.

Step 12: Given a training set, for each Class $c_i \in C$

i. Estimate the prior probability: $P(c_i)$

ii. For each feature x_j, estimate the probability of that feature value given Class c_i: $P(x_j/c_i)$

Step 13: for each Class $c_i \in C$, compute: $P(c_i) * \prod_{j=1}^{n} P(x_j/c_i)$

Step 14: Select the most probable Class $C = \underset{c_i \in C}{\operatorname{argmax}} P(c_i) * \prod_{j=1}^{n} P(x_j/c_i)$

EXPERIMENTAL SETUP

The experiment run on an Intel® Core™ i5-2410M CPU @2.45Ghz,~2.4GHz with 4.00 GB memory running on 64-bit Windows 10. The experiment was carried out with the aid of JAVA programming language, WEKA 3.8 machine learning apparatus and Weka Library functions for feature selection techniques. We used a well-known NSL-KDD benchmark dataset created by the MIT Lincoln Lab for the experiment with aim of juxtaposing the performance of different intrusion detection techniques. Dataset of NSL-KDD containing classes which are grouped into five, namely: normal and four types of attacks such as R2, Probing, DoS, and U2R.

20% NSL-KDD dataset is utilized in the experiment for both training and testing with further splitting of the 20% dataset into 30% of the instances as training instance and the rest 70% as testing instance. Table 1 demonstrates the details of the 41 features of the dataset [16].

A. Performance Metric

True Positive (TP): TP is an Alarms setup to be alerted when there is successful and accurate identification of normal behaviours.

False Positive (FP): FP is an Alarm setup to go on immediately an abnormal behaviouris incorrectly identified as normal.

Accuracy: It is the proportion of correctly classified classes.

Table 1. 41 Features of NSL-KDD Data Set [16]

Feature No.	Feature Name	Type	Feature No.	Feature Name	Type
1.	Duration	Con.	22.	is_guest_login	Dis.
2.	protocol_type	Dis.	23.	Count	Con.
3.	Service	Dis.	24.	srv_count	Con.
4.	Flag	Dis.	25.	serror_rate	Con.
5.	src_bytes	Con.	26.	srv_serror_rate	Con.
6.	dst_bytes	Con.	27.	rerror_rate	Con.
7.	Land	Dis.	28.	srv_rerror_rate	Con.
8.	wrong_fragment	Con.	29.	same_srv_rate	Con.
9.	Urgent	Con.	30.	diff_srv_rate	Con.
10.	Hot	Con.	31.	srv_diff_host_rate	Con.
11.	num_failed_logins	Con.	32.	dst_host_count	Con.
12.	logged_in	Dis.	33.	dst_host_srv_count	Con.
13.	num_compromised	Con.	34.	dst_host_same_srv_rate	Con.
14.	root_shell	Con.	35.	dst_host_diff_srv_rate	Con.
15.	su_attempted	Con.	36.	dst_host_same_src_port_rate	Con.
16.	num_root	Con.	37.	dst_host_srv_diff_host_rate	Con.
17.	num_file_creations	Con.	38.	dst_host_serror_rate	Con.
18.	num_shells	Con.	39.	dst_host_srv_serror_rate	Con.
19.	num_access_files	Con.	40.	dst_host_rerror_rate	Con.
20.	num_outbound_cmd	Con.	41.	dst_host_srv_rerror_rate	Con.
21.	is_host_login	Dis.			

Precision: It estimate the probability of a positive prediction that are being correct.

It is paramount to keep the false alarm rates as low as possible and to ensure the security of the system, the false negative alarms should be at the barest minimum

B. Experimental Result and Evaluation

With respect to the NSL-KDD dataset used which comprised of a normal type of class label and class label for 4 attack type such as R2, Probing, DoS, and U2R. A well-known classification system called k-fold cross validation that is capable of eliminating over-fitted classification was used based on 10-fold cross validation

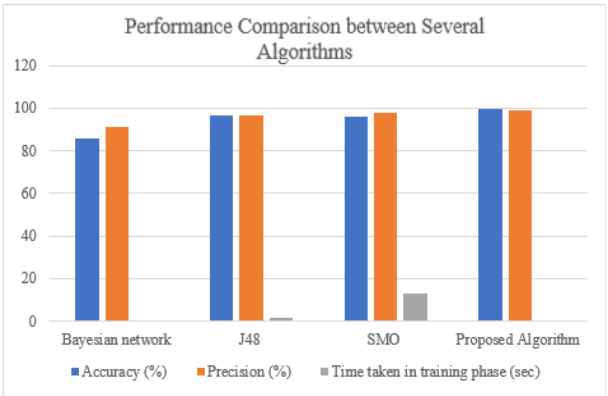

Fig. 3. Performance Comparison between Several Algorithms

Table 2 demonstrated the general performance of the proposed IDS model. Clearly the proposed model performed better with the follow results: true positive rate of 97.3%; low false positive rate of 0.6%; and ROC area of 99.7% as compared to the other models marking our model to have

performed excellently. It suffices to know that the benchmark for ROC area is greater or equal to 95%.

Table 3 below shows the result of proposed algorithm as

Table 2. Overall Performance of the Proposed IDS

Class	True Positive Rate (TPR) (%)	False Positive Rate (FPR) (%)	ROC Area (%)
Normal	97.5	0.6	99.7
U2R	73.5	0.2	93.5
R2L	77.1	0.1	99.1
DoS	96.9	0.6	99.7
Probing	93.4	0.4	99.2
Average Weight	98.1	0.6	99.7

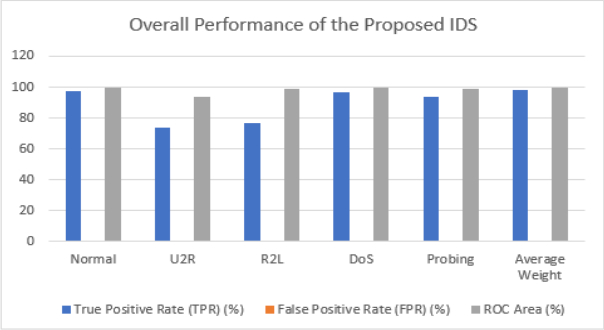

Fig. 2. Overall Performance of the Proposed IDS

compared to some other algorithms. It is evident that the proposed system performed better with an accuracy rate of 99.73% whereas other algorithms such as Bayesian Network gave an accuracy rate of 85.76%, algorithm SMO gave an accuracy of 95.99% and a decision tree J48 algorithm gave 96.43%. The time taken for training phase of the classification model in the proposed algorithm is very low, 0.18 sec compared to Naive Bayes, J48 and SMO which takes 0.2, 1.73, and 13.1 respectively as graphically represented in Fig. 3.

Table 3. Performance Comparison between Several

Algorithms	Bayesian Network	J48	SMO	Proposed Algorithm
Accuracy (%)	85.76	96.43	95.99	99.73
Precision (%)	91.4	96.5	97.6	99. 1
Time taken in training phase (sec)	0.20	1.73	13.01	0.18

Our proposed wrapper approach in terms of performance as compared with some other well-known feature selection techniques is demonstrated in Table 4 and depicted in Fig. 4. Out of 41 features, our proposed wrapper approach performed better than a Consistency Feature Selection (CFS) technique with 16 important features selected. CFS technique using rank search gave 93.13% accuracy while CFS using filter approach gave 94.88 % accuracy rate and finally, 91.13% was recorded using CFS type filter based genetic search which obviously is considerably low as compared to our proposed wrapper approach for feature space searching.

IV. Conclusion and Future Work

In this research work, a novel model termed Wrapper Based Naïve Bayes Attack Detector (WBNAD) for intrusion detection is proposed. WBNAD is based on wrapper approach for feature selection and Naïve Bayes Classifier. The process involved the preparation of a proper NSL-KDD train dataset with features16 out of 41 as final features selected. Classification of test instances followed using Naïve Bayes classifier. Our proposed model recorded 0.006 as False Positive Rate (FPR) and a 98.1% True Positive Rate (TPR). The result of the proposed model appeared to be reliable and outdone other classifiers with respect to their performances in efficiency and accuracy. Conclusively, the wrapper approach using reasonable features performs excellently as regards to anomaly intrusion detection.

The study from this experiment revealed a method in which an intrusion detection can be observed by using fewer features leading to the reduction of time as well as the

Table 4. Performance Comparison between Several Feature Selection Techniques

Algorithm	Feature Selected	Accuracy (%)
BestFirst+ConsistencySubsetEval	9	96.99
GeneticSearch+CfsSubsetEval	23	91.13
GreedyStepwise+CfsSubsetEval	11	92.81
RankSearch+CfsSubsetEval	14	94.88
RankSearch+ConsistencySubsetEval	26	93.13
Nil	41	92.68
Proposed Wrapper Approach	16	99.73

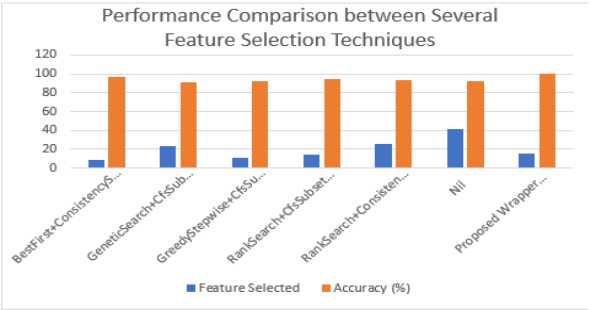

Fig. 4. Performance Comparison between Several Feature Selection Techniques

complexity involved in both the training and testing stage. Future research areas can be in the following aspects: An easy feature selection approach should be developed by exploring other techniques for efficient and effective feature selection. Experimenting this proposed method using actual cloud data for the purpose analysis real-time results.

References

[1] S. E. Adel, O. Zeynep, and M. A. B. Adnan, "A Novel Feature-Selection Approach Based on the Cuttlefish Optimization Algorithm for Intrusion

Detection Systems," Expert Systems with Applications, Vol. 42, pp. 2670-2679, April 2015.

[2] M. Anbarasi, E. Anupriya and N. Iyengar, "Enhanced Prediction of Heart Disease with Feature Subset Selection using Genetic Algorithm," International Journal of Engineering Science and Technology, Vo. 2, pp. 5370–5376, October 2010.

[3] C. Anuradha and T. Velmurugan, "A Comparative Analysis on the Evaluation of Classification Algorithms in the Prediction of Students Performance," Indian Journal of Science and Technology, Vol. 8, pp. 1 – 12, July 2015.

[4] T. Chih-Fong, E. William and C. Chi-Yuan, "Genetic Algorithms in Feature and Instance Selection,". Expert Systems with Applications, Vol. 39, pp. 240 – 247, February 2013.

[5] Y. Y. Chung and N. Wahid, "A Hybrid Network Intrusion Detection System using Simplified Swarm Optimization (SSO)", Applied Soft Computing Journal, Vol. 12, pp. 3014 – 3022, September 2012.

[6] G. Feng, J. Guo, B.-Y. Jing, and L. Hao, "A Bayesian Feature Selection Paradigm for Text Classification," Information Processing and Management, Vol. 48, pp. 283–302, March 2012.

[7] G. Wang, J. Hao, M. Jian and Huang L., "A New Approach to Intrusion Detection using Artificial Neural Networks and Fuzzy Clustering," Expert Systems with Applications vol. 37 pp. 6225–6232, September 2010.

[8] M. Gaurav and R. C. Ravi, "A Review Paper on IDS Classification using KDD 99 and NSL KDD Dataset in WEKA. International Conference on Computer", Communications and Electronics, Vol. pp. 553 – 558, July 2017.

[9] M. Govindarajan, and R. M. Chandrasekaram, "Intrusion Detection using Neural based Hybrid Classification Methods," Computer Network, Vol. 55, pp. 1662 – 1671, June 2011.

[10] H. T. T. Nguyen and D. K. Le, "An Approach to Improving Quality of Crawlers using Naïve Bayes for Classifier and Hyperlink Filter," Computational Collective Intelligence. Technologies and Applications, pp. 525 – 532, 2012.

[11] T. Karthikeyan and P. Thangaraju, "Genetic Algorithm based CFS and Naive Bayes Algorithm to Enhance the Predictive Accuracy," Indian Journal of Science and Technology, Vol. 8, pp. 1 – 8, October 2015.

[12] K. Levent, A. M. Thomas and S. Shahram, "A Network Intrusion Detection System Based on a Hidden Naïve Bayesian Multiclass Classifier," Expert Systems with Applications, vol. 39, pp. 13492–13500, December 2012.

[13] S. Ming-Yang, "Real-time anomaly detection systems for Denial-of-Service Attacks by Weighted K-nearest-Neighbor Classifiers," Expert Systems with Applications, vol. 38, pp. 3492–3498, April 2011.

[14] P. Muniyandi, R. Rajeswari and R. Rajaram, "Network Anomaly Detection by Cascading K-Means Clustering and C.45 Decision Tree Algorithm," Procedia Engineering, Vol. 30, pp. 174 – 182, 2012.

[15] P. B. Natesan and G. Gowrison, "Improving the Attack Detection Rate Intrusion Detection using AdaBoost Algorithm," Journal of Computer Science, Vol. 8, pp. 1041 – 1048, August 2012.

[16] F. H. Nutan, R. O. Abdul and M. S. Faisal, "An Ensemble Framework of Anomaly Detection using Hybridized Feature Selection Approach (HFSA)," SAI Intelligent Systems Conference, pp. 689 – 995, November 2015.

[17] S. Sharma, S. Kumar, and M. Kaur, "Recent Trend in Intrusion Detection Using Fuzzy-Genetic Algorithm," International Journal of Advanced Research in Computer and Communication Engineering, Vol. 3, April 2014.

[18] S. Selvakumar and A. P. R. Kumar, "Detection of Distributed Denial of Service Attacks using an Ensemble of Adaptive and Hybrid Neuro-Fuzzy Systems", Computer Communications, vol. 36, pp. 303–319, February 2013.

[19] L. Seungmin, K. Hyunwoo and K. Sehun, "Advanced Probabilistic Approach for Network Intrusion Forecasting and Detection. Expert Systems with Applications, Vol.40, pp. 315 – 322, January 2013.

[20] H. Shi-Jinn, S. Ming-Yang, C. Yuan-Hsin, K. Tzong-Wann, C. Rong-Jian, L. Jui-Lin, and C. D. Perkasa, "A Novel Intrusion Detection System Based on Hierarchical Clustering and Support Vector Machines," Expert Systems with Applications, Vol. 38, pp. 306–313, January 2011.

[21] W. Shun-Sheng, Y. Kuo-Qin, W. Shu-Ching and L. Chia-Wei, "An Integrated Intrusion Detection System for Cluster-based Wireless Sensor Networks", xpert Systems with Applications, Vol. 38, pp. 15234 – 152443, December 2011.

[22] S. Siva, S. Sivatha, S. Geetha and A. Kannan, "Decision Tree Based Light Weight Intrusion Detection Using a Wrapper Approach," Expert Systems with Applications, Vol. 39 pp.129–141, January 2012.

[23] M. C. Yang, C. S. Huang, J. H. Chen, and R. F. Chang, "Whole Breast Lesion Detection Using Naive Bayes Classifier for Portable Ultrasound," Ultrasound in Medicine and Biology, Vol. 38, pp. 1870–1880, November 2012.

[24] S. Ming-Yang, "Real-Time Anomaly Detection Systems for Denial-of-Service Wttacks by Weighted K-Nearest-Neighbor Classifiers," Expert Systems with Applications, Vol. 38, pp. 3492 – 3498, April 2011.

[25] H. Yoon, P. Cheong-Sool, K. Jun-Seok and B. Jun-Geol, "Algorithm Learning Based Neural Network Integrating Feature Selection and Classification". Expert Systems with Applications, Vol. 40, pp. 231–41, January 2013.

[26] H. Yung-Tsung, C. Yimeng, C. Tsuhan, L. Chi-Sung and C. Chia-Mei, "Malicious Web Content Detection by Machine Learning," Expert Systems with Applications, Vol. 37, pp. 55-60, January 2010.

Z. Zhang, Q. Zhu, and Y. Xie, "A Novel Image Matting Approach Based on Naïve Bayes Classifier," Intelligent Computing Technology, pp. 433–441, July 2012

Development of Low Cost Heart Beat Monitoring Device using Arduino uno.

Charles JoeGarba,Abdullahi Z. M., Agada Peter, Amos Ataguba
Department of Communication Engineering ABU Zaria, Kaduna Nigeria
charlesjoegarba@yahoo.com, amzanna@gmail.com, Petag5ray@yahoo.com, ephraimamos62@gmail.com

ABSTRACT— the aim of this project is to develop a low cost heart beat monitoring device. The system consists of three main parts: 1) the optical sensor: consisting of the optical transmitter and receiver for emitting the light and receiving it; 2) the Arduino Uno section: which receives and processes the signal to display the heart rate and will be obtained by measuring the time between signal peaks and then calculating the frequency of the peaks in units of beats per minute. 3) The LCD section which show the reading of heart beat and the implementation of the heart monitor.

KEYWORDS – LCD, Optical Sensor, Low Cost, Heart Beat

INTRODUCTION

Heart beat rate measurement could show the condition of the heart. Heart rate is varying according to age, person physical and activity condition. Human heart rate of healthy adult is around 60 to 100 beats per minute (BPM). While for an athlete, his/her heart rate is slower than an active adult, for baby is on the other hand, the heart rate is higher which is around 120 to 160 BPM and for children's heart rate is around 75 to 110 BPM. Abnormal heart rate such as lower heart rate than the normal rate is called bradycardia whereas for a higher heart rate, which is higher than the normal, is called tachycardia. The traditional method of heart rate is measurable by putting finger above pulse artery and count pulse rate within 30 second and heart rate (BPM) can be found with multiplying with 2. This way is easy but inaccurate especially when artery pulse state in high rate. The most accurate method to measure heart rate is by using electrocardiogram machine (ECG) but this equipment is expensive and not affordable by individuals

HEART BEAT RATE

The heart is the organ that is responsible for pumping blood throughout the body. It is located slightly offset to the left and surrounded by the lungs, the human heart is composed of four chambers which are two atriums and two ventricles. The right atrium receives blood returning to the heart from the whole body. That blood passes through the right ventricle and is pumped to the lungs where it is oxygenated and goes back to the heart through the left atrium, and then the blood passes through the left ventricle and is pumped again to be distributed to the entire body through the arteries.

Heart rate is the number of heartbeats per unit of time, typically expressed as beats per minute (BPM). Heart rate can vary as the body's need to absorb oxygen and excrete carbon dioxide changes during exercise or sleep. The heart rate of a healthy adult at rest is around 72 beats per minute (bpm). Athletes normally have lower heart rates than less active people. Babies have a much higher heart rate at around 120 bpm, while older children have heart rates at around 90 bpm. Lower than normal heart rates are usually an indication of a condition known as bradycardia, while higher than normal heart rates are known as tachycardia. The measurement of heart rate is used by medical professionals to assist in the diagnosis and tracking of medical conditions. It is also used by individuals.

HEART RATE MEASUREMENT METHOD

The heart rate can be measure at any spot on the body at which an artery is close to the surface and a pulse can be felt. The most common places to measure heart rate using the palpation method is at the wrist (radial artery) and the neck (carotid artery). There are several others places that can measure heart rate such as elbow (brachial artery) and groin (femoral artery). The methods of measuring heart rate can be divided into two:
1: manual method, 2: monitor method.

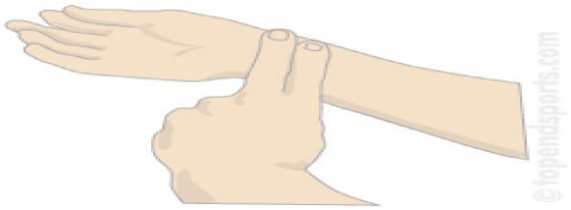

Fig. 1 Manual Method

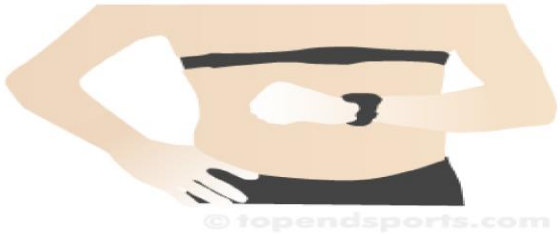

Fig. 2: Monitor Method

The monitor method can be perform by using electrocardiogram (ECG) machines. The standard Electrocardiogram (ECG) machine normally found in big hospitals, due to the high cost and requires a specialist to handle the machine. The ECG concept also applied on several gadgets such as watch and Smartphone but the demand is not good due to the high price.

FINGERTIP SENSOR

Heart beat sensor is a device designed to give digital output of heart beat when a finger is placed on it. When the heart beat detector is working, the beat LED flashes in unison with each

heartbeat. It works on the principle of light modulation by blood flow.

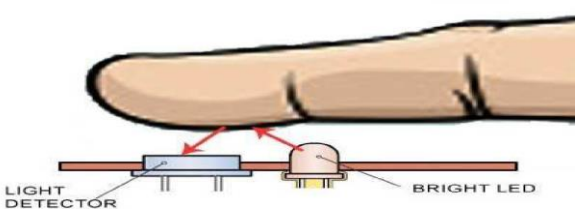

Fig. 5 Fingertip Sensor

Fingertip sensor has been done in two methods: transmittance and reflectance of light. In transmittance fingertip sensor, light is shone through the tissue using an LED and is detected on the other end using a photo detector. In contrast, reflectance fingertip sensor uses a photo detector on the same side as the LED to detect the light reflected by the tissue.

V. ARDUINO UNO

Arduino Uno is a widely used open-source microcontroller board based on the Microchip ATmega328P microcontroller and developed by Arduino-cc.The board is equipped with sets of digital and analog input/output (I/O) pins that may be interfaced to various expansion boards (shields) and other circuits.The board features 14 Digital pins and 6 Analog pins. It is programmable with the Arduino IDE (Integrated Development Environment) via a type B USB cable.It can be powered by a USB cable or by an external 9 volt battery, though it accepts voltages between 7 and 20 volts.

Figure 6: Arduino Uno

VI LCD (Liquid Crystal Display)

A Liquid-Crystal Display (LCD) is a flat-panel display or other electronically modulated optical device that uses the light-modulating properties of liquid crystals. It does not emit light directly, instead it uses a backlight or reflector to produce images in color or monochrome.LCDs are available to display arbitrary images (as in a general-purpose computer display) or fixed images with low information content, which can be displayed or hidden, such as preset words, digits, and seven-segment displays.

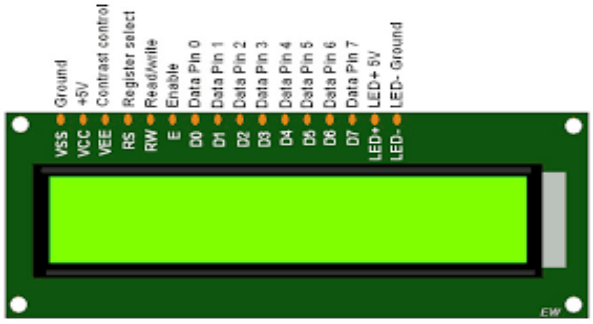

Figure 7: LCD (Liquid Crystal Display).

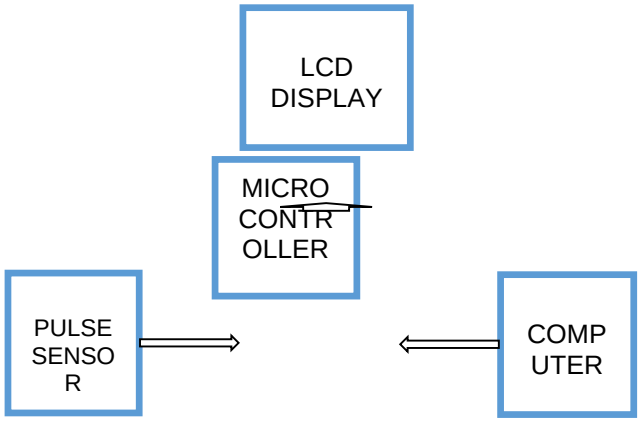

Figure 8: Heartbeat Monitor Device Block Diagram

VII. MATERIAL AND METHOD

The component used was selected based on the design which would provide optimistic low cost, and availability. The components are coupled in the design to complete the circuit of heart beat monitoring device where by the circuit were run to ensure it services.

A. List of Material Used

The materials used for this work are listed below.

1 Atmega328.
2 Resistors.
3 Capacitors.
4 Push button.
5 Jumper wires.
6 National instrumentation (NI) multism.
7 Arduino Uno (Integrated Development Environment (IDE))
8 Soldering iron.
9 Soldering lead.
10 LCD.
11 Fingertip sensor.
12 Bread board.
13 Casing.
14 IC socket.

B. pulse sensor circuit.

Heart beat sensor is designed to give digital output of heart beat when a finger is placed on it. When the heart beat detector is working, the beat LED flashes in unison with each heartbeat

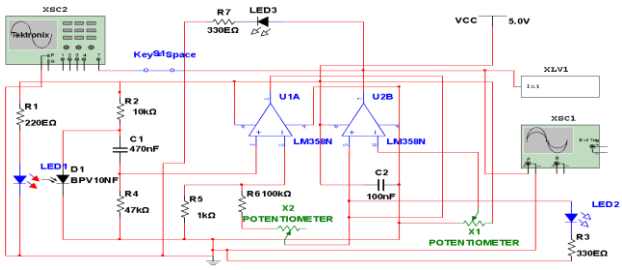

Figure 9: Heartbeat Sensor Circuit

VIII. RESULTS

Through various test procedures and techniques, many parts of this project were improved. Initially, basic features were tested to ensure that each component or block worked, as testing progressed, modifications or adjustments were made to the circuits so they functioned well practically.

Figure 10: shows the result obtained at 10 kHz sampling rate and linear interpolation at time domain.

Figure 11: shows the result obtained for spline interpolation at time domain

Figure 12: shows the result obtained at 10 kHz sampling rate for spline interpolation at time domain.

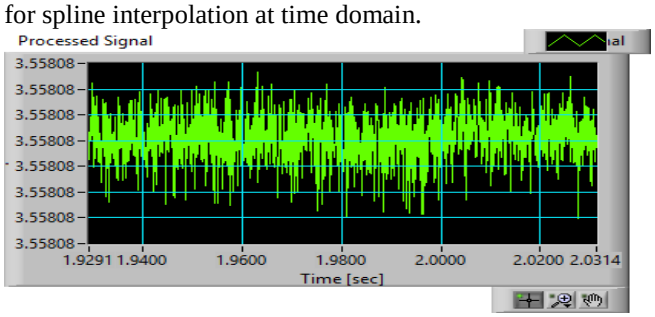

Figure 10: Linear Interpolation at Time Domain for 10 kHz Sampling Rate.

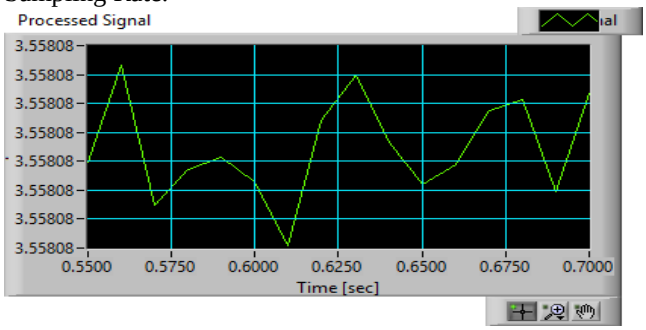

Figure11: Spline Interpolation at Time Domain for 100 Hz sampling rate.

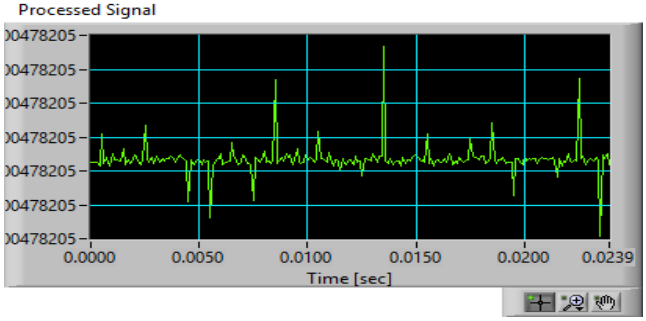

Figure12: Result at 10 kHz sampling rate, spline interpolation at time domain

IX. cost of hardwares (components)

The costs for all the parts used in the design and implementation of the heartbeat monitor device sensors are listed below. The costs outlined below are for only the parts used to build the actual circuits. Additional costs related to other parts used in older models of these circuits are not attached

Table 1: Bill of Quantity (BOQ)

PARTS	QUANTITY	PRICE
Microcontroller	1	#1000
LCD	1	#700
(male to male)/male to female jumper	1 dozens each	#700
Thumb sensor(pulse sensor)	1	#1800
Casing	1	#200
Chip socket	1	#1200
Female connector	1	#100
Total cost		#5700

X. CONCLUSION

This implementation of a heart monitor involves low cost components coupled with a sophisticated microcontroller and LCD screen. The device is useful as it is portable, it was designed with use of 5volt. In doing this the output voltage was found to be strongly related to the quality of contact between the sensor and the thumb and was observed to be highly variable. This project was successfully implemented as digital heart rate monitoring device.

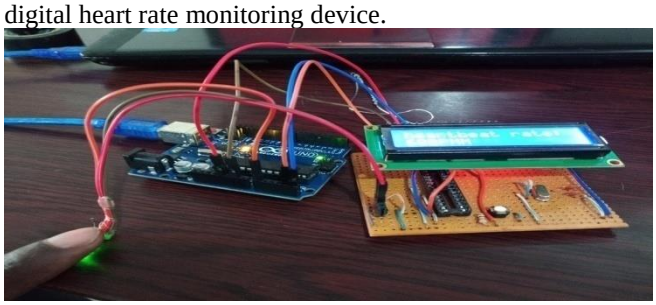

Figure 13: Constructed Project

REFERENCES

[1] T. G, D. Greenspan, M. Welsh, R. R. Juang, and A. Alm. *Vital Signs Monitoring and Patient Tracking Over a Wireless Network*. IEEE Engineering in Medicine andBiology 27th Annual Conference, Shanghai, China, September 2005

[2] Brian Dolan. *Home health monitoring was 11b market in 2008*. Berg Insight,
September 2009. <http://mobihealthnews.com/4568/home-health-monitoring-was-11bmarket-

In-2008/>
[3] Mundt, Carsten. *Lifeguard – A Wearable Vital Signs Monitoring System*. NASA AMES Astrobionics, February 2004. <http://lifeguard.stanford.edu/lifeguard_writeup_medium.pdf
[4] Anon. *Spot Vital Signs LXi*. WelchAllyn, 2010.<http://www.welchallyn.com/products/en-us/x-11-ac-100-0000000001118.htm>
[5] Anon. *740 Vital Signs Monitor*. CASMED. <http://www.casmed.com/740Rev02.pdf>
[6] V*ital Signs Monitor*. EBay, March 12, 2010. <http://shop.ebay.ca/?_from=R40&_trksid=m38&_nkw=vital+signs+monitor>
[7] Anon. *ECG Measurement*. Biomedical signals of the human body, 2004.

Developmentof a Propagation Model for IEEE 802.11 Wireless Networks: Case of GidanKwano Campus, FUT MINNA

Sunday OgunjideUsman Abraham Usman, Henry Ohize, Umar Suleiman Dauda
Department of Electrical and Electronics Engineering
Federal University of Technology, Minna, Nigeria
favouredben78@gmail.com,usman.abraham@futminna.edu.ng, usdauda@gmail.com

ABSTRACT—Wireless propagation modeling is an essential task in planning wireless networks. In the last few decades, the use of Wireless Local Area Network (WLAN) popularly referred to as Wi-Fi(Wireless Fidelity) in communication system has been on the increase with the exponential usage of handheld cell phones, laptops, and palm-tops to mention but a few. Notwithstanding, WLAN faces a peculiar propagation issue which lies in its changing propagation environment and this affects the quality of service. Poor quality of service is experienced on WLAN of GidanKwano campus of Federal university of technology, Minna. This arises due to signal propagation impairment caused by the terrain and the structures within the campus. Received Signal Strength (RSS) measurements were conducted at different locations away from the selected Access Points (APs) both in Line of Sight (LOS) and Non- Line of Sight (NLOS) situations. The path loss exponent (n) and standard deviation (σ) were estimated for the environment. The obtained results were contrasted with the already published work to show the level of agreement. The empirical models were developed for LOS and NLOS situations and compared with the existing standard models.

KEYWORDS—Wireless Local Area Network, Path loss model, Path loss exponent, Propagation impairment, Access Points (APs)

INTRODUCTION

Wireless Local Area Networks (WLANs) popularly referred to as Wi-Fi (Wireless Fidelity) have recently gained prominence in various walks of life, including medical centre, retail, assembling, warehousing, and academic environment [2] [4][9]. These sectors have benefitted immensely by utilizing hand-held gadgets and notebook computers for real time data transmission [13]. Wireless communication offers clients and associations numerous advantages, for example, compactness and adaptability, increment profitability, and lower cost of installation when compared to the wire line communication systems [18] [23]. WLAN gadgets enable clients to move their cell phones from place to place without the requirement for wires [5]. Less wiring implies more noteworthy adaptability and increment proficiency. Handheld gadgets, such as, Personal Digital Assistants (PDA) and mobile phones permit remote clients to synchronize individual databases and give access to network services, for example, remote email, web browsing, and other web administrations [6]. However, as wireless signals move from a transmitter to a receiver, they get diffracted, scattered, and absorbed by the territory, trees, building, vehicles and individuals which constitute the environment of propagation [1] [3] [11] [20] [21] [23]. The nearness of obstacles along the path of wireless signal may cause great signal attenuation more noteworthy than it would under free space conditions [8] [12] [14]. Radio signal attenuation and path losses are greatly due to the terrain of propagation [10] [15] [16] [17]. Poor network planning is a factor responsible for WLAN poor quality of service [18] [19] [20] [24]. For accurate network planning, a good knowledge of propagation characteristics is of great importance [22] [25]. In the literature, empirical propagation models are most prevalently used for handling network planning issues. However, due to changes in the environment of propagation, the empirical models are not globally applicable [1] [21]. Accordingly, it is important to determine the particular radio propagation characteristics that will be ideal for the environment under study while carrying out network planning [23].The Gidan Kwano campus of FUT, Minna often times encounter poor quality of service arising from the signal propagation impairment. The accurate prediction of well-known propagation models is not suitable to evaluate the propagation characteristic of this campus due to the peculiarity of its terrain. This paper is geared toward developing a propagation model for this campus using received signal strength measurements from a selected access points within the campus.

METHODOLOGY

Many techniques and materials have been utilised in taking information from an access point (or a base station) [17] [22]. These techniques include radio frequency (RF) overview and drive test among others [18] [7] [2]. For this work, the technique for RF overview was utilised and this section describes the materials and strategies used to achieve this investigation. Figure 1 shows the summary of the methodology deployed.

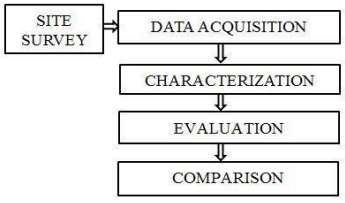

Fig.1. Summary of the methodology

A. Study area description

The GidanKwano campus of Federal University of Technology (F.U.T) Minna is situated in Minna, the Niger state capital, Nigeria. It lies on Longitude 6.50*E* and Latitude 9.70*N*. The campus is moderately sized with complex terrain because of the presence of tall structures, classrooms and trees within it. The attenuation of the Wi-Fi signal within the campus is attributed to numerous reflections, absorption and diffractions off rooftops, trees, cars and so on [**?**]. The access points (APs) utilised for this work are referenced with respect to the campus building they were mounted on, in particular, ITS Wi-Fi, LIB. Wi-Fi, SEM Wi-Fi, SEET2 Wi-Fi, PTDF Wi-Fi, AGRIC-AP, CON-Wi-Fi, SICT Wi-Fi, ABE Wi-Fi, and SET Wi-Fi. These APs were picked as a result of accessibility of their hardware specifications and configuration.

B. Radio Frequency Site Survey

An RF site review is the initial phase in the deployment of a Wireless network and the most significant advance to guarantee wanted operation [22]. A site study is a step-by step process by which the surveyor thinks about the facility to understand the RF behaviour, finds RF coverage areas and decides the appropriate placement of Wireless devices [18]. There is no viable alternative for measuring real-world obstruction, blockage and Received Signal Strength Indicator (RSSI) at a site, just on-location measurements and overviews can give the total picture. RF site over view were led utilising studying apparatus that enable data to be gathered from an access point, example of such data is the RSSI.

C. Surveying Tools

In carrying out the site survey, Air Check Wi-Fi Tester 2.4GHz and 5.0GHz was utilised to capture wireless packets from an ad-hoc or infrastructure network setup utilising an access point. The specifications of the software and hardware equipment utilised for this study are given below.

1) Software specifications:

i. Inssider software
ii. Matlab version R2014a
iii. Microsoft window 8 Pro.

2) Hardware specifications:

a: Air Check Wi-Fi Tester 2.4GHz and 5.0GHz

*b:*Laptop

i. Vendor Hp
ii. Model: Note book 15
iii. CPU Speed: 2.7GHz
iv. Memory: 2GHz
v. Wireless Card: Intel PRO/Wireless 2200BG

c: IEEE 802.11b/g Access Point

i. Vendor: Mikrotik RB Metal G52SHPacn
ii. Range: $\approx 183m = 600ft$
iii. Transmitter reference Power: *1W*
iv. Bands: *2.4GHz* to *2.4835GHz*
v. Transmission speed-Wi-Fi 2.4GHz: 150Mb/s

d: Global Positioning System (GPS)

i. Vendor: Magellan
ii. Model: Explorist 500

e: 25-foot measuring tape.

D. Data Collection Methods

An Hp laptop with a Network Interface Card (NIC) installed and running on Microsoft Windows 8 Pro with Inssider software was utilised to obtain RSSI information at varying radial distance from the chosen APs on the campus. The following privacy guidelines were observed during data collection:

1) The Inssider software did not attempt gaining access to the network.
2) The Inssider software sees all the access points publiclycommunicating their Service Set Identifier (SSID).

Ten (10) APs were chosen on the Campus at distinctive areas. The chosen APs were from a similar vendor and with similar specifications utilising IEEE 802.11 b/g standard. At each AP, straight ways were stamped out at various bearings from the AP to the laptop. On every one of these ways, test points were physically estimated at a 10m interval utilizing a measuring tape estimating to a 100m stamp from the AP.

1) Line of Sight (LOS) data collection procedure scenario:

In a LOS environment, the receiving antenna is detectable to the transmitting antenna with an exceptionally minimal obstacle. The origins of attenuations are essentially from the movement of individuals and vehicles over the path of signal transmission. This is so since the human body is made of around 70 percent water, hence, it ingests some amount of signal accordingly causing loss of strength of the signal being transmitted. Signal information with relating separations fromthe APs were measured, and at each measured separation, a few estimation of RSSI were gathered. The APs in a LOS environment situation are FUT Wi-Fi (ITS), FUTLIB. WiFi, SEM MBB Wi-Fi, SEET2-Wi-Fi and GOOGLE Wi-Fi (PTDF).

2) Non-Line of Sight (NLOS) data collection procedure scenario: For NLOS condition, there were no visual observable pathway between the receiving and the transmitting antennas. The radio transmission way is mostly or completely impeded by the nearness of physical obstructions, for example,tall structures, trees, slopes, individuals, vehicles and so on[16]. These interference bodies weaken the signal strength by method of absorption, reflection, scattering and diffraction.

RSSI values were gathered from five (5) APs on the campusat estimated separations from the APs in a NLOS domainsituation. The APs in a NLOS situation are FUTAGRIC-AP,CON-FUT Wi-Fi, GOOGLE Wi-Fi (SICT), ABE-Wi-FiandGOOGLE WIFI (SET). Data were gathered between the hours of 10 am and 12 pm and between 2 pm and 4 pm from Monday through Friday. Themovement of

individuals and vehicles is reduced at these hoursof the day being the lecture hours. This is aimed at reducingthe attenuation caused by individuals and car movement. There is an interior antenna situated behind the laptop screen, so the laptop screen was directed toward the apex sky keeping in mind the end goal to improve the probability that the direct beams signal path falls on the beam width of the antenna.

II. RESULTS, DISCUSSION AND ANALYSIS

In the study of wireless data communication networks, the path loss exponent is the principal parameter of interest [2]. The path loss exponent relies greatly upon the environment of propagation. High path loss exponent symbolizes how quick the signal strength drops with respect to the distance between the transmitter and the receiver [19] [21]. Therefore, in carrying out signal propagation modeling for a given study area, the path loss exponent for such study area has to be determined. This section shows results, discussion and analysis of information gathered on RSSI from the environment of propagation.

A. Presentation of results

The ranges of the signal strength measurements and the corresponding signal quality from Inssider software is presented in Table I based on the standard [18]. The measurement surveyed signal strength obtained for some of the APs in LOS and NLOS are presented in Tables II and III respectively.

TABLE ISURVEY OF THE RSSI

Received Signal Strength in dBm	Signal quality
-60<RSSI≤-20	Excellent signal
-75<RSSI≤-60	Good signals
-85<RSSI≤-75	Low signal
-90<RSSI≤-85	Very Low signal
-108<RSSI≤-90	No signal

TABLE II MEAN RSSI FOR LOS ENVIRONMENT SCENARIO

d(m)	Mean RSSI FUT Wi-Fi (ITS)	Mean RSSI FUT_LIB. Wi-Fi	Mean RSSI SEM MBB Wi-Fi	Mean RSSI SEET2 -Wi-Fi (ITS)	Mean RSSI GOOGLE Wi-Fi(PTDF)
1	-14.03	-14.03	-14.03	-14.03	-14.03
10	-41.65	-42.70	-43.45	-42.35	-42.75
20	-42.35	-44.45	-45.85	-46.40	-43.90
30	-43.25	-42.65	-46.75	-44.35	-45.80
40	-42.85	-44.35	-47.50	-47.10	-48.65
50	-48.05	-47.40	-45.90	-54.90	-47.55
60	-53.75	-51.30	-53.05	-57.85	-53.65
70	-52.90	-52.85	-56.95	-56.75	-62.25
80	-56.55	-54.70	-54.85	-62.50	-52.60
90	-61.80	-52.40	-65.75	-65.00	-65.40
100	-67.85	-60.25	-63.55	-66.75	-69.40

TABLE III. MEAN RSSI FOR NLOS ENVIRONMENT SCENARIO

d(m)	Mean RSSI FUTAGRIC-AP	Mean RSSI CON-FUT Wi-Fi	Mean RSSI GOOGLE Wi-Fi (SICT)	Mean RSSI ABE-WIFI	Mean RSSI GOOGLE WIFI (SET)
1	-14.03	-14.03	-14.03	-14.03	-14.03
10	-54.10	-52.60	-48.85	-50.80	-48.35
20	-57.15	-57.85	-52.50	-55.40	-54.50
30	-62.25	-56.80	-55.75	-59.65	-57.20
40	-68.60	-58.50	-62.90	-61.50	-56.95
50	-65.65	-66.20	-70.25	-59.05	-59.95
60	-67.75	-62.35	-67.30	-63.20	-66.45
70	-74.20	-83.85	-66.60	-71.10	-70.45
80	-73.30	-81.40	-74.85	-69.00	-75.85
90	-86.25	-85.70	-81.90	-79.15	-79.85
100	-84.90	-87.80	-79.85	-84.05	-78.95

B. Computation of path loss exponent using Log distance path loss propagation model

Where $P_t$is the reference transmitter power of *1W*, W_m *equals* 10^{-3} *W*, P_T is the transmitter power in dBm, $P_L(d)$ is the Path Loss at distance *d* and $P_L(do)$ is the Path Loss at reference distance 1m.

RSSI are the measured data against distance at the various locations.With reference to RSSI expression of (1), (4) is obtained.Utilizing (4) obtained the path losses. With reference to (4) at reference distance of 1m away from the access point, RSSI is -14.03dBm. From which P_L (*do*) is solved to be 44.03dB. Hence (3) becomes,the path lose exponent for both LOS and NLOS were obtained using (5). The standard deviation (σ) and Sum of Square Error (SSE) of the developed models from the established standard model were computed by applying (6) and (7) utilizing MATLAB tool.

Where $y_i$is the measured path loss at a particular interval, $\bar{y}$ is the developed model path loss and *M* is the data length. Table IV and V show the mean path loss exponents for LOS and NLOS scenarios respectively.

TABLE IVTHE MEAN PATH LOSS EXPONENTS FOR LOS

Location	Mean Path Loss Exponent(n)
FUT Wi-Fi(ITS)	2.24
FUT_LIB Wi-Fi	2.16
SEM MBB Wi-Fi	2.34
SEET2 Wi-Fi	2.44
GOOGLE Wi-Fi(PTDF)	2.36

TABLE VTHE MEAN PATH LOSS EXPONENTS FOR NLOS

Location	Mean Path Loss Exponent(n)
FUTAGRIC-AP	3.36
CON-FUT Wi-Fi	3.34
GOOGLE Wi-Fi(SICT)	3.14
ABE Wi-Fi	3.11
GOOGLE Wi-Fi (SET)	3.07

DISCUSSION OF RESULTS

The standard deviation σ and SSE of the developed models from the field measurements were the parameters used to evaluate the models quality. In this analysis, the standard deviation of the measured LOS path loss and the developed model LOS path loss was 2.81dB as opposed to 5.60dB of the measured LOS path loss and Free Space Lose. Also, the standard deviation of the measured NLOS path loss and the developed NLOS model was 3.23dB while that of Hata model and the measured NLOS path loss was 7.04dB. The SSE of the measured LOS path loss and the developed model LOS path loss was 8.87dB while that of the free space model and themeasured LOS path loss was 17.71dB. The measured NLOS path loss and the developed model NLOS SSE was 10.20dB while that of Hata model and the measured NLOS path loss was 22.26dB. Path loss exponent is the most imperative model parameter obtained from the analysis. This parameter gives noteworthy knowledge into how wireless signals attenuate with respect to the distance between the access point and the mobile receiver. In the analysis, it was gathered that, the path loss exponent for NLOS scenario was higher when compared to that of the LOS environment. This shows that, the signal strength for NLOS scenario decreases faster due to the presence of obstructions along the path of propagation than for LOS scenario. The obtained path loss exponent in this analysis falls within the range of the most researchers published results [7][12][22]. Table VI gives the summary of the path loss exponents for both LOS and NLOS scenarios.

TABLE VISUMMARY OF THE PATH LOSS EXPONENTS FOR BOTH LOS AND NLOS SCENARIOS.

Environment	Mean Path Loss exponent (n)
LOS	2.31
NLOS	3.20

(8) and (9) are the derived mean path loss models for LOS and NLOS scenarios.

Comparison with standard models

Propagation path loss exponents obtained from the empirical measurements were contrasted with that of the free space loss and Hata model (Refer table VII and VIII) and depicted in Figures 2 and 3. Obviously, the path loss exponents from the empirical measurements as contrasted with the free space loss appeared to be higher, and this was seen to be caused by extra losses from the environment of propagation, which attenuates the signal quickly than in free space.

TABLE VII COMPARISON BETWEEN MEASURED DATA, DEVELOPED MODEL AND FREE SPACE LOSS

d (m)	Measured data [PL_{LOS}]	PL (d) [LOS] For n=2.31	PL (d) [FSL] For n=2.0
10	71.95	67.13	64.03
20	75.90	74.08	70.05
30	73.80	78.15	73.57
40	75.95	81.03	76.07
50	83.30	83.27	78.01
60	86.25	85.11	79.60
70	84.40	86.65	80.93
80	88.50	87.99	82.09
90	89.80	89.17	83.11
100	90.85	90.23	84.03

TABLEVIIICOMPARISON BETWEEN MEASURED DATA, DEVELOPED MODEL ANDHATA MODEL

d (m)	**Measured data [PL_{NLOS}]**	**P L (dB) [NLOS] For n=**3.20	**PL(dB) Hata Model**
10	83.60	76.03	72.46
20	89.10	85.66	81.44
30	92.25	91.30	86.69
40	98.45	95.29	90.42
50	97.70	98.39	93.31
60	98.25	100.93	95.67
70	105.30	103.07	97.67
80	103.15	104.93	99.40
90	108.75	106.57	100.92
100	109.90	108.03	102.29

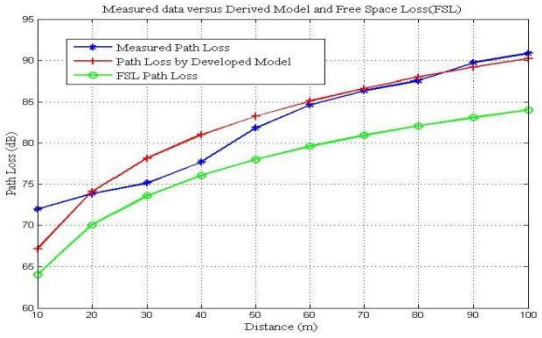

Fig. 2. Comparison of the measured data with the derived model and Free Space Loss (FSL).

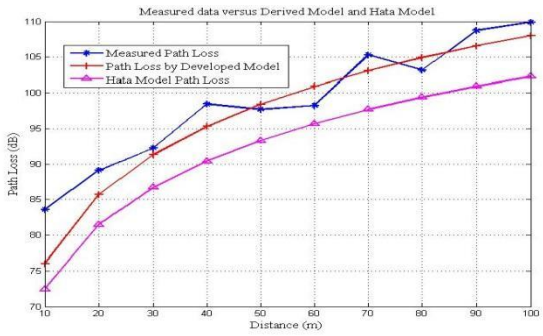

Fig. 3. Comparison of the measured data with the derived model and Hata Model.

CONCLUSION

This work has developed a propagation model that can be utilised in describing the signal attenuation within the GidanKwano campus of FUT, Minna. This was actualised by investigating the effect of the environment on radio frequency signal quality. It was discovered that the nearness of obstructions attenuates the signal strength which degrades the performance of the wireless network. RSSI data were gathered in a LOS and NLOS situations. The path loss exponents and standard deviations acquired for the obstructed environment (NLOS) were seen to be higher than those obtained for unhampered (LOS) condition. This perception demonstrated that the nearness of hindrances truly have effects on radio frequency signal quality. Based on the empirical data gathered, propagation models were determined for both NLOS and LOS conditions. The obtained results were then contrasted with the existing standard models and the outcome demonstrated high level of agreement. The results were satisfactory, showing the developed models can effectively be utilised for APs deployment at FUT Minna to accomplish high quality signal coverage for optimal performance.

REFERENCES

[1] Aremu, O.A. (2016).Experimental study of variation of Path Loss with respect to Heights at GSM frequency band. *3, Nigeria :s.n., IJSRSET* 2, 19-21.

[2] Rodrigues, R.C., Mateus, G.R.andLouriro, A.A.F. (2012). On the Design and Capacity Planning of a Wireless Management Symposium Noms. *(IEEE / IFIP, ed.)*, 335-348.

[3] Bejide, O., Onumanyi, A., and Onwuka, E. (2017). Empirical Path loss Models for the 802.11a/b/g Propagation Channel at the Bosso Campus of the Federal University of Technology, Minna. *2nd International Engineering Conference (IEC 2017) Federal University of Technology, Minna, Nigeria*, 2.

[4] Bidgoli, H. (2013). The Internet Encyclopedia. *John Wiley and Sons, Inc. Hoboken, New Jersey*, 4, 183 185.

[5] Saveeda, P. (2013). Received signal strength(RSS) Calculation for GSM cellular system at BSNL Pondicherry using modified HATA model. *1,International Journal of Science, Engineering and Technology Research*, 2, 10-13.

[6] Shelly, G.B., Cashman, T. J.and Rosenblatt, H.J. (2012). Systems Analysis and Design. *7th ed., 425, ISBN-13: 978-1-4239-1222-4.*

[7] Eibert, T. F. and Kuhlman, P, (2013). Notes on Semi empirical wave propagation modeling for microcellular environments comparison with measurements. *IEEE Trans. Antenna and Propagation*, 51, 2253-2259.

[8] Tarokh, V. (2014). New Directions in Wireless Communication Research. *Springer Dordrecht Heidelberg London New York,* 1, ISBN 978- 1-4419-0672-4.

[9] Goransson, P.andGreenlaw, R. (2011). Secure Roaming in 802.11 *Networks. 128, ISBN 978-0-7506-8211-4.*

[10] Green, D. B and Obaidat, M. S. (2011). An Accurate Line of Sight Propagation performance model for Ad-Hoc 802 11 wireless LAN (WLAN) Devices. *SRI Internal and Mon mouth University*, 2, 12-13.

[11] Terplan, K. and Morrwle, P. (2014). The Telecommunication Handbook. *2-4, IEEE Press, ISBN 0-8493-3137-4.*

[12] Sun, L., Fu, C., Zhang, Z. C. (2010). Wireless Communications, Networking and Mobile Computing 2010. *IEEE Wicom. International Conference*, 5, 1060.

[13] http://en.wikipedia.org/wiki/Empierical model , date accessed: March 10, 2010.

[14] http://www.telecomspace.com/wirelessnw-wsecurity.html. Wireless security. Date accessed: 23th April, 2011.

[15] Idim, A.I and Anyasi, F.I. (2014). Determination of building penetration loss of GSM signals using selected buildings in Orhuwhorun,DeltaState,Nigeria as a case study. *5, IOSR Journal of Electronics and Communication Engineering*, 9, 01-05.

[16] Zaballos, A., Corral, G., Carne, A. and Pijoan, J. L. (2015). Modeling new indoor and outdoor propagation models for WLAN. *University Ramon Llull, Barcelona Spain. www.salle.url.eduRetrieved date:* 2nd August, 2015.

[17] Sun, L., Fu, C., Zhang, Z. C. (2010). Wireless Communications, Networking and Mobile Computing 2010. *IEEE Wicom. International Conference*, 5, 1060.

[18] Liechty, C. L., Reifsnider, E. and Durgin, G. (2013). Developing the Best 2.4 Propagation Model from Active Network Measurements. *George Institute of Technology, Atlanta.*

[19] Llorete, J., Lopez, J. J., Turro, C. and Flores, S. (2012). A fast design model for indoor radio coverage in the 24GHz wireless LAN. *In Proc. International symposium on Wireless Communications Systems, Maeritus*, 408412.

[20] Mishra, A., Shrivastava, V., Banorjee, S., and Arbaugh, W. (2006). Partially Overlapped Channels Not Considered Harmful. *ACM SIGMETRICS Performance Evaluation Review*, 34, 6374.

[21] Nwalozie, D. (2014). Path loss prediction for GSM mobile networks for Urbanregion of ABA, South - East, Nigeria. *2, International journal of computer science and mobile computing*, 3, 267-281.

[22] Ogbulezie, J.C. (2013). Site specific measurements and propagation models for GSM in three cities in Northern Nigeria. *American Journal of Scientific And Industrial Research*, 3, 40-41.

[23] Okumura, Y., Ohmori, E., Kawano, T. and Fukuda, K. (1968). Field Strength and its variability in VHF and UHF Land-Mobile Radio Services. Rev. *Electronic Communications Lab*, 16, 825-873.

[24] Oyetunji, S.A. (2013). Determination of Propagation Path Loss and Contour Map for FUTA FM Radio Federal University of Technology. *3,IOSR Journal of Electronics and Communication Engineering,*, 6, 04-09.

[25] Situn, H. (2011). Radio Wave Propagation for Telecommunication Applications. *9, Springer ISBN: 3-540-40758-8*

Design of an L-Shape Slanted Dual-Band Microstrip Patch Antenna for Long-Term Evolution Wireless Application

Muhammad Surajo, Abdulmalik Shehu Yaro, Isiyaku Yau,
Department of Communications Engineering,
Ahmadu Bello University, Zaria
muhammads@abu.edu.ng,asyaro@abu.edu.ng,isiyakuyau@abu.edu.ng

S. M. Yusuf
Department of Computer Engineering
Ahmadu Bello University Zaria, Nigeria
sheikullahi@gmail.com

ABSTRACT—In this paper, an L-shape slanted dual-band microstrip patch antenna operating at the 2.1 GHz and 2.6 GHz bands for long term evolution (LTE) application is proposed. The flame-resistant type 4 (FR-4) substrate having a relative permittivity of 4.30 and loss tangent of 0.002 is considered for the design, which is probe feed by a 50-Ω microstrip, feed line. To achieve the lower band mode of 2.1 GHz and improve resonance at the upper band mode of 2.6 GHz, a slanted L-shaped slot is loaded onto the patch. Simulation results obtained using the computer simulation technology (CST) software shows that the -10 dB operation bandwidth at the 2.1 GHz and 2.6 GHz bands are 40 MHz and 110 MHz respectively. Furthermore, the gains achieved in the lower and upper resonance frequencies are 1.79 dB and 3.06 dB respectively.

KEYWORDS—microstrip patch, antenna, reflection coefficient magnitudes, radiation pattern, L-shape slot.

INTRODUCTION

Microstrip antennas are used in several wireless applications such as wireless local area network (WLAN) [1], Wi-Fi [2, 3], and Bluetooth [4, 5]. The development of wireless technology has grown to very large extent and it has been forecasted that increase in human population will lead to increase in internet access. The presence of service for higher data rate will be the solution to answer the needs. To overcome this issue, Long Term Evolution (LTE) technology was launched. The LTE will be the stride towards the fourth generation (4G) originated from radio technology, which is designed to enhance network capacity and speed [6, 7].

The 4G a successor of second generation (2G) and third generation (3G), promises a 100 Mbps data rates in mobile devices and is yet to shower its wonders on. In the case of 4G, extra features besides that 3G are included such as multimedia newspapers and the ability to watch T.V programs with the clarity as to that of an ordinary terrestrial TV. Unlike the 3G, which is based on two parallel infrastructures consisting of circuit switching and packet switching network nodes, the 4G is based on only packet switching thus, requires low latency data transmission. Furthermore, data are sent much faster than that of the previous 2G and 3G generations. It is expected to provide a comprehensive and secure all Internet Protocol (IP) based solutions [8]. The LTE provides downlink capacity of at least 100 Mbps and uplink capacity of at least 50 Mbps [4, 9]. It has been shown that through the years, since the very first mobile phone device (1G), the cellular mobile networks have had several changes to cope with user increase, system coverage, and the necessity to transfer different kind of data such as voice, video and data packets, and the desire to make the human-machine interface more amenable. At the same time, 3G technology was reaching its limit boundary and getting full of users. The necessity to create a new technology which increments the bandwidth and the data transfer rates was compulsory. The 4G technology appears as a framework established to try to accomplish new levels of user experience and multi-service capacity by integrating all the mobile technologies that exist. Even though the 4G and 3G technologies are at different frequency bands, mobile devices must be capable of working at both frequencies. This is because there is the risk of 4G signal loss at certain areas and some countries are yet to implement the 4G technology [8].

In the wireless communication system, the role of antenna is very crucial. Wireless technology application requires a small, light weighted, cheap and easy to install antenna, without compromising its performance [6, 9], the Microstrip antenna meets some of these requirements. A special quality of Microstrip antenna is its low profile and easy in realization. In this paper, a slanted L-Shaped dual band Microstrip patch antenna for LTE wireless application is proposed, the bandwidth of the propose antenna was improved by cutting away an L-shaped slot on the rectangular patch. Two resonant modes were achieved at 2.45GHz ad 2.6GHz. The antenna was design and simulated using computer simulation technology (CST).

The remainder of the paper is organized as follows: Section 2 presents the methodology for the design of the antenna while in Section 3, the simulation result and discussion is presented. Finally, the conclusion is presented in Section 4.

METHODOLOGY

In this section of the paper, the methodology for the design of the proposed antenna is presented. The rectangular Microstrip patch antennas is the commonly adopted shape in the design of a wideband antenna capable of operating in the microwave and millimeter wave frequency bands which is considered in this paper. Fig. 1 shows the structure of the proposed slanted L-shaped antenna on the rectangular Microstrip patch. The front view of the antenna contains a rectangular radiator of about 26.78 × 33.8 mm^2 in dimension which is fed through a 50 Ω feed line probe of about 11.6 × 1 mm^2 in dimension. On the back view, there is a ground plane of about 38 × 36 mm^2 in dimension with a substrate between it (ground plane) and the radiator. A flame-retardant type 4 (FR-4) substrate with a height of 1.6 mm having a dielectric constant of 4.30 and loss tangent of 0.002 is used due to its

low cost and light weight. The larger dielectric constant in FR-4 helps in reducing the size of the patch.

The patch radiator is designed using closed-form equations for the fundamental mode in the following steps:

i. The width (W1) of the patch is calculated using (1).

$$W = \frac{c}{2f_o\sqrt{\frac{\varepsilon_r+1}{2}}} \quad (1)$$

where: $\varepsilon_r = 4.30$ is the relative permittivity of the dielectric substrate, c = speed of light in vacuum, and f_o= 2.6 GHz is the resonant frequency of the antenna.

ii. The length (L1) of the patch is determined using (2).

$$L = L_{eff} - 2\Delta L \quad (2)$$

Where: L_{eff} and ΔL are the effective length of the patch and the path length extension which are determined using (3) and (4) respectively.

$$L_{eff} = \frac{c}{2f_o\sqrt{\varepsilon_{eff}}} \quad (3)$$

$$\Delta L = 0.412h\frac{(\varepsilon_{eff}+0.3)\left(\frac{W}{h}+0.264\right)}{(\varepsilon_{eff}-0.258)\left(\frac{W}{h}+0.8\right)} \quad (4)$$

where: ε_{eff} is the effective relative permittivity of the dielectric substrate and is determined using (5).

$$\varepsilon_{eff} = \frac{\varepsilon_r+1}{2} + \frac{\varepsilon_r-1}{2}\left[\frac{1}{\sqrt{1+\frac{12h}{W}}}\right] \quad (5)$$

The h =1.6 mm in (5) is the height of the dielectric substrate.

iii. To achieve lower band of 2.1 GHz, the feed line is carefully placed at about 9 mm from the center of the patch.

iv. The length of the slanted-L slot is appropriately selected at about λ/4 of the 2.6 GHz fundamental mode, which corresponds to 7 mm (2*Ls*).

Based on the aforementioned design process, the parameters are transferred to the CST simulation software. The inclusion of the slanted-L stub can improve the upper resonant mode and by also moving the feed line of the antenna to the right-hand side (RHS) of the patch another resonance mode is achieved at 2.1 GHz. Specifically, the effects of the length *Ls* on the upper resonant mode is obvious from the concept of λ/4 slot antenna. As the length is extended above the *Ls*, it results in total rejection in the upper frequency [11]. Additionally, the lower resonance mode is achieved by shifting the long narrow feed line to the RHS of the patch. The W2 in Fig. 1a provides the position of the feed line on the antenna [9].

Other parameters like *L*, *L1*, *Lf*, *W*, *W1*, *Ws*, and*Wf*, were adjusted through parameter tuning and the final sizes f the designed slanted-L Microstrip patch antenna is shown in Table I.

TABLE I. DIMENSION OF THE PROPOSED ANTENNA

Parameter	W	W_1	W_2	W_f	W_s	L	$L1$	L_s	L_f
Values (mm)	36	33.8	25.4	1	2	38	*26.78*	*3.5*	*11.6*

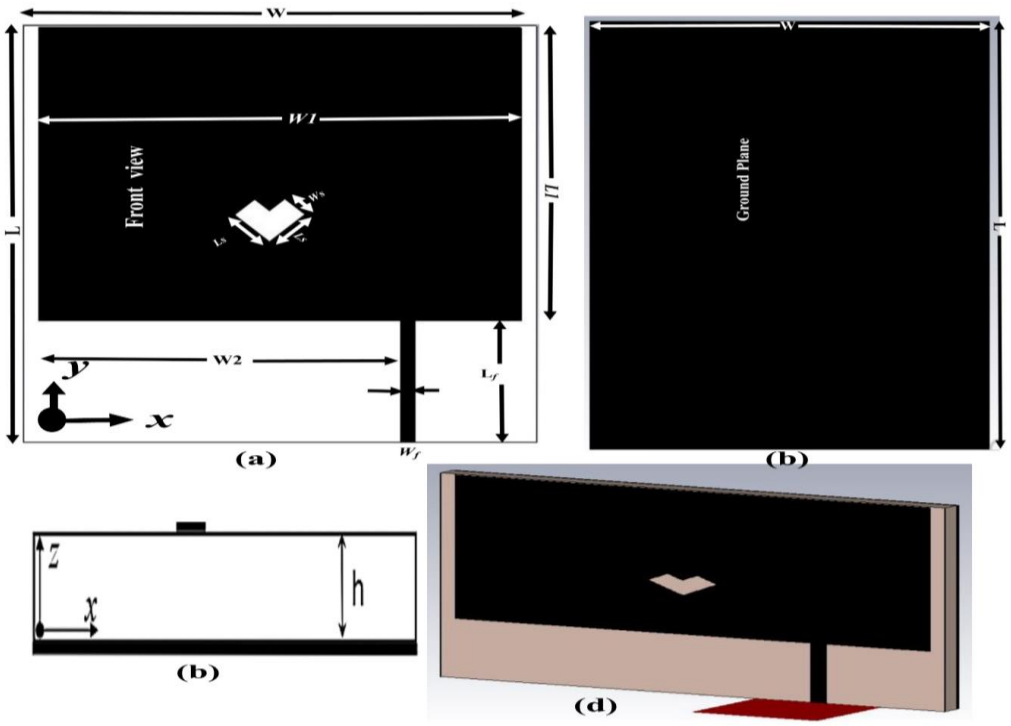

Fig. 1. Geometry of the proposed Antenna (a) Front view (b) Back View and (c) Side view. (d) Perspective view

SIMULATION RESULTS AND DISCUSSION

The initial characteristics and performance of the proposed antenna at -10 dB return loss that covers 2.08 – 2.12 GHz and 2.57 – 2.64 GHz as the lower and upper resonance frequency modes respectively, are presented in this section.

Fig. 2 shows the result of the reflection coefficient magnitude against frequency of proposed antenna and that of the background antenna obtained from the closed form model equations with its feed line at the center of the patch. The

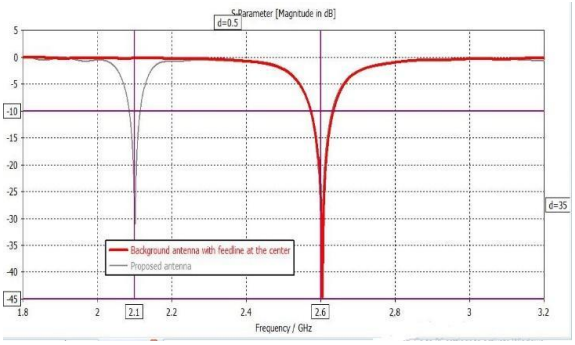

background antenna has only one resonant mode at around 2.6 GHz that correspond to $|S_{11}|$ of about -28 dB. When the feed line is tuned to about 9 mm from the center of the patch a second lower resonance mode at about 2.1 GHz is achieved.

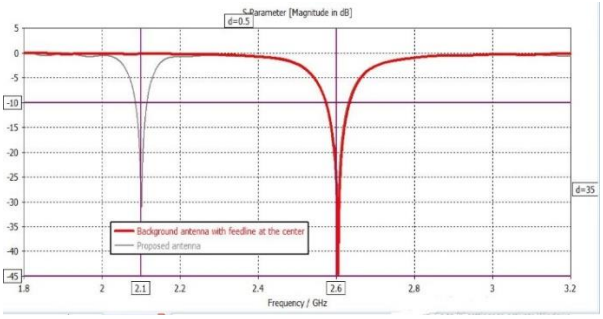

Fig. 2. Reflection coefficient magnitude against frequency for proposed and background antenna.

Fig. 3 shows the effect of the slanted-L slot cut at about λ/4 of the fundamental 2.6 GHz frequency band, and the $|S_{11}|$ increase from -28 dB to about -36.5 dB, which is presented in Fig. 4.

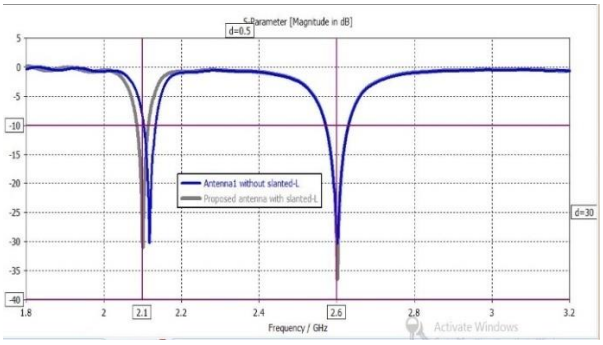

Fig. 3. Reflection coefficient magnitude against frequency showing the effects of slanted L-shape on the proposed antenna.

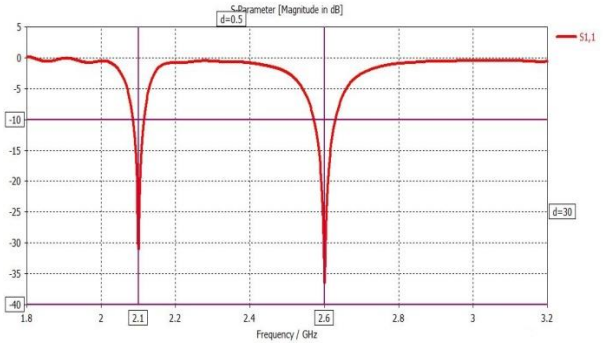

Fig. 4. Reflection coefficient magnitude against frequency for proposed antenna.

The radiation pattern shown in Fig. 5 indicate that, the proposed antenna has a maximum gain of about 1.79 dB and 3.06 dB at 2.1 GHz and 2.6 GHz respectively with a nearly omnidirectional pattern that can be used for wireless application in LTE access technology.

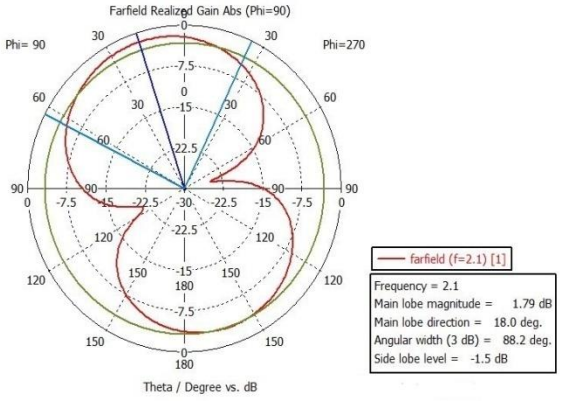

(a)

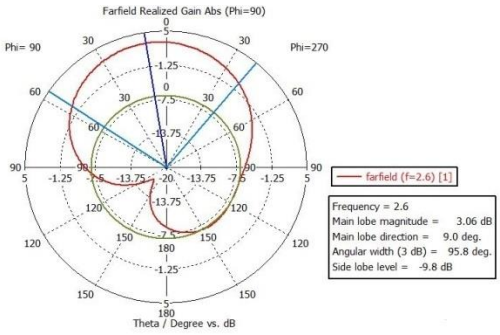

(b)

Fig. 5. Simulated 2-D radiation patterns (a) 2100MHZ (b) 2600MHz.

CONCLUSION

A new dual band slanted-L shaped antenna that operates at UMTS2100 and LTE2.6GHz frequency for LTE technology is proposed. The design antenna introduces a slanted L-shape at the center of the radiator to achieve the lower frequency. To improve the impedance matching, a 50 Ω feed line probe is shifted to right side of the patch. The total dimension of the proposed antenna is about 38 × 36 × 1.6 mm^3 which reasonable enough for wireless application. The proposed gain of the antenna in the lower and upper mode are around 1.79 dB and 3.06 dB respectively.

REFERENCES

[1] C. K. Ghosh, and S.K. Parui, "Design, analysis and optimization of a slotted microstrip patch antenna array at frequency 5.25 GHz for WLAN-SDMA system" International Journal on Electrical Engineering and Informatics, vol. 2, no. 2, pp. 106 - 110, 2010.

[2] J. G. Vera-Dimas, M. Tecpoyotl-Torres, P. Vargas-Chable, J. A. Damián-Morales J. Escobedo-Alatorre and S. Koshevaya "Individual Patch antenna and antenna patch array for Wi-Fi communication" Center for Research of Engineering and Applied Sciences (CIICAp), Autonomous University of Morelos State (UAEM), 62209, Av. Universidad No.1001, Col Chamilpa, Cuernavaca, Morelos, México.

[3] C. Ubeda Castellanos et al., "Performance of Uplink Fractional Power Control in UTRAN LTE," VTC Spring 2008 - IEEE Vehicular Technology Conference, Singapore, 2008, pp. 2517-2521.

[4] A. Majumder, "Design of an h-shaped microstrip patch antenna for bluetooth applications. International Journal of Innovation and Applied Studies, vol. 3, no. 4, pp. 987-994, 2013.

[5] S. V Doraisamy. "Design of microstrip array antenna at 5.8GHz," Department of Electrical Engineering. thesis, University Technology Malaysia. 2005.

[6] R Garg, et al., Microstrip antenna design handbook. Artech house, 2001

[7] P. Bhartia et al., Microstrip Antenna Design Handbook, Artech House Antennas and Propagation Library, 2000.

[8] D. M. Pozar and D.H. Schaubert, Microstrip antennas: the analysis and design of microstrip antennas and arrays, John Wiley & Sons, 1995.

[9] S. Muhammad., A.S. Yaro, and I. B. Alhassan, "Wide-band 4G mobile device planar antenna using couple feeding technique. ATBU Journal of Science, Technology and Education, vol. 5, no. 4, pp. 107-116, 2018.

[10] H. Liu, et al., "A multi-broadband planar antenna for GSM/UMTS/LTE and WLAN/WiMAX handsets," IEEE Transactions on Antennas and Propagation, vol. 62, no. 5, pp. 2856 – 2860, 2014.

[11] P. A. Ambresh, P. M. Hadalgi and P. V. Hunagund, "Effect of slots on microstrip patch antenna characteristics," 2011 International Conference on Computer, Communication and Electrical Technology (ICCCET), Tamilnadu, 2011, pp. 239-241

Digital Forensics Model for Mobile VoIP Cloud Computing Investigation

Joshua Edward Mamza, Ismaila Idris
Cyber Security Science Department, Federal University of Technology, Minna, Nigeria.
joshua.pg6759@st.futminna.edu.ng, ismi.idris@futminna.edu.ng

ABSTRACT—Voice over IP on Mobile Cloud Computing (mVoIPcc) is gaining acceptance as a technology for transmitting voice or video data over IP based cloud networks. This can be attributed to the ability to rapidly develop and deploy VoIP application by mobile application developers and the free billing features of VoIP in correlation to the traditional circuit switch network. This creates two precarious precedents, first of which is attack associated with vulnerability on VoIP protocols such as call management protocols (SIP) and Media Delivery Protocols (RTP). Secondly is the forensics analysis challenge to investigators due to the converged attribute of mVoIPcc communications which are not bounded to any physical location. The latter is further complicated by Cloud Service Providers (CSPs) reluctance to provide vital digital forensics data within the CSPs internal networks. This paper reveals VoIP Digital Forensics Models (f VoIP-DEFSOP and VoIP-NFDE) for detecting, reconstructing and investigating compromised VoIP systems. A hybrid cloud forensics investigation model, which consist of Forensic-as-a-Service provided by the CSPs, and investigation model that can be adapted to cloud forensics called mVoIPc-IM.

KEYWORDS – CloudService Provider, Protocols, VoIP, Forensics Analysis Models, Mobile Cloud Computing

INTRODUCTION

Voice over Internet Protocol (VoIP) calls is common in existing telecommunications modus with bright potentials as the next century generational telephone of choice or preferred. The prodigious increase in the use of VoIP application has advanced the increased research by academia and telecommunication companies or Network Service Providers (NSP). This is not in part because of the growing acceptance of VoIP application, the benefits of using this kind of technology include but not limited to low call cost for locals, long distance and international. Most people now usually use telephone calls with IP mobile devices such as (WhatsApp calls, Facebook Video Calls, Skype, Imo etc) which synchronizes speech and video data to be transmitted over a long distance with data packets. . The cost is reduced drastically with the arrival of Mobile Cloud Computing (MCC). Mobile Clouding Computing allows mobile application to be deployed on the cloud, such applications can then be accessed on multiple platforms [1]. Mobile VoIP over Cloud (mVoIPc) enables VoIP Application operates in a virtualized environment independent of the mobile devices. Using APIs on mobile devices, users connect to the virtualized VoIP services in the cloud across multiple platforms via IP networks. The proliferation VoIP applications over the cloud on multiple mobile operating systems is an exemplification of how the two technologies (VoIP & cloud computing) have completely revolutionized how users communicate [2] over IP based network.

Detecting attacks or misuse of VoIP application requires the use Network Forensics Analysis Tools (NFAT). The tools uses network traffic and log files from other network applications such as IDS and firewalls to detect and reconstruct attacks [3]. Investigating attacks or misuse of mVoIPc using current NFAT is next to impossible due to the privacy concerns from the Cloud Service Providers (CSPs). The privacy concerns leave forensics investigators restricted to only log files from the compromised mobile devices and access points and mobile base stations used by the mobile device. This is because there is little or no access to the CSPs internal networks infrastructure where vital forensic evidence that will assist in reconstruction of attacks is located. The growth of mVoIPc has created a wealth of research in to different areas of mVoIPc, one such area is forensic pattern analysis. As of the time of writing of the paper, there is no unified research paper that has exam forensic pattern analysis in respect to mVoIPc.

This paper aim to address these by critically review and analyze security architecture, threats, vulnerability and current forensics investigation models of detecting, reconstructing and investigating VoIP attacks over Mobile cloud computing. Section 2 provides overview into VoIP, Mobile Cloud Computing and implementing VoIP over Mobile Cloud Computing. Section 3 takes a critically reviews at current VoIP Forensics Model and Patterns Analysis Frameworks, we also review current forensic evidence detection and reconstruction models. Section 4 we proposed mVoIPc forensics model for investigating VoIP attacks over cloud. Lastly is the conclusion in Section 5

OVERVIEW

Voice over IP is a technology that allows communication over broadband internet. Using IP networks, VoIP allows voice and video packet to be transmitted over public network such as the internet instead of the traditional fixed or mobile telephony. VoIP can be use to make audio or video calls between two points that is the source terminal and the destination terminal, which can be personal computer workstations, VoIP phones, mobile

devices or two or more traditional phones provided they are connected to an IP network. The cost for user or an actor is neglibale compared to the use of VoIP applications is rapidly changing how users communicate universally. VoIP can be used for both business and domestic purpose. The emergency of MCC has greatly increased the proliferation of VoIP applications on mobile platforms. Operating in client-server architecture, MCC allows VoIP users connect to VoIP server installed virtually on the cloud. Using an APIs installed on mobile devices, VoIP phones, Computers, calls are initiated which is then routed through the cloud server to the destination user. In these section we critically examine current SIP based VoIP architecture, we also exam MCC and implementation of VoIP on MCC.

A. Voice over IP Architecture

The traditional phones system is based on copper wires carrying analog voice data over the dedicated circuits. Calls are transmitted over a dedicated channel between two points for the duration of the call. In SIP based VoIP, analog voice packets are converted into to digital voice packet using voice codecs. User calls are initiated and authenticated using Signaling Protocols (SIP) and Media Transfer Protocols such as Real-Time Transport Protocol (RTP) are used to transmit digitized voice packets over IP network. In SIP based VoIP consist of different component which includes User Agents and Proxy Server. SIP supported VoIP architecture uses proxy servers for call routing. The proxy server provides security mechanism for the terminal or mobile devices such as Authorization, Authentication and Accountability [4]. Below shows a hybrid VoIP SIP based architecture.

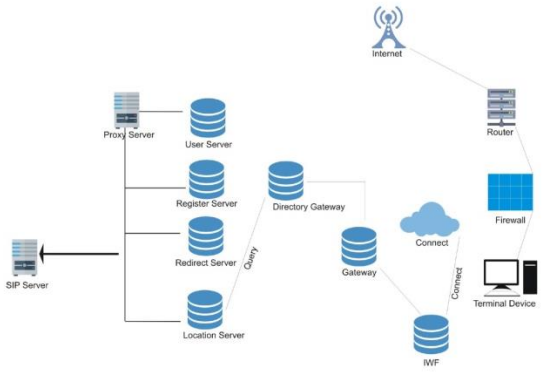

Fig. 1. Hybrid VoIP Signaling Protocol Architecture

The SIP User Agents (UAs) represents the phone and there are two parts to UAs: client and server, the client portion is called the User Agents Client (UAC) while the server portion is called the User Agent Service (UAS) [5]. The Register Server receives registration and requests update of Location Server which keeps track of UAs. The UAC is responsible for initiating a call by sending a URL-Addressed INVITE to the intended recipient UAC, while UAs receives the request and send back responses [6]. The proxy server is connected to a VoIP gateway and other proxy servers. In most cases the Location and Register Server are integrated into the Proxy Server. The Redirect Server functions as a router, it receives request, determines the next-hop server and return's the address of the next-t-hop server to the client instead of forwarding the request.

B. Mobile Cloud Computing (MCC) Architecture

Cloud computing also refer to as grid computing or virtualization is exemplify by [7] as a model of convenient, on-demand network access to computing resources such as network, servers, storage, applications, and services that can be rapidly deployed with little management by CSPs. Based on the IT resource been provided, cloud computing are classified into three (3) category which are Infrastructure as a Service (IaaS), Software as a Service (SaaS) and Platform as a Service (PaaS). Cloud computing has completely transform how users consume IT across different platforms, one field cloud computing has transformed user IT usage is Mobile Cloud Computing (MCC). This is fast emerging as one of most exceptional branch of cloud computing and is expected to broaden the mobile eco system. [8]. MCC can be described as an on-Demand model of access IT resource over mobile networks. MCC enable applications operate autonomous of the mobile device by mitigating device data, processing power and storage. As a result mobile applications are rapidly developed and deployed with minimal efforts or CSPs reciprocal action. Using APIs on the mobile device, the mobile device send service request to the cloud server via access points, the cloud server allocates resources to the received request to establish connection [9]. Figure 2 shows an example of MCC architecture.

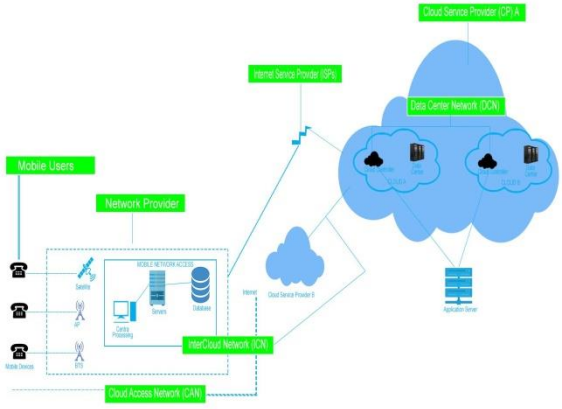

Fig. 2. Architectures of Mobile Cloud Computing

As seen on Figure 1, MCC architecture consist of mobile devices, mobile networks service (BTS and Access Point) provided by the mobile operator, the internet access provided by the Internet Service Provider (ISP) and lastly the CSPs infrastructure which contains the application server, Cloud Controller and the Cloud Data

Center. The critical elements interconnecting the various MCC architecture is the networking. As shown in Figure 2, we divided the network into three (3) segments, which are Cloud Access Network (CAN), Data Center Network (DCN) and Intercloud Network (ICN) [10].

CAN enable mobile device user's access to the cloud network, the segment consist of the wireless access point and satellites, it also consist of central processing, home agent and security (Authorization, Authentication and Accountability) servers which is provided by the mobile network operator. The DCN enables clusters of computers or application server interconnects with each other, in a sense DCN allows data center to data center intercommunication. The Application servers are located in these network segment include cloud controllers. The ICN enables two cloud infrastructure communicate with each other. Similar to DCN, it is located and controlled by the CSPs [10]

C. Architecture of Mobile Cloud based Voice over IP

Migrating storage space and computing power to the cloud service provider sees Mobile Cloud Computing (MCC) applications gaining popularity across the global. One such application that is retrieving due to the emergency of MCC is VoIP. The early VoIP system mirrors the architecture of legacy telephone network system and other VoIP system such as skype are based on closed private p2p secure networks. Depending how VoIP is implemented on MCC, VoIP services can be offered to user as Platforms as a Service (Paas) and Software as a Services (SaaS). Figure 3 shows the deployment of mVoIPc over Cloud Computing.

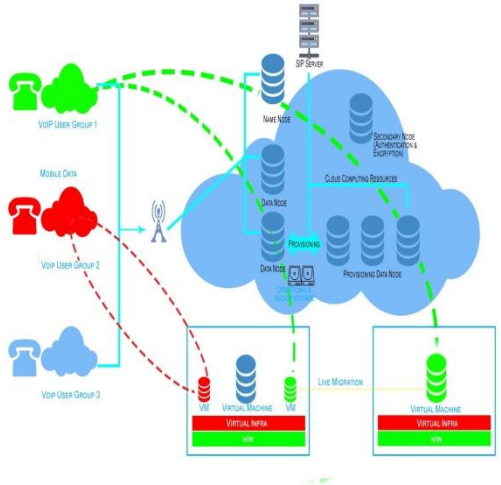

Fig. 3. Architecture Mobile Cloud based Voice over IP

In MCC based mVoIPc, the SIP proxy, Registration Servers are installed and configured on the CSPs servers. Using heterogeneous networks (wireless network, mobile network operators) Users access the VoIP cloud on smartphones, personal computers and other devices with internet access.

VOIP FORENSICS MODEL AND PATTERNS ANALYSIS FRAMEWORKS

The openness nature of VoIP protocols (SIP and H.323) and the inherit vulnerability associated with IP based real-time services such as VoIP permits such systems susceptibility to attacks by malicious users. Identifying, collecting, preserving and analyzing legal digital evidence is the primary aim of Network Forensics. In VoIP forensics, network patterns are used to analyze voice packet based on collected VoIP network traffic [11]. These method helps investigator to identify, detects, trace, investigate and determine attack point of origin and attack behavior [12]. Detecting VoIP digital evidence requires comparing normal and abnormal VoIP network traffic, when insufficient information for investigation is lacking, VoIP model employs the use Secure Temporal logic of action (S-TLA). S-TLA enable VoIP forensics model reconstruct digital evidence where lack of sufficient information about an attack is not available [13] [14]. This model also provides reliability and integrity for the collected information, validates the authenticity of the provided evidence, and allows NFIs to capture unknown attacks undetected by other network forensics methods [10]. In this section, we critically review current VoIP forensics analysis models and we review current network traffic capturing techniques used during VoIP forensics.

Current Network Forensics on wired and wireless networks can rapidly access compromised networks and network devices, but reverse is the case when investigating similar attacks on system over MCC [15]. This is because Network Forensics Investigators (NFI) restricted access to the internal networks and other resources of the CSPs, these in turn complicate acquisitions of forensics data and other critical forensics investigation procedure such as Access to Artifact and Chain of Custody respectively.

Another area of concern is user data privacy on the cloud, such as alteration of data by unauthorized users on the cloud, privacy of user data during forensics investigations' and integrity of user data during migrating between cloud networks. In this section, we take a critically look at current forensic mode and pattern analysis framework, in relation to detecting, collecting, examine and analyzing digital evidence at different segments of MCC (CAN, DCN and ICN) network [10]

Table I. VoIP Forensic and Pattern Analysis Framework

VOIP FORENSIC MODEL	
VOIP FORENSIC MODEL & PATTERN ANALYSIS FRAMEWORKS	
1	VoIP Network Forensic Digital Evidence (VoIP-NFDE)

2	VoIP Digital Evidence Forensics Standard Operating Procedure (VoIP -DEFSOP)

As seen from the Table I current VoIP network forensics model and pattern analysis frameworks. We grouped the models into two namely VoIP Forensics model and VoIP forensic pattern analysis frameworks.

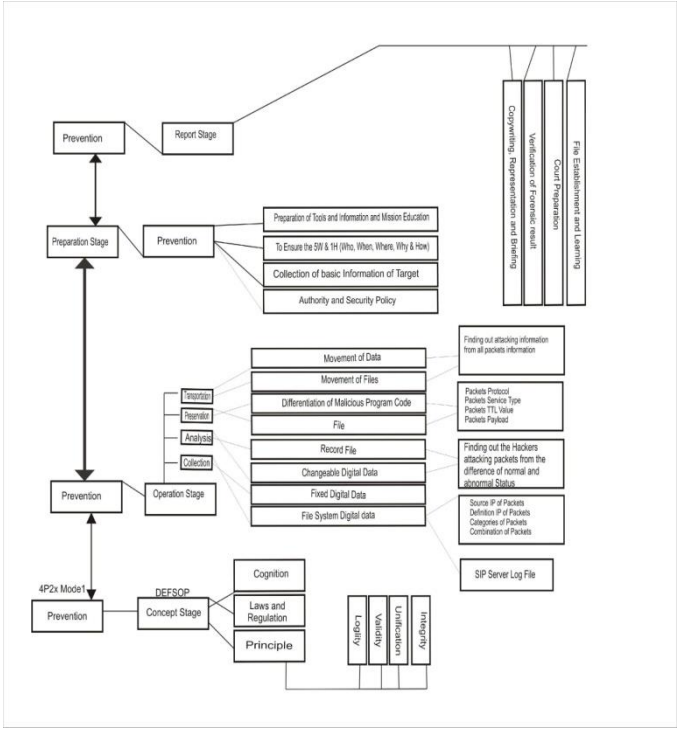

Fig. 4. DEFSOP Model

The first responders must exercise with caution when they seize any electronic device. The second stage is the Preparation Stage; the stage involves preparations before forensics investigation in order to prepare for the Operational stage of the VoIP-DFESOP. The preparation stage involves having basic information about the crime scene, preparing forensics tools needed, identifying forensic team members and a proper briefing relating to the crime scene. The third stage is the Operation Stage; this is the most important state on the VoIP-DEFSOP. It deals with the precaution taken in collection, preservation and transporting of digital evidence. More

mVoIPc FORENSICS ANALYSIS

Digital forensic is a technology to identify, collect, examine, analyze, and still preserve the integrity of the digital evidence such as data, finger prints etc. These crimes are usually in modern high technology. [23]. Cloud computing, which is designed to support and provide large-scale data processing, to support on-demand services. However, to support forensic investigation and examination on the cloud, especially on real time

A. VoIP Network Forensic Digital Evidence (VoIP-NFDE)

Due to the nature of openness of VoIP protocols (SIP and H.323) and the vulnerably that is associated with IP based real-time services such as VoIP permits attacks by malicious users or clients. VoIP evidence are identified by comparing the abnormal and normal voice packets during VoIP communication [10]. [20] proposed a digital forensics evidence procedure for VoIP network forensics. One such digital forensics evidence procedure is Digital Evidence Forensics Standard Operating Procedure (DEFSOP) for VoIP network forensics. VoIP DEFSOP is based on [21] Prevention and Protection are connected to security, while Preservation and Presentation are connected digital forensics. These is called the Four P's i.e 4Ps. [22] DEFSOP is made up of four (4) stages namely Concept Stage, Preparation stage, Operation stage and Report stage. These four stages form are broken down as shown in Figure 4 which shows VoIP-DEFSOP structure with 4P's Model.

The Concept Stageis the first stage of VoIP-DEFSOP, the concept stage deals with a set of procedural rules for forensics by the first responder (an Investigator) to abide by. The first responder should be familiar with the information in forensic guide and perform his duties and responsibilities ascircumstances dictate. This ensures evidences collection is done following procedural rules with warrant and also ensures obtaining digital evidence legally without violating other information found on the compromised devices.

so, it can also be determine by court judgment. The operation stage recognize, identify, seize and secure all digital evidence at the scene. Documents the entire scene and the specific location of the evidence found. Collect, label and preserve the digital evidence and finally package and transport digital evidence in a secure manner. The Report Stage is the final stage of the VoIP-DEFSOP. This is where courts make judgments based on collected and analyzed forensics evidence obtained at the scene of the crime [21, 22]. In other to identify or collect forensic evidence and investigates, VoIP packet need to be collected in real-time and stored for forensics analysis. In the next section, we discuss VoIP network traffic capturing techniques.

applications such as VoIP, multiple challenges such as the inability of computer systems to make use of information among current forensic investigation tools, technique and models must be overcome[24, 25]. Current VoIP forensics analysis (VoIPEM, VoIP-NFDE and VoIP-DEFSOP) outlines and models depend on network traffic analysis techniques such as Logging, packet marking, forensics intrusion tolerance, forensics Examination, and interaction. VoIP forensics investigator or first responder adopt these network traffic analysis techniques to record, store,

examine VoIP packet, and may be reconstruction attack situations.

The distributed nature and the layered network structure of the cloud presents two critically challenge to digital forensics investigators, first, is the large surface area of investigation due to the distributed nature of the cloud and secondly the restrict access of the internal Document Control Number and Internal Control Number (DCN and ICN) cloud network to forensics network traffic analysis techniques. The latter further complicated evidence identification, gathering and analysis on MVoIPc because critically VoIP component such as Registration server, SIP server are placed within the internal network. To overcome these cloud forensics challenge, we propose to develop a hybrid digital forensics investigation framework, which consist of Forensics-as-a-Service from the Cloud Service Providers (CSPs) and a VoIP forensic investigation model called VoIP-Cloud Forensics Evidence Model (VoIP-CFEM). This proposed model enables forensic investigators access too critically analyzes forensics evidence without compromising the internal CSPs network and most specially the privacy of the cloud users or clients.

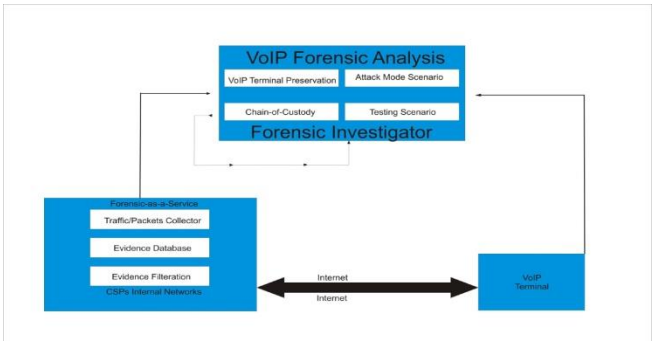

Fig. 5. VoIP Forensic Analysis Model

From the Figure 5 shown, the proposed cloud forensics MVoIPc-IM. The proposed model consists of two components, the Forensics-as-a-Service Evidence Accumulator FEA and Forensics Investigation Procedure (FIP). The proposed model is designed to ensure critically forensics data are collected, stored and filtered without compromising the privacy of a user or client. The proposed model also eliminated the interoperability of current VoIP forensics investigation techniques. We take a critically look at each of the component of the proposed model. First component (FEA) of the proposed model is designed to collect, stores and fitter VoIP data in real-time. It collects VoIP packet from different VoIP components that resides within the CSPs internal network. The FEA consist of three components namely the Traffic/Packet Collector, Evidence Database and Evidence Filtration.

The Traffic/Packet Collector component of the FEA gathers network traffic request and VoIP packet the Real Time Transport Protocol (*which delivers audio and videos over IP network)* and Real Time Control Protocol *(use to monitor transmission and quality of service)* (RTP and RTCP) between user VoIP terminal and VoIP server. Such component includes SIP Authentication and Registration server. Evidence Database, this stores collected VoIP network packet. Evidence Filtration, the stores data is filtered in other to ensure the privacy of other users. The second component of the proposed MVoIPc-IM is the Forensics Investigation Procedure (FIP). The procedure aims to address the challenges of interoperability of current VoIP forensics investigation models by granting access to CSPs data. FIP consist of four (4) sub-components namely Chain-of-Custody, VoIP Terminal Preservation, Attack Mode Scenario and Reporting.

Chain-of-Custody: The chain of custody refers to the documentation or paper trail, showing the seizure, collection, control, transfer, receipt, analysis, storage, and disposition of the digital and electronics evidence. A chain of custody is also validating how any kind of evidence (Digital or Electronics) have been collected, tracked and protected. Chain of custody must answer the following questions. Where is the evidence? How did the analyst get it? When was it collected, who and who handled it? Why the mentioned person did handled it? Where the evidence was ultimately stored? The investigator should ensure that he knows each step the person to whom the evidence was handled over. He must also ensure that such persons has an approved authority to have the evidence in his custody. This ensures that any results we report relate beyond all reasonable doubt to a particular crime in a court of law [26]. In this paper, the author will consider forensics cloud data collected from CSPs has a tool for forensics investigations.

CONCLUSION

Due to increase in the use of VoIP application has advanced the increased research by academia and Telecommunication Companies (TC) or Network Service Providers (NSP). Using the Cloud, VoIP are virtualized on servers to be accessed on-demand. This make VoIP application over the cloud easily installed, configure and rapidly deployed with little management by CSPs. The openness nature of VoIP protocols (SIP and H.323) and the inherit vulnerability associated with IP based real-time services such as VoIP permits such systems susceptibility to attacks by malleolus users. The benefits of using VoIP over cloud, presents forensics challenge to digital forensics investigator. In conducting network forensics investigations in a VoIP environment, the collection of voice packets in real time and the use of automatic mechanisms are fundamental.

This presents three critically challenge forensics investigators. The first is the distributed characteristics of the cloud, secondly the large investigation area covering different location geographically. Thirdly the restrictive nature of the internal cloud network infrastructure and the lack of interoperability of current VoIP forensics (VoIP-NFDE and VoIP-DEFSOP) investigation framework and models. We proposal developing a hybrid digital forensics

investigation framework which consist providing Forensics-as-a-Service from the CSPs. This proposed model enables forensic investigators access to critically forensics evidence without compromising the internal CSPs network and most specially the privacy of the cloud users or clients.

REFERENCE

[1] P. Andriotis, G. Oikonomou, and T. Tryfonas, "*Forensic analysis of wireless networking evidence of Android smartphones*," in *Information Forensics and Security (WIFS), 2012 IEEE International Workshop on*. 2012..

[2] R. Bhadauria, "A Survey on Security issues in cloud computing and preprint," arXiv: 1109.5388, 2011.

[3] R. Bhadauria, S. Sanyal, "Survey on Security issues in cloud computing and associated mitigation techniques,".

[4] A. J. Duncan, S. Creese, M. Goldsmith, "Insider Attacks in cloud computing. In: proceeding of the trust," Security and Privacy in Computing and Communications (TrustCom), 2012 IEEE 11th International Conference on 2012. IEEE

[5] E.B. Fernandez, J.C.P., and M.M. Larrondo-Petrie, "*Security patterns for voice over IP networks,"* Proceedings. of the 2nd IEEE Int. Multiconference on Computing in the Global Information Technology, 2007.

[6] J. C. Fernandez, P.a.E.B., "*VoIP network forensic patterns"*.in Proceedings of the 4th International Multi-Conference onComputing in theGlobalInformationTechnology (ICCGI '09),, August 2009. 180: p. 175.

[7] N. Gupta, and A. Agarwal. "*Context aware Mobile Cloud Computing: Review,"* in *Computing for Sustainable Global Development (INDIACom), 2015 2nd International Conference on*. 2015.

[8] Y. Guang, , B. Jun, and A.V. Vasilakos, "*Passive IP Traceback: Disclosing the Locations of IP Spoofers From Path Backscatter,"*. Information Forensics and Security, IEEE Transactions on, 2015. 10(3): p. 471-484.

[9] F. GEREA,,"*Implementation of Cloud Computing into VoIP"*. Database Systems Journal, 2012. III, no. 2.

[10] SH Madni, M. S. Latiff, Y. Coulibaly "Recent advancements in resource allocation techniques for cloud computing environment: a systematic review," Cluster Computing. 2017 Sep 1;20(3), pp. 2489-533.

[11] M. M. Ibrahim, M.T. Abdullah, and A. Dehghantanha. "*VoIP evidence model: A new forensic method for investigating VoIP malicious attacks"*. in*Cyber Security, Cyber Warfare and Digital Forensic (CyberSec), 2012 International Conference on*. 2012.

[12] I-Long Lin, Y.-S.Y., Bo-Lin Wu, Hsiang-Yu Wang, *VoIP Digital Evidence Forensics Standard Operating Procedure (DEFSOP).* International Conference on Broadband, Wireless Computing, Communication and Applications, IEEE, 2010.

[13] Juan C. Pelaez, E.B.F., *Network Forensics Models for Converged Architectures.* International Journal on Advances in Security, 2010,.vol 3 no 1 & 2.

[14] J, et al. *(Im)proving chain of custody and digital evidence integrity with time stamp*. in*MIPRO, 2010 Proceedings of the 33rd International Convention*. 2010.

[15] SH Madni, Latiff MS, Abdullahi M, Usman MJ. Performance comparison of heuristic algorithms for task scheduling in IaaS cloud computing environment. PloS one. 2017 May 3;12(5):e0176321.

[16] Kotwal, P.A. and A.R. Singh. *Evolution and effects of mobile cloud computing, middleware services on cloud, future prospects: A peek into the mobile cloud operating systems*. in*Computational Intelligence & Computing Research (ICCIC), 2012 IEEE International Conference on*. 2012.

[17] Khan, S., et al., *A Comprehensive Review on Adaptability of Network Forensics Frameworks for Mobile Cloud Computing.* The Scientific World Journal, 2014. 2014: p. 27.

[18] Kuhn, D.R. Walsh, T.J; Fries, S. Special Publication 800-58: Security Considerations for Voice Over IP Systems; NIST: Gaithersburg, MD.USA,2005.

[19] Latiff MS, Abdul-Salaam G, Madni SH. Secure scientific applications scheduling technique for cloud computing environment using global league championship algorithm. PloS one. 2016 Jul 6;11(7):e0158102.

[20] Kumar, R. and S. Rajalakshmi. *Mobile Cloud Computing: Standard Approach to Protecting and Securing of Mobile Cloud Ecosystems*. in*Computer Sciences and Applications (CSA), 2013 International Conference on*. 2013.

[21] Lin, I.L., et al. *VoIP network forensic analysis with digital evidence procedure*. in*Networked Computing and Advanced Information Management (NCM), 2010 Sixth International Conference on*. 2010.

[22] Osanaiye, O., Choo K-K.R., Dlodlo , M. 2016. Distributed Denial of Service (DDOS) resilience in cloud: review and conceptual cloud ddos mitigating frame work

[23] Pelaez, J.C. and E.B. Fernandez. *VoIP Network Forensic Patterns*. in*Computing in the Global Information Technology, 2009. ICCGI '09. Fourth International Multi-Conference on*. 2009.

[24] Pelaez, J.C., *Voip network security and forensic models using patterns*. 2007, Florida Atlantic University. p. 187.

[25] RohasNagpal. Introduction to cyber crime investigation, Asian School of Cyber Laws published in 2012 p.19-23

[26] SitiRahayuSelamat, R.Y., Shaharin Sahib, Nor Hafeizah Hassan, MohdFaizalAbdollah,

ZaheeraZainalAbidin, *Traceability in Digital Forensic Investigation Process.* IEEE conference publication, 2011: p. 101-106

[27] Sally, J., *Major Reasearch Issues in Forensic Computing.*nineth "2007 Internet Space: Information, Laws and Society," TheoriticalReasearch and Practice Coriference,, 2007.

[28] W. Ren, H.J., *Distributed Agent-based Real Time Network Intrusion Forensics System Architecture Design.* Proceedings of the 19th International Conference on Advanced Information Networking and Applications, 2005

[29] Yanik, T., et al. *Evaluating SIP proxy servers based on real performance data*. in*Performance Evaluation of Computer and Telecommunication Systems, 2008. SPECTS 2008. International Symposium on*. 2008.

Development Of A Microcontroller Sun Tracker For Efficient Photovoltaic Electricity Generation

H. A. Abdulkareem, A. M. S. Tekanyi, and U. N. Chkeluba
Communication Engineering Department
Ahmadu Bello University, Zaria, Nigeria
ha2zx@yahoo.com; amtekanyi@abu.edu.ng

ABSTRACT: ***Solar energy is rapidly gaining importance as an alternative source of energy. To make solar energy more viable, the efficiency of the solar panel system must be maximized. A feasible approach to maximize the efficiency of the solar panel system depends on the accurate and effective sunlight tracking mechanism of the system. This paper developed a system that accurately moves and positions the solar panel directly with the sunlight so that maximum sunlight intensity falls on the panel. The system uses a motor to change the position of the solar panel to be in line with the falling light intensity of the sun. The motor is controlled by Atmel 89c51 microcontroller that has the ability to detect the sunlight using photocells. The Liquid Crystal Display (LCD) integrated into the developed system displays the charging voltage of the PV module at every point in time.***

INDEX TERMS: ***Microcontroller, Sunlight, solar cell, luminous intensity, and solar energy electricity generation***.

INTRODUCTION

Concerned individuals, scientist's governments, and other agencies nowadays feel uncomfortable about the global warming situation and started researching into other forms of clean energy generation. One of the ways to reduce global warming is to reduce the utilization of electrical energy and change to a natural energy source from wind, water, sunlight, and geothermal heat. For example, this change is achieved by converting sunlight energy from solar panel, wind energy from wind turbines or that of water from water turbines into electrical energy. The conversion is feasible through solar panel installations, wind turbine installations, etc. Every solar energy project installation has the solar panel, battery bank, charging control unit, and an inverter. The sun that provides the photon energy required for electricity generation is directly affected by the weather condition each day. Hence, weather condition is the contributing factor that affect the performance of (amount of energy generated by) the solar panel. Electricity is produced directly from photovoltaic (PV) cells. These PV cells are made from material (for example silicon) that when sunshine falls on it, the photons of light excite their electrons and cause them to flow as electric current or electricity [1*; 3*]. Sunlight photons are small particles of light energy which are absorbed when they fall on material of a solar cell or photovoltaic panel. Photovoltaic light energy is used in a number of ways, but primarily to power homes that are connected to the public utility grid [4]. Atoms of material that makes up a photovoltaic cell absorb energy from light wavelengths corresponding to the visible spectrum. The silicon that makes up the solar panel cells is mixed with two different impurities that produce positive and negative charges (moving electrons or current) in the form of electricity [5*; 8*]. The change of light intensity falling on a solar cell changes all the parameters, including the open circuit voltage, short circuit current, the field factor, panel efficiency, and impact on the entire series and shunt resistances, that is, the increase or decrease of the light intensity has a proportional effect on the amount of power output from the panel [6]. The solar cell is a semiconductor material that converts visible light into direct current for usable electricity [*7*]. Through the use of solar arrays, a series of solar cells are electrically connected to generate a DC voltage that can be used on a load and an increase of solar arrays results in higher output of usable electricity [*6*].

2. METHODOLOGY AND DESIGN

In order to achieve the set objective of sun movement tracker, a physical prototype model is developed using locally sourced materials, which comprise the microcontroller circuit that provides the logic function that determines when to accurately tilt the PV cell to the direction of the sun and the mechanical unit that takes control instruction from the log control circuit and carry out the required task. The to achieve the prototype also covers the software aspect. The step by step procedure adopted in this paper to develop the microcontroller sun tracker is highlighted as follows:

1. Design Specification
2. Input Interface Design
3. Process Flow Chart
4. Output Interface Design
5. Integrating the Sub units to form a Module

2.1 Design Specification

The project was designed to fulfill the following three conditions for efficient output delivery:

1. Input voltage 12V.
2. Input current 6A.
3. Maximum angle of rotation of 240 degrees.

2.2 Input Interface Design

The input interface of this work is the sensor made of Light Dependent Resistor (LDR), two of which were used. The configuration of each sensor is as shown in Figure 1. The LDR is a variable resistor, whose resistance decreases (vary) with the increase in light intensity. The varying resistance is converted into varying voltage that the microcontroller can measure. The LDR and the resistor act as a potential divider to the input of the comparator as shown in Figure 1. The supply voltage, V_{cc} is 5V and connected to port 1 of pin 4 and 6 of the microcontroller. This arrangement makes the LDR resistance varies according to the light intensity.
The current through the resistors is given by:

$I = V_{cc}/(R_1 + R_{2)}$ (1)

From Ohm's law, at the positive pin of the comparator:

$V_o = I \times R_1$ (2)

The comparators output voltage can be determined by substituting equation (1) into equation (2):

$V_o = V_{cc} \times R_1/(R_1 + R_2)$ (3)

where, V_o is the output voltage of the comparator and R_2 is the LDR resistor value, R_1 is the resistor in series with the LDR resistor.

$V_o = 5 \times 10/(10+5)$

$= 3.33V$

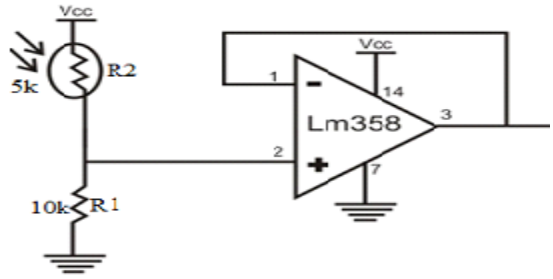

Figure 1 Input Interface Design [6].

The LDR is interfaced with a dual single supply LM 358 operational amplifier as shown in Figure1 and the output of the amplifier is connected to the microcontroller port of pin what? One of the sensors acts as a pilot or tracker that always looks for the direction of the sun's highest intensity to position the panel. The second sensor acts as omnidirectional sensor, which detects the presence of sun light at all times.

2.3 Process Flow Chart

The process control flowchart shows the flow sequence that determines when the solar panel tray should rotate and in which direction. Other sequences not presented on Table 1 are not valid in the design. The following logic table is used in the development of the flow chart.

Table 1: Logic Table of Sensor

Pilot Sensor	**Omni Sensor**	**Action**
0	0	Resting Position
0	1	Tracking Sun
1	0	Stop Tracking

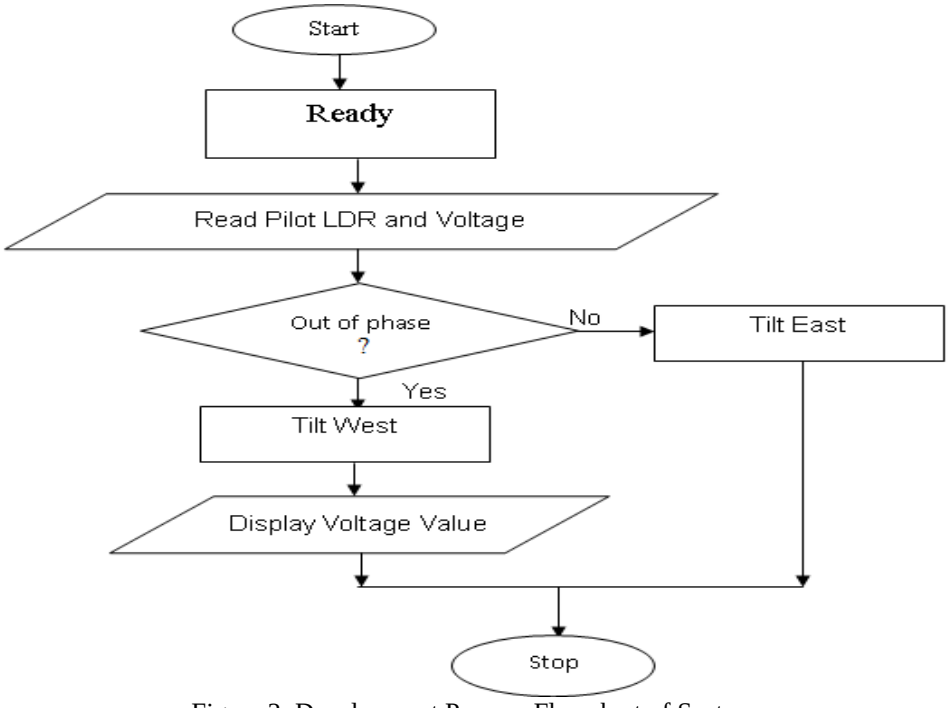

Figure 2: Development Process Flowchart of System

Figure 2 represents the flow sequence of actions to be taken as indicated in Table 1. The flowchart shows the design logic followed in the development of the program that determines the direction of the tracker. At start, microcontroller reads the state of pilot LDR in order to know what action is required taking and an appropriate instruction given. If solar module

is out of phase with light intensity, microcontroller commands the motor to tilt the solar module to the West position (assuming that the module was in the East position) and stops once it senses high intensity of light and displays the voltage value of the solar module at that point. If pilot LDR is in phase with the light intensity, microcontroller commands the motor to tilt the solar module to East position, stops it, and displays the charging voltage.

2.4 Output Interface Design

The output interface consists of a DC motor configuration used in the implementation of the motorized jack that is made of two transistors coupled with relay as shown in Figure 3. The relay enables mechanical switching to activate the motor.

At the base, a pull-up resistor is used to switch the transistor on when the system is powered "ON". The operating mode of the transistor in digital form is that the collector produces logic 1 when the base is not biased. When the base is biased, the output of the collector is logic 0. Now the relay is connected to Vcc on one terminal and the other terminal is controlled by the collector output of the transistor as shown in Figure 3. In this case, the transistor is biased, the collector reads 0, and thus completes the circuit for the relay to switch "ON".

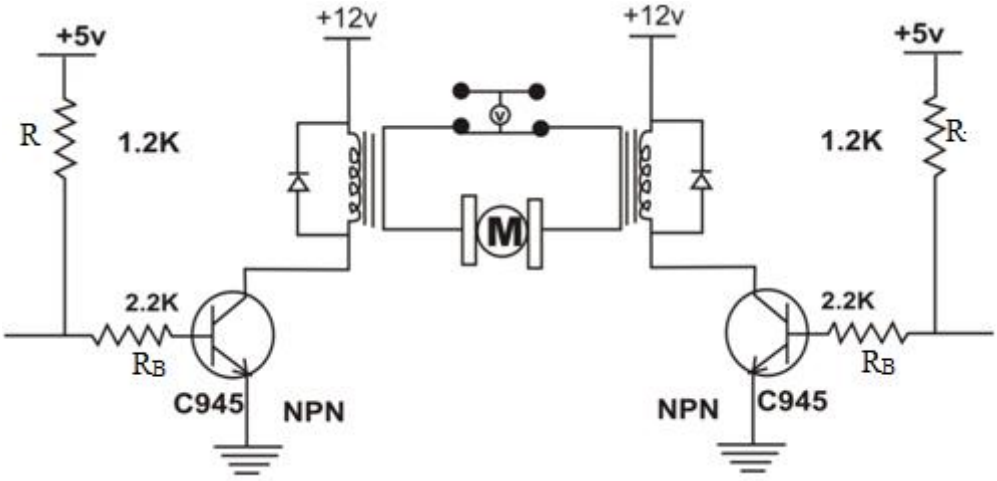

Figure 3. DC Motor Configuration [6]

The value of the base resistor, R_B is calculated as follows:

$$R_B = \frac{V_{CE} - V_{BE}}{I_B} \quad (4)$$

Q_1= C945
$I_{C\,max}$ = 100mA
$h_{fe\,(min)}$ = 40
$h_{fe\,(max)}$ =500
where, $I_{C\,max}$, $h_{fe\,(min)}$ and $h_{fe\,(max)}$ are determined from the data book.

$$I_E = I_C + I_B \quad (5)$$

$$h_{fe} = \frac{I_C}{I_B} \quad (6)$$

$$V_B = V_{CC} - V_{BE} \quad (7)$$

where, I_E is emitter current, I_C iscollector current, I_B is base current, and $I_E = I_C$, h_{fe} is current ratio transfer.

Assuming that h_{fe} for Q_1 is 40, substituting the values of equation (6) gives base current, I_B as:

$I_B = \frac{100mA}{40}$
= 2.5mA.

When Q_1 is "ON" (saturation point), $V_B = V_{CC}$, but at any point the two are not equal. Hence from equation (7):

$V_B = 5 - 0.7$
= 4.3V.

Substituting the value of V_B (4.3V) into equation (4) yields:

$R_B = \frac{4.3}{2.5mA} = 1720\Omega$

But 2.2kΩ was chosen as the closest resistor value from the data book. Give reasons

2.5 Integrating the Sub Units to form a Single Module

The complete circuit diagram of Figure 4 shows the integration of all the sub units to the microcontroller. The microcontroller ports are used to interface the various sub units. The Analog to Digital Converter (ADC) is interfaced to port 0, the LCD is interfaced to the port 2, the motor unit is interfaced to port 3, and the operational amplifier is connected to port 1 of the microcontroller.

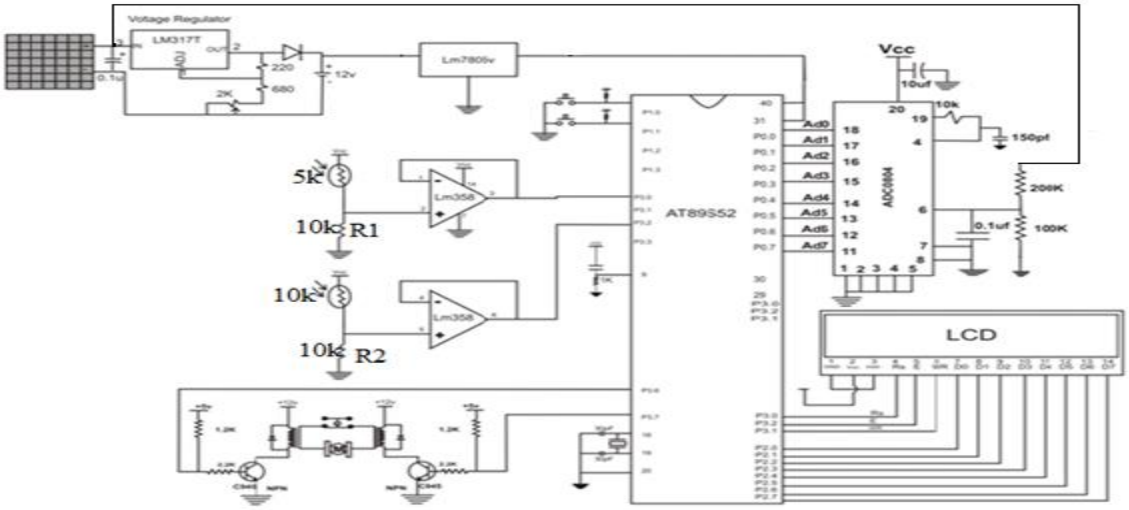

Figure 4: System Complete Circuit Diagram [1

RESULTS AND DISCUSSION

This section covers the results obtained after testing the prototype that was produced. Each result obtained from the test was adequately discussed. Such discussion brought about an complete summary of contributions achieved from this work.

Testing and Result

The developed system was completed and the control program downloaded into the microcontroller. The system was then installed and tested. While tracing the sun, the values of the LDR of both fixed panel and tracking panel at various instances were read through the ADC. The programs on the microcontroller converted the values back to voltage value and were hence displayed on the LCD.

The values both tracking panel and fixed panels were obtained at different hours from 6:30am to 6:30pm in the month of July, 2018 and recorded accordingly as shown in Table 2. The month of July, 2018 was chosen because this is the month when average cloud and sun conditions were observed in Kaduna.

Table 2 shows the voltage increase that was recorded by the panel that was tracking the sun when compared to those of the panel (static flat panel) that was not tracking the sun movement. It was observed that at that point when both panels were at the same inclination to the sun, their respective voltages were the same. It happened at midday when the sun is directly overhead.

Time of the day in July, 2018	**Readings of Voltage**	
	Static Flat Panel	**Tracking Panel**
06:30Hrs	0.196	1.477
07:30Hrs	0.249	2.104
08:30Hrs	0.225	3.411
09:30Hrs	0.723	3.783
10:30Hrs	2.011	3.900
11:30Hrs	3.910	4.657
12:30Hrs	4.888	4.990
13:30Hrs	3.803	4.990
14:30Hrs	3.456	4.985
15:30Hrs	3.930	4.892
16:30Hrs	1.544	4.694
17:30Hrs	0.980	2.456
18:30Hrs	0.718	0.968

Table 2: Results of voltage obtained in July, 2018

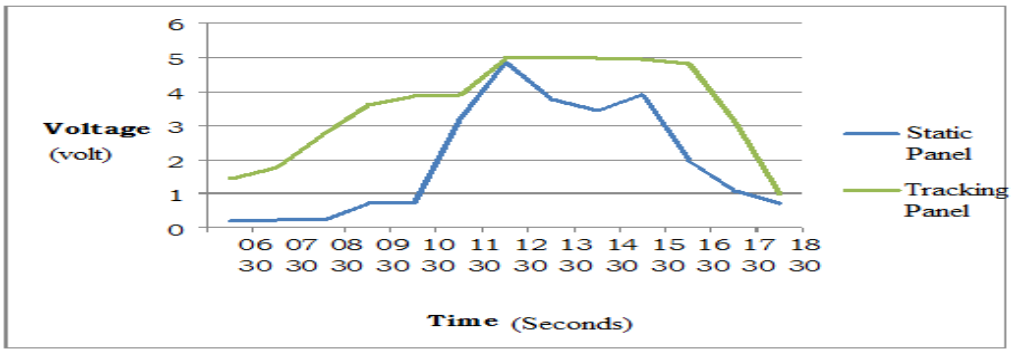

Figure 5: Voltage versus Time Results for Both Panels

The graphical representation of voltages of both panels against the time of the day is shown in Figure 5. From the graph, it is observed that solar intensity increases as the sun rises with the increase of the time of the day to its maximum intensity at 12 pm and then starts to decrease as the sun begins to fall toward evening hours. Some fluctuations are noticed in the graphs which were as a result of cloudy sky and abnormal atmospheric conditions at some instances during the day.

3.2 Analysis

The maximum sunlight occurs at around midday, with these values extending between 12 noon hours and 2 pm when the sun is very hot. In the morning and late evening, intensity of sunlight diminishes and the values obtained are less than those obtained during the day. The tracking system is on during the day and is switched off at sunset to save energy.

For the panel equipped with the tracking system, the values of the LDRs are expected to be close because whenever they are in different positions there is an error generated that enables its movement to adjust the panel inclination in direct contact with the sun. The motion of the panel is stopped when the values are the same, meaning the LDRs receive the same intensity of sunlight. For the fixed panel, the values vary because the panel is at a fixed position and most times the LDRs are not facing the sun at the same inclination. The graphs also show that at a particular point (midday) when both panels are facing the sun at the same time and at the same inclination, the voltages of both panels are the same.

The tracking system's solar panel has increased power output than the fixed panel system as the day progresses because the power generated by its panel is dependent on the intensity of light and the system's panel is adjustable so that it is always in direct contact with the sun. The more the light intensity the more the power that is generated by the solar panel. Since the panels of the tracking system is always in direct contact with the sun, its power is bound to be more than the fixed panel system that may be out of phase with the sun it moves from its rise to its fall in the evening. Therefore, the developed sun tracking system collects maximum energy than a fixed panel system at any time of the day because its panels are always in direct contact with maximum sun light intensity. This is the reason why it is an efficiency tracking system for solar energy collection.

4. RELIABILITY ASSESSMENT OF THE DEVICE

The method adopted in assessing the reliability of the sun tracking system is stress failure rates of components (parts) used in the design of the device. The method is based on obtaining the failure rate of each component from the standard tables of failure rates. The weighing factors for environment, operating stress, and temperature are determined and then the overall failure rate is computed using the following relationship:

$$\boldsymbol{\lambda_{oi} = n_i \lambda_i W_E W_T W_R} (\%/\mathbf{10^3}\text{hr}) \quad (8)$$

where:

$\lambda_{oi}\ is\ overall failure rate.$
n_i is number of the component used.
$\lambda_i\ is$ failure rate of individual component.
W_E is enviromental weighing factor.
W_R is operating stress weighing factor.
W_T is temperature weighing factor.

The reliability is then calculated using the relation

$$\boldsymbol{R = e^{-\lambda t}} \quad (9)$$

where, $\lambda = \Sigma\lambda_{oi}$ and t is time of operation of the device.

Table 3 gives the components used in this work, their number, their failure rates, their weighing factors, and the overall failure rate of the device.

Component	Number used n_i	Failure rate λ(%/10^3hr)	Weighing factors due to:			Overall failure Rate $\lambda_{oi} = n_i\lambda_i W_E W_T W_R$(%/$10^3$hr)
			Environment W_E	Temperature W_T	Rating W_R	
Integrated circuit (IC)	4	0.02	2.0	1.5	1.5	0.18
Capacitors	1	0.2	2.0	1.5	3.0	12.6
Electrolytic Ceramic	5	0.01	2.0	1.5	3.0	0.36
Resistors (gen. purp)	11	0.01	2.0	1.5	1.5	0.765
Transistor	2	0.08	2.0	1.5	2.0	3.84
Soldered	1	0.001	2.0	1.5	2.0	0.006
Motor	1					
						$\lambda = \sum\lambda_{oi}$ = 17.811

Table 3.1. Components and Their Failure Rates.

The overall failure rate is 17.811%/10^3hr. The reliability of the device that operates for one year
(t = 24 x 365
=8760hr) is calculated from equation (9) as follows:

$$\boldsymbol{R = e^{-(0.17811x10^{-3}x8760)} = 0.61 or 61\%}$$

RECOMMENDATION

For maximum power used for charging solar batteries to be attained, there is need to install solar panels equipped with a solar tracker in order to make the best use of the energy the sun produces. This will enable users save cost of installing many solar panels facing different positions to gain more energy for a single purpose.

CONCLUSION

.

At the end of this project, microcontroller based solar tracker using Atmel AT89S51 was actualized. The system was able to track the position of the sun where maximum intensity could be found. The system was also able to measure and display the current battery level.

REFERENCES

[1] Abdulateef Kaisl I. (2012), "Single-Axial sun tracker system using PIC micontroller", Diyala journal of Engineering Science,Vol 05, No.01.

[2] Greenough River Solar Farm (2016), "*What is solar energy",* Retrieved from: http://www.greenoughsolarfarm.com.au/solar-energy/

[3] Hemlata B. Nirmal, Syed A. Naveed. (2013), microcontroller based automatic solar power tracking system (IJEET), Volume4,issue1, Jan-Feb(2013),pp.109-114.

[4] Jamaludin NurKhuzairy Bin (2008), "*Solar Tracking System",* Faculty of Electrical & Electronic EngineeringUniversity Malaysia Pahang.

[5] Kumar M.N., Saini H.S., AnjaneyuluK.S.R., Singh K. (2014), "*Solar Power Analysis Based on Light Intensity",* The International Journal of Engineering and Science, pp. 01 – 05.

[6] Oloka R. O. (2015), "*Solar Tracker for Solar Panel",* University of Nairobi, Faculty of Engineering.

[7] Prodik Kumas Das, Mir Ahasan Habib, Mohammed, Mynuddin (2015). "Microcontroller Based Automatic solar tracking system with mirror booster" International journal of sustainable and Green energy Vol 4.No4.pp.125-136.

[8] Visha Bhote, Jaikaran Singh (2012) "Implementation of dual axis solar tracker model by using micro controller. "International journal of Engineering Keas peach and General science Volume 2, Issue 4, june-july, 2008.

Proceedings of the 1st National Communication Engineering Conference 2018

Attenuation Analysis due to Rain at Satellite Frequencies

Yerima A.M.
Department of Communications Engineering
Ahmadu Bello Universty
Zaria, Nigeria
aminuyerima@yahoo.com

Abdullahi Z.M.
Department of Communications Engineering
Ahmadu Bello University
Zaria, Nigeria
amZanna@gmail.com

Abubakar Kabir
Department of Communications Engineering
Ahmadu Bello Universty
Zaria, Nigeria
aakabeer9@gmail.com

ABSTRACT

Rain attenuation is a major source of signal degradation in microwave satellite communication resulting in unavailability of satellite reception during heavy rainfall. The knowledge of attenuation due to rain and its analyses is an essential consideration while setting up a satellite communication link in order to optimize system capacity and provides quality of service (QoS). In this project, a three year Rain rate data was obtained from the Nigeria Meteorological Agency (NIMET) database for all its centers in Northern Nigeria, the rain intensity was derived by converting the rain statistics obtain from NIMET, the converted data to rain intensity and the ITU-R recommended rain intensity models were used to estimate the deviation of rain attenuations at satellite frequencies (C, Ku and Ka-bands). The attenuation result at lower frequency spectrum especially C-band transponders (4-7.5) GHz are lower, while at higher frequencies above 10GHz, Ku-bands (10.7-12.75) GHz and Ka-band (20-30) GHz the attenuation are high, nevertheless, the research shows that rain attenuation is less severe in the Northern part of Nigeria and require lower fade margin for satellite link design purposes at all frequencies.

Keywords—Annual rainfall, rain intensity, satellite frequencies,

1. INTRODUCTION

The rapid growth in communication systems has brought saturation to the most desirable frequency bands (1 to 10 GHz). This fact has led to the utilization of higher frequencies extending the radio frequency spectrum from the cm into the millimeter wavelength region. (Khandaker L. and Mohammad M., 2014).

The presence of various forms of precipitation such as rain, snow, cloud and fog in a radio wave or microwave path is always capable of producing major impairment to terrestrial communications. Hydrometeors can introduce significant attenuation and depolarization, through their ability to absorb and scatter radio waves (Shoewu, O. and Edeko, F., 2011). Attenuation due to rain at microwave frequencies mainly leads to outages that compromise the availability and quality of service, making it one of the most critical factors in designing microwave link in tropical and subtropical regions. The design of new telecommunication systems requires the knowledge of rain fade in that region in order to optimize system capacity and meet quality and reliability criteria (Chebil, J. and Rahman, T., 1999).

For a reliable communication system, unavailability time during a year has to be kept at 0.01%. This corresponds to availability time of 99.99% during a year. Therefore rainfall with one-minute integration time is very important parameter to predict attenuation at 0.01% of time availability (ITU-R, P., 2003).

In this project, three years annual rainfall data was collected at various meteorological stations across Northern Nigerian States from the Agency Headquarter in Abuja. Common rain attenuation prediction methods require 1-min rain rate data, which is scarce in the tropical and subtropical regions. However, annual rainfall data are available at many meteorological stations. **A** method for converting the available rainfall data to the equivalent 1 min rain rate cumulative distribution (CD) was used. This allow for the usage of long-term mean annual rainfall data M at the location of interest (Khandaker L. and Mohammad M., 2014).

2. METHODOLOGY

The annual rainfall statistics (mm) collected from all the meteorological stations was converted first to rain intensity in order to calculate the rain attenuation; some selected rain models recommended by the ITU-R were used and integrated with the ITU-R model which is the most widely accepted international method and benchmark for comparative studies.

3. CONVERSION OF RAIN STATISTICS TO RAIN INTENSITIES

The Moupfouma model, a method for converting the available rainfall data to the equivalent 1 min rain rate cumulative distribution (CD) was used. Several studies have shown that the Moupfouma model with refined parameters can best describe the 1 min rain rate cumulative distribution in temperate and tropical regions. Moupfouma found that the 1 min rain rate CD could be expressed as (Khandaker L. and Mohammad M., 2014).

$$P(R \geq r) = 10^{-4}\left(\frac{R0.01+1}{r+1}\right)^{b} \exp(u[R_{0.01} - r]) \quad (1)$$

Where P is the probability of a rain event at 0.01%of the time, r (mm/h) represents the rain rate exceeded for a fraction of the time, $R_{0.01}$ (mm/h) is the rain intensity exceeded at 0.01 percent of time in an average year, and b is approximated by the following expression:

$$b = \left(\frac{r-R0.01}{R0.01}\right) \ln\left(1+\frac{r}{R0.01}\right) \quad (2)$$

The parameter *U* in eqn. 1 governs the slope of rain rate CD, and depends on the local climatic conditions and geographical features. For tropical and subtropical localities

$$U = \frac{4\,In\,10}{R0.01} exp\left(-\lambda\left[\frac{r}{R0.01}\right]^{\gamma}\right) \quad (3)$$

Where λ and γ are positive constants and are given as
λ= 1.066 and γ = 0.214.
$R_{0.01}$ is the rain rate exceeded for 0.01% which is obtained using Chebil model.
Thus, the Moupfouma model requires three parameters; λ, γ and $R_{0.01}$. While the first two parameters λ and γ, have been provided. $R_{0.01}$, is estimated using the Chebil's model. This allows for the usage of long-time mean annual accumulation, M, at the location of interest.
The power law relationship of the model is given by Equation (4):

$$R_{0.01} = \alpha M^{\beta} \quad (4)$$

Where α and β are regression coefficients defined as
α= 12.2903 and β = 0.2973.

However, using the Chebil model, the 1-minute rain-rate cumulative distribution for 20 locations was fully determined from the long term mean annual rainfall data, as presented in table (1).

4. PROJECT PROCEDURES

The ITU-R 618-10gives summarized procedures for the computation of satellite path rain attenuation. In order to compute the slant-path rain attenuation using point rainfall rate, the following parameters are required:

$R_{0.01}$: point rainfall rate for the location for 0.01% of an average year (mm/h)
hs: height above mean sea level of the earth station (km)
θ: elevation angle (degrees)
φ: latitude of the earth station (degrees)
f: frequency (GHz)
Re: effective radius of the Earth (8500 km).

The following steps are used for estimating the long-term statistics of rain attenuation for the design of earth to satellite systems (Khandaker, L. and Mohammad, M., 2014).

Step 1: Determine the rain height, h_R, from the latitude of the earth station φ, from the formula
$h_R = h_0 + 0.36$ km(Recommendation ITU-R P.839).
Where;
$h_0 = 5.0$ for $0^o \leq \varphi < 23^o$ km (5)
$h_0 = 5.0 - 0.075(\varphi - 23)$ for $\varphi > 23^o$ km

Step 2: For $\theta \geq 5^o$ compute the slant-path length L_s below the freezing rain height from:

$$Ls = \frac{(hR - hS)}{\sin\theta} \text{ km} \quad (6)$$

For $\theta < 5^o$, the following formula is used:

$$Ls = \frac{2(hR - hS)}{\left[\sin^2\theta + \frac{2(hR - hS)}{Rs}\right]^{1/2} + \sin\theta} \text{ km}$$

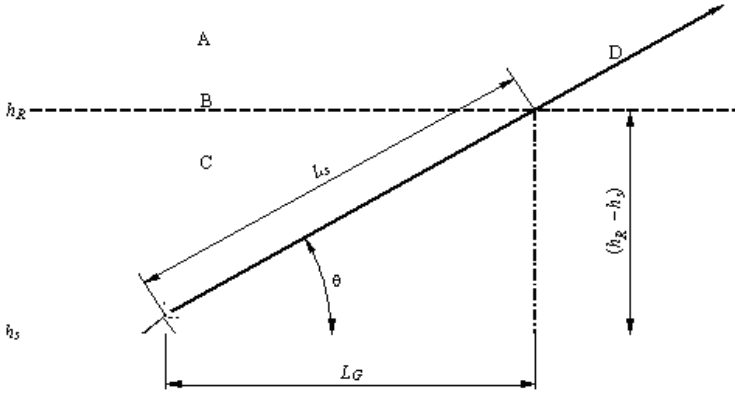

Fig 1: Schematic presentation of an earth-space path given the parameters to be input to the attenuation prediction process.

Where;
A: Frozen precipitation
B: Rain height
C: Liquid precipitation
D: Earth-space path

If $h_R - h_s$ is less than or equal to zero, the predicted rain attenuation for any time percentage is zero and the following steps are not required.

Step3: Calculate the horizontal projection, L_G, of the slant-path length from:

$L_G = L_s \cos\theta$ km (7)

Step4: Obtain the rainfall rate, $R_{0.01}$, exceeded for 0.01% of an average year (with an integration time of 1 min).

Step5: Obtain the specific attenuation γ_R, using the frequency-dependent coefficients given in Recommendation ITU-R P.838 and the rainfall rate, $R_{0.01}$, determined from

Step4, by using:

$\gamma_R = k\,(R_{0.01})^{\alpha}$ dB/km (8)

Step 6: Calculate the horizontal reduction factor, for $r_{0.01}$, for 0.01% of the time:

$$r_{0.01} = \frac{1}{1 + 0.78\sqrt{\frac{L_G\,\gamma_R}{f}} - 0.3(1-e^{-2L_G})} \quad (9)$$

Step 7**:** Calculate the vertical adjustment factor, $v_{0.01}$, for 0.01% of the time:

$$\zeta = \tan^{-1}\left[\frac{(hR - hS)}{L_G\, r0.01}\right] degrees$$

For $\zeta > \theta$, $L_R = \frac{L_G\, r0.01}{\cos\theta}$ km

Else,

$$L_R = \frac{(hR - hS)}{\sin\theta} \quad km$$

If $|\varphi| < 36^{o}$, $\chi = 36 - |\varphi|$ degrees

Else, $\chi = 0$ degrees

$$v_{0.01} = \frac{1}{1+\sqrt{\sin\theta}\left[31\,(1-e^{-(\theta/(1+\chi))})\sqrt{\frac{L_R\,\gamma_R}{f2}} - 0.45\right]} \quad (10)$$

Step 8: The effective path length is:

$L_E = L_R V_{0.01}$ Km (11)

It is worth noting that the effective path length L_E can also be obtained by using the unified method for slant paths and terrestrial links model by skipping steps 6-8, where the effective path length can be extended for the slant path case by considering the rain height (Da Silva M., Marlene S., 2012).

The rain height is defined as a function of the zero degree isotherm height, which is mapped all over the world and given in Rec. ITU-R P.839-3.

For a slant path with an elevation angle θ, the effective path length will be given by;

$$L_E = (L) = \frac{1}{L_G + L_S\cos\theta}\int_{-L_G}^{L_S\cos\theta} Ls(x)dx = \frac{1}{\frac{1+L_s\cos\theta}{L_G}}\,.\,L_S \quad (12)$$

Step 9: The predicted attenuation exceeded for 0.01% of an average year is obtained from:

$A_{0.01} = \gamma_R L_E$ dB (12)

Step 10: The estimated attenuation to be exceeded for other percentages of an average year, in the range 0.001% to 5%, is determined from the attenuation to be exceeded for 0.01% for an average year:

$$A_{\%P} = A_{0.01}\left[\frac{P}{0.01}\right]^{[0.065 + 0.033\ln(P) - 0.045\ln(A0.01\%) - \beta(1-P)\sin\theta]} \quad (13)$$

4. RESULT AND DISCUSSION

This chapter presents results obtained at each stage of this project in both tabular and graphical forms.

Table -1 shows how the long-term mean annual rainfall data M (mm/year) obtained from NIMET was converted to 1 min rain rate data $R_{0.01}$ (mm/h) using the Chebil's power law relationship. The model is applicable to both tropical and subtropical localities. Thus;

$R_{0.01} = \alpha M^{\beta}$

Where α and β are regression coefficients defined as α = 12.2903 and β = 0.2973.

Table 1: Measured mean annual rainfall and converted rain intensity(Nigerian Metrological Agency, 2018).

Stations location	Average annual cumulative rainfall data for 3 years M (mm/year)	Converted rain rate $R_{0.01}$ (mm/hr)
ADAMAWA	1489.5	107.9
ABUJA (FCT)	2184.9	120.9
BAUCHI	2153.5	120.4
BENUE	1805.3	114.3
BORNO	1328.5	104.3
GOMBE	1635.1	111.0
JIGAWA	2195.1	121.0
KADUNA	2315.5	123.0
KANO	1641.2	111.1
KATSINA	1192.7	100.9
KEBBI	1652.0	111.3
KOGI	1977.5	117.4
KWARA	2815.0	130.3
NASARAWA	1997.2	117.8
NIGER	1961.4	117.1
PLATEAU	1809.0	114.3
SOKOTO	1459.5	107.2
TARABA	1532.8	108.7
YOBE	1341.9	104.5
ZAMFARA	1569.7	110.0

5. COORDINATES AND ELEVATION ANGLES

The ground station look angle calculator in figure 4.1is a an online software used for calculating satellite azimuth and elavation angles. It was used in conjunction with the coordinates in table 4.2 obtained from the world atlas to calculate the elevation angles of each location.
The first parameters inputed into the calculator was the coordinate of Adamawa State, which has latitude of 9.208390˚ and longitude of 12.481460˚. The result displayed as the elevation angle was 71.7931˚.

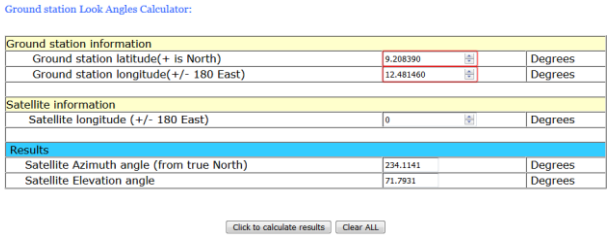

Fig 2: Ground station look angle calculator (Satcom, 2018).

Table 2: Result showing the coordinates and elevation angles obtained (world atlas, 2018).

Stations Location	Latitude $(N)^0$	Longitude $(E)^0$	Height Above Sea Level h_S (m)	Elevation Angle (θ)
ADAMAWA	9.208390	12.481460	162	71.7931
ABUJA (FCT)	9.057850	7.495080	476	76.1586
BAUCHI	10.310320	9.843880	616	73.2531
BENUE	7.733750	8.521390	104	76.4498
BORNO	11.846920	13.157120	325	69.2649
GOMBE	10.289690	11.167290	460	72.1746
JIGAWA	12.453470	10.041150	359	71.2326
KADUNA	10.526410	7.438790	626	74.8364
KANO	12.000120	8.516720	484	72.7143
KATSINA	12.990820	7.601770	519	72.3176
KEBBI	12.453890	4.197500	234	74.5246
KOGI	7.796880	6.740480	53	77.8522
KWARA	8.496640	4.542140	320	78.6344
NASARAWA	8.493900	8.515320	179	75.844
NIGER	9.615240	6.547760	243	76.3007
PLATEAU	9.928490	8.892120	1,186	74.3291
SOKOTO	13.062690	5.243220	296	73.4397
TARABA	8.893670	11.359600	349	73.051
YOBE	11.713910	11.081080	427	71.0879
ZAMFARA	12.170240	6.664120	451	73.6825

6. RAIN HEIGHT, HORIZONTAL PROJECTION AND SLANT PATH LENGTH

Steps 2 and 3 from the project procedure was used to calculate the rain height, the minimum and maximum values of the horizontal projection and the slant height as shown in table 4.3;

Table 3: Rain height, horizontal projection slant path and lengths

h_R (km)	Ls at maximum rain rate (km)	Ls at minimum rain rate (km)	L_G at maximum rain rate (km)	L_G at minimum rain rate (km)
4.64	4.6	4.3	0.9	1.3

7. SPECIFIC RAIN ATTENUATION

The specific rain attenuation on satellite frequencies (C, Ku and Ka bands) for both the horizontal and vertical polarities were determined using the equation in step5 $\gamma_R = k\,(R_{0.01})^{\alpha}$

dB/km. The minimum and maximum values of rain rates $R_{0.01,}$ (100.9 mm/hr) and (130.3 mm/hr) dB/km respectively and the ITU-R predicted rain rate 111.49 mm/hr served as an input.

The ITU-R recommended frequency dependent coefficients for estimating specific rain attenuation and the results obtained were as shown in tables 4 to 10.

Table 4: Recommended ITU-R P.838-3 Frequency-dependent coefficients

Freq. (GHz)	k_H	α_H	k_V	α_V
1	0.0000259	0.9691	0.0000308	0.8592
1.5	0.0000443	1.0185	0.0000574	0.8957
2	0.0000847	1.0664	0.0000998	0.9490
2.5	0.0001321	1.1209	0.0001464	1.0085
3	0.0001390	1.2322	0.0001942	1.0688
3.5	0.0001155	1.4189	0.0002346	1.1387
4	0.0001071	1.6009	0.0002461	1.2476
4.5	0.0001340	1.6948	0.0002347	1.3987
5	0.0002162	1.6969	0.0002428	1.5317
5.5	0.0003909	1.6499	0.0003115	1.5882
6	0.0007056	1.5900	0.0004878	1.5728
7	0.001915	1.4810	0.001425	1.4745
8	0.004115	1.3905	0.003450	1.3797
9	0.007535	1.3155	0.006691	1.2895
10	0.01217	1.2571	0.01129	1.2156
11	0.01772	1.2140	0.01731	1.1617
12	0.02386	1.1825	0.02455	1.1216
13	0.03041	1.1586	0.03266	1.0901
14	0.03738	1.1396	0.04126	1.0646
15	0.04481	1.1233	0.05008	1.0440
16	0.05282	1.1086	0.05899	1.0273
17	0.06146	1.0949	0.06797	1.0137
17	0.06146	1.0949	0.06797	1.0137
18	0.07078	1.0818	0.07708	1.0025
19	0.08084	1.0691	0.08642	0.9930
20	0.09164	1.0568	0.09611	0.9847
21	0.1032	1.0447	0.1063	0.9771
22	0.1155	1.0329	0.1170	0.9700
23	0.1286	1.0214	0.1284	0.9630
24	0.1425	1.0101	0.1404	0.9561
25	0.1571	0.9991	0.1533	0.9491
26	0.1724	0.9884	0.1669	0.9421
27	0.1884	0.9780	0.1813	0.9349
28	0.2051	0.9679	0.1964	0.9277
29	0.2224	0.9580	0.2124	0.9203
30	0.2403	0.9485	0.2291	0.9129
31	0.2588	0.9392	0.2465	0.9055
32	0.2778	0.9302	0.2646	0.8981
33	0.2972	0.9214	0.2833	0.8907
34	0.3171	0.9129	0.3026	0.8834
35	0.3374	0.9047	0.3224	0.8761
36	0.3580	0.8967	0.3427	0.8690
37	0.3789	0.8890	0.3633	0.8621
38	0.4001	0.8816	0.3844	0.8552
39	0.4215	0.8743	0.4058	0.8486
40	0.4431	0.8673	0.4274	0.8421
41	0.4647	0.8605	0.4492	0.8357
42	0.4865	0.8539	0.4712	0.8296
43	0.5084	0.8476	0.4932	0.8236
44	0.5302	0.8414	0.5153	0.8179
45	0.5521	0.8355	0.5375	0.8123
46	0.5738	0.8297	0.5596	0.8069
47	0.5956	0.8241	0.5817	0.8017

Table 5: Specific attenuation (γ_R) for C, Ku and Ka bands on horizontal at ITU-R ($R_{0.01}$)

ITU-R Horizontal	C-band (4GHz)	Ku-band (12GHz)	Ka-band (20GHz)
α_H	1.6009	1.1825	1.0568
k_H	0.0001071	0.02386	0.09164
$\gamma_{R\ Db/km}$	0.2029	6.2882	13.3537

Table 6: Specific attenuation (γ_R) for C, Ku and Ka bands on horizontal at minimum $R_{0.01}$

Horizontal	C-band (4GHz)	Ku-band (12GHz)	Ka-band (20GHz)
α_H	1.6009	1.1825	1.0568
k_H	0.0001071	0.02386	0.09164
$\gamma_{R\ Db/km}$	0.1729	5.5881	12.0170

Table 7: Specific attenuation (γ_R) for C, Ku and Ka bands on horizontal at maximum $R_{0.01}$

Horizontal	C-band (4GHz)	Ku-band (12GHz)	Ka-band (20GHz)
α_H	1.6009	1.1825	1.0568
k_H	0.0001071	0.02386	0.09164
$\gamma_{R\ Db/km}$	0.2635	7.5612	15.7456

Table 8: Specific attenuation (γ_R) for C, Ku and Ka bands on vertical at ITU-R ($R_{0.01}$)

ITU-R vertical	C-band (4GHz)	Ku-band (12GHz)	Ka-band (20GHz)
α_H	1.2476	1.1216	0.9847
k_H	0.0002461	0.02455	0.09611
$\gamma_{R\ Db/km}$	0.0882	4.8554	9.9696

Table 9: Specific attenuation (γ_R) for C, Ku and Ka bands on vertical at minimum $R_{0.01}$

Vertical	C-band (4GHz)	Ku-band (12GHz)	Ka-band (20GHz)
α_V	1.2476	1.1216	0.9847
k_V	0.0002461	0.02455	0.09611
$\gamma_{R\ Db/km}$	0.0779	4.3412	9.0365

Table 10: Specific attenuation (γ_R) for C, Ku and Ka bands on vertical at maximum $R_{0.01}$

Vertcal	C-band (4GHz)	Ku-band (12GHz)	Ka-band (20GHz)
α_V	1.2476	1.1216	0.9847
k_V	0.0002461	0.02455	0.09611
$\gamma_{R\ Db/km}$	0.1071	5.7833	11.6239

8. THE EFFECTIVE PATH LENGTH

Table 11 shows the average effective path length which was calculated using the formula in step 8, values obtained earlier for the elevation angle, the horizontal projection and slant height length at minimum and maximum rain rates served as inputs for the equation.

Table 11: Effective path length (L_E) calculated at minimum rain rate

L_E minimum (km)	L_E maximum (km)	L_E average (km)
1.0183	0.7598	0.8891

9. Estimated rain attenuation compared with predicted ITU-R values

Tables 12 and 13 shows the estimated rain attenuation obtained using the formula $A_{0.01}= \gamma_R L_E$,in step10, for measured minimum and maximum rain rates ($R_{0.01}$) values at Katsina and Kwara states respectively on both horizontal and vertical polarization as compared with predicted ITU-R values.

ITU-R recommendation P.837-6 contains annexes and maps of meteorological parameters that have been obtained using the European Centre for Medium-Range Weather Forecast (ECMWF) ERA-40 re-analysis database, which are recommended for the prediction of rainfall rate statistics with a 1-minute integration time, when local measurements are not available. The model uses a database of parameters (Pr6, Mt and β), available from the ITU's 3M Group, each of which is matched to a pair of longitude and latitude. This model was used to measure rain rate for comparison purposes (Afahakan I., Udofia K., and Umoren M., 2018). From ITU-RP837-6 mm/hr (A), the recommended rain rate is 111.49 which was used in calculating the attenuation at the predicted ITU-R predicted rain attenuation, while he maximum and minimum rain rates were obtained using rain rates from Kwara mm/hr (130.3) mm/hr and Katsina (100.9) mm/hr respectively.

Table 12: Estimated rain attenuation for all three frequency bands at horizontal polarization

Frequency	$A_{0.01}$ (dB) at Measured Minimum $R_{0.01}$	$A_{0.01}$ (dB) at Measured Maximum $R_{0.01}$	ITU-R Predicted values
4 GHz	0.1538	0.2343	0.1804
12 GHz	4.9683	6.7226	5.5908
20 GHz	10.6844	13.9995	11.8728

Table 13: Estimated rain attenuation for all three frequency bands at vertical polarization

Frequency	$A_{0.01}$ (dB) at Measured Minimum $R_{0.01}$	$A_{0.01}$ (dB) at Measured Maximum $R_{0.01}$	ITU-R Predicted values
4 GHz	0.0693	0.07674	0.0784
12 GHz	4.4207	3.8597	4.3169
20 GHz	9.2019	8.0344	8.8640

10. ATTENUATION

The graphical display showing the results obtained for the attenuation at minimum and maximum measured rainfall as compared with predicted ITU-R values as given in figures 3 to 5.

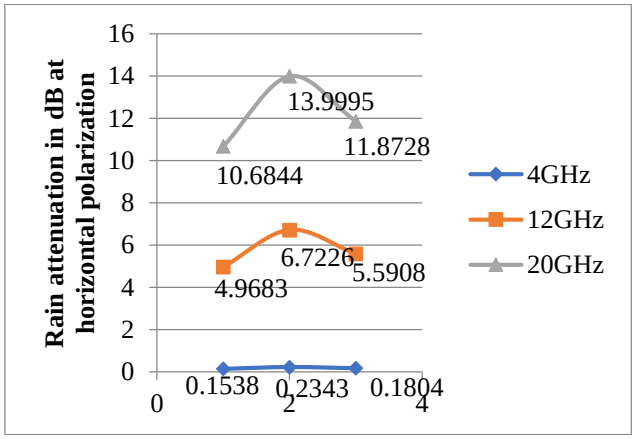

Fig 3: Estimated rain attenuation at minimum and maximum rain rate on horizontal polarization.

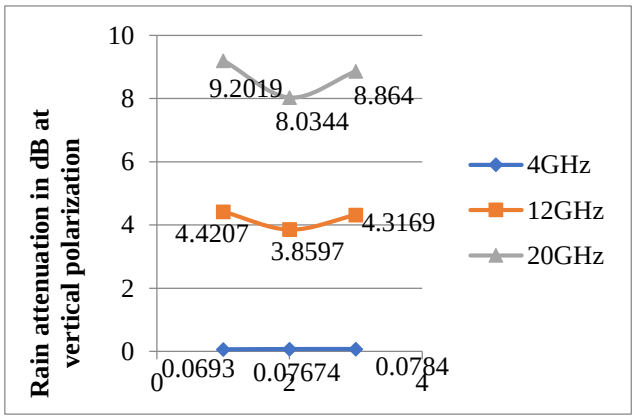

Fig 4: Estimated rain attenuation at minimum and maximum rain rate on vertical polarization.

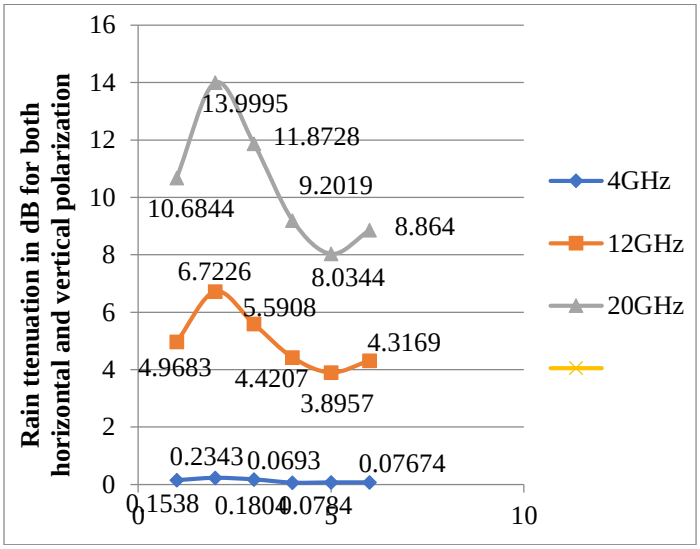

Fig 5: Comparison with predicted attenuations on both horizontal and vertical polarizations

For all the three bands, rain attenuation was estimated and compared with the ITU-R recommended rain attenuation for those regions. It is obvious that attenuation is lower at C-band on both horizontal and vertical polarization than the higher frequencies at Ku-band and Ka-band respectively.
The vertical polarization shows lower attenuation at all frequencies as compared to the horizontal polarization.
Hence to design a reliable microwave link, it is very critical because of higher attenuation at Ku and Ka- bands and needs careful and accurate estimation of rain attenuation, Kwara state has the highest rainfall cumulative distribution and rain rate at (130.3 mm/hr) with Katsina state having the lowest at (100.9 mm/hr) while the recommended ITU-R rain rate is 111.49 mm/hr.

10 CONCLUSION

Rain is a dominant source of attenuation at satellite frequencies in tropical and subtropical regions. Therefore accurate estimation of rain fade is very essential in order to design reliable microwave links in such regions. This was based on the cumulative rainfall data collected for three years in different parts of Northern Nigeria. Using appropriate conversion model, the long-term annual rainfall data was converted to rain intensity data. The rain intensity proposed by the International Telecommunications Union and Radio (ITU-R) as well as the converted data was used to investigate rain attenuation for microwave propagation in these regions at all frequencies.

From the results presented in tables and graphs in chapter 4, it is obvious to note that the level of attenuation due to rain on satellite frequencies was very small on lower frequency (C-band), while it was significantly high on higher frequencies (Ka and Ka) bands, It also shows that attenuation was less on the vertical polarization as compared to the horizontal polarization.
Attenuation at those frequencies was lower in the Northern region as compared to the Southern part of this country, which may serve as a good location to site Fixed Satellite Earth Station.

11 RECOMMENDATION

There was lot of difficulties and delay associated with sourcing data from the Nigerian Metrological Agency to execute this project. Long time research and rain studies should be deployed in future in order to get a more accurate effect of attenuation due to rain on satellite frequencies, also project of this nature needs funding.

REFERENCES

Afahakan I., Udofia K., and Umoren M., (2018) Nigerian Journal of Technology (NIJOTECH) Vol. 35 No. 1, January 2016, pp. 137 – 143.

Chebil J. and Rahman, T.: 'Rain rate statistical conversion for the prediction of rain attenuation in Malaysia', Electron. Lett., 1999, 35, (12), pp. 1019-1021.

Da Silva M., Marlene S. Journal of Microwaves, Optoelectronics and Electromagnetic Applications, Vol. 11, No.1, June 2012.

ITU–R, "Propagation Data and Prediction Methods Required for the Design of Earth–Space Telecommunication Systems," Recommendation

ITU–R P.618–8, vol. 12, pp. 1–24, 2015.

ITU-R, P. Recommendation ITU-R P.837-4, "Characteristics of precipitation for propagation modeling", ITU, Geneva, Switzerland, 2003.

Khandaker, L. and Mohammad, M., (2014) Performance Analysis of Rain Fades on Microwave Earth-to-Satellite Links in Bangladesh. International Journal of Engineering and Technology, Volume 4, No 7.

Nigerian Metrological Agency, (2018). ' Cummulative rainfall distraibution from 2014-2016'

Moupfouma, F., and Martin, L.: 'Modeling of the rainfall rate cumulative distribution for the design of satellite and terrestrial communication systems', Int. J. Sat. Communication., 1995, 13, pp. 105-115.

Shoewu, O. and Edeko, F., (2011).'Microwave Signal Attenuation at 7.2GHz in Rain and HarmattanWeather', American Journal of Scientific and Industrial Research. ISSN: 2153-649X.

https://www.worldatlas.com/webimage/countrys/africa/nigeria/nglatlog.htm, 2018.

https://www.tutorialsweb.com/satcom/calculation-of-satellite-look-angles.htm, 2018.